THE EFFECT OF STORAGE UPON SEDIMENT TRANSFER PROCESSES IN A SMALL SCOTTISH GRAVEL-BED RIVER

Simon John Wathen

A Thesis Submitted for the Degree of PhD
at the
University of St Andrews

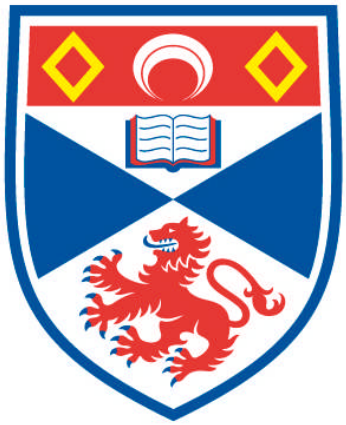

1995

THE EFFECT OF STORAGE UPON SEDIMENT TRANSFER PROCESSES IN A SMALL SCOTTISH GRAVEL-BED RIVER

A thesis submitted as fulfilment of the requirements for the degree of Doctor of Philosophy in the University of St. Andrews

SIMON JOHN WATHEN

VOLUME I

JANUARY 1995

Declaration

I, Simon John Wathen, hereby certify that this thesis, which is approximately 71000 words in length, has been written by me, that it is a record of work carried out by me and that it has not been submitted in any previous application for a higher degree.

date.12/1/95 signature of candidate. [redacted]

I was admitted as a research student in October 1990 and as a candidate for the degree of Ph.D. in October 1991; the higher study for which this is a record was carried out in the University of St. Andrews between 1990 and 1994.

date.12/1/95 signature of candidate. [redacted]

I hereby certify that the candidate has fulfilled the conditions of the Resolution and Regulations appropriate for the degree of Ph.D. in the University of St. Andrews and that the candidate is qualified to submit this thesis in application for that degree.

date.12/1/95 signature of supervisor. [redacted]

In submitting this thesis to the University of St. Andrews I understand that I am giving permission for it to be made available for use in accordance with the regulations of the University Library for the time being in force, subject to any copyright vested in the work not being affected thereby. I also understand that the title and abstract will be published, and that a copy of the work may be made and supplied to any bona fide library or research worker.

date.12/1/95 signature of candidate. [redacted]

Abstract

A detailed morphological approach is used to determine the effect of storage location upon sediment mobility, providing partial explanation for previously reported non systematic characteristics of sediment transfer. Data were collected over a period of 2 years from a small river in the Highlands of Scotland. Sediment transfer fluxes and volumetric storage were measured using an integrated data collection programme utilising 990 magnetic tracers and 225 cross sections spaced at c1 m intervals over two contrasting reaches (A and B).

Scaled tracer fluxes were monitored between 6 numerically defined storage types (very active, active, semi active, stable, inactive and dormant). Storage characteristics were determined using response time, defined as the time at which cumulative output from a store exceeds sediment in storage. Activity progressively declined from very active to inactive stores, the exact magnitude being a function of local morphology, particularly the presence of fixed bars.

Inter store exchanges of sediment were assessed using descriptive matrices categorised into individual types according to transfer and storage proportions. A relative dimensionless shear stress scale used to differentiate the storage conditions responsible for the occurrence of each matrix type indicated that transfer in reach A is a function of hydraulic conditions, grain size and storage, in reach B grain size is the only dominant factor. These controlling factors were sub divided into peak stage, duration, relative and absolute grain size, morphology and burial and assessed with reference to fractional transfer distances. The relative importance of each factor to transfer depends upon storage location and the incidence of morphological change. Comparison between tracer and volumetric fluxes provides explanation for sediment transfer distributions and allows assessment of morphological controls upon channel pattern maintenance. The results from this study were summarised in two conceptual models describing downstream and within reach sediment transfer.

Acknowledgements

This study was self funded, finance being derived/scrounged from various sources. I am particularly grateful to my father for paying the unreasonable level of fees imposed by the University of St. Andrews. The author also received financial assistance from the School of Geography and Geology and advice from the Registrar, Miss S. Taylor. Field data collection was carried out whilst the author was a Research Assistant (NERC Grant No. GR3/7407); permission and support from Rob Ferguson is gratefully acknowledged.

This study has considerably benefited from the supervision and critical review of Alan Werritty and Trevor Hoey, their time and patience is gratefully acknowledged. Hania Allan provided advice about interpolation techniques, Graham Sandeman assisted with the use of Adobe Illustrator and subsequent map production, Colin Cameron and Jack Jarvis ensured equipment availability and Andy Mackie provided reliable transport (usually!). The Department of Geography and Environmental Management at Middlesex University provided the resources and support for completion of this thesis. Use of a PC, loaned from the School of Geography and Geology in St. Andrews during 1994 allowed efficient data processing and considerably reduced production time.

Field assistance in all manner of unreasonable climatic conditions was provided by the following: Stuart Allison, Andrew Black, Bill Dietrich, Rob Ferguson, Michelle Forsyth, Richard Foster, Helen Grew, Mhari Harvey, Trevor Hoey, David Knighton, Kath Leys, Hamish Ross, Greg Sambrook Smith, Alex Sutherland and Alan Werritty. Their contribution and in some cases useful discussion is gratefully acknowledged. Access to the field site was provided by Scottish Natural Heritage, Mr. P. Adams and Mr. J. Kennedy. Reliable local weather reports, crucial to the study, were provided by Mrs. M Kennedy. Alastair and Sarah Oag are to be thanked for their wonderful hospitality, provision of a semi-permanent base for fieldwork and the venison.

TABLE OF CONTENTS

CONTENTS

LIST OF FIGURES

LIST OF TABLES

LIST OF PLATES

1. Introduction

Sediment transfer within gravel-bed rivers is often explained and/or predicted with reference to reach or section averaged parameters (e.g. Parker and Klingeman 1982, Pickup et al. 1983, Ferguson and Ashworth 1992, Hoey and Ferguson 1994). Alternatively, the distribution and magnitude of sediment fluxes have been documented and in some cases predicted using floodplain scale sediment budgets where sediment transfer between broadly defined stores is examined (Dietrich et al. 1982, Nakamura 1986, Kelsey et al. 1987). Whilst such simplifications may be practically justifiable, they overlook detailed small scale processes. Grain scale experiments have demonstrated that local factors are important to the magnitude and distribution of transfer fluxes (e.g. Hassan 1990, Laronne and Duncan 1992). Tracer particle transfer distances during contrasting flood events have been related to bed packing, grain size and burial depth (e.g. Church and Hassan 1992, Hassan and Church 1994). However, the distribution of transfer distances is not a simple deterministic function (Laronne and Carson 1976), and stochastic explanations have been advocated (e.g. Hassan et al. 1991). Tracer studies have not considered the role of channel morphology in any detail, regarding it only as a factor which may provide explanation for some of the stochastic behaviour (Hassan and Church 1992). Drew (1992) noted that bar storage was an important determinant of the distribution of transfer distances, the magnitude of this effect varying between rivers according to the dominant bar type. Hassan and Church (1992) suggest that adoption of a three dimensional morphological approach is necessary to explain sediment transfer. This study aims to provide this additional undocumented analytical dimension through detailed analysis of sediment transfer patterns relative to storage locations in two small reaches of a gravel-bed stream.

Sediment entrainment and transport are together defined as transfer since the processes are impossible to adequately separate during measurement and analysis. All movement of sediment documented in this study is deemed to be transfer, the magnitude of which is a function of depositional conditions at the location of entrainment and factors operating during transport.

This study aims to describe and explain sediment transfer patterns at high levels of resolution. Specific objectives are to:

1. Document and explain the magnitude and distribution of sediment transfer within two reaches of contrasting activity; assess the importance of morphology and local hydraulic conditions to patterns of fractional sediment transfer.

2. Provide an objective division of each reach into physically meaningful sediment stores; monitor sediment fluxes between these stores using magnetic tracers (e.g. Hassan et al. 1984), and construct a reach scale sediment budget based upon sediment exchange between stores.

3. Describe the activity and function of the stores; assess the importance of storage for sediment transfer fluxes with reference to parameters of sediment transfer distributions (Dietrich et al. 1982).

4. Assess the relative importance of local entrainment from the bed (Hassan 1990) and morphological change to sediment transfer.

5. Develop a three dimensional morphological approach to evaluate the magnitude and distribution of transfer, and assess the effect of conditions at entrainment in each storage type (morphology and sediment elevation) upon fractional transfer distances; determine the distribution of sediment sources in contrasting flood events.

6. Evaluate the importance of local morphology to sediment transfer, particularly the presence of fixed and free bars (Seminara and Tubino 1989).

7. Determine at the grain scale the relative importance of motion and inertial forces upon sediment transfer expressed as the dimensionless shear stress, τ^*, at a depositional location.

8. Develop a conceptual model to describe, explain and summarise sediment transfer fluxes. The scope of this study prevents numerical implementation of this model, instead, this will form the basis for future work.

The Allt Dubhaig, the site used in this work, has also been used to determine the significance of selective transfer to overall downstream fining (NERC Grant Ref. GR3/7407) with sediment transfer only considered in the downstream dimension (Hoey and Ferguson 1994). The present study augments this work and additionally evaluates the importance of lateral storage effects. Some data from the fining project are used in this study. In such cases, the relevant sample locations are described.

Analysis of sediment transfer according to lateral and vertical effects has not been the subject of intensive study. Lateral sorting effects were considered by Seal et al. (1993) who related downstream fining rates to the cross sectional distribution of sediment patches. Numerous other studies briefly describe the importance of lateral storage upon transfer without being specific. For example, Laronne and Duncan (1992) state that sediment mobility is greater from low elevation bars than high elevation bar surfaces. Elevation effects are important factors determining sediment

mobility (Williams and Rust 1969, Lekach et al. 1992) and require detailed analysis in contrasting systems. Lateral storage attributable to bars results in an irregular spatial and temporal distribution of transfer distances in the downstream direction (Hassan and Church 1992). This study addresses these factors detailing entrainment and transfer from storage locations in a structured manner. Chapter 2 reviews the current extent of research into sediment transfer, focusing upon factors which may be responsible for the random distributions thus far reported. Chapter 3 introduces the field site, and describes the hydraulic and sedimentological characteristics of the two study reaches to be used. In addition, historical evidence is used to assess previous reach activity. The methods used to determine sediment and volumetric fluxes are introduced in chapter 4 along with grain size and stage measurement. Chapter 5 describes the numerical method used to categorise storage within each reach. Relative activity is assessed at reach, sub-reach, storage type and sub-reach storage type scales. Tracer and volumetric fluxes are linked in chapter 6 providing explanation for the observed transfer distributions. Transition matrices (e.g. Kelsey et al. 1987) are used to describe fluxes of sediment between stores according to contrasting flow conditions. The effect of sediment storage upon the mode of transfer is described in chapter 7. Entrainment and transport are separated and the relative magnitude of each assessed, along with discussion of the importance of burial according to storage type. The results of the main analytical chapters are summarised and conceptualised in chapter 8. A semi-quantitative model is suggested describing the main components of the sediment transfer process. Conclusions are presented in chapter 9 where the significance of this study in the wider context is evaluated.

2. Sediment transfer and storage

This chapter introduces the extent of current understanding into sediment transfer processes and reviews controls upon transfer patterns, particularly the importance of sediment sorting and horizontal and vertical exchange. A review of sediment budget studies and the previously used descriptive variables in conceptualising transfer at the reach scale is also presented.

2.1 The bedload transfer process

Fluvial geomorphologists and engineers have attempted to document and predict bedload transfer through the study of entrainment and transport for a number of years, depositional effects being rarely studied. Bedload can be defined as the component of the fluvial sediment load that moves via rolling or saltation (Gomez 1991). It is arbitrarily defined in gravel-bed rivers to exclude material less than 0.2 mm in diameter (Gomez and Church 1989) as finer sediment is assumed to go directly into suspension when disturbed (Leeder 1982).

All predictions of bedload involve a number of simplifying assumptions which essentially define an equilibrium state. This may be possible to define in flume conditions but is rarely attained in the field (Gomez 1991). Flume experiments have shown that even equilibrium bedload transfer is a highly irregular process when viewed at short timescales (Kuhnle and Southard 1988, Gomez et al. 1989). For these reasons there is no universal formula for the prediction of bedload transfer (Gomez and Church 1989).

2.1.1 Historical overview

Bedload transfer was first examined by du Boys (1879) adopting an excess shear stress approach and conceptualising the bed as a series of layers with the most mobile layer found at the surface. Gilbert (1914) noted that transfer capacity increases with steeper gradient, higher discharge and lower calibre of bedload. Much early work concentrated upon transfer until Hjulström (1935) introduced deposition in the form of an empirical curve documenting particle movement and deposition according to a size related critical velocity.

The fluid force acting to move a particle is the shear stress τ, defined for uniform flow in wide channels by du Boys (1879) as

$$\tau = \rho g h S \tag{2.1}$$

where ρ is the density of water, g is acceleration due to gravity, h is mean depth and S is slope. Shields (1936) defined a dimensionless shear stress, τ* as,

$$\tau^* = \frac{hS}{\gamma D_i} \tag{2.2}$$

where, τ*, is the ratio between forces acting to move a particle of diameter D_i and those keeping it at rest. γ is the sediment submerged weight equal to $(\rho_s-\rho)/\rho$ where ρ_s is sediment density.

Shields (1936) defined a critical dimensionless shear stress τ^*_c as the point at which incipient motion occurred. This definition has been criticised since it is arbitrary and is a difficult state to objectively define (Richards 1982). Shields experiments with uniform grain sizes defined a relationship between τ^*_c and particle Reynolds number, Re_p (Figure 2.1). Re_p was defined as

$$\mathrm{Re}_p = v_* D_i / v \approx 11.6 D_i / \delta_{sub} \tag{2.3}$$

where v_* is shear velocity, D_i is particle diameter, v is kinematic viscosity and δ_{sub} is the thickness of the laminar sub layer. Shields suggestion of a constant τ^*_c of 0.06 (Figure 2.1) at high values of Re_p (above approximately 100) indicates a direct relation between shear stress and particle diameter (obtained by substitution of 0.06 into Eq. 2.2), suggesting that sediment entrainment (and hence transfer) is size selective. Shields concluded that motion did not occur at τ^*_c values below 0.06.

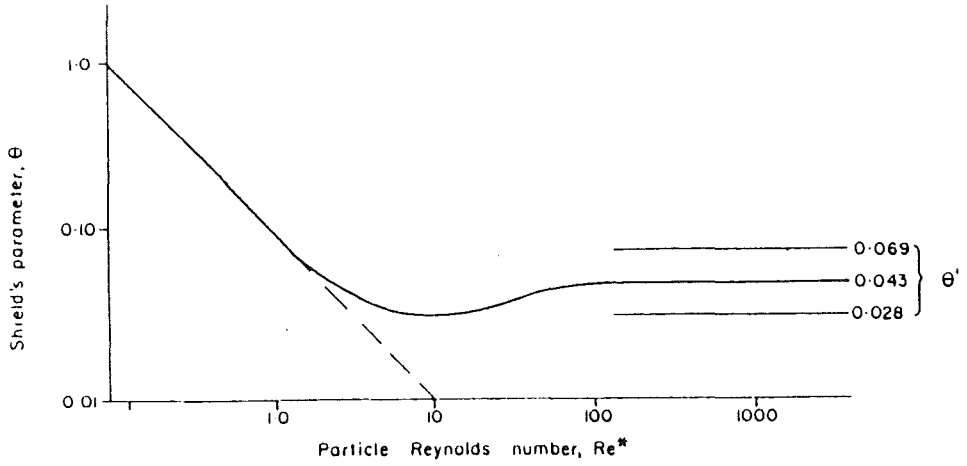

Figure 2.1. Shields entrainment function relating τ^*_c (Shields parameter, θ) to Re_p for uniform sediment. Envelope of published data where Re_p>100 is indicated (after Yalin and Karahan 1979).

The development of the excess shear stress concept led to the derivation of a number of empirical equations to predict bedload transfer rates (e.g. Meyer-Peter and Müller 1948 (MPM), Brown 1950, Parker 1979). Parker (1979) used data from 278 rivers to produce an approximation of the Einstein - Brown relation (Brown 1950) predicting dimensionless transfer rate, Φ

$$\Phi = \frac{11.2(\tau^* - 0.03)^{4.3}}{\tau^{*3}} \qquad (2.4)$$

The value of 0.03 is the critical value of τ^*, prior to which no transfer occurs. This contradicts Shields who calculated the critical value as 0.06. The variability in reported values for τ^*_c (e.g. MPM critical value is 0.047) reflects experimental and derivational assumptions. Yalin and Karahan (1979) provide an envelope for uniform grain τ^*_c data of 0.028 - 0.069 with a best fit at 0.043 (Figure 2.1).

Einstein (1942) began to break down the simplified view of size selectivity. In a semi-theoretical approach, a hiding factor was introduced which took into account smaller particles requiring higher critical shear stresses due to coarser material shielding them from the flow. Protrusion of coarser particles was not considered. Einstein (1950) elaborated upon these ideas and discussed the stochastic nature of bedload transfer where material moved in a series of hops each with a length approximately 100 times the particle diameter. This led to a transfer intensity function based upon the probability of particle exchange at the bed.

The assumption that saltation hop length is 100 times the particle diameter has been proved to be inaccurate since step length increases with stream power (Grigg 1970) and transfer stage (Abbot and Francis 1970). Einstein's unusual approach has the advantage over other formulae in that it contains no threshold value (Richards 1982). Although this formula is still used, it is of more use as a conceptual tool than for application. In this regard, the potential of Einstein's approach has yet to be fully realised.

2.1.2 Particle entrainment studies and bedload transfer prediction

Shields' analysis on uniform sediment crucially excluded relative size effects (Egiazaroff 1965). Fine sediment mobility is reduced due to hiding effects (Einstein 1942) and conversely, coarser sediment protrusion into the flow increases mobility (Fenton and Abbott 1977). A further problem with Shields' analysis was demonstrated by Baker and Ritter (1975) who noted that lift forces are reduced where depth is large since the bed only experiences a fraction of the mean velocity. Conversely, low flows were found to be more competent than expected since lift forces were greater. Shields' analysis did not directly consider lift forces.

The importance of relative size effects has led to the derivation of alternative approaches to the explanation of entrainment and bedload transfer. Parker and co-workers initially assumed that once shear stress was above a critical value, all sizes on the bed became potentially mobile (Parker et al. 1982a, Andrews 1983). This theory of equal mobility forms the basis for prediction of bedload transfer using shear stress and the median diameter of the subsurface. Implicit in this is the concept of mobile armour, defined as a mobile bed phenomenon (Parker and Klingeman 1982) present even during large flood events where all sizes are in motion yet only a small fraction of surface grains of a given size are actually moving. The presence and maintenance of such a feature was demonstrated in laboratory experiments by Parker et al. (1982b). Parker and Klingeman (1982) hypothesised that the armour regulates bedload transfer such that the stream can transfer both the coarse and fine halves of its bedload supply at equal rates implying that the bedload size distribution should approximate that of the subsurface.

In the course of their analysis Parker et al. (1982a) developed a relation to describe the mobility of material once shear stress is sufficient. This entrainment function is given by

$$\tau_c^* = a\left(\frac{D_i}{D_{50}}\right)^b \tag{2.5}$$

where D_{50} is the median grain size, in this case of the sub armour (D_{50sub}). Data presented by Parker et al., suggested that b, the entrainment coefficient, = -0.982 and a = 0.0876. The approximation of b to -1 indicated that once shear stress was above a threshold value, all grain sizes were equally mobile allowing development of an empirical bedload transfer relation (Parker et al. 1982a) based upon D_{50sub}. It is important to note that this approach to particle mobility was only a first order approximation. The results from this model were compared with actual Oak Creek data (Milhous 1973) and found to perform considerably better than Meyer-Peter and Müller and Einstein models. Carson and Griffiths (1987) discuss some drawbacks of this model, principally that it was developed using very low transfer rates such that application to rivers with high transfer rates may be more problematic.

Andrews (1983) and Andrews and Erman (1986) developed a similar relationship to Eq. 2.5 using the coarsest particle on the bed, which was taken to be a surrogate representative of the limit of the critical condition. The b value was -0.872 (Figure 2.2), however, most of their plots contained only 6 - 8 points causing the 95% confidence limits to be quite large (Ashworth and Ferguson 1989). Also, D_i appears on both sides of their derived equation overemphasising the approach of b towards 1. The value of -0.872 was less than that of Parker et al. indicating that deviation away from perfect equal mobility did take place. However, any comparison between the results of Andrews

and Parker et al. must be viewed with caution since the methods were not strictly comparable (Carson and Griffiths 1985). The analysis of Andrews also used the maximum grain size to represent competence, an approach criticised by Wilcock (1992a).

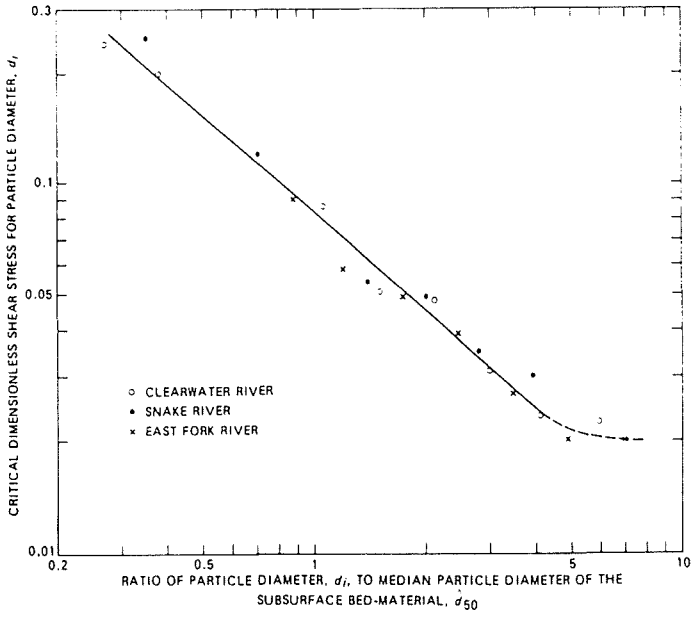

Figure 2.2. Relation between relative grain size and critical dimensionless shear stress. b = -0.872 (After Andrews 1983).

The predictive model of Parker et al. assumed equal mobility, the b value was modified to -1 instead of -0.982 as derived. A development on this has been models which go further than a first approximation and utilise some size selectivity principles. Diplas (1987) refined this model by including a constant proportional to grain size. Whilst based upon deviation away from perfect equal mobility, this refinement reproduced the characteristic asymmetric bedload size distribution of Oak Creek more effectively. Parker (1990) also adopted the view that deviation away from perfect equal mobility did occur. This was incorporated into a surface based model utilising some of the principles from the subsurface based model of 1982, with $b \approx -0.9$.

Acknowledgement of deviation away from perfect equal mobility arose from widespread debate concerning particle entrainment. Komar (1987) suggested that the Oak Creek data used by Parker and Andrews suggests a b value of only -0.68 when analysed in a different way. Wilcock (1988) while conceding that Andrews analysis was flawed suggested that Parker et al. were correct and that equal mobility was the dominant transfer characteristic. In support of this, Wilcock and Southard (1988) used flume experiments to demonstrate that all size fractions begin moving at a similar shear stress. Theoretical proof for equal mobility was provided by Wiberg and Smith (1987). These theories led to contrasting explanations regarding the formation and maintenance of mobile and static armours (Andrews and Parker 1987). During this period, the literature was contradictory and no clear answer was apparent.

Further evidence for the absence of perfect equal mobility was provided by Ashworth and Ferguson (1989) who reported b values of less than -1 from numerous field data sources (support for perfect equal mobility was based upon results from very narrowly defined experimental conditions). Such a deviation was advocated as a possible cause of downstream fining (Paola and Wilcock 1989). Komar and Shih (1992) suggested that equal mobility took place at an early transitional stage during transfer, subsequent to which the distribution of transferred sediment became coarser as discharge increased (Kuhnle 1992, 1993, Wathen et al. in prep.). Shih and Komar (1990a, b) have developed a model based upon fitting a Rosin distribution to the grain size distribution of bedload and apportioning the total gravel transfer rate accordingly. This makes no assumption about relative mobility at entrainment.

The analyses of Diplas and Shih and Komar produce good fits between observed and predicted data, however, as a first approximation, the model of Parker et al. was perfectly adequate. The principle of equal mobility was developed as an approximation and subsequent argument has resulted in a conclusion that was already acknowledged by Parker et al., namely that equal mobility can occur but some degree of size selectivity is usually present. The magnitude of this depends upon a number of hydraulic and morphological factors. The causes of this deviation are an implicit aim of this study.

The general conclusion from this section is that equal mobility is a suitable first approximation in the prediction of bedload transfer, however, selective transfer is also important and is most obvious over a range of discharges (Wilcock 1992b). It is important to note most research documents transfer (e.g. Ashworth and Ferguson 1989, Kuhnle 1992), at present no studies have documented local depositional effects upon size selectivity and transfer. Hassan and Church (1992) suggest that adoption of a morphological approach is essential to understand the mechanisms responsible for within channel fluxes and hence bedload transfer patterns and the dominant mode of transfer.

2.2 Sediment sorting

Fractional transfer fluxes (and hence the dominant mode of transfer) at the reach scale are the result of the interaction of local sorting processes and distribution of controls upon them. Sediment sorting processes may be described at two scales: (1) overall long profile scale sorting, often a result of size selectivity and an associated downstream decline in competence (e.g. Ferguson and Ashworth 1991, Werritty 1992); (2) local reach scale sorting. Downstream changes in the hydraulic properties of a river, manifested as (1), alter local sediment supply and the grain sizes available in the bed for local sorting processes. The dominant control on the magnitude and distribution of local sorting are morphology, hydraulics, sediment supply and grain size. Within

sorting (Ashworth et al. 1992). Upstream sediment supply affects morphological stability and channel pattern maintenance and may therefore alter local sediment sorting processes (Goff and Ashmore 1994). Local sorting patterns are therefore the result of complex interaction and may be documented and explained with reference to transfer fluxes (Laronne and Duncan 1992). This study aims to assess the extent of these controls upon local transfer fluxes and ascertain the importance of local processes to the mode of transfer and fractional mobility.

2.2.1 Reach scale sorting

Local sediment sorting and size segregation have been advocated as explanations for bar formation (Krigström 1962, Bluck 1979, Hein and Walker 1977, Rundle 1985, Ashworth et al 1992). Sorting patterns may indicate the stage of development of bars within a particular reach. Bluck (1979) suggested an evolutionary sequence of bar types (Figure 2.3), due to dissection of existing sediments and contrasting patterns of sediment redistribution. Ashworth et al. (1992) used

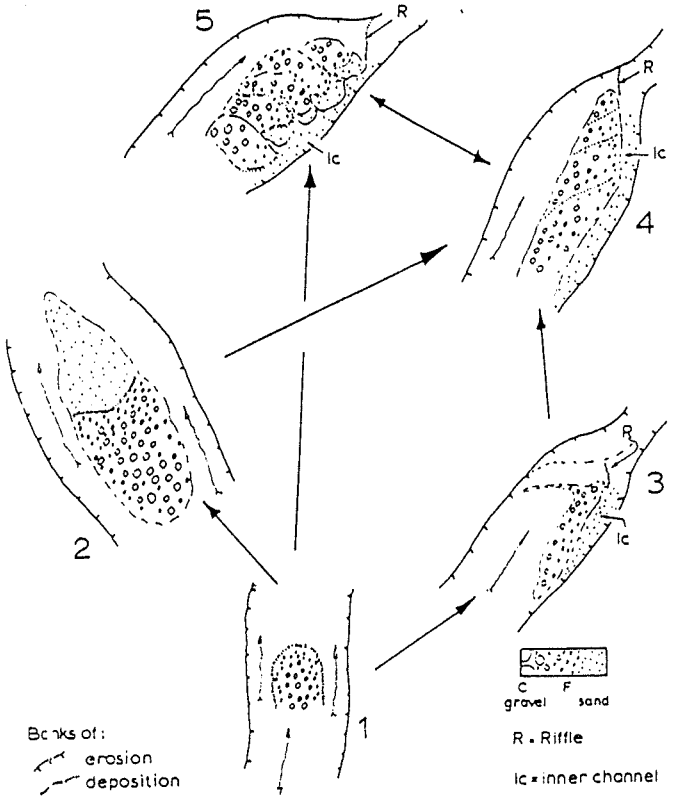

Figure 2.3. Development of bar types, multiple results are dependant upon hydraulics and sedimentology (after Bluck 1979). The basic unit is a linguoid bar which may be transformed into various bar assemblages as indicated by the arrows.

a combination of field and flume data to demonstrate bar development and size segregation resulting in downstream fining sequences across bar surfaces (e.g. Williams and Rust 1969, Rust 1972, Hein and Walker 1977). Such fining sequences were not a result of sorting in transfer, but may have been due to selective deposition where a 'like seeks like' scenario takes place (Kuenan 1956, Bluck 1982, Allen 1965), an example of roughness induced sorting.

Sediment sorting takes place in horizontal and vertical directions (tracer evidence for this is presented in section 2.4). Elevational effects operate at the bed surface where particles are subject to varying depths of flow. Laronne and Duncan (1992) noted that tracer particles deposited on lower elevation bars were more likely to be entrained than material on high bars where attainment of sufficient depth for entrainment was less frequent. Bars formed in large scale events of higher recurrence interval tend to remain until a comparable flood recurs.

Sediment sorting at the reach scale can be examined by looking at fractional movement fluxes. These fluxes are attributable to 4 factors (Ashworth et al. 1992):

1. Initial Size Mix: Iseya and Ikeda (1987) recognised 3 zones of bed configuration, the distribution of which varies according to the actual size mix of sediment. These are analogous to gravel sheets or lobes (Hein and Walker 1977, Whiting et al. 1988, Dietrich et al. 1989). Such features may explain the observed temporal variations in transfer rates (Kuhnle and Southard 1988, Gomez et al. 1989). The influence of sheets and lobes upon movement fluxes is uncertain, however, these bedforms must be considered when examining lateral and downstream distributions. It is possible that poorly sorted initial size distributions (according to storage location) may provide increased potential for downstream sorting.

2. Sediment Supply: Sediment supply from upstream has been advocated as a cause of morphological change (Goff and Ashmore 1994). Lane et al. (in prep) introduce the concept of over aggraded reaches characterised by instability and morphological change. In addition upstream supply affects the degree of armour development, with the degree of armouring inversely related to the rate of supply (Little and Meyer 1976, Sutherland 1987, Dietrich et al. 1989, Sear 1992). Surface coarsening via a gradual reduction in fine material through either vertical (Parker and Klingeman 1982, Diplas and Parker 1992) or downstream winnowing (Parker and Sutherland 1990) results in coarse surface layers which in the case of static armour are rarely broken down at high stage. Sediment supply varies spatially (Church and Jones 1982) and the propensity for morphological change and distribution of static armour may also vary accordingly (Lisle and Madej 1992).

3. Flow Hydraulics: The rate of downstream sorting at the reach scale is a function of the effect of excess shear stress upon dominant sorting processes of abrasion and/or selective transfer (Parker 1991a, Hoey and Ferguson 1994). Ferguson et al. (1989) reported the effects of interaction between flow and bed roughness upon local sorting processes. Using a braided study reach of the White River, they compared the hydraulics and bedload movement between a gravel-bed and a sand ribbon. The effect of the differences of roughness for the same depth of flow allowed attainment of greater τ on the gravel, however, the large D_i/D_{50surf} ratio (D_{50surf} - median grain size of surface) on the sand offset this. The effect of D_{50surf} outweighed the roughness differences, resulting in the sand ribbon acting as a traction carpet with a larger bedload transfer capacity and competence than the gravel.

The velocity reversal hypothesis (Keller 1971) is a further example of the effects of flow hydraulics on bed material and size segregation. Riffle and pool grain size distributions are a result of high velocities in pools and lower values over riffles during flood stages (Andrews 1979), although evidence for such a reversal is somewhat sparse (Carling 1991). Bhomik and Demissie (1982) argued that in some cases pools contained lag coarse deposits which could not be attributed to velocity reversal. Recent research based upon numerical simulation suggests that the occurrence of velocity reversal is a function of the relative difference between pool and riffle roughness at varying stage (Carling and Wood 1994). At the bar scale, flow convergence and divergence (Ferguson and Werritty 1983, Ashworth and Ferguson 1986) are linked to size segregation and modes of bar formation (e.g. Ashworth et al. 1992).

Secondary circulation within pools associated with super elevation at bends affect fractional transfer fluxes with secondary currents locally competent to transfer finer sediment. Saunders (1988) illustrated this for a riffle pool bar unit on the River Feshie. Finer material moved onto the bar from the riffle whilst coarser material remained in the channel. Unfortunately, the original tracer positions were not accounted for thus precise movement directions were unclear. Thorne and Lewin (1979) used painted tracer pebbles to examine material movement out of a pool in a meander bend and found that particles eroded from adjacent to the outer bank moved downstream without crossing the channel and were deposited on the point bar at the next bend. Material seeded on the inner bend was influenced by the inner flow cell resulting in movement up the point bar face. These patterns are dependant upon the distributions of the main, inner and outer bank cells (Carson 1986), a function of the width:depth ratio of the bend (Markham and Thorne 1992).

4. Channel Patterns: Channel pattern, particularly the effect of bar assemblages influence the distribution of sediment fluxes. Brierley (1989) has documented contrasting facies distributions on the Squamish River according to channel pattern and Laronne and Duncan (1992) demonstrated contrasting sediment flux in braided and alternate bar reaches. Their explanations were related to

hydraulic effects and the influence of bars upon the distribution of flow. On this basis it is useful to classify bars according to formation mechanism as free or forced bars (Seminara and Tubino 1989). A free bar develops within the channel spontaneously due to sediment supply while forced bars (hereafter referred to as fixed bars) are a response to channel curvature and hydraulics (Whiting and Dietrich 1991). Church and Jones (1982) developed a similar dichotomy with bars divided up into hydraulic element (fixed) and sediment storage (free) bars. Fixed features such as point bars rarely migrate, but dominate local flow and sediment transfer patterns (e.g. Hooke 1975, Bridge and Jarvis 1982, Dietrich and Smith 1983, 1984, Thorne et al. 1985). Alternate bars are free bars and tend to migrate; the patterns of flow around these morphological units act to drive sediment transfer and bar migration (Whiting and Dietrich 1991). Examination of fluxes relative to bar storage may provide an insight into the mechanisms causing channel change. For example, avulsion documented on the River Feshie by Ferguson and Werritty (1983) was due to aggradation and dissection, processes which can be described and explained by analysis of movement fluxes.

All four factors are interrelated and determine the magnitude and distribution of sediment flux pathways. For example, sediment fluxes particular to a channel pattern (4) depend upon flood magnitude (3), the magnitude and calibre of upstream supply (1, 2), the distribution of morphology (4) and the associated propensity for morphological change. The combined effect of these sorting factors at the local scale may be quantified with reference to sediment flux characteristics and transit time distributions. The effect of these reach scale factors may be complicated by the importance of local grain scale effects (e.g. pocket geometry) upon documented tracer fluxes (Church and Hassan 1992).

2.2.2 Inter reach sorting

This section describes the factors influencing long profile grain size distributions, predominantly the presence/absence of downstream fining. The mechanisms responsible for this downstream decrease in grain size are important not only at the broad long profile scale, but also to the local reach scale since they influence sediment availability.

Many rivers demonstrate a characteristic decline in mean grain size with progression in the downstream direction away from sediment sources. Numerous authors have documented this in a variety of fluvial environments (e.g. Yatsu 1955, Church 1972, Church and Kellerhals 1978, Frostick and Reid 1980, Brierley and Hickin 1985, Dawson 1988, Werritty 1992, Kodama 1992). Sternberg (1875) described the downstream decrease in particle weight on the Rhine by a function of the form,

$$\omega = \omega_o \exp(-a_w x) \tag{2.6}$$

where ω_o is initial weight, ω is the weight at distance x downstream and a_w is a coefficient related to the weight reduction. Downstream fining has been attributed to abrasion, tested in field and laboratory situations (Krumbein 1941, Kuenen 1956, Bradley 1970, Schumm and Stevens 1973). However, in some cases the documented decrease in grain size has been very rapid over a short distance (Adams 1979). Rotating drum experiments (Lewin 1989, Brewer et al. 1992) have suggested that such rates cannot always be explained by abrasion alone. The downstream decrease in grain size can be explained by a second mechanism, selective transfer. Bradley et al. (1972) hinted at this by discussing sediment transfer and flow competence as controlling factors. Only a slight deviation away from perfect equal mobility is required to explain the observed rates of downstream fining in rivers with abrasion resistant bed material (Brierley and Hickin 1985, Ferguson and Ashworth 1991).

The two processes responsible for downstream fining are not mutually exclusive. Werritty (1992) found both processes to be operative on the Czarny Dunajec River in S. Poland. Trends in grain size for various lithologies were used to separate out the relative magnitudes of the two. Parker (1991a, b) developed a 1D model for prediction of downstream fining on the basis of selective transfer of an aggradational wave and abrasion.

Abrasion has been ruled out as a major factor on the Allt Dubhaig by laboratory testing by Brewer and Lewin (see Brewer et al. 1992 for a full experimental description). Downstream fining at this site may be primarily attributed to selective transfer (Ferguson and Ashworth 1991, Hoey and Ferguson 1994). Seal et al. (1993) advocate that fining may be produced by the occurrence of grain size patches and lateral sorting even in the presence of perfect equal mobility. The patches of mixed grain size act to remove coarser size fractions (dependant upon patch grain size distribution) from the transfer system, a type of selective deposition, hence promoting downstream fining. A model was formulated where the rate of fining is governed by the variance in cross channel shear stress and the ratio of the standard deviation of within patch grain size to the standard deviation of patch means. The importance of lateral sorting to downstream fining on the Allt Dubhaig is not yet known.

The above discussion is based upon downstream fining at a general scale. At a finer resolution, a regular downstream decline in grain size is rarely observed. Tributary inputs and other lateral inputs such as landslides and bank erosion may result in downstream fining profiles 'nested' within the overall profile (Miller 1958, Church and Kellerhals 1978, Dawson 1988).

The above discussion illustrates the larger scale factors which influence inter reach sorting. These are overall factors and local sorting is derived from local scale processes acting upon these general

inputs. All these factors must be considered when examining sorting processes and sediment fluxes within and between individual reaches.

2.3 Sediment budgets: conceptual framework

Sediment budgets have been extensively studied at a wide range of scales detailing a number of processes at varying levels of spatial and temporal resolution. A sediment budget structure is useful for description and analysis of the factors responsible for within channel sediment transfer. Small scale reaches may be considered as systems to which a sediment budget may be applied. This section briefly reviews basin scale budgets before concentrating upon local scale studies. Application of basin scale analytical variables such as transit time (Dietrich et al. 1982) to the smaller channel scale is described.

2.3.1 The basin scale

Dietrich et al. (1982) define the sediment budget for a drainage basin as a 'quantitative statement of the rates of production, transport and discharge of detritus'. Large scale sediment budget studies applying these principles are numerous and range from the continental (Wilkin and Hebel 1982, Meade 1982) to the more common development of a budget for a specific basin (e.g. Dietrich and Dunne 1978, Kelsey 1980, Trimble 1981, Stott et al. 1986, Kelsey et al. 1987).

Dietrich et al. (1982) summarise 3 requirements to be fulfilled in the development of a sediment budget:

1) recognition and quantification of transfer processes;
2) recognition and quantification of storage elements;
3) identification of linkages between transfer processes and storage elements.

Dietrich and Dunne (1978) illustrate the above in a detailed flow diagram recognising storage, transfer and linkages (Figure 2.4). This type of detail is essential to any sediment budget study. The result of many sediment budget studies is a predictive empirical model (e.g. Dietrich and Dunne 1978, Kelsey et al. 1987) involving quantification of the storage characteristics of the elements within the budget and calculation of residence times (Nakamura 1986), transit times (Dietrich et al. 1982) and/or erosion rates (Nakamura et al. 1987). In the case of Dietrich and Dunne, such model development allowed predictions of sediment transfer and soil formation processes.

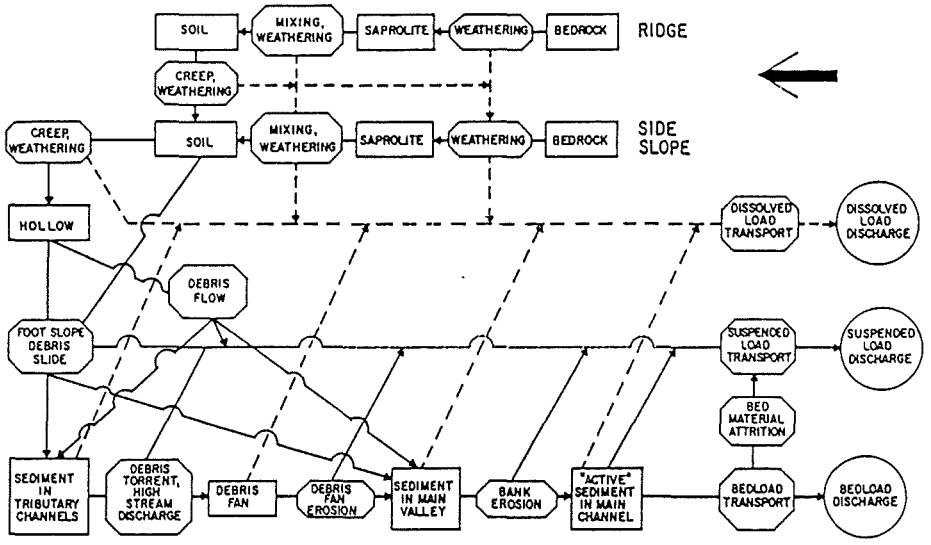

Figure 2.4: Sediment budget structure and interrelationships derived for Rock Creek. Rectangles indicate storage, octagons are transfer processes, circles are outputs. Solid and dashed lines are transfers of sediment and solutes respectively (After Dietrich and Dunne, 1978).

2.3.2 The reach scale

At the reach scale, the only sediment inputs are bedload transfer and bank erosion. Storage, output, and subsequent redistribution of sediment within the reach is then quantified and predictions can be made. Few examples of this scale of sediment budget exist. The development of small scale budgets within a gravel-bed river utilises principles from basin scale models to describe and predict the processes operating. Essential to this is the division of the reach into discrete storage units and quantification of storage characteristics (Eriksson 1971, Bolin and Rohde 1973, Dietrich et al. 1982). A store is defined in this study as *a volume or area of sediment bordered by numerically defined boundaries representing a specific range of potential transfer conditions.* Reservoir theory (Eriksson 1971) provides a framework for characterisation of these stores according to sediment age and hence activity using descriptive variables such as residence time providing quantitative assessment of storage within the reach system.

Within channel storage has been classified using a number of variables including elevation, potential activity, vegetation age and the distribution of sediment transfer. An early attempt at defining sediment storage was carried out by Williams and Rust (1969) who classified the active channel according to elevation, vegetation and flow activity. Similarly, Lekach et al. (1992) examined basin scale inputs to a reach where storage was arbitrarily divided up into high and low elevation bars. Kelsey et al. (1987) defined four fluvial sediment stores across a floodplain according to potential activity (Figure 2.5).

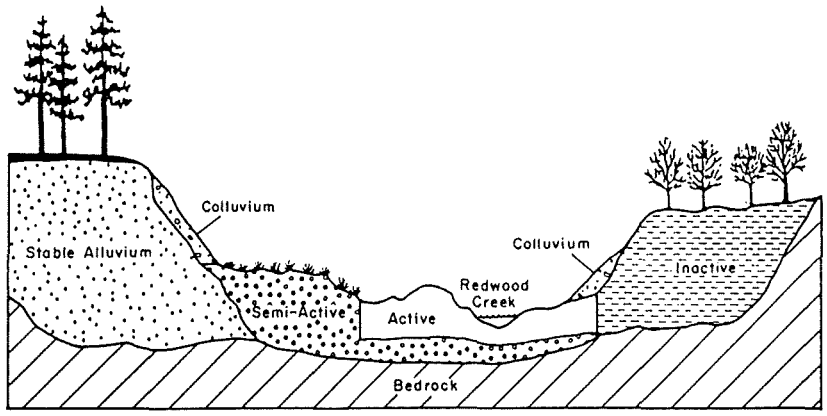

Figure 2.5. Sediment storage reservoirs in Redwood Creek. A predictive model was based upon volumetric transfers of sediment between these stores. (After Kelsey et al. 1987).

In the absence of tracer information or process measurement, vegetation age has been used to quantify stores according to previous activity (Everitt 1968, Nakamura 1986). Hoey (1989) and Hoey and Sutherland (1991) classified reservoirs according to elevation and direct observation of the frequency of bedload transfer (Figure 2.6). These methods meet criteria 2 of Dietrich et al., as unlike the basin scale, most emphasis at the reach scale is placed upon determination of storage. Inputs into the system are often not known so are assumed, for example, using a bedload equation (Kelsey et al. 1987). For reach scale sediment budget studies, accurate determination of storage and linkages between stores (the distribution of transfer fluxes) is essential.

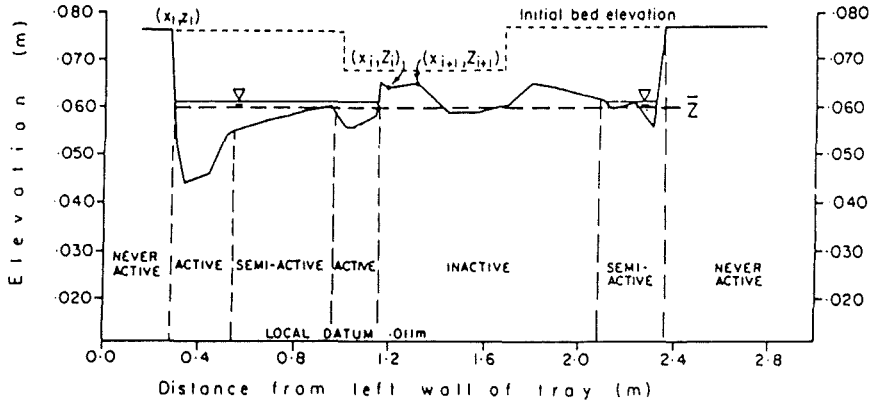

Figure 2.6: Sediment storage classified according to elevation and frequency of bedload transfer. (After Hoey 1989). Active reservoirs - sediment stored in frequently activated channels. Semi - active - very little bedload activation, yet are water covered. Inactive - Emergent bars. Never active - bank material never mobilised.

2.3.3 Descriptive variables

The preceding discussion details criteria 1 and 2 of Dietrich et al. (1982), identification of dominant processes and quantification of storage. Analysis of linkages and storage characteristics usually utilises a number of descriptive variables. This sub section describes these variables, particularly those available from particle movement data within a reach scale study.

2.3.3.1 Transit and residence times

Storage reservoirs can be characterised by the age distribution of sediment within them (Nakamura 1986, Nakamura et al. 1987). The following discussion is based upon the theory described in Dietrich et al. (1982) and assumes that storage is pre defined. If the sediment within a store is dated then a cumulative curve of the mass M of sediment of age t or less (Figure 2.7, a) can be calculated where,

$$\lim_{t \longrightarrow \infty} M(t) = M_o \tag{2.7}$$

where M_0 is the total sediment mass. The form of the relationship varies according to channel morphology and stability. Nakamura (1986) demonstrates this using three contrasting reaches (Figure 2.8): a) a single channel in a narrow cross section. The break in the curve represents large scale discontinuous sediment movement 15 years ago. The active channel contains a small proportion of the total sediment; b) a wide braided cross section, with frequent reworking of sediments; c) a deep gulley channel. The majority of the sediment is in the gully and frequently activated, with remaining sediment in stable gulley walls. Taking the derivative of Eq. 2.7 with respect to age provides an age distribution function ψ (Figure 2.7, b),

$$\psi(t) = \frac{1}{M_o}\frac{dM(t)}{dt} \tag{2.8}$$

The average age of sediment, T_a, can also be computed by integrating the cumulative curve with respect to mass and dividing by the total mass,

$$T_a = \frac{1}{M_o}\int_0^\infty t dM(t) \tag{2.9}$$

$$T_a = \int_0^\infty t\psi(t)dt \tag{2.10}$$

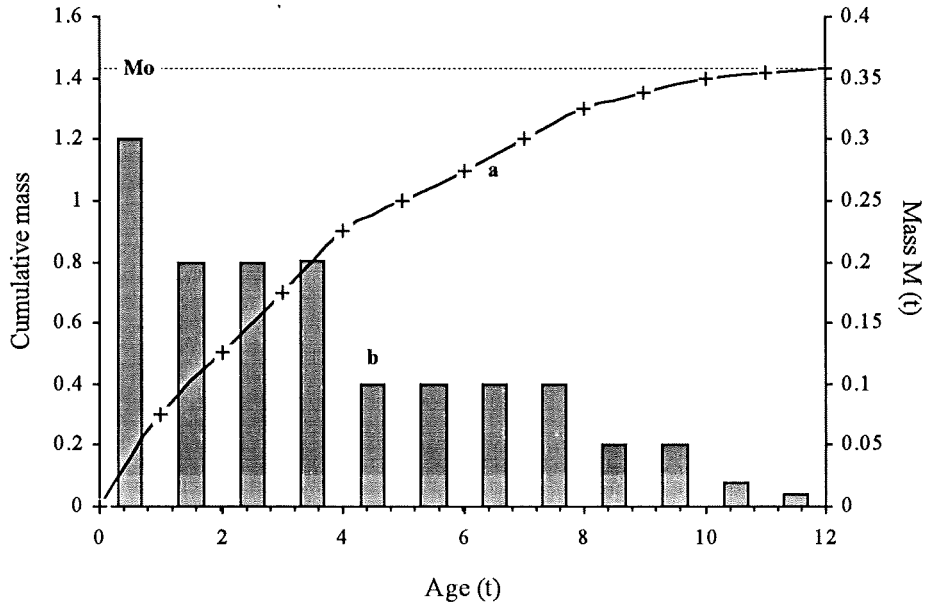

Figure 2.7: Mass M of sediment stored in a hypothetical reservoir. a - Cumulative mass as a function of time t. b - Age distribution calculated from derivation of Eq. 2.7 with respect to age.

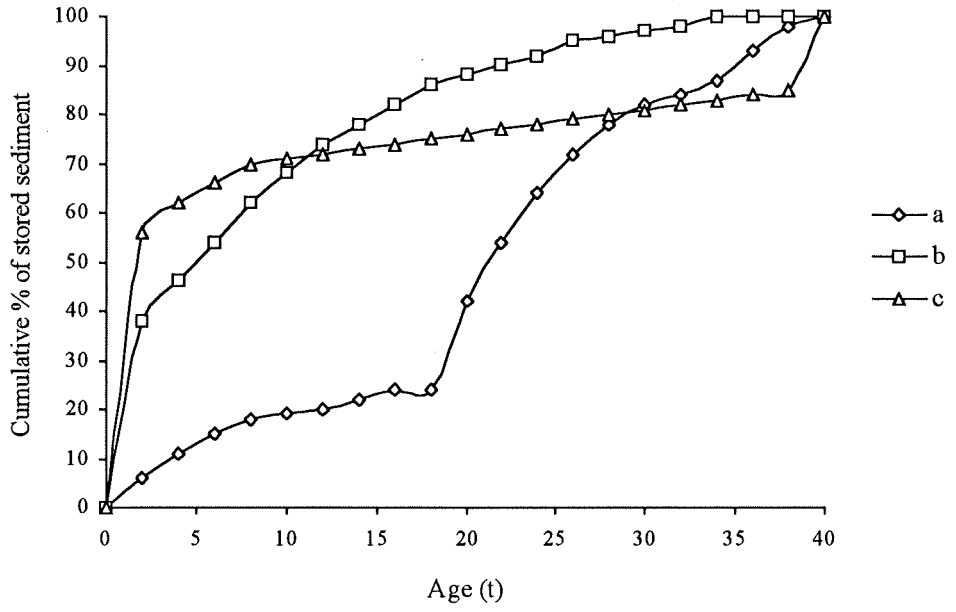

Figure 2.8: Cumulative curves for different reaches of the Furana River (After Nakamura 1986).

The above data may be obtained using natural or artificial tracers, for example radioactive fallout (Ritchie et al. 1975), painted tracers (Laronne and Carson 1976) and the age distribution within forestry overlying fluvial sediments (Nakamura 1986). However, in order to solve Eq. 2.10 with any degree of accuracy, the tracers must have been in the store for a considerable period (dependant upon system activity), this makes the determination of the age distribution of a store extremely difficult.

An alternative method involves using tracers to characterise transit times, the time spent in storage for each particle that leaves the store. The average transit time T_t is the residence time of material in the reservoir, this is based upon Eq. 2.9 where,

$$T_t = \frac{1}{F_o}\int_0^\infty t dF(t) \tag{2.11}$$

$$T_t = \int_0^\infty t\phi(t)dt \tag{2.12}$$

where F_o is the total flux out of the reservoir, F(t) is the mass of discharged sediment of age t or less and ϕ is the transit time distribution function. Calculation of transit time is difficult, requiring accurate tracer information. Dietrich et al. (1982) discuss three prerequisites for any programme of data collection used to determine transit times.

1. Definition of physically meaningful storage reservoirs within the channel. An arbitrary classification is not satisfactory since a number of factors influence transfer and redistribution within different areas of a reach.

2. Tracers must be representative of the bed material distribution, be integrated within the bed and be of sufficient number to obtain valid results.

3. 100% recovery must be obtained from the tracers. In 1982, this was deemed unobtainable since only painted tracers with very low recovery rates were available thus the transit time distribution could not be estimated with any certainty. However, the advent of new techniques such as magnetic tracers (Hassan et al. 1984) allow this criterion be met and it is now possible to obtain accurate data to determine transit times. This is particularly important for the reach scale where detailed information on sediment redistribution can be calculated from tracers.

In addition to using transit times, other methods are available to determine residence time and characterise storage activity. Most of these variables rely upon a steady state assumption where

sediment input to storage is equal to the amount output ensuring a constant residence time. Bolin and Rohde (1973) derived the turnover time T_t, which under steady state conditions was equal to the residence time of sediment where,

$$T_r = \frac{M_o}{F_o} \tag{2.13}$$

The assumption of a steady state is rarely valid, as in reality, mixing is commonplace. In addition, the age distribution is time and space dependant (Dietrich et al. 1982). Figure 2.9 illustrates a conceptual model with the channel in three contrasting positions. Floodplain age distributions differ according to previous migration. The average age of floodplain sediment with the channel in positions 1 to 3 according to Eq. 2.9 would be 5.5, 8 and 6.4 years respectively. This time dependency may be overcome by extending outer boundaries to allow unconstrained migration of the channel across the floodplain at any time (Dietrich et al. 1982).

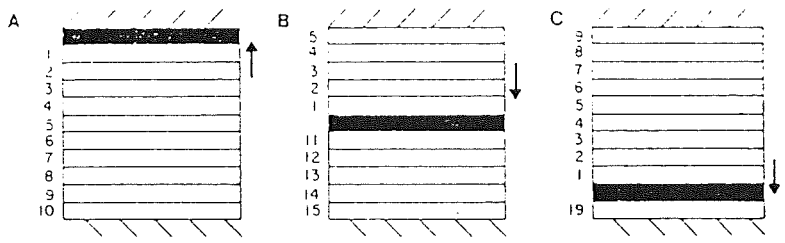

Figure 2.9: The effect of channel migration across the floodplain. Numerical values give age for each increment of flood plain deposit (After Dietrich et al. 1982).

A further method of residence time calculation was suggested by Dietrich and Dunne (1978) where,

$$Q_B \propto A^n \tag{2.14}$$

$$A \propto X^P \tag{2.15}$$

$$V \propto A^m \tag{2.16}$$

where Q_B is bedload discharge, A is drainage area, V is volume of sediment per m of flood plain and X is reservoir or channel length with n, p and m exponents which vary according to the system. For example, m = 1.35 for the main channel, 1.07 for active sediments and 1.37 for gravel bars. From the above power laws it is possible to calculate the residence time per km as

$$\frac{1}{V} \propto A^{m-n} = \alpha P^{m-n} = \frac{V}{Q_B} \tag{2.17}$$

where α is a constant. The residence time between two points, x_1 and x_2 is given by,

$$T = \alpha \int_{x1}^{x2} x^{p(m-n)} dx \tag{2.18}$$

This method was used for defining the residence time of the channel store. Transit times present a more accurate method for characterising within reach scale stores. However, transit times distributions are usually skewed and the average transit time may not be a good indicator of the time spent in storage. The transit time distribution must be defined (Dietrich et al. 1982) and the accuracy of any estimate of residence time assessed. All the above formulae were derived for the basin scale. The principles remain exactly the same for the smaller reach scale, but the field methods differ. Transit time distributions calculated from output tracers will be used to determine storage characteristics. In addition, local variations in morphology and hydraulics may be assessed with reference to the form of the transit time distribution function.

2.3.3.2 Particle velocities

Meland and Norrman (1966) used rhombohedrally packed 'beds' of spherical glass beads in a flume to calculate velocities for individual particles. Particle velocities were determined in relation to shear velocity, bed roughness and grain size. Meland and Norrman (1969) listed six variables impacting upon velocity: water velocity; particle interactions; bed surface stability; particle characteristics (size, shape, sorting); bed roughness; and bed forms. Bridge and Dominic (1984) developed a predictive relation for grain size velocities in terms of excess shear velocity (equivalent to excess shear stress) and boundary roughness.

Within a sediment budget it is possible to apply the above particle scale ideas to broader levels where velocity can be simply taken as,

$$U_b = L/E_t \tag{2.19}$$

where L is the distance moved and E_t is the time over a threshold. The threshold refers to the shear stress above which bedload transfer takes place. A number of authors have plotted tracer trajectories (e.g. Laronne and Duncan 1992), however, these distances have not been used to calculate velocity relative to morphology and transfer pathways in a detailed field study. In addition, particle velocities are sensitive to rest periods which tend to be randomly distributed (Schmidt and Ergenzinger 1992); morphology along the transport pathway may provide explanation for this.

2.4 Horizontal and vertical exchange

This section discusses the factors responsible for sediment transfer fluxes (hence transit times and velocities) and primarily focuses upon data from tracer studies. Previous analysis suggests that flux distributions are random (Hassan et al. 1991), examination of the importance of horizontal and vertical exchange (a function of local sorting processes, section 2.2), particularly with reference to local morphology may provide explanation for this irregularity and demonstrate systematic controls upon fractional transfer.

2.4.1 Movement fluxes

Preferential sediment movement will produce relatively young transit time distributions for more active stores (Figure 2.10a) while inactive stores (Figure 2.10b) exhibit much older distributions. Particle velocities are also affected as material is slowed down on bars as a result of lower shear stresses and increased rest periods.

Downstream sorting within reaches is variable and reflects detailed reach morphology. Sorting is defined by fractional movement fluxes of all particles. For example, size segregation occurs as a result of hydraulics and results in surface coarsening in locations where water surface slopes are steep such as riffles (Prestegaard 1983) and in mountain streams (Ergenzinger 1992). Preferential transfer can also take place around bars producing local fining (Ashworth et al. 1992). The factors affecting sorting were discussed in section 2.2, all influence transfer fluxes and transit times.

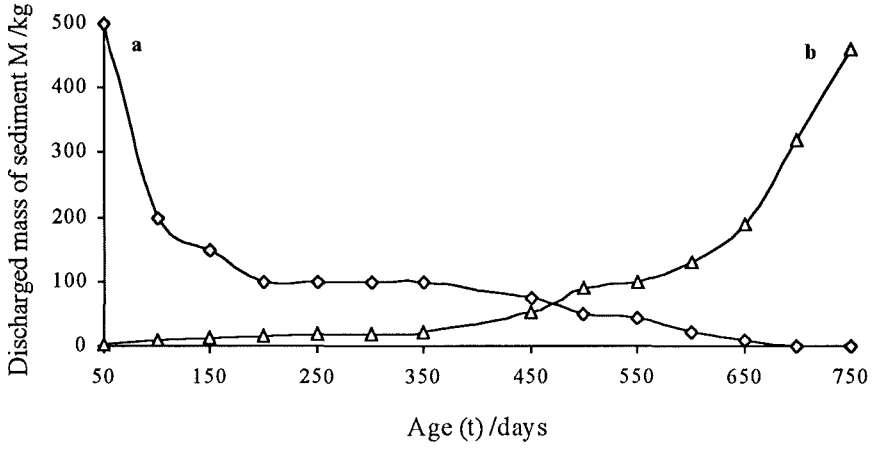

Figure 2.10: Transit time distribution for two hypothetical reservoirs. a - Active store where sediment is predominantly young. b - Inactive store where material is removed from transfer for a substantial period.

Distributions of distances moved are more stochastic than ordered (Hassan and Church 1992) and most plots of distance against particle size show little correlation. Larger particles (>2*D_{50}) display some regularity as selective transfer results in decreasing distances of transfer as size increases (Parker 1991a). However, for the majority of material, stochastic tendencies dominate, within this certain factors operate at the reach scale producing the observed scatter. Hassan et al. (1991) suggested that three factors influence bedload movement:

1. Sedimentary characteristics of the bed.
2. Hydraulic conditions of the flow.
3. Characteristics of the individual moving particles.

The overlap and interaction of such factors is responsible for the large data scatter so often observed when particle movement is documented (e.g. Einstein 1937, Hubbel and Sayre 1964, Carling 1987). This almost stochastic nature enabled Hassan et al. (1991) to successfully fit a compound Poisson model and a simple gamma function to observed distance distributions (Figure 2.11).

The stochastic overall pattern is made up of a series of deterministic processes operating at different scales, partial disaggregation of which is an aim of this study. Laronne and Carson (1976) noted a feedback effect whereby morphological features are determined by transfer paths but at the same time also act to influence such paths. This reductionist approach will be useful to identify specific patterns and can be used together with more traditional and general mechanistic explanation. Hassan and Church (1992) recommend the adoption of such a morphological approach to provide explanation for the distribution of transfer distances.

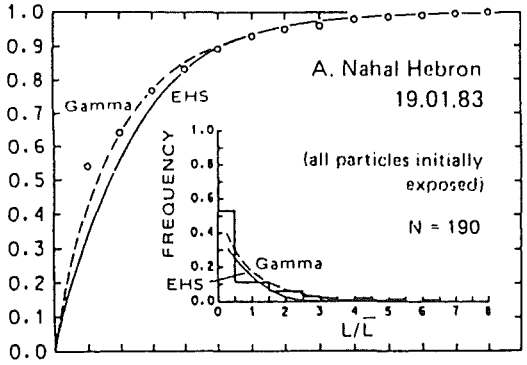

Figure 2.11: Prediction of normalised distances using Gamma function and Einstein-Hubbel-Sayre model. Abscissa values are normalised distance, ordinate values represent cumulative frequency. (After Hassan et al. 1991).

Few studies have made direct observations of particle transfer paths at the reach scale. However, studies concerned with transfer paths have yielded information regarding reach dynamics and patterns of sediment supply (e.g. Thorne and Lewin 1979). Brewster (1986 in Ashworth 1987) demonstrated that a bar head on the River Feshie did not develop from successive increments of locally derived sediment, but that, the material source was far upstream. Laronne and Duncan (1992) use movement as an indicator of the mechanisms of bar development on the North Ashburton River, New Zealand. Tracer material moved along anabranches within a braided system during small flood events while material within an alternate reach was transferred onto bar platforms suggesting that gravel sheets or lobes (Iseya and Ikeda 1987, Whiting et al. 1988) may be responsible for bar propagation and formation at higher stages.

2.4.2 Bar storage

The influence of bars upon material movement paths was dealt with in the preceding subsection. This subsection discusses studies which have examined the importance of bar storage. It is generally accepted that transit times vary within the channel (Dietrich et al. 1982) with bars having older transit time distributions than for example, pools. Hassan (1990) noted material movement from bar surfaces, but, very little material was transferred from within the bar. Scour was generally restricted to the thalweg, suggesting temporary storage of material within bar frameworks. Two mechanisms explain how material may be reincorporated within the transfer system.

1. Repeated degradation of a bar surface or margins (e.g. Hassan 1990).
2. Channel change (e.g. Goff and Ashmore 1994, Lane et al. in prep).

Facies models provide further evidence for the stability of bars detailing sedimentary sequences characteristic of a number of channel patterns and barforms (e.g. Allen 1965, Miall 1977). Such evidence also supports the contention that in the absence of morphological change, bars act as stores of sediment delaying particle transfer through a reach.

2.4.3 Pocket geometry effects

Both entrainment and deposition are affected by interaction between individual particles and bed sediments. Imbrication (Li and Komar 1986), hiding (Einstein 1942), protrusion (Fenton and Abbot 1977), packing (Church 1978) and clustering (Reid et al. 1992) all promote or reduce the value of τ^*_c for a particular particle. Surface material is usually more mobile than material locked into the surface or buried (Hassan et al. 1991, Church and Hassan 1992, Hassan and Church 1994). Carling et al. (1992) argue that entrainment of particles from natural beds is influenced by: (1) interlocking of irregular shaped particles; (2) the impact of mobile material on static particles.

These sedimentological interactions alter the transit times and velocities of tracers and are dependant upon depositional characteristics. Study in the field is difficult. Buffington et al. (1992) used peels of surface material and analysed pivoting angles in the lab. At present, an entirely field based study has not been undertaken, however such small scale effects may be important if packing correlates with storage, such effects may therefore be indirectly determined in this study.

2.4.4 Vertical exchange processes

Previous discussion in this section dealt with the processes influencing transfer fluxes operating in the horizontal plane. Associated vertical effects include elevation, vertical winnowing and burial.

The importance of absolute elevation was described in section 2.3.2 in relation to storage definition. Elevation is often used as a surrogate for activity where material on high bar surfaces is assumed to be less mobile than sediment in the thalweg (Williams and Rust 1969, Laronne and Duncan 1992, Lekach et al. 1992).

Vertical winnowing describes the process where fine material infiltrates into the surface and becomes incorporated within the subsurface (Parker et al. 1982b, Frostick et al. 1984, Carling and McCahon 1987, Diplas and Parker 1992). This process has not been documented for gravel sized tracers in the field. In the absence of perfect equal mobility, finer particles are the most mobile. Any infiltration into the surface (where $D_i < D_{50}$) would increase transit times and reduce velocity as the material is defined as buried.

Improved recovery rates associated with magnetic tracers (Hassan et al. 1984, Laronne 1987) have allowed 3 dimensional examination of bed material and transfer fluxes to be carried out with a greater degree of accuracy. Schick et al. (1987a, b) used tracers to examine vertical fluxes of material within Nahal Hebron and Nahal Og concluding that the time a particle remains at rest, buried or exposed is dependant upon the position within the channel. The probability of movement for a deep buried particle was less than that for a shallow buried one. Such principles were included within a vertical exchange model which documented fluxes between three vertical zones within a river bed. Drew (1992) carried out field tracing experiments and developed a model similar to that of Schick et al. (1987a). However, in direct contradiction with Schick et al. and Hassan (1990), Drew noted that buried particles were more mobile than surface clasts. Such studies are characterised by two inaccuracies: (1) surface and buried tracers are not comparable due to different starting xy positions (in planform) and hence hydraulic and morphological conditions; (2) the importance of burial is a function of morphology. Drew noted a contrast in mobility from bar locations on two Scottish rivers. Bar particles on the Monochyle Burn were more mobile than on the Allt Dubhaig, as the former was characterised by lower elevation bars.

Drew (1992) observed that preferential scour and fill took place with a random break-up of the bed surface at flood stage. Conversely, Hassan (1990) noted more systematic scour and fill across scour chain sections due to bedform migration and erosion. Such contrasting evidence suggests that the probability of burial is stochastic, however, the data was derived from different rivers with contrasting morphology. Comparison between the burial characteristics for given morphological types may allow better understanding of controls upon burial and its importance to sediment transfer. The distribution of burial depths, was considered to be exponential by Hassan and Church 1994 who developed a model predicting burial depth for a single event accounting for sediment mixing, non uniform scour depths (Hassan 1990) and fractional trends. This study will compare burial characteristics with morphology to assess whether it is an entirely stochastic process or whether it is a function of shear stress (hence active layer depth) and storage location.

2.5 Sediment budgets: field methods

Dietrich et al. (1982) suggest that identification of transfer and storage characteristics and the linkages between them is crucial in a sediment budget study. In the fluvial environment at the reach scale, tracers particles are the obvious choice for identification of the transfer processes while surveying is used to characterise storage. Grain size measurement is required to accurately characterise storage.

2.5.1 The tracing technique

The use of tracer particles within a fluvial environment was instigated almost 30 years ago in North America (Leopold et al. 1964) and Japan (Takayama 1965). Material was painted and labelled prior to introduction and relocation within a river. This method was widely used for the examination of fractional mobility and its controlling factors (e.g. Leopold et al. 1966, Laronne and Carson 1976, Ashworth 1987). One inherent problem with all particle tracing work using paint only methods was the low recovery rate associated with non-location of buried tracers. Leopold et al. (1966) reported recovery rates varying from 0 to 88% while Laronne and Carson (1976) recovered only 5%. Low recovery prompted a number of attempts to adapt tracers for subsurface relocation. For example, Butler (1977) used metal strips attached to tracers and attempted to relocate the tracers using a metal detector, but recovered only 35%.

A major development in tracing techniques was made with the use of magnetism. Oldfield et al. (1981) enhanced the natural magnetism of particles while Ergenzinger and Custer (1983) monitored bedload transfer rates using magnets within particles and a fixed detector. Hassan et al. (1984) suggested a more practical method for the development and usage of magnetic tracers.

They placed magnets within holes drilled into the tracers and used numbers within the hole as labels. The holes were then sealed using epoxy resin or an appropriate substitute. The change in weight caused by this was only 0.2 %. The positions of both surface and buried tracers could then be determined by using a magnetic locator with documented recovery rates up to 93%. It should be noted that conditions on the ephemeral Nahal Hebron, Israel, where relocation of particles took place were favourable for the usage of this technique. Recovery rates in excess of 90 % are rarely achieved on perennial gravel-bed rivers.

Schmidt and Ergenzinger (1992) used magnetic tracers to examine size effects and the influence of channel morphology upon particle mobility in a steep headwater step pool system. In addition, radio tracers (the pebble transmitter system, PETS, Ergenzinger et al. 1989) were used to assess rest periods and hop location. Such clasts allow continuous monitoring of particle location via a transmitter within the tracer. However, a major problem is the expense of individual tracers, therefore, the experiments of Schmidt and Ergenzinger were restricted to only 7 transmitting particles. Development of this technique would represent a considerable improvement upon existing tracing methods.

Magnetic tracers will be used in this study to determine fractional transfer fluxes and transit times for particular stores. The data will also allow an evaluation of horizontal and vertical exchange effects upon transfer.

2.5.2 Survey techniques

Surveying will be used to quantitatively define the stores and storage volumes. The field techniques involved are simple and require no further review. Lane et al. (1994) used Digital terrain mapping (DTM) to provide a level of temporal and spatial resolution which cannot be attained from conventional survey methods. However, data collection reflected the need for detailed information regarding aggradation relative to diurnal flow fluctuations in a proglacial river.

Survey data can be used to calculate volumetric fluxes and bedload transfer rates (e.g. Carson and Griffiths 1989, Ferguson and Ashworth 1992), usually at small scales such as riffle bar units. Bedload transfer data are available from volumetric information using one of three methods (Goff and Ashmore 1994): the step length approach (Ferguson and Ashworth 1992); erosion zones (Carson and Griffiths 1989, Kussner 1992); and a within reach sediment budget (Ferguson and Ashworth 1992). The first two use an average step length and match up erosive and depositional cells. The latter uses a sediment continuity equation to determine the rate of change of bedload transfer given by either

$$\Delta q_s / \Delta x = -V(w.\Delta x.T) \tag{2.20}$$

or,

$$\Delta Q_s / \Delta x = V(\Delta x.T) \tag{2.21}$$

where V is the volume of erosion (negative) or deposition (positive) over channel length Δx and time T, w is width of erosion or deposition, q_s is volumetric transfer rate per unit length and time and Q_s is totalled over w and averaged over T.

This analysis uses zones between successive cross sections. The total volume V_i of erosion within each zone is obtained by superimposing the cross section data at each site between t_1 - t_2. The value of w is calculated by comparison between the sections. V_i is determined on the basis of the assumption that w and d, the depth of erosion, vary linearly with distance (the prism formula) between sections i-1 and i, and is calculated as

$$V_i = (x_i - x_{i-1})(2w_i d_i + w_i d_{i-1} + w_{i-1} d_i + 2w_{i-1} d_{i-1}) / 6 \tag{2.22}$$

An input transfer rate is specified for the first cross section. Downstream, transfer rates can be calculated between all sections as long as V and w are known. If no transfer data are available then an up or downstream boundary condition of non-zero transfer can be set (Griffiths 1979).

2.6 Sediment budget modelling

Modelling at the reach scale has received very little attention, probably due to the inherent complexity of such a system and lack of detailed field data to facilitate model construction and verification. Dietrich et al. (1982) suggested a conceptual model providing a mass balance per unit length,

$$V - S^T V + Q_i = Q_o + \Delta V \tag{2.23}$$

where V is the sediment stored per unit length, $S^T V$ is the redistributed volume changes per unit length, Q_i is the upstream input (usually redistributed between stores using S^T), Q_o the output and ΔV the change in storage. The variables are easily described from field data, however, the model has a strictly conceptual basis requiring modification to become predictive.

Transition matrix S^T describes the probability of transfer between stores, in the following example, 2 stores are used,

$$S = \begin{pmatrix} a & b \\ c & d \end{pmatrix} \tag{2.24}$$

where, S represents the change between two stores. The components of the matrix are represented by: a- proportion of sediment that remains in store 1; b- proportion of sediment that is transferred from store 1 to 2; c- proportion of sediment that is transferred from store 2 to 1; d- proportion of sediment that remains in store 2.

If a transpose of this matrix is taken and multiplied by V then the amount of sediment in each reservoir due to the fluxes described in S is given. The net change can then be calculated. Kelsey et al. (1987) and Hoey (1989) replaced a-d with probabilities based upon field and flume observations respectively. A certain degree of success was attained in fitting observed to predicted data. This study will use transition matrices to describe sediment transfer between stores.

Cellular modelling techniques (Smith 1991) may be used to describe and predict sediment transfer. Murray and Paola (1994) divided up a reach into a $1m^2$ grid and routed discharge from upstream to downstream cells. Sediment routing was based upon the discharge within a cell and probabilistic rules governing transfer directions. Using a near homogeneous plane as a start point, the model successfully replicated braided channel patterns. This modelling technique is ideal for sediment transfer description and prediction since transfer from each cell is a function of local rather than reach average conditions.

A further approach to modelling such sediment redistribution may be to employ stochastic techniques. Singh et al. (1988) review such methods in relation to rainfall runoff processes and suggest that stochastic treatment of variables in a modelling situation may act to reproduce natural variability better than purely deterministic methods.

Sediment routing models (e.g. HEC-6) provide an additional insight into movement and variability of sediment fluxes, however, any information yielded is fairly limited since such models are 1-D and lateral variation is not accounted for. Pickup et al. (1983) suggested a different approach to the usual hydraulics driven model. The Braided River (BR) model is sediment driven where the sediment flow is predicted allowing control of deposition and transfer with limits set by the transfer capacity (Pickup 1988). This approach may be utilised when within reach downstream and lateral sediment redistribution is described, but unlike cellular models, it does not account for local conditions.

2.7 The morphological approach

Numerous sorting and flux processes determine within reach sediment transfer patterns, the combination of which result in the reported stochastic distributions (e.g. Hassan and Church 1992). Previous studies concentrate upon each process in isolation, but this study will use overall tracer dispersion to determine which sorting and flux related factors are relevant to transfer. Most of the processes described in this chapter are a direct (e.g. bar storage) or indirect (secondary currents) result of morphology therefore a morphological approach will be adopted to determine systematic morphology induced trends in the transfer system. Within reach storage will be categorised and flux characteristics relative to each store determined. Detailed examination of these between store transfer fluxes using tracers and volumetric data should permit a breakdown of these stochastic transfer patterns and identify the relative importance of some of the flux and sorting processes described herein.

3. The Field Site

This chapter introduces the field area and the two study reaches. Each reach is described in terms of overall fluvial characteristics, historical change, morphology at the start of the study and morphological adjustment during the study.

3.1 Choice of site

Data were collected between July 1991 and July 1993 on the Allt Dubhaig, a headwater tributary of the River Tay in the Central Highlands of Scotland draining 17 km^2 of schist and granulite upland terrain to the south of the main watershed between the Tay and Spey river systems (Figure 3.1). The river has been studied by a number of authors and has been intensively studied in two Ph.D. theses (Ashworth 1987, Drew 1992) which document the characteristics of the channel at several locations. Ashworth discussed downstream changes in shear stress and bedload transfer in relation to changing channel pattern (Ashworth and Ferguson 1989, Ferguson and Ashworth 1991) and Drew completed a sediment tracing study, concentrating upon vertical exchange.

Individual reaches of the Allt Dubhaig display contrasting hydraulic and sedimentological characteristics within short distances down the long profile providing a number of potential study sites. Data concerning sediment redistribution were collected using magnetic tracers (e.g. Hassan et al. 1984). The Allt Dubhaig is extremely well suited to tracer recovery being sufficiently shallow to allow access within the channel even during intermediate floods. In addition, burial depths are restricted to a maximum of 0.5 m allowing relatively easy relocation of material.

The alluvial gravel-bed stretch of the Allt Dubhaig begins at an arbitrarily defined location of 0 m where the river emerges from the hills (upstream, the channel is a confined upland stream with a pronounced step pool sequence) and continues downstream until a transition from a gravel to sand bed at 2500 m. The river displays a highly concave long profile with slope decreasing from 0.02 to 0.001 (see Figure 3.3). Associated with the decrease in slope is a reduction in grain size and a progressive change in channel pattern (Ferguson and Ashworth, 1991). Upstream reaches are typified by high energy wandering channels with D_{50} in the order of 115 mm. As slope declines, the channel pattern becomes more transitional displaying both wandering and meandering reaches. This unstable part of the river exhibits the highest rates of channel change before the onset of meandering at approximately 1400 m. As the slope continues to decline, lower energy channel patterns occur alternating between meandering, transitional and straight reaches with D_{50} ranging from 40 to 25 mm. The straight reaches show alternate bar development with an associated meandering thalweg. At the lowest part of the long profile, local base level control in the form of natural (two tributary alluvial fans) and artificial (~1 m high dam) constraints generate

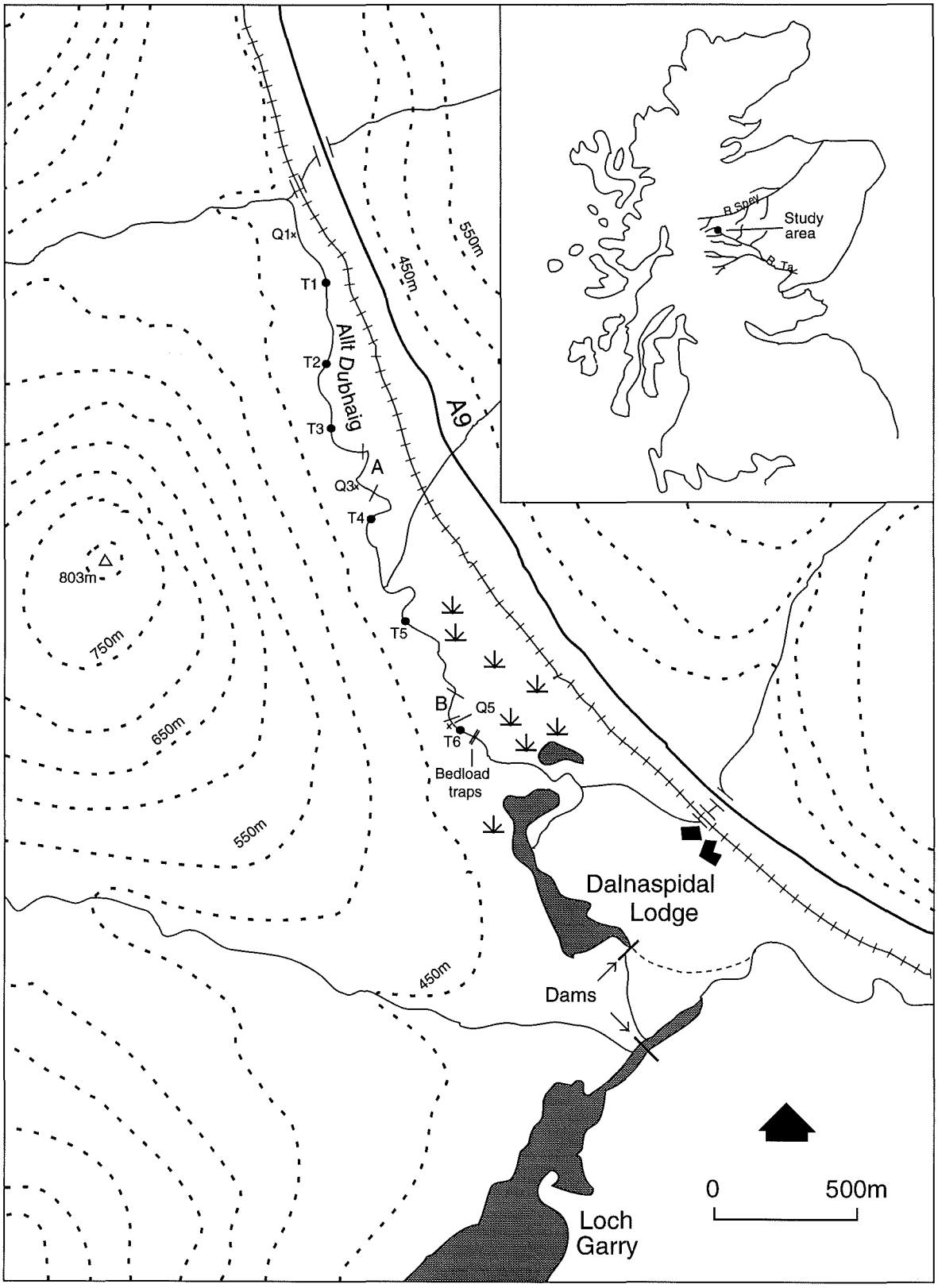

Figure 3.1. Study reaches and additional field installations. Map based upon Ferguson and Ashworth (1991). T and Q notation refers to tracer sets (T) and gauging stations (Q) associated with the fining project. Study reaches are A and B. OS Grid Ref. of Dalnaspidal Lodge: NN646729.

a 'lowland' style of channel with backswamp areas, pronounced levees and crevasse splays. The gravel to sand bed transition at approximately 2500 m is due to the imposed base level control (Sambrook Smith and Ferguson, in press, 1995). Non abrupt changes in channel pattern along the long profile of the Allt Dubhaig demonstrate a continuum of channel types (Ferguson 1987). This progression is influenced by, but also affects, the gradual downstream changes in hydraulic, sedimentological and morphological variables.

The dominant metamorphic nature of the surrounding geology gives rise to abrasion resistant bed sediments. Circular flume experiments suggest that, on average, samples of Allt Dubhaig bed material decrease in weight by 0.08 % per km (P. Brewer and J. Lewin, University of Aberystwyth, pers. comm. 1993).

Overbank flow regularly occurs in the lower reaches at discharges > 6 m^3s^{-1}, whereas flow in the upper reaches does not exceed the channel capacity until discharges of > 8 m^3s^{-1} are attained, reflecting the reduction in slope and decline in channel capacity in the downstream direction. The absence of any significant tributary inputs ensures that discharge remains almost constant along the 2.5 km of river studied, although drainage area increases from 13.4 km^2 at the head of the river to 16.4 km^2 at the dam.

Magnetic tracers were installed at six sites along the Allt Dubhaig for use in the downstream fining project (Figure 3.1). Some of these data will be compared with tracer data collected from the present study. These six sets were labelled with a prefix 'T' and a number referring to the relative installation position downstream. Sets T1 and T2 were placed in the high energy upstream wandering reaches of the river, T3 was in a more transitional pattern, alternating between wandering and meandering, T4 tracers within a meandering site, and T5 and T6 in low energy meandering and straight reaches respectively.

Bedload transfer data used in this study are derived from bedload traps used in the downstream fining project (Wathen et al. in prep.). Data were collected in a 200 m straight reach with a stable rectangular cross section and no erosion of the near vertical vegetated banks. The site is at 2400 m, 100 m upstream of the gravel to sand bed transition and 150 m downstream of the end of the lower reach to be used in this study (see section 3.4).

3.2 Choice of study reaches

The study reaches were selected according to morphological criteria. Each site had to be sufficiently well defined to allow analysis of sediment redistribution between sediment stores of contrasting activity. In order to make significant comparisons concerning sediment fluxes, the reaches had to be hydraulically and sedimentologically distinct. Inferences can therefore be made regarding the relative importance of the processes determining sediment storage and redistribution in contrasting reaches.

Each reach had to be short enough to allow detailed study. To achieve the required level of detail the maximum practical reach length was about 125 m. Reaches without deep pools were selected for convenience in surveying and tracer mapping. Tracer seeding sites and gauging station location associated with the fining project also impacted on the selection of reaches for this study. Each reach had to be near to or contain a gauging station and sufficiently far from the existing tracer sets T1 - T6 to prevent overlap between magnetic particles.

The above criteria resulted in the selection of two study reaches, hereafter referred to as reaches A and B. These reaches are well defined with the input or start point taken as the channel downstream of the apex of a sharp 90^{0} bend. Output or end points are represented by undifferentiated channel approximately 120 m downstream of the input. Each reach exhibits morphological variability and both are prone to bank erosion. Lateral erosion changes the volume of sediment stored as the active cross section width increases; this issue will be more fully addressed in chapter 5. Reaches A and B are located approximately 1 km apart (Figure 3.2) which, given the rapid downstream changes in channel type, will allow hydraulic and sedimentological comparisons to be made.

3.3 Reach A

3.3.1 Hydraulics and sedimentology

This site is a 120 m transitional reach located at 1000 m (Figure 3.3, 3.4) with a meandering thalweg and associated bank attached bars. Reach slope is 0.011, based on the mean slope through 12 cross sections (Figure 3.3). Ferguson and Ashworth (1991) reported a median shear stress of 30 Nm^{-2} for this site on the basis of velocity profiles measured at discharges ranging from 2.5 to 5.5 m^3s^{-1}. Peak discharge on the Allt Dubhaig is of the order of 10 m^3s^{-1}. Together, the relatively low grain size and local depth and slope variation provides a partial explanation of why this part of the Allt Dubhaig displays the greatest morphological activity (e.g. Drew 1992). This can be demonstrated with reference to an estimate of bankfull shear stress, τ_{BF}, (Eq. 2.1) in the deepest

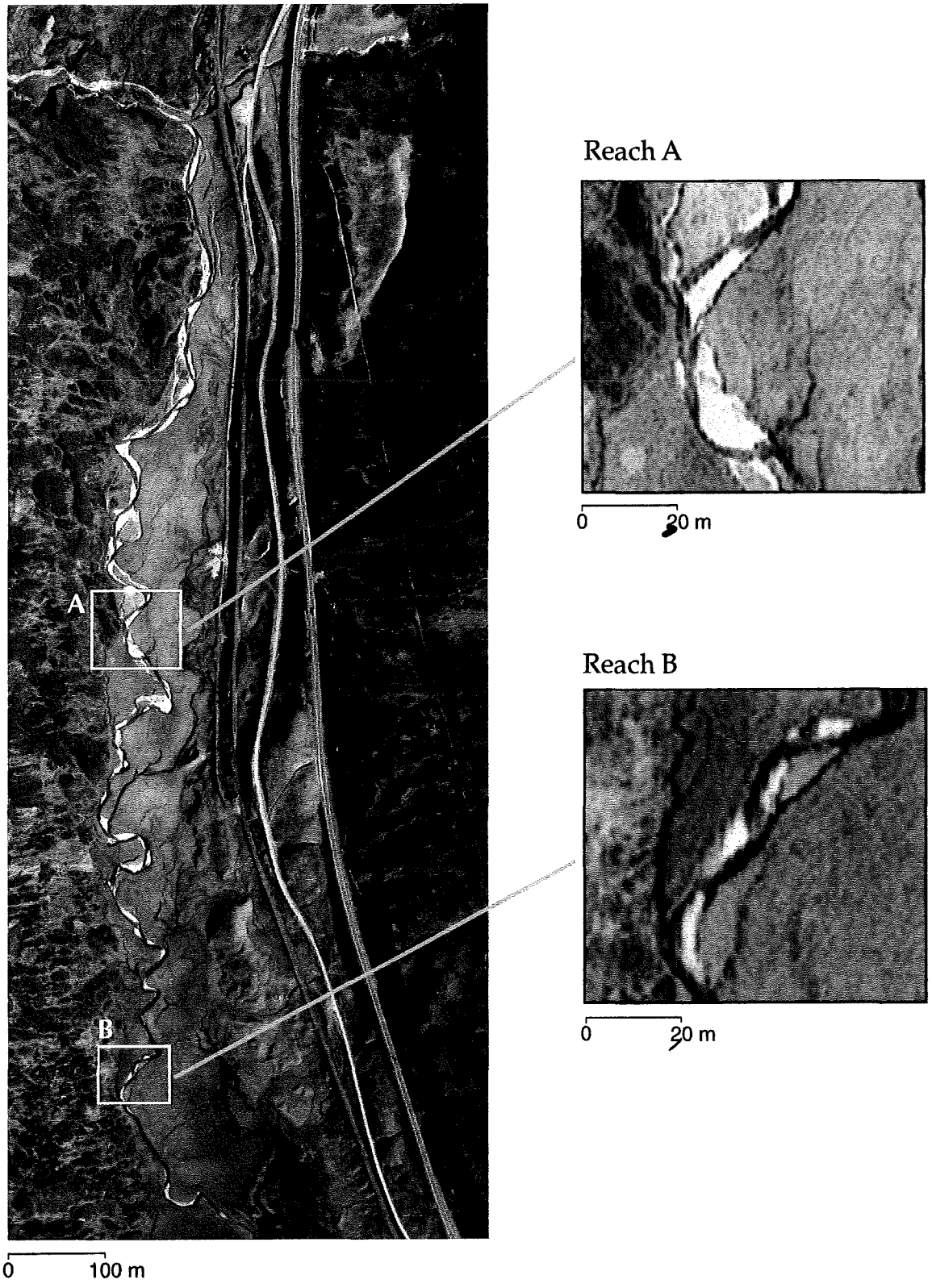

Figure 3.2 Location of Reaches A and B

Data source: 1988 air photo

pool. Assuming that water surface slope equals bed slope at high stage (0.011) and that maximum bankfull depth is 1.4 m (taken from cross sections), $\tau_{BF} \approx 150$ Nm^{-2}. Using the maximum surface D_{50} (106.2 mm, see Appendix A) the dimensionless shear stress (Eq. 2.2) is 0.09. This exceeds the usual range of critical dimensionless stress values of 0.02 - 0.06 reported for gravel-bed rivers (e.g. Church 1978) indicating entrainment at stresses somewhat below bankfull.

Figure 3.3. Location of reaches A and B in relation to the long profile of the unconfined alluvial Allt Dubhaig. The profile was obtained from thalweg elevations at 120 cross-section sites.

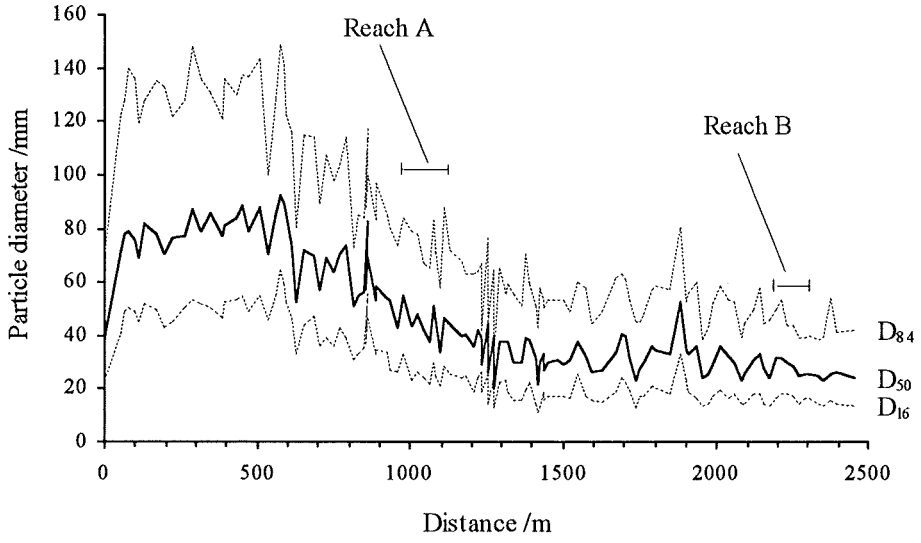

Figure 3.4. The location of Reaches A and B in relation to the downstream decrease in D_{84}, D_{50} and D_{16} on the Allt Dubhaig. Data from surface count (Wolman) samples of 100 particles.

For the descriptive purposes of this chapter, a single bulk grain size measurement taken within the reach is sufficient to characterise the bed sediment (Figure 3.5). The distributions are unimodal with a pronounced gravel mode. Surface D_{50} is 66.4 mm and subsurface D_{50} is 26.7 mm, indicating a degree of armouring with a surface to subsurface D_{50} ratio of 2.5. This armour is frequently broken resulting in large scale bed mobilisation and associated bedload transfer (Drew 1992).

3.3.2 Reach A morphology at the start of the study

The following discussion details the significant morphological characteristics of reach A. All numerical labels used in this sub section refer to Figure 3.6. Reach A was first mapped in June 1991, and was dominated by three main bars or storage units (Figure 3.6). The first of these was a bank attached, fixed (Seminara and Tubino 1989) lateral bar (I) at the head of the reach (Plate 3.1), which had prograded in the downstream direction since 1988 (see Figure 3.7d). A deep pool in the channel to the left (looking downstream) (1) was associated with this bar. This pool was responsible for repeated undercutting of the left bank (Ashworth pers. comm., 1991), flow striking the bank at an oblique angle, especially downstream of the riffle at the head of bar I. The second main bar (II) was a fixed point bar on the main leftward bend in the centre of the reach (Plate 3.2). This feature appeared to be a result of scour out of the upstream pool (1), which was also the likely mechanism responsible for formation of the riffle (2) which joined the two main bars in this upstream part of the reach. The point bar (II) and riffle (2) diverted flow towards the right bank resulting in minor undercutting. As Figures 3.7a - d indicate, this bank is part of a fossil bar which tended to dominate this reach when it was active.

At the apex of the bend, flow struck an outcrop of hummocky moraine at almost 90^{o} (3). This resulted in bank collapse and an input of coarse (b axis > 1 m) angular debris, which has remained *in situ* as flow in this reach is not competent to transfer such particles. Also located at the apex of the bend was a deep pool (4) with considerable patches of fine material on the bed. Secondary circulation effects out of the pool may have resulted in the formation of a fine grained low elevation bar (5) attached to the point bar.

A pronounced riffle (6) joined the point bar to the shallow head of the third and final major bar (III) in the reach. Vegetation growth at the bar head suggested that this bar was stabilising. Flow was diverted round this former bank attached bar (III) (the bar was attached to the left bank in 1988, Drew 1992) with the left anabranch accounting for most water (7). This anabranch was congested by turf blocks from upstream bank erosion (Plate 3.3). In the left of this channel was a smaller left-bank attached bar (IV) which formed after dissection of the major bar (see section 3.4.3). Vegetation growth on the bar head suggested that this was a fairly stable feature. This bar

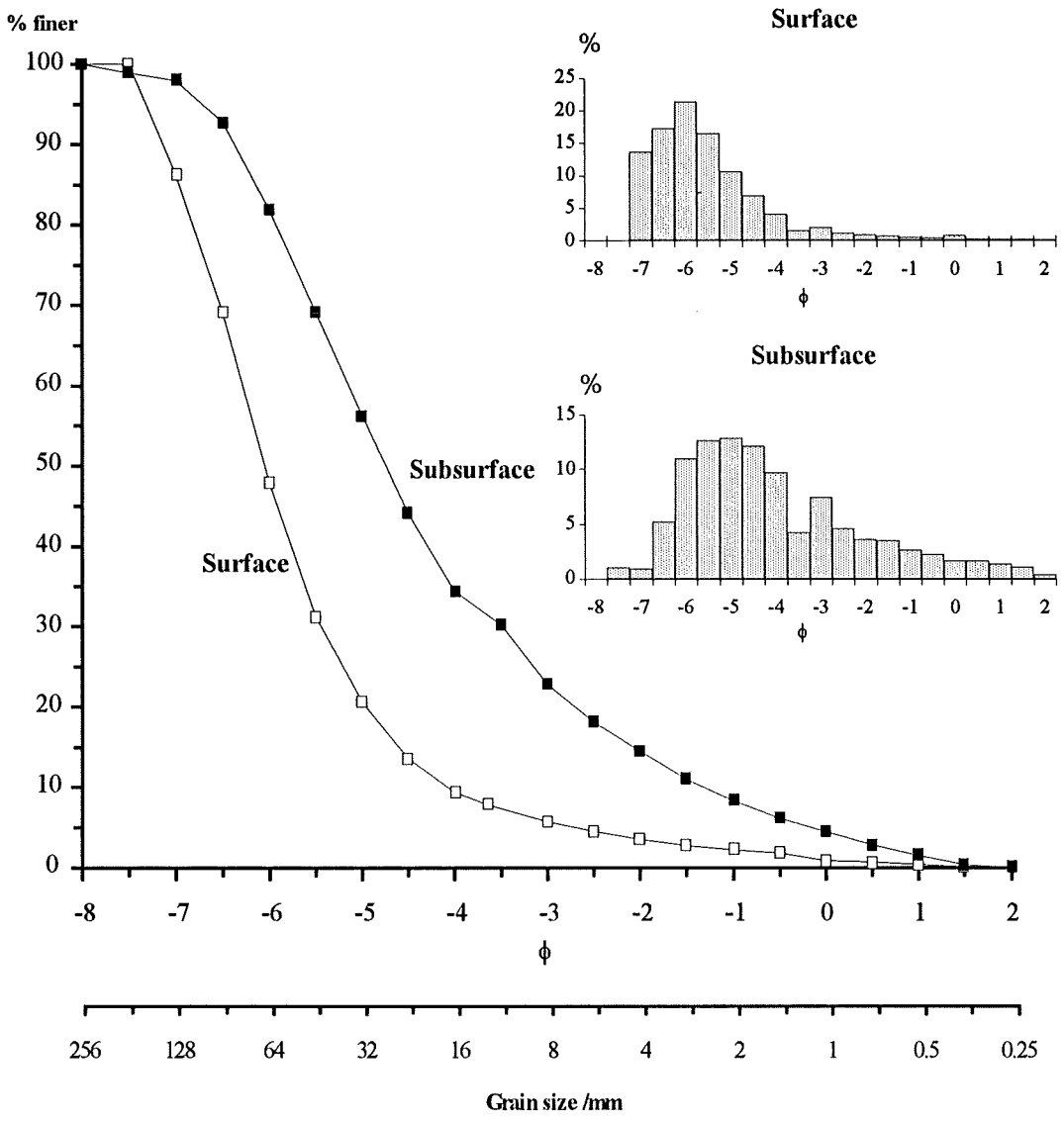

Figure 3.5. Reach A single representative grain size distribution. Sample taken from a cross section at the head of the reach. Inset bar charts illustrate the grain size proportions for surface and subsurface sediments.

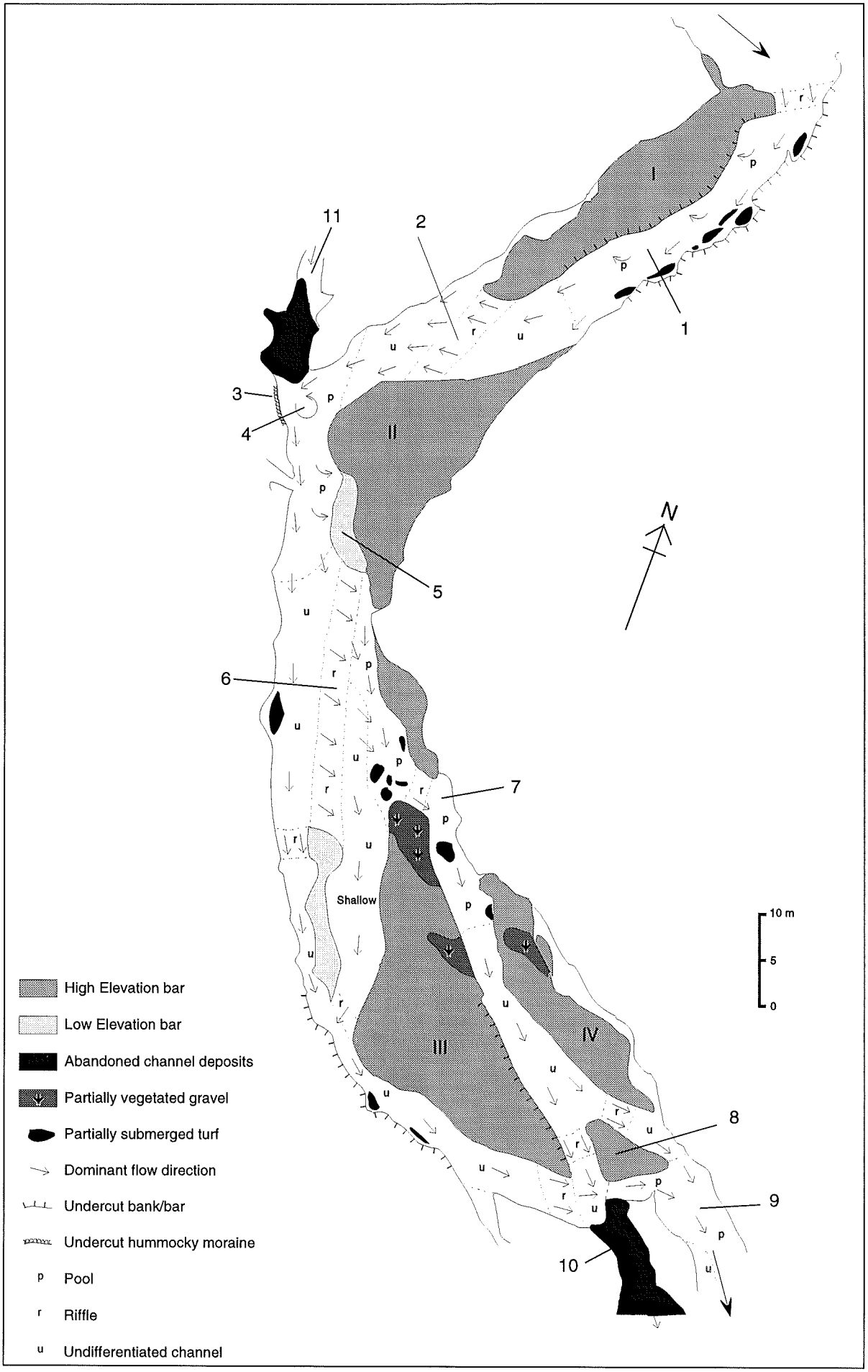

Figure 3.6. Planimetric map of Reach A, June 1991. Stage (Q3) = 24 cm, Q = c0.5 cumecs.

Plate 3.1. Downstream view of the alternate bar (I) at the head of reach A, December 1991. $Q = c1\ m^3s^{-1}$.

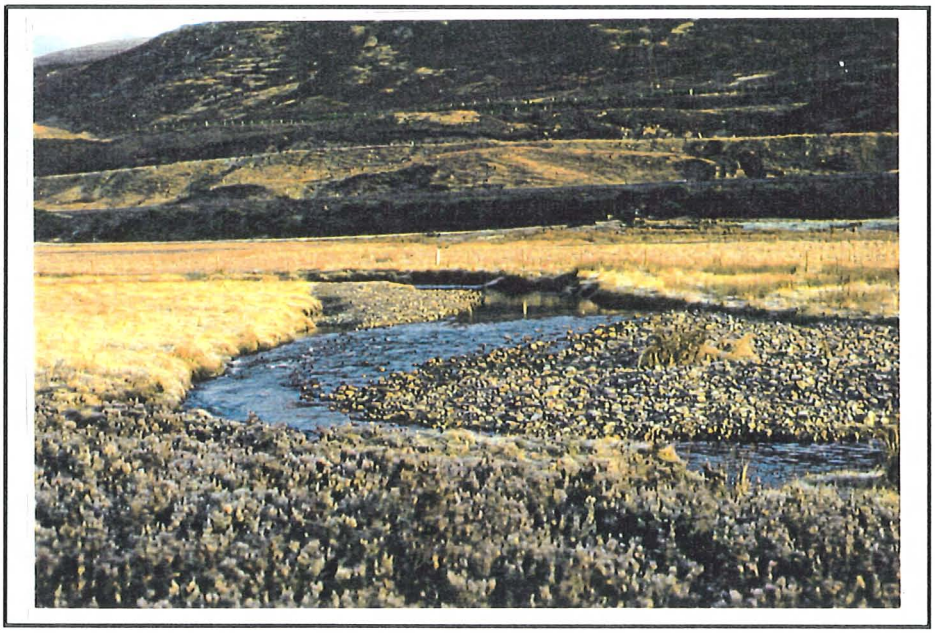

Plate 3.2. Upstream view of the point bar (II) at the apex of the central bend, reach A, December 1991. $Q = c1\ m^3s^{-1}$.

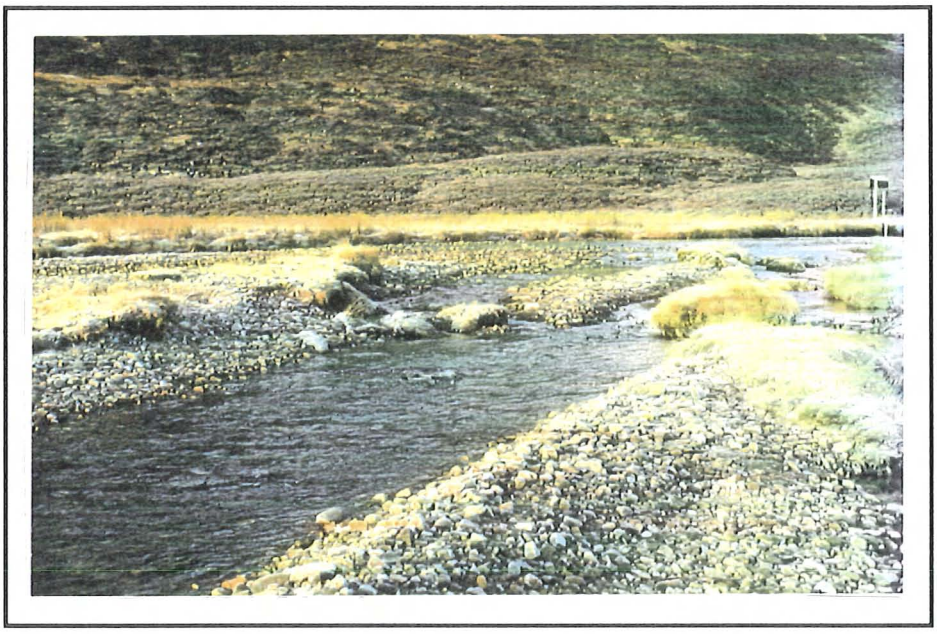

Plate 3.3. Turf congested channel, head of bar III is to the left, bar IV is right, Reach A, December 1991. $Q = c1\ m^3s^{-1}$. Flow towards the camera.

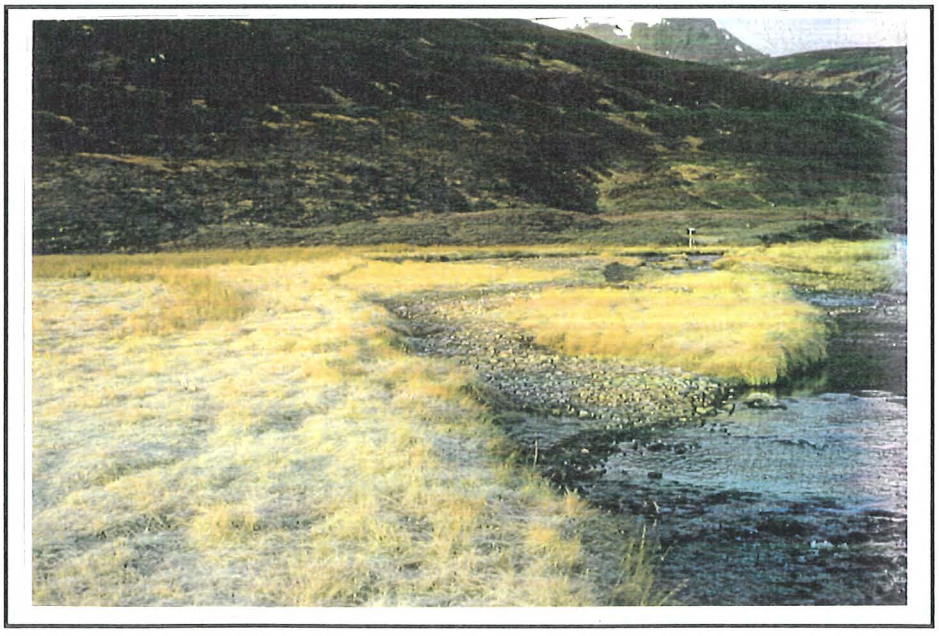

Plate 3.4. Inactive channel deposits downstream of reach A. $Q = c1\ m^3s^{-1}$. Flow towards the camera.

was aggrading in June 1991 as the left channel widened at the expense of the main bar, therefore decreasing flow depth and increasing the potential for deposition. Opposite, the major bar (III) repeatedly cut back revealing a steep exposed face. A temporary bar downstream of this erosion (8) represented some of the sediment lost from bar III. This low elevation feature was the last bar in the reach before the final pool (9) which subsequently shallowed towards the end of the reach. The bars in the lower half of the reach appear to be free formed in response to sediment supply rather than channel curvature and hydraulics.

In addition to the active gravel features there are two areas of less active sediments. There was (and still is) a high flow chute (10) to the right of the final pool (Plate 3.4) which contains exposed sediments (which show signs of vegetation colonisation) representing areas of the channel which used to be active (see subsection 3.3.3). A similar abandoned channel is located upstream of the apex of the bend (11). This was a previously important chute diverting flow behind the abandoned bar, but was only moderately active at high flow and is unlikely to be responsible for any direct sediment input (this feature was temporarily re-activated in January 1994 as a direct result of a long duration snow melt flood). These abandoned channel deposits will not be considered during this study since they are unimportant to the current reach morphology.

3.3.3 Historical channel change, 1946 - 1988

This subsection presents evidence for past morphological change in reach A and assesses the relevance of this to present day conditions. The data presented are based upon 4 good quality air photographs taken from 1946 (Ref. 106G/SCOT/UK/64.RP, Scale 1:8400), 1959 (Ref. OS/59/107, Scale 1:24000), 1971 (Photo. No. 654 772-775, Scale 1:8400) and 1988 (Ref. 19 88 124, Scale 1:24000).

The 1946 air photo, being particularly detailed, was used as the basis for the reach outline. This remained consistent throughout the 42 years of study, except for the gradual tightening of the bend at the start of the reach. The general outline of the reach in 1946 was traced and the morphological detail filled in for subsequent photographs. This method ensures that the overall scale is consistent and that sketches taken from each photo are directly comparable.

In 1946, the overall channel pattern was reasonably simple (Figure 3.7a). Flow entered the reach striking the outer bank of the bend at almost 90^{o} (1a). Adjacent to this, on the inner of the bend was a large area of active and vegetated gravel in the form of a complex point bar assemblage (2a). An active chute (3a) bypassed some flow behind this bar. The medial bar (4a) diverted flow at the apex of the central leftward bend, together with associated point (5a) and bank attached (6a) bars. The lower half of the reach (much wider than today) contained a right-bank attached bar

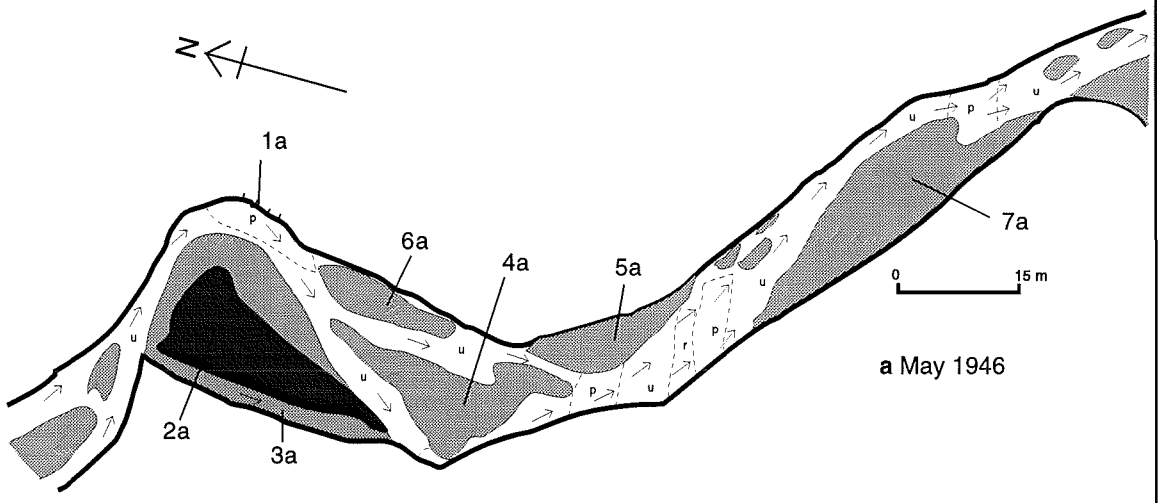

Key: See Figure caption.

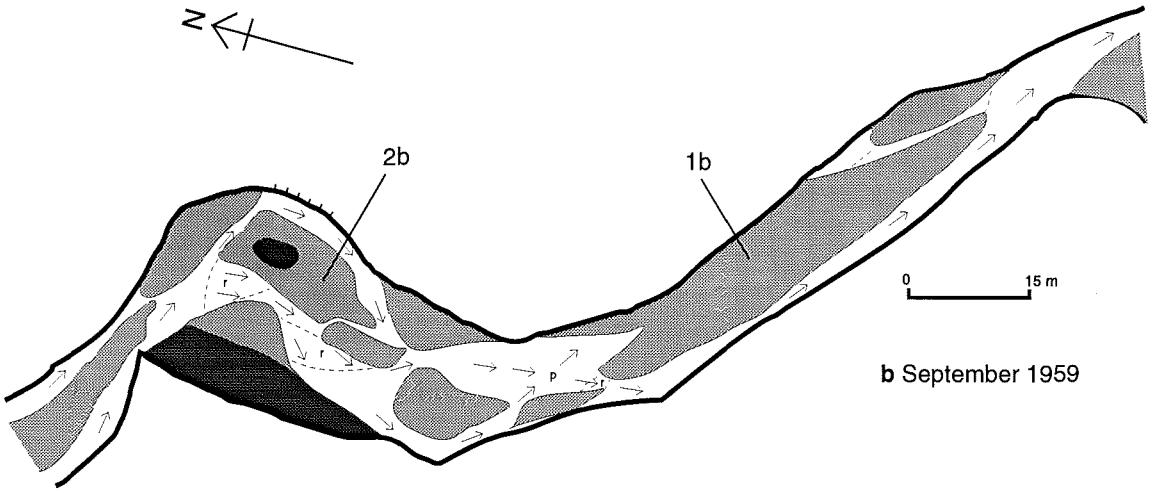

Key: See Figure caption.

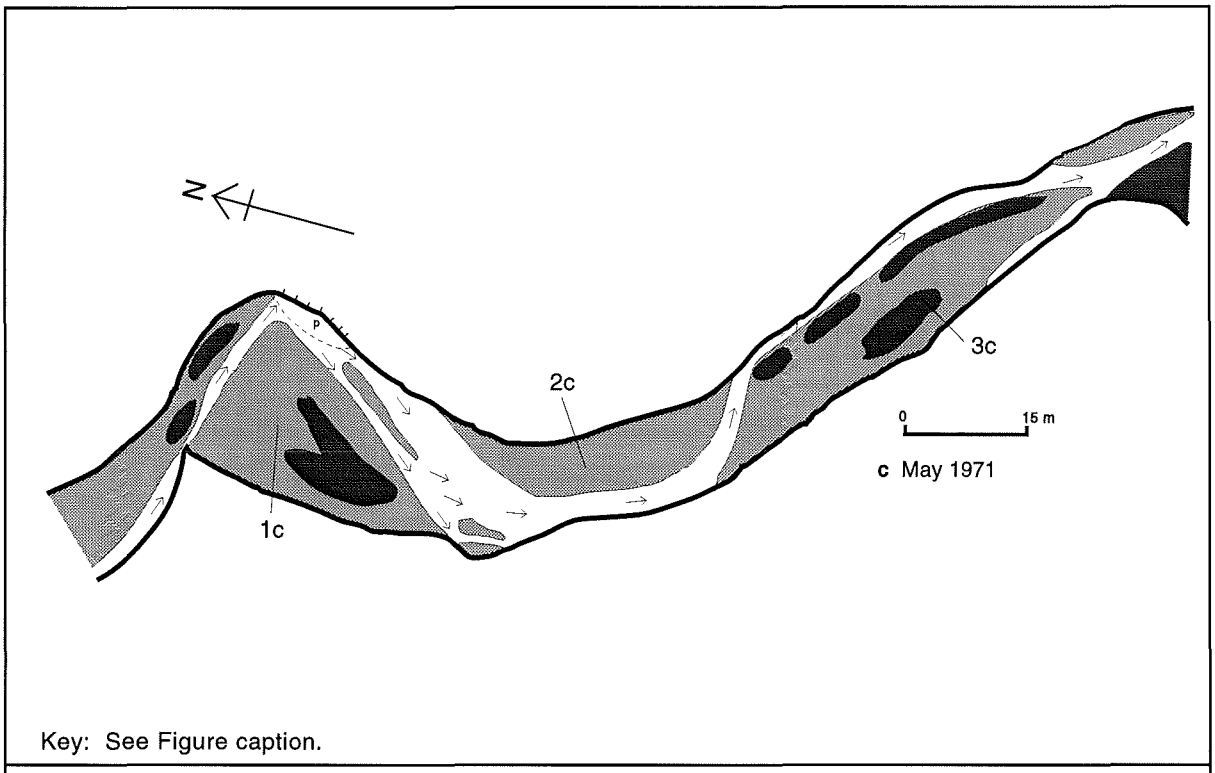

Key: See Figure caption.

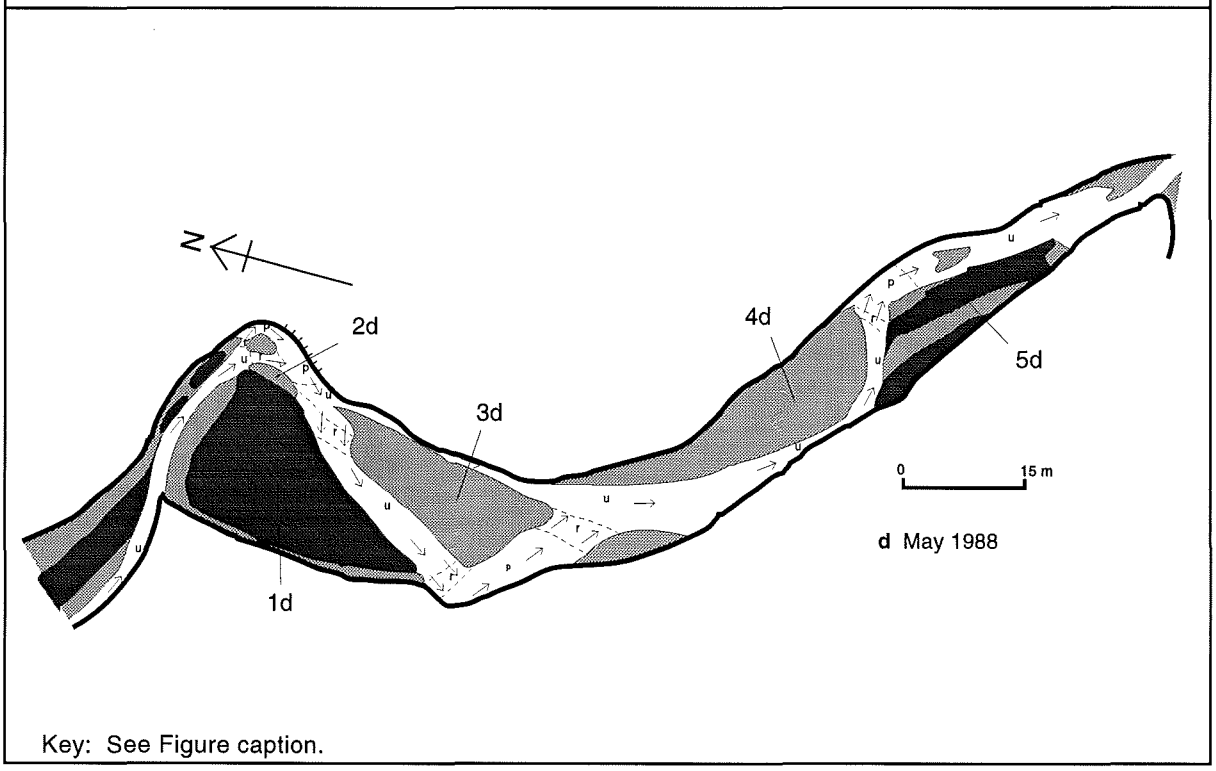

Key: See Figure caption.

Figure 3.7. Reach A historical channel change, 1946 - 1988. Bold shading - Fossil bars. Light shading - active gravel. p - Pool. r - Riffle. u - Undifferentiated channel. Arrows indicate probable flow direction. Bold line - Reach outline. Refer to Figure 3.6 for key.

containing most of the stored sediment (7a). By 1959, this bar had changed position, becoming attached to the left bank (Figure 3.7b) (1b). The most notable change since 1946 was the development of a complex of braid bars at the head of the reach (2b). These may have formed as a response to reactivation and subsequent dissection of the previously partly active point bar (2a). It is possible that this upstream change was responsible for the switch of the large downstream bar.

The channel pattern in 1971 (Figure 3.7c) was much less complex than in 1959, although large expanses of active gravel were still present. The braided complexes at the first bend were replaced by a large area of active gravel which was beginning to show signs of stabilisation by vegetation (1c). A large point bar developed on the central bend (2c). The bar downstream of the central bend (3c) had again switched sides and was beginning to show signs of vegetation stabilisation.

The situation in 1988 again revealed significant morphological change (Figure 3.7d). The point bar at the head of the reach (1d) was vegetated indicating a significant reduction in the width of the active channel. Flow at the apex of the first bend continued to erode the outer bank with a small point bar forming (2d) opposite, attached to the fossil bar. At the next bend, a point bar (in a contrasting position to the 1971 point bar (2c)) and active chute (3d) were located with associated pool riffle sequences. The bar in the lower half of the reach was further upstream than in 1971, much depleted and attached to the left bank (4d). Downstream of this, the once active deposits were vegetated (5d) reducing the active channel width by almost two thirds. This date records the smallest area of active gravel in each of the four photographs, this reach scale constriction may reflect reduced sediment supply and possibly explain the activity at this site at the present time when compared with other reaches of the Allt Dubhaig. Earlier activity when constriction was less may have been a result of increased sediment supply from upstream.

The preceding description has illustrated a cycle of instability with reactivation and subsequent stabilisation of the major point bar (2a, 2b, 1c, 1d). This cycle is possibly a consequence of changing upstream sediment supply (e.g. Church and Jones 1982). Upstream changes and their effects upon downstream morphology will be examined for present day channel change and are the basis for a major part of this work.

Comparison between figures 3.7d and 3.6 reveals that between 1988 and 1991 the trend of morphological change continued, although comparisons made between an air photograph sketch and a detailed reach map cannot be totally accurate. Since 1988, the new bar (2d) at the start of the reach has prograded downstream, and the chute behind the point bar (3d) has aggraded. However, the major differences are found downstream where the major alternate bar (4d) changed considerably. By November 1990, the bar had been dissected and was detached from the bank

(Plate 3.5). Between then and July 1991 (Figure 3.6), the left channel widened and a new smaller left-bank attached bar formed, and the detached bar (III) was progressively cut back.

3.3.4 Channel change during this study (June 1991 - July 1993)

The preceding discussion indicates the morphological changes which have taken place over the past half century. This is still a very active reach which has also altered considerably during the 2 years of study. This reach affords an ideal location to study the dynamics of sediment redistribution and volumetric changes since these are significant at both present and historical time scales. Figure 3.6 will be used as the start point to introduce the major morphological changes which will be quantitatively examined in subsequent chapters. Minor changes to the distribution of pools and riffles are largely omitted. Bars are labelled according to the notation introduced in Figure 3.6. The stage and discharge figures used in this subsection are intended as an illustrative guideline only. Exact flood magnitudes are discussed in relation to field measurements in Chapter 4.

December 1991. After mapping the reach, the first significant floods took place in October 1991 (peak stage at Q3, c.0.7 m, $Q \approx 6$ m^3s^{-1}). These caused only minor changes, but did identify the areas most likely to be susceptible to alteration during floods. In describing changes in morphology, these subsections will deal with the reach progressively in the downstream direction.

By December 1991, there had been no change in the upstream half of the reach, namely, the area of channel upstream of the apex of the leftward bend. Downstream of here the dominant bar (III) had again cut back resulting in the formation of a low elevation 'protective' platform (Plate 3.6). Bar IV remained unaltered since the turf blocks which afforded it protection had not been disturbed. The most notable change in reach A at this time was the absence of the temporary storage bar (8) at the tail of the reach. This wide region was prone to changes throughout the study where temporary instability arose due to the deposition of sediment from upstream effectively 'choking' the channel (analogous to the 'over aggraded' state introduced by Lane et al., in prep.).

January 1992. Two of the largest floods recorded during this study occurred during December 1991 and January 1992 (peak stage at Q3, c0.75 m, $Q \approx 7$ m^3s^{-1}). The reach was re-examined in January 1992 and again, the upstream half showed little change except for bank erosion. The downstream part of reach A experienced aggradation at the head of the major bar (III) and on the riffle (6), thus effectively blocking the right channel. All turf in the left channel had been removed allowing reworking and reformation of the bar (IV) attached to the left bank. The low elevation 'protective' platform previously adjacent to the cut bar (III) had also been removed and the bar further eroded (Plate 3.7). Some of the eroded material was found in unstable temporary storage at the foot of the reach deposited as a dissected area of sediment forming two temporary

Plate 3.5. Reach A, November 1990. Note the detachment of bar III from the left bank. $Q = c2\ m^3s^{-1}$. Flow is from left to right.

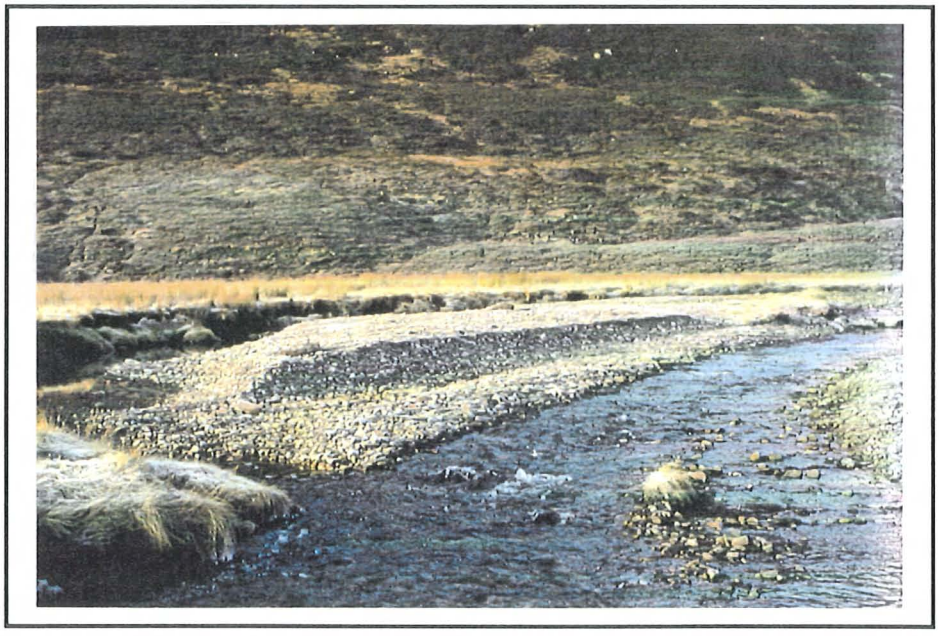

Plate 3.6. Eroding bar III, reach A, December 1991. Eroded material formed a low elevation 'protective' platform. $Q = c1\ m^3s^{-1}$. Flow towards the camera.

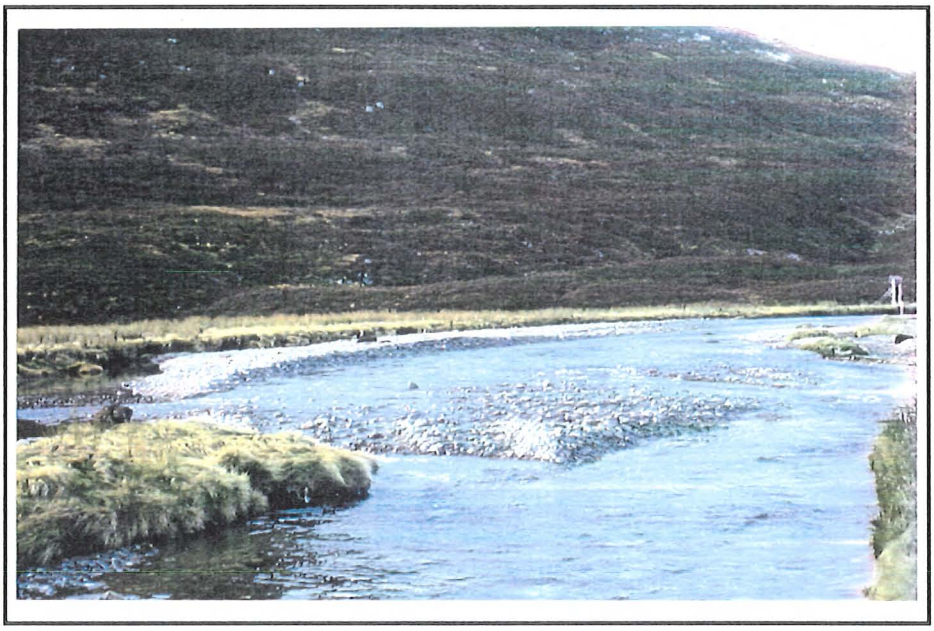

Plate 3.7. Eroding bar III, reach A, January 1992. Note the temporary accumulations of eroded sediment downstream of the bar. Q = c3.5 m^3s^{-1}. Flow towards the camera.

Plate 3.8. Eroding bar III, and dissected temporary accumulations of sediment, reach A, October 1992. Q = c1 m^3s^{-1}. Flow towards the camera.

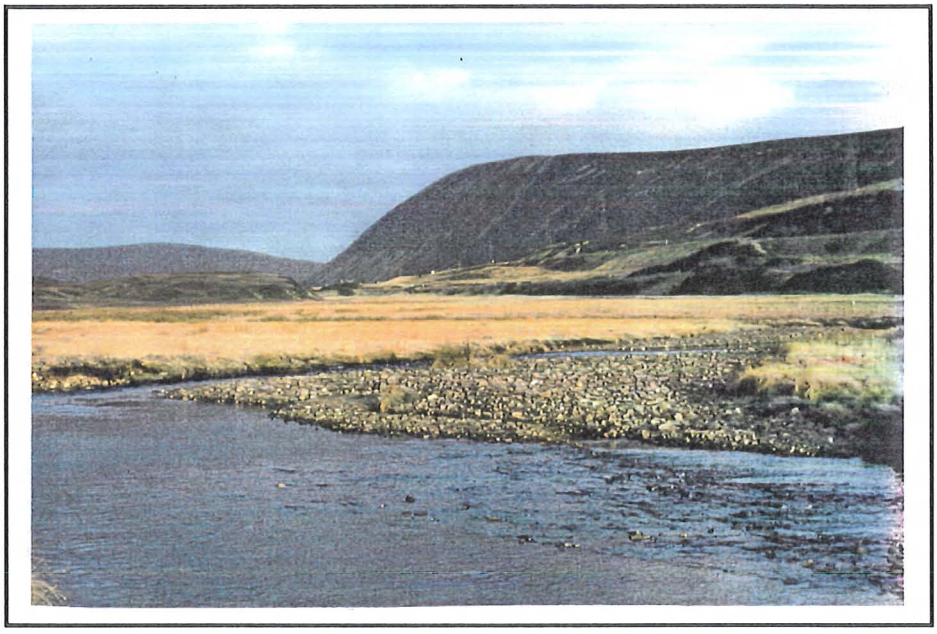

Plate 3.9. Point bar (II) at the apex of the central bend, reach A, December 1991. $Q = c1\ m^3s^{-1}$.

Plate 3.10. Point bar (II) at the apex of the central bend, reach A, February 1993. $Q = c2\ m^3s^{-1}$.

Plate 3.11. Upstream view from below reach A, February 1993. Q = c2 m^3s^{-1}.

Plate 3.12. Temporary sediment storage lobe attached to the remains of dissected bar IV, reach A, February 1993. Q = c2 m^3s^{-1}.

accumulations. Once again, the lower half of the reach had undergone considerable morphological change, apparently not at the expense of the upper half. Minor autumn floods in 1992 caused further erosion of the bar (III) and dissection of the material stored at the tail of the reach (Plate 3.8)

February 1993. The next notable channel change occurred in January 1993. This was the result of a snow melt flood which resulted in widespread disruption and damage further down the network of the River Tay. This flood (peak at Q3 was in excess of 0.8 m Q $\approx$ 10 m^3s^{-1}) caused the largest amounts of channel activity seen during the study period. The prograding bar (I) at the head of the reach aggraded by up to 60 cm. In the adjacent channel (1) the downstream part of the pool filled while the upstream pool at the head of the reach deepened. Associated with this was bank retreat of up to 1 m. Eroded bank material was deposited on the downstream point bar (II) together with up to 40 cm vertical accumulation of sediment (Plates 3.9 and 3.10). This bar also prograded towards the right bank (the abandoned bar). It is probable that the source for this sediment was 100 m upstream where an avulsion caused erosion of a substantial amount of sediment from an abandoned channel.

The downstream part of reach A experienced further aggradation at the head of the cut bar (III), suggesting that switching of the channel back to its old position (pre 1990) on the right was unlikely, at least in the short term. The cut bar face was also eroded. At the start of the study it was a major feature (III), by February 1993 it was a shallow small scale bar (Plate 3.11). Opposite this, the left bar (IV) was heavily dissected and became attached to an aggraded temporary storage lobe downstream, now a more permanent feature (Plate 3.12). The other storage lobe was eroded with a remnant attached to the tail of the cut bar. This lower half of reach A was now a shallow wide area of channel, the well defined morphological differentiation evident at the start of the study having disappeared.

3.4 Reach B

3.4.1 Hydraulics and sedimentology

Reach B is a low energy transitional reach displaying both meandering and straight channel characteristics. The reach is situated in a limb of a wide meander bend containing a meandering thalweg. This 100 m reach begins at 2300 m, over 1 km downstream of A. Reference to the long profile (Figure 3.3) illustrates the low local bed slope for this reach. The mean reach slope (calculated in the same way as for A) is 0.004, slightly higher than for reaches immediately up and downstream which flow parallel to the valley whilst reach B is almost perpendicular. Peak shear stress in a straight reach downstream for a $7m^3s^{-1}$ flood was 34.9 Nm^{-2} (Wathen et al. in prep.).

Local shear stress values for B are likely to be slightly higher due to the larger overall bed slope and within reach local variations (Figure 3.8). An estimate of critical dimensionless shear stress for the deepest pool can be made in the same way as for reach A. A slope of 0.004, at a bankfull depth of 1.2 m with a D_{50} of 35.3 mm suggests $\tau_{BF} \approx 47$ Nm^{-2}. The resultant value of τ^* is 0.08 suggesting a lower degree of activity than in reach A.

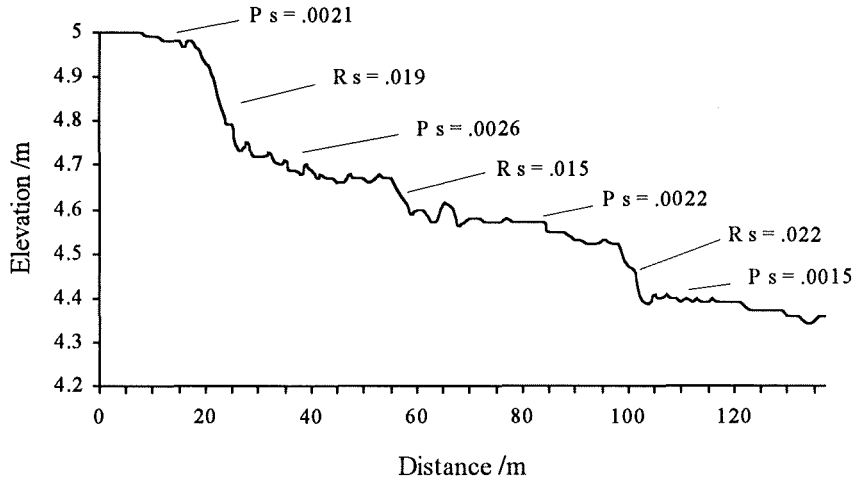

Figure 3.8. Reach B thalweg water surface slope. Stage at Q5 = 0.28 m, Q ≈ 0.7 m^{3}s^{-1}. Ps - Pool slope, Rs - riffle slope. Data expressed in m/m.

This reach can be thought of as a low activity site, as evidenced by incipient levees. The degree of fining in this part of the river is small (Figure 3.4). The grain size distributions taken from a single bulk sample at reach B (Figure 3.9) indicate weakly bimodal surface sediments and a unimodal subsurface. The gravel mode for the subsurface is less pronounced than the surface due to the larger proportion of sand in the former. D_{50} of the surface is 21.3 mm, and 13.9 mm for the subsurface. The D_{50} ratio of 1.67 suggests slight armouring. Despite the low slope and shear stress values, significant bedload transfer does take place in these lower reaches (Wathen et al. in prep.), and the extent to which this influences sediment redistribution in reach B will be addressed later.

3.4.2 Reach B morphology at the start of the study

Reach B was first mapped in July 1991 (Figure 3.10). The reach consisted of well defined bars and an associated complex arrangement of pools and riffles (Plate 3.13). The first notable feature upstream of the start of the reach was a lobe of sediment (1) advancing towards the outer bank. The bank showed no sign of recent erosion, yet cohesive eroded bank material formed part of the channel bed extending 3 m into the centre of the bend. The occurrence of a non-gravel bed for part of the bend suggests a limited area of gravel for input to the reach.

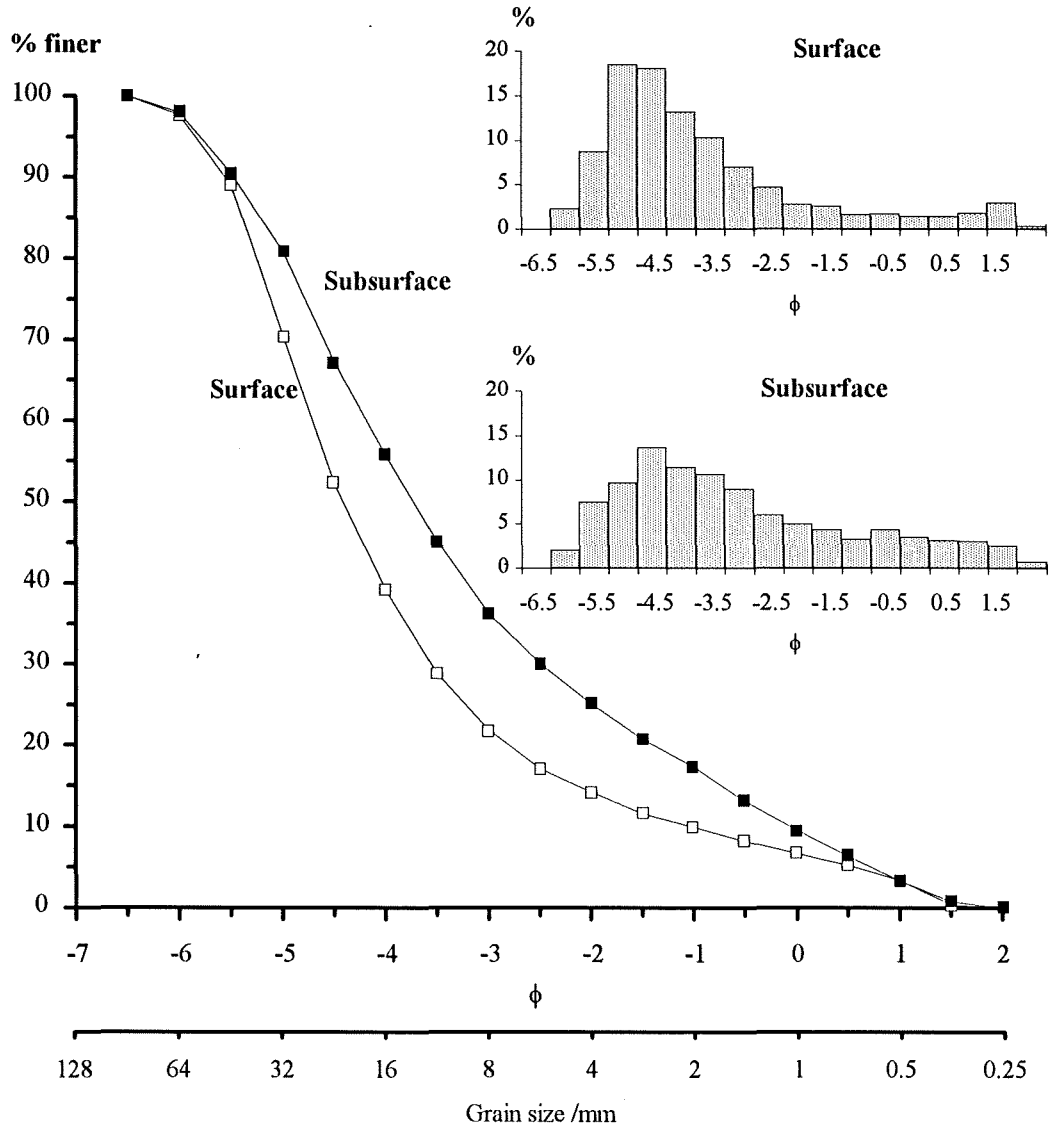

Figure 3.9. Reach B single representative grain size distribution. Sample taken from a cross section 10 m downstream of the reach.

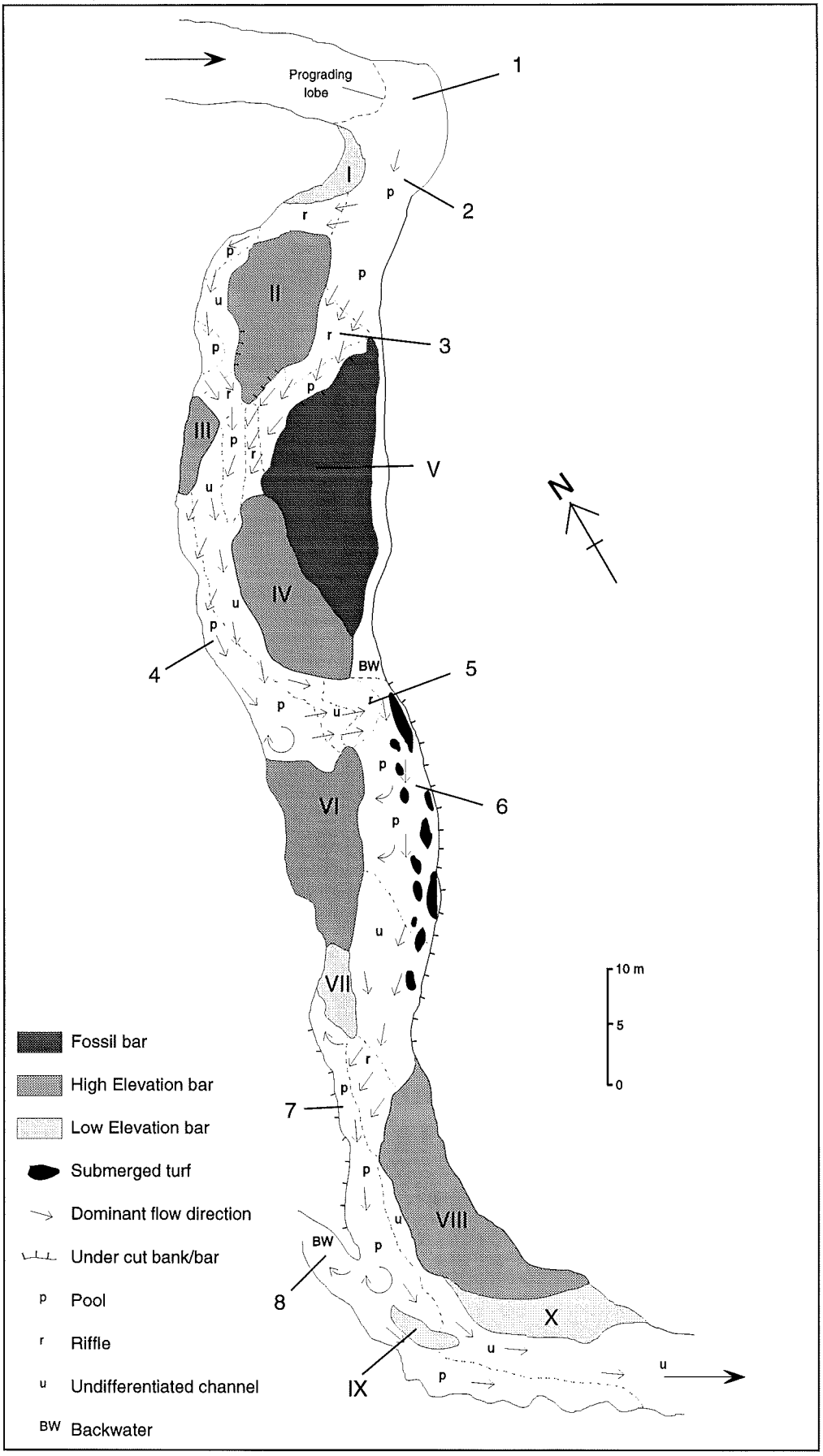

Figure 3.10. Planimetric map of Reach B, July 1991. Stage (Q5) = 20.4 cm, Q = c0.2 cumecs.

At the top of the reach a fine grained point bar (I) was located adjacent to a pool (2). This pool starts at the apex of the bend on the cohesive bed, extending downstream onto the gravel bed. Scour from this area and sediment from upstream may be responsible for formation of the medial bar downstream (II) (Plate 3.14). Photographs taken from 1988 suggest that this bar enlarged considerably by the time the map was constructed (Plate 3.15). The bar divided flow into two anabranch channels. The right channel was fine grained and partly active with considerable ponding, although it was important for the maintenance of the fine grained bar (III) at the tail of the medial bar. This channel was often abandoned during periods of low flow. The left channel contained a steep well defined riffle (3) leading into a pool. Downstream of this feature was an alternate bar (IV) attached to a fossil bar/vegetated island (V) (Plate 3.16). The bar margins (IV) showed the greatest activity, the high elevation plateau being fine grained and rarely submerged. The fossil bar is an indication of past activity across a greater area of activated gravel (see 3.4.3).

Adjacent to the high elevation bar (IV) was a pool extending along the right bank (4). This pool was responsible for sediment supply to an active bank attached bar (VI), the coarse nature of the bar head reflecting the depth of the pool (source area) and hence competence. At the head of this bar, the submerged channel turned 90^{o} over a riffle step (5) where it flowed perpendicular to the left bank prior to turning almost parallel to the bank. The oblique angle of flow relative to the bank resulted in erosion and deposition of turf blocks within the channel (6). This was the only evidence of bank retreat in this reach. Secondary currents from this pool resulted in a fine grained low elevation bar (VII) attached to the tail of bar VI.

On the apex of the bend downstream of the bank erosion, a point bar (VIII) diverted flow across a riffle into an elongated pool (7) adjacent to the right bank (Plate 3.17). Scour from this pool formed a migrating lobe represented by a partially submerged bar (IX). Secondary circulation resulted in another fine bar tail (X), this time attached to the point bar.

The lower half of reach B is directly comparable, in morphological terms, to the upper half of reach A. Each has fixed alternate point bars. The associated pool and riffle units are also located in similar positions. Comparison between these parts of each reach will help to isolate morphological effects, although hydraulics will differ.

3.4.3 Historical channel change 1946 - 1988

Reach B appears inactive, but reference to the air photographs (section 3.3.3) reveals that this has not always been the case. This analysis is based upon the same method adopted for reach A where the 1946 outline is used as the basis for the sketches.

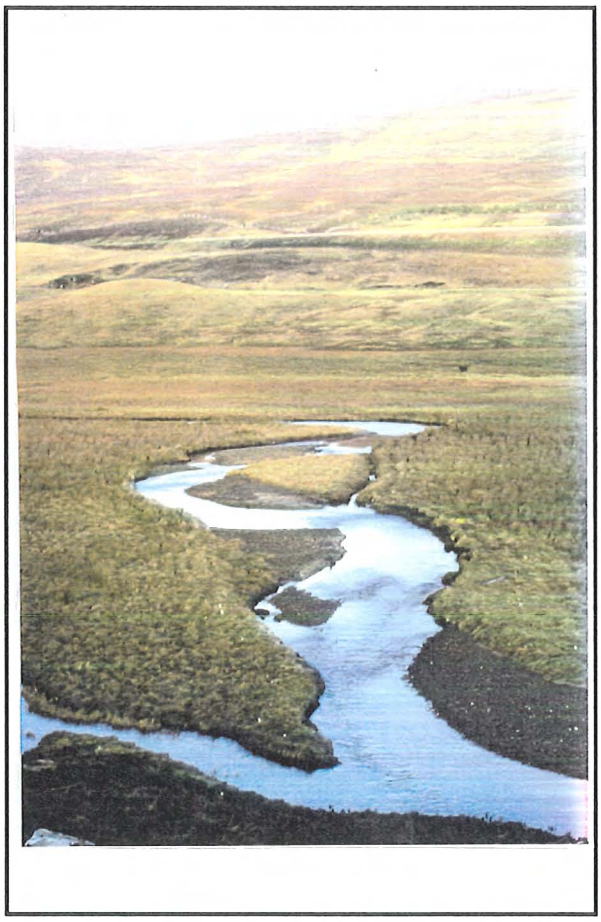

Plate 3.13. Planimetric view of reach B, December 1991. Q = c1 $m^3 s^{-1}$. Flow towards the camera.

Plate 3.14. Medial bar (II) with bank attached bar (III) in foreground, reach B, July 1991. Q = c0.5 $m^3 s^{-1}$. Flow towards the camera.

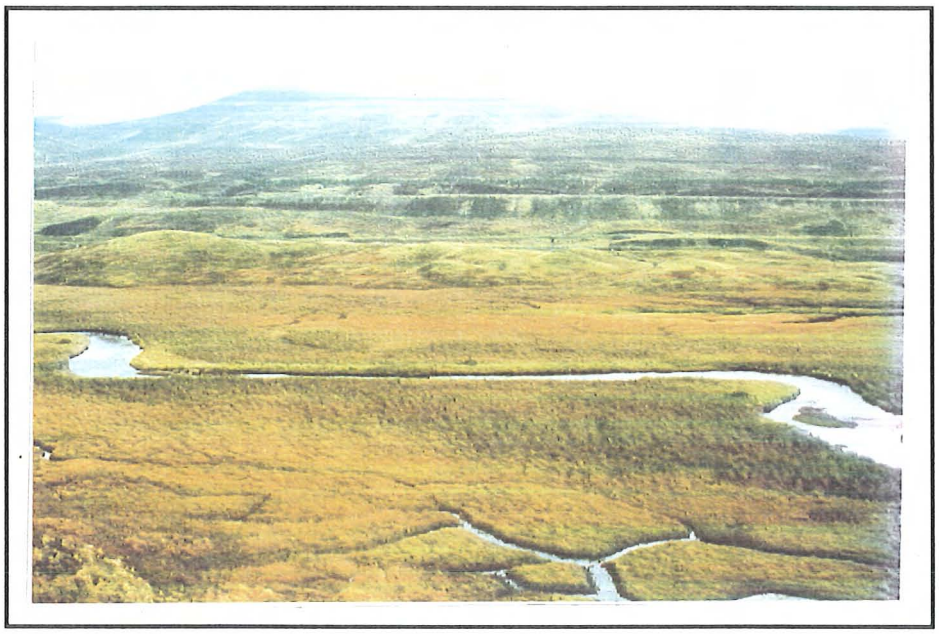

Plate 3.15. Medial bar (II), reach B, May 1988. Q = c1 m^3s^{-1}. Flow is from left to right (source: H. Ross).

Plate 3.16. High elevation alternate bar (IV) attached to the fossil bar (V), reach B, July 1991. Q = c0.5 m^3s^{-1}. Flow towards the camera.

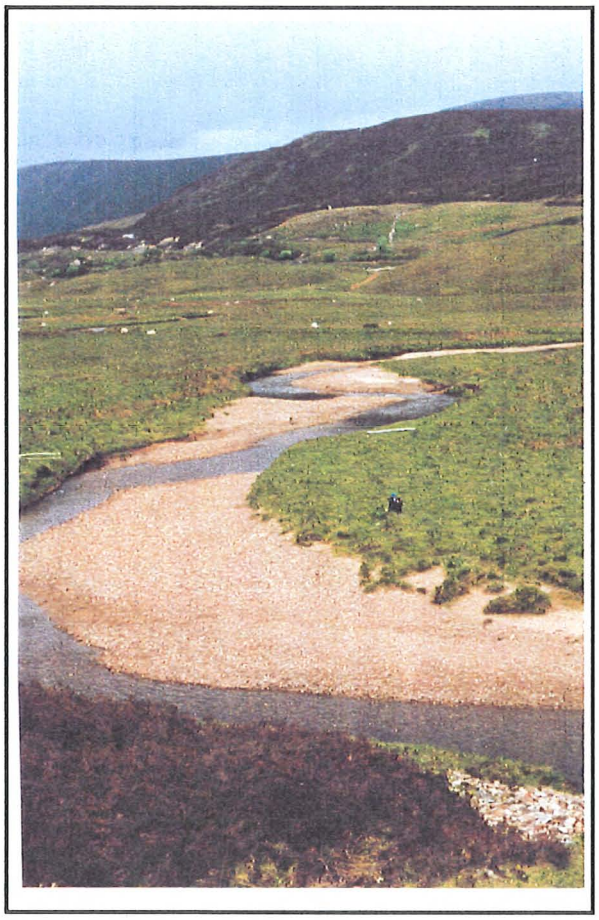

Plate 3.17. Upstream view of bar alternate bars VIII (foreground) and VI (background), reach B, July 1991. Q = c0.5 m^3s^{-1}.

In 1946 the active channel was much wider and more complex than at present (Figure 3.11a). Flow from the pool at the apex of the bend resulted in the formation of three bars, the most prominent of which was a medial bar (1a). Adjacent to this was a vegetated bank attached bar (2a), although this is not a part of the fossil bar found (V) today. Like the present situation, most of the bars were joined by a series of riffles. Downstream of 1a was a larger bar (3a) which may have been attached to the vegetated bar. Flow convergence downstream forced the formation of a smaller bar (4a) in an area of the river much wider than today.

By 1959 the morphology of reach B was less complex (Figure 3.11b). Pool scour at the start of the reach formed a single left bank attached bar (1b), the centre of which was vegetated. This area represents the nucleus of fossil bar (V). Downstream of this bar, an aggrading riffle (2b) diverted flow towards the left where the active width had narrowed as a result of stabilisation of the point bar head attached to the apex of the bend (3b). The situation was similar in 1971 (Figure 3.11c). The positions of the main bars were comparable and the extent of the vegetated bars had increased. The only major changes since 1959 were the development of a right-bank attached bar (1c) at the tail of the main riffle (this bar is still in evidence today) and the stabilisation of the fine sediment attached to the tail of the right bank (2c).

The 1971 pattern formed the basis for the 1988 channel morphology (Figure 3.11d). The dominant bar at the head of the reach (1d) became dissected forming the medial bar (Figure 3.10, II) and the fossil bar increased in size together with the bar attached to its downstream face (2d) forming the high elevation low activity bar (IV). In 1971 a considerable area of channel upstream was available for scour and sediment supply to this bar. By 1988 the upstream medial bar (II) had altered this with flow directed away towards the left bank, bar IV being left as an inactive feature. Downstream, the aggradation of the major riffle (3d) continued after 1971 causing bar development (V) and eventual narrowing of flow resulting in deviation towards the left bank. Additional vegetating of the downstream point bar (4d) has decreased the channel width to its present levels.

This section has concentrated upon well defined morphological features. The location of smaller pools and riffles on the sketches is based upon bar position and slight hue changes in the channel on the air photos. Reach B has gradually evolved to its present state since 1959, changing from a straight channel with braid bars to one with a meandering thalweg and associated alternate bars (e.g. Lewin 1976).

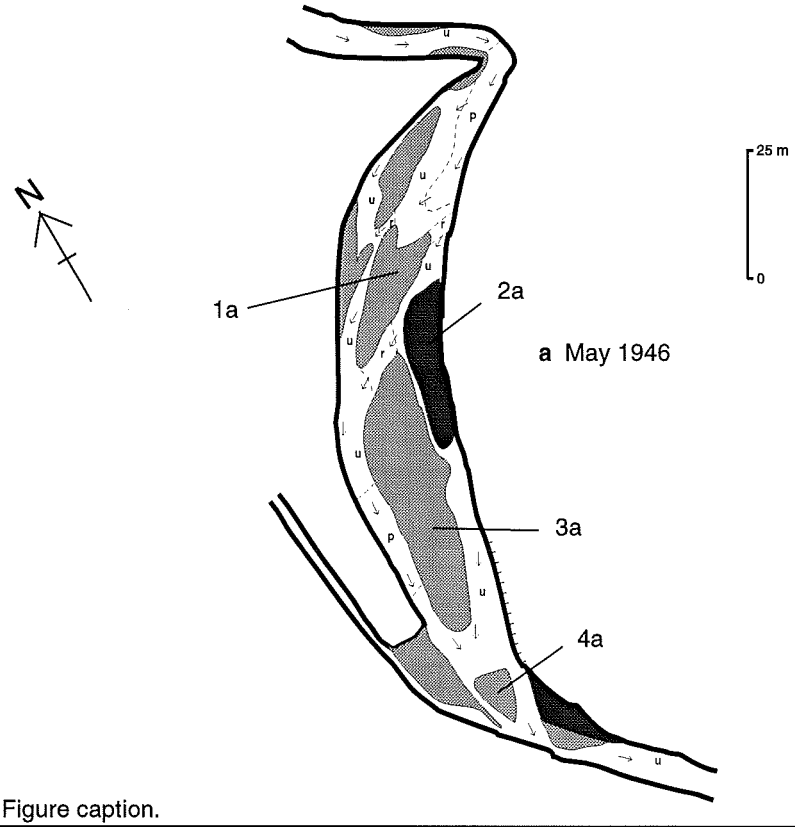

Key: See Figure caption.

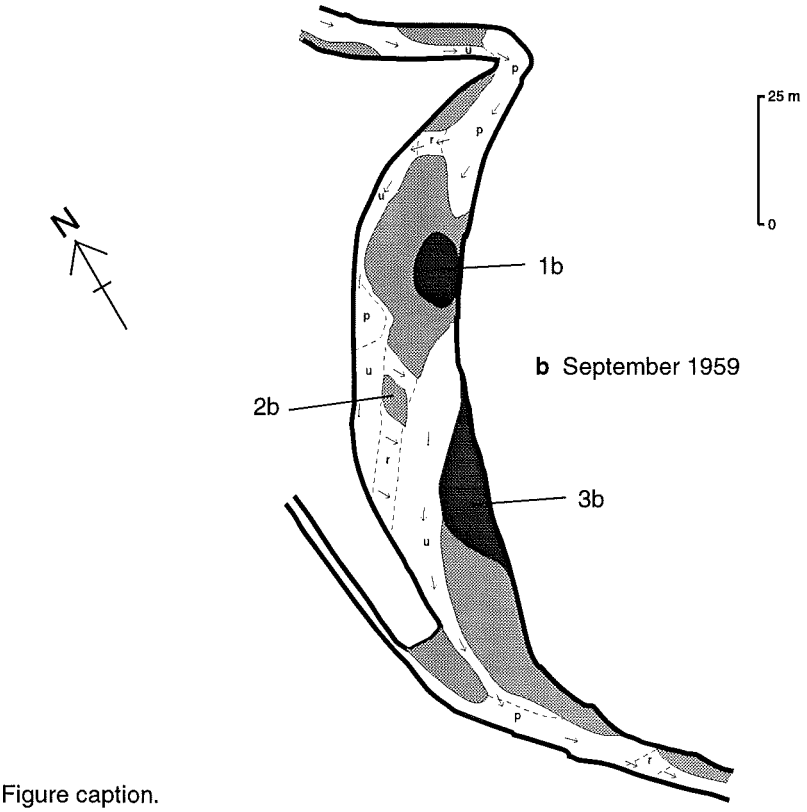

Key: See Figure caption.

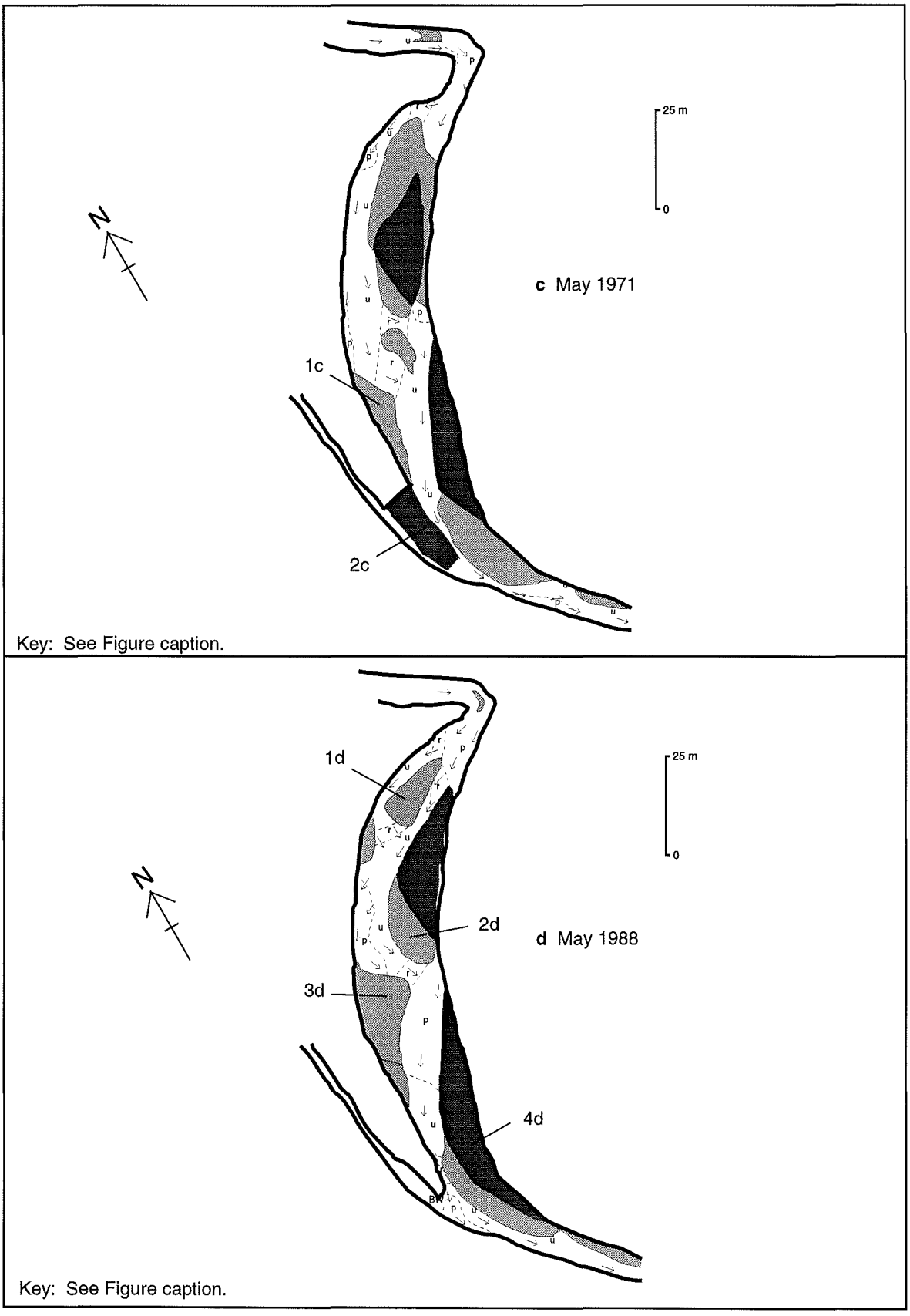

Figure 3.11. Reach B historical channel change, 1946 - 1988. Bold shading - Fossil bars. Light shading - Active gravel. p - pool. r - riffle. u - undifferentiated channel. Arrows indictate probable flow direction. Bold line - Reach outline. Refer to Figure 3.10 for key.

3.4.4 Channel change during this study (June 1991 - July 1993)

The situation in 1993 was broadly the same as it was in 1988. Over the course of the study the only alteration to the bars was slight surface aggradation arising due to the deposition of gravel sheets, a few particles thick, scoured out of pools during periods of high flow. There was negligible erosion of the cohesive banks, although, there is evidence for past erosion in the form of submerged turf blocks. In one case a turf block adjacent to the vegetated island did influence pool migration. Subsequent scour around the block filled a downstream pool, the scoured area taking the place of the original pool.

The pool at the apex of the bend (Figure 3.10, 7) moved 5 m upstream after a flood in January 1993. Similarly, the pool tail (downstream of 3) opposite the fossil bar (V) filled while the deepest part of the pool migrated upstream. The riffle downstream aggraded forming an emergent bar at low flow hence reducing the width of flow. These are all minor changes compared to reach A, which are indicative of how this reach continues to slowly evolve.

Although apparently broadly similar in planform, reaches A and B show contrasting hydraulic and grain size characteristics. Both reaches are dominated by bank attached bars and a meandering thalweg, however, the contrasting slopes result in very different levels of activity at each site. Reach B represents an ideal site to compare with the unstable active reach A.

4. Data Collection

This chapter describes the techniques used to document and explain reach scale sediment storage and transfer fluxes. Cross sections are used to determine the extent and volume of sediment stores, surveys being repeated after significant channel change. Bedload transfer is the linkage between these stores and is determined from magnetic tracing of gravel sized material. All data are presented relative to a bedload threshold defined from stage data. Each method is described in detail together with its relevance to the overall aims of the project. In order to describe sediment budgets at the reach scale, emphasis must be placed upon detailed data collection but this has to be balanced with logistical constraints.

4.1 The particle tracing programme

Magnetic tracer particles were used to document sediment transfer within the two study reaches. These data are the basis for calculation of transit time distributions (characterising storage) and replicate fluxes of sediment between stores (linkages). In order to fully characterise the transit time distribution of a particular store, a 100% recovery rate is necessary (Dietrich et al. 1982). Prior to 1984, recovery rates from tracer studies were often poor (see section 2.4.1), but usage of magnetic tracers (Hassan et al. 1984) permits higher recovery rates, sometimes in excess of 90 %.

4.1.1 Tracer particle number

In order to accurately represent reach sediment fluxes, the size distribution of each tracer set should match that of the bed (Dietrich et al. 1982). However, initial attempts at scaling using surface pebble count data suggested 2 problems: (1) tracer numbers required for half phi classes less than reach D_{50} were in excess of what was possible to manufacture (for example, 500 16 - 23 mm tracers were required); (2) the grain size distribution used represented the bed surface, not the active layer (defined as the layer of episodically mobilised material on the stream bed, Hassan and Church 1994). This is usually a few particles diameters thick and is a source of bedload, therefore scaling should be relative to the active layer.

Tracer numbers may be determined from the mean reach surface bulk samples discussed in chapter 3 (Figure 3.5 and 3.9). However, these surface samples taken to a depth of the maximum particle b axis, D_{MAX}, are not representative of the active layer thickness. Limited field data suggest that this varies with transfer intensity (Hassan 1990, Hassan and Church 1992). Sediment routing models allow it to vary relative to flow competence (Borah et al. 1982) or grain size (Parker 1990, Hoey and Ferguson, 1994). Even if the active layer could be reliably determined from bulk

data, it would still be necessary to convert to particle number (e.g. Kellerhals and Bray 1971, Bunte 1992), which still poses the problem of excessive tracer numbers required to match the bed.

Instead of scaling tracer numbers to match the bed prior to determining sample sizes, this study used an almost uniform distribution of tracers for different size classes in each reach. The tracers were then scaled to match the active layer such that 1 tracer in fraction *i* represented x_i bed particles (chapter 5). The main justification for this is logistical as usage of such a distribution prevented the manufacture of vast numbers of tracers for the modal half phi class. Tracers thus over-represented coarse fractions (by number) and under-represented the fines. Scaling is necessary to provide accurate fractional transfer flux data from each store.

530 tracers were used in reach A and 460 in B. The total of 990 was the maximum possible for practical reasons. The numbers used in this study were sufficient to allow a detailed coverage of the reach although no statistical basis for determination of the number of tracers to be used was possible since transit time data had not been previously calculated on the Allt Dubhaig.

Each tracer set was divided into three subsets for seeding purposes, with each half phi class (except the coarsest) containing the same number of particles (Table 4.1). The tracers in the coarsest half phi class for each reach were non magnetic (<180 mm A, <90 mm B). These classes contained fewer tracers than the other half phi classes and were painted only. The absence of a magnet was based upon the premise that this material is less mobile and thus the least likely to be buried.

	Reach A			**Reach B**		
	I	**II**	**III**	**I**	**II**	**III**
<180	20	10	20	0	0	0
<128	32	16	32	0	0	0
<90	32	16	32	30	15	15
<64	32	16	32	50	25	25
<45	32	16	32	50	25	25
<32	32	16	32	50	25	25
<22	32	16	32	50	25	25

Table 4.1. Distribution of tracer particles seeded in Reaches A and B as subsets I, II and II.

Comparison between tracer distributions and surface count data (Figure 4.1) reveals the full extent of the discrepancy between tracers and actual bed material. Reach B tracers were closer in proportion to the bed material, but there is a considerable disparity between reach A tracers and the bed, this will be adjusted when the data are scaled.

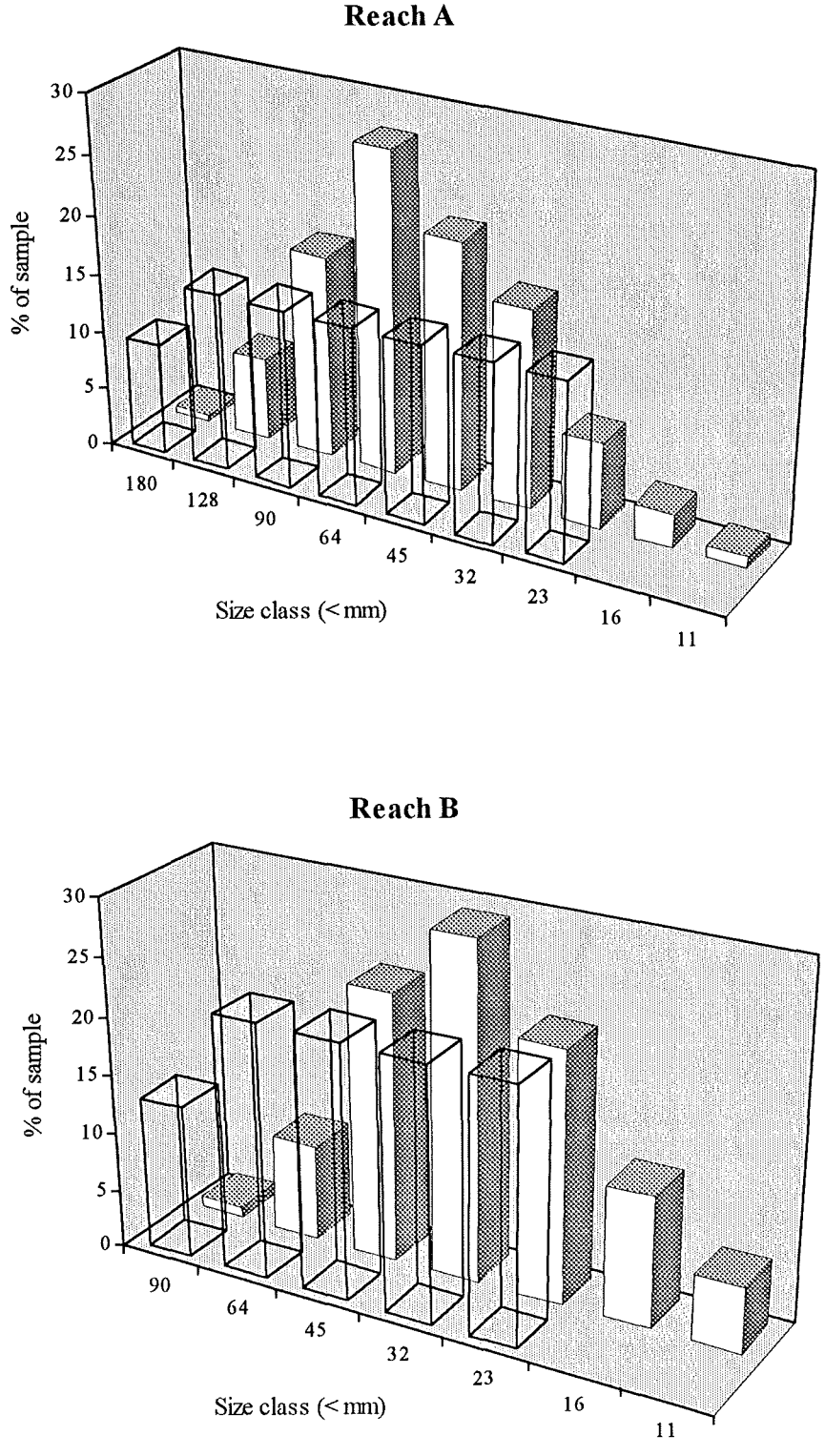

Figure 4.1. Comparison between tracer and bed surface grain size. Bold columns represent tracers, fine columns represent surface grain size distribution derived from surface pebble counts.

4.1.2 Tracer production

The procedure for the production of a magnetic tracer is described in more detail elsewhere (e.g. Hassan et al. 1984, Laronne 1987, Drew 1992). The tracer clasts were randomly selected from sites in the upper reaches of the river, predominantly on a bar upstream of T1 (see Figure 3.1). Many more than were actually required were taken to allow for breakage. The random sampling procedure ensured the sample contained no bias in terms of lithology or particle shape.

Ceramic ferrite magnets (10 * 6 mm) were used for material > 45 mm and Neodymium Iron Boron (6.4 * 2 mm) for particles < 45 mm. Smaller holes were drilled in the finer particles to minimise breakage during production and reduce the zones of weakness (this also lowers the potential for the tracer to crack once installed in the river). A hole was drilled in each particle, which was then given two coats of paint. Each set (I - III) was colour coded to allow easier visual interpretation. A single magnet was placed in the hole and sealed with epoxy resin to within 2 mm of the pebble surface. A numerical label was placed over this dry resin with the remaining void subsequently sealed by a further application of resin. The tracers were labelled using black enamel paint and a permanent marker pen. Once prepared, all the tracers were measured (a,b,c axes) and weighed to aid with identification in case label numbers were removed.

4.1.3 Tracer seeding

The most important factor governing the installation positions of the tracers was the need to ensure rapid incorporation within the reach transfer system. In addition, the tracers should be distributed throughout the study reaches, not just the upstream areas since tracer dispersion from an initial seeding point increases rapidly downstream (e.g. Mosley, 1978, Pickup et. al., 1983, Hoey, in press 1995). Inadequate coverage over the downstream areas of the reaches was avoided by seeding the tracers at three locations in the upstream half of each reach. In order to ensure rapid entrainment the tracers were seeded in pools where the probability of entrainment was high (Laronne and Carson 1976, Schmidt and Ergenzinger 1992).

4.1.3.1 Reach A tracer seeding sites

The three seeding locations in reach A are illustrated in relation to the rest of the reach in Figure 4.2. A brief description of each is given below.

Reach A site I: 212 orange tracers seeded in four 2 m parallel lines in a deep pool at the head of the reach (Plate 4.1). It was anticipated that secondary currents from this pool would transfer some material into storage in the tail of bar I. In addition, material would be incorporated within the

Figure 4.2. Reach A tracer seeding positions, Dec. 1991.

Bankfull depth based upon Sept. 1991 survey.

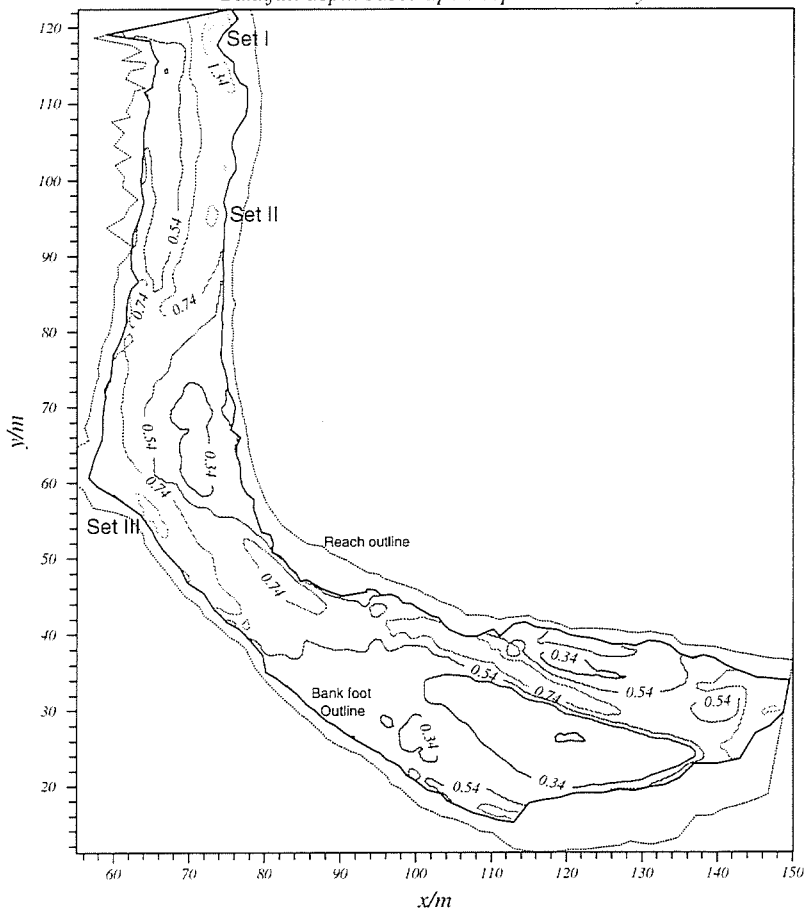

B.Full depth /m

1.84
1.34
0.74
0.54
0.34
0.00

Plate 4.1. Installation position of tracer set I, reach A, December 1991. Q = c1 m^3s^{-1}. All material was entrained by January 1992. Flow is from right to left.

Plate 4.2. Upstream view of set II installation site, reach A, December 1991. Q = c1 m^3s^{-1}.

Plate 4.3. Installation position of tracer set III, reach A, December 1991. Q = c1 m^3s^{-1}. Flow is from right to left.

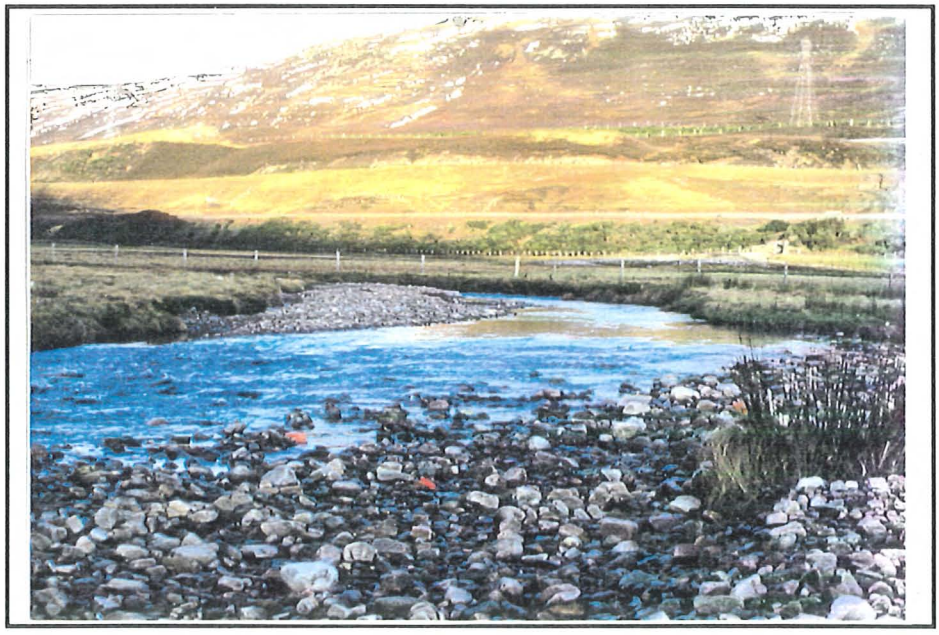

Plate 4.4. Upstream view of reach A demonstrating incorporation of tracers within the storage system after the first flood events, January 1992. Q = c2 m^3s^{-1}.

upstream part of the reach. Selection of this site was vindicated by only five tracers remaining in the pool after the first flood events.

Reach A, Site II: 106 green tracers seeded in two 3 m parallel lines in a shallow pool 25 m downstream of set I (Plate 4.2). Seeding aimed to ensure tracer coverage within the central regions of the reach and incorporation of material into the point bar (II) at the apex of the bend. Most tracers were entrained from this site although some coarse particles remained suggesting lower competence than the deeper pool site I.

Reach A, Site III: 212 red tracers seeded in five 1.5 m parallel lines (Plate 4.3) in the pool site downstream of the central bend. This was the last available pool before the wide gravel expanses of the lower half of the reach. Seeding in this pool site ensured entrainment of most tracers.

The programme of tracer seeding was successful for the active reach A. In excess of 95% of tracers were entrained into the storage system after the first flood (Plate 4.4).

4.1.3.2 Reach B tracer seeding sites

Again, the tracer sets were located in three pool sites at separate locations along reach B (Figure 4.3). A brief description of each seeding site is given below.

Reach B, site I: 230 orange tracers seeded in four 3 m parallel lines (Plate 4.5) in the tail of the pool at the head of the reach. The aim was to incorporate most of the tracers into the upstream part of the reach and into storage within the associated bars. However, only 50% of the tracers were entrained, a large proportion of the remainder being buried by c10 cm of sediment.

Reach B, site II: 115 red tracers seeded in two 4 m parallel lines in a deep pool in the centre of the reach, downstream of the fossil bar. This pool is a major source of material for the pronounced right bank attached bar (Plate 4.6). Again, approximately 50% of the tracers remained in situ buried by c10 cm of sediment.

Reach B, site III: 115 green tracers seeded in two 4 m parallel lines in the deep pool below the riffle step. Tracers at this site were intended to cover the lower half of the reach. No coarse clasts > 64 mm moved out of this pool indicating low competence.

The seeding programme was not entirely successful due to the low activity of this reach. A large proportion of material (c50%) remained in the pools after the first floods. Solutions to this problem will be discussed in section 4.1.5.

Figure 4.3. Reach B tracer seeding positions, Dec. 1991.

Bankfull depth based upon July 1991 survey.

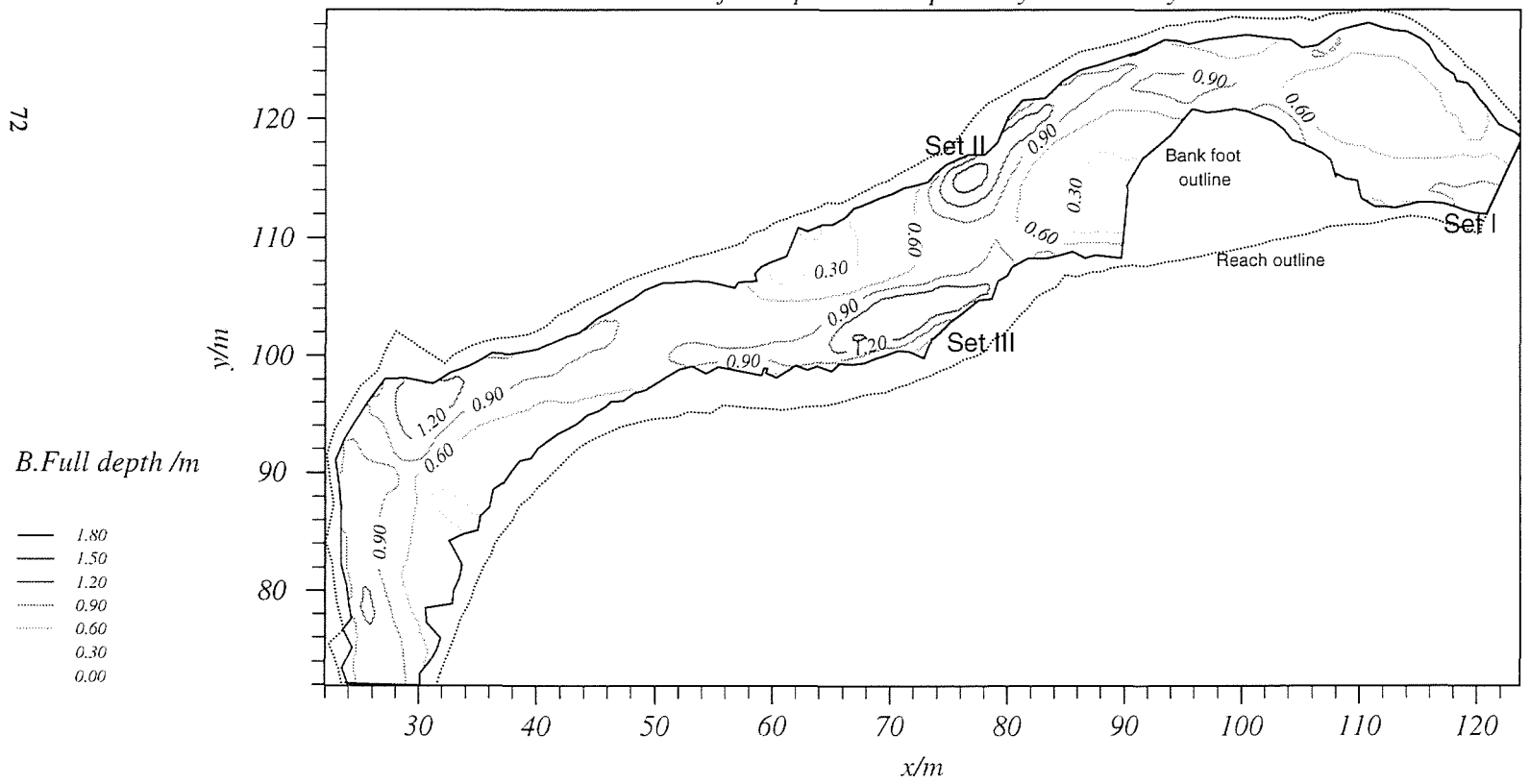

Plate 4.5. Installation position of tracer set I, reach B, December 1991. Q = c1 m^3s^{-1}. Flow is from right to left.

Plate 4.6. Lobe of sediment containing set II tracers scoured out from the installation pool site, Reach B. Q = c1.5 m^3s^{-1}. Flow is towards the camera.

4.1.4 Tracer searching

Once incorporated within the reach system, tracers were mapped using one of two techniques. When only one person was searching, two tapes were used to measure the distance of the tracer particle from two known points, usually cross section survey pegs. Cartesian co-ordinates were calculated from the cosine rule. With two people a total station Wild T1000 EDM (Electronic Distance Measurement) and theodolite was used. This equipment automatically calculated and stored tracer co-ordinates accurate to 0.01 m. The accuracy of the former method was ± 0.75 m, the latter, ± 0.2 m. Tracer burial depths were measured to within ± 0.025m.

Tracers not visible on the surface were searched for with a Schonstedt Heliflux Magnetic Locator (Plate 4.7) up to depths of 50 cm (Plate 4.8). In such cases it has been argued that minimal disturbance to the bed occurs as long as the excavated material is carefully replaced (Drew 1992). However, disturbance is unavoidable where tracer particles accumulate in storage zones (Plate 4.9). This should not be a hindrance to the present study providing such zones are carefully repaired.

The nature of flooding on the Allt Dubhaig precluded frequent searching; floods often follow in rapid succession allowing insufficient time for a full data collection programme of tracers and cross sections. Instead, this project relied upon the occurrence of weather 'windows' to carry out the 10 days needed for data collection. A total of 8 searches were carried out in reach A and 7 in reach B (Table 4.2).

	Reach A		**Reach B**	
Date	**Search No.**	**Type**	**Search No.**	**Type**
Dec. 1991	1	Installation	1	Installation
Jan. 1992	2	All tracers	2	All tracers
Mar. 1992	3	All tracers	3	All tracers
Sept. 1992	4	All tracers	4	All tracers
Oct. 1992	5	All tracers		
Dec. 1992	6	Surface only	5	All tracers
Feb. 1993	7	All tracers	6	All tracers
July 1993	8	All tracers	7	All tracers

Table 4.2. Tracer search details.

It was inevitable that during the course of the study some tracers would be output from the reaches. This material represents part of the overall transit time distribution of the whole reach (Plate 4.10). In order to account for this, the areas up to 250 m downstream of A and 80 m downstream of B were searched. Relocated material was replaced back in the reaches. The clasts

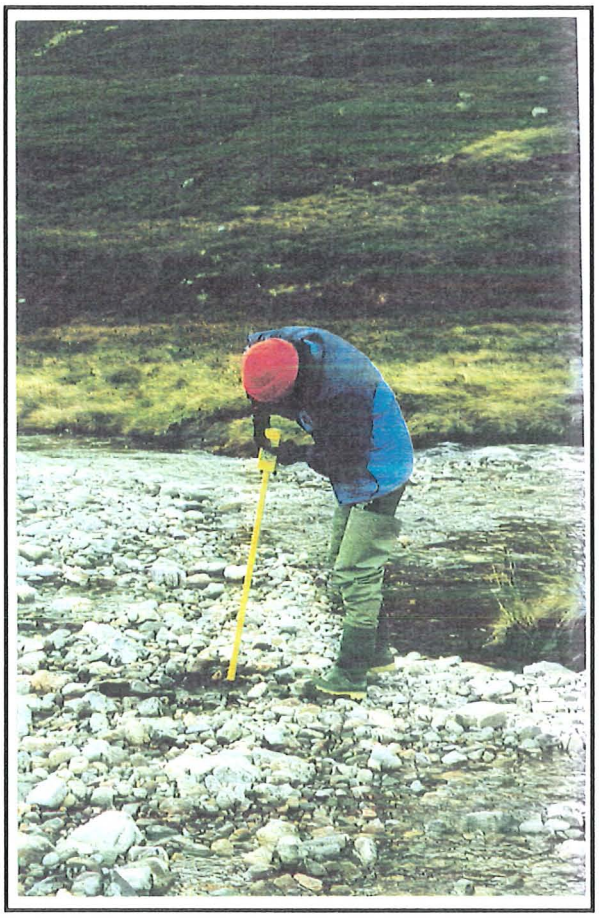

Plate 4.7. Determination of tracer position using a magnetic locator.

Plate 4.8. Buried particle located at a depth of 40 cm.

Plate 4.9. The impact of concentrated tracer relocation upon a temporary storage lobe in reach A.

Plate 4.10. Tracers relocated downstream of reach A after the floods of January 1993 forming part of the reach transit time distribution. This material was reseeded in the upstream half of the reach.

were usually reinstalled in the initial source pools, although, some were seeded on bars where tracer coverage was sparse.

4.1.5 Data availability

Tracer installation in seeding pools is termed search 1. Where possible, all subsequent searches refer to the same floods for reaches A and B. No search was carried out in reach B in October 1992, where minimal numbers of tracers had moved since search 4 during intermediate magnitude events. There was slight evidence of movement at reach A, therefore a search was undertaken. Reach A search 6 involved only surface tracers as it was curtailed by rising stage. The corresponding search in reach B (5) took place prior to this.

There are two drawbacks associated with the tracer derived data: firstly, the length of study was not sufficient to characterise transit times in the long term and secondly, attainment of a 100% recovery rate was not feasible. The temporal problem is overcome by the fact that all transit time distributions will be subject to the same constraints and will therefore be relatively comparable. The recovery rates may be more problematic, however, simplifying assumptions regarding tracer location may somewhat alleviate the problem. The following two subsections will present and analyse the recovery rates for both reaches and make an assessment of the quality and quantity of data available.

4.1.5.1 Reach A recovery rates

The data presented in this section will be broken down into sets I, II and III allowing a detailed examination of the factors influencing the tracer results. All the sets display a consistently high recovery rate for material > 32 mm until search 6 (Table 4.3). Recovery from surface only search 6 was low and it also declines with size suggesting increased burial of the finer fractions (particularly < 32 mm). Recovery for searches 7 and 8 was small due to morphological change between searches 6 and 7. Appreciable aggradation in some areas ensured that some tracers were out of range of the locator.

The most notable exception to the general trends in recovery for each set are the low values for < 32 mm clasts associated with set III. No definite explanation can be offered for this. It is reasonable to assume that these fine tracers are the most mobile but this does not explain the low recovery. The areas downstream of the reaches were thoroughly searched yet tracers were still missing. Reach B and the results from the downstream fining project show similar trends of low recovery for finer clasts. The answer may lie in the choice of magnets. A very intense signal is obtained from the small magnets used in these particles, but the magnetic field is fairly low. These

fine particles are more mobile and tend to be buried more frequently (Hassan and Church 1994); once deeply buried, the field of the magnet is too weak to detect possibly explaining the low recovery rates for fine material from all three sets.

Search No.	% Recovery						
Set I	**<180**	**<128**	**<90**	**<64**	**<45**	**<32**	**<23**
1	100	100	100	100	100	100	100
2	100	100	97	94	81	75	66
3	100	97	91	100	84	75	59
4	100	94	91	97	91	72	66
5	100	97	84	91	84	72	66
6	79	75	47	44	28	18	13
7	37	75	72	81	78	69	72
8	32	75	47	81	59	53	56
Set II							
1	100	100	100	100	100	100	100
2	100	100	75	87	81	94	62
3	100	90	94	87	69	81	56
4	100	100	100	100	81	81	69
5	100	100	100	100	100	81	63
6	70	69	56	19	25	25	13
7	70	69	100	75	69	75	50
8	30	87	87	69	63	63	50
Set III							
1	100	100	100	100	100	100	100
2	100	100	84	81	78	34	34
3	100	100	87	81	72	47	44
4	100	94	84	91	78	62	66
5	100	94	91	87	91	66	69
6	85	84	41	28	31	19	16
7	100	91	66	72	69	53	69
8	65	91	78	66	62	56	53

Table 4.3. Reach A tracer recover rates.

4.1.5.2 Reach B recovery rates

The recovery rates for reach B are considerably higher than in reach A (Table 4.4), partly reflecting the reduced clast mobility. Lower recovery in reach A was a result of better incorporation of tracers within the system. The high recovery rates at B are affected by the assumption that if a particle was not found within 30 m of the pool and it was known to have been in the pool in the preceding search then it had not moved. The basis for this was the location of a large number of buried particles in the seeding pools (especially sets I and II) which could not be recovered due to the water depth. A process of elimination was used to identify these particles. At set III, this immobility assumption was not necessary since most material was transferred from the pool or remained on the pool surface. The recovery rates from B whilst good, are a symptom of the inactivity at this site. It was not until search 6 that material became well incorporated in this reach.

Search No.	% recovery				
Set I	**<90**	**<64**	**<45**	**<32**	**<23**
1	100	100	100	100	100
2	100	98	98	96	96
3	97	94	88	90	76
4	97	100	84	75	59
5	100	100	88	84	86
6	97	94	86	80	86
7	100	96	88	86	92
Set II					
1	100	100	100	100	100
2	100	100	100	100	100
3	93	100	96	96	92
4	93	100	92	88	88
5	93	100	96	88	88
6	87	100	96	92	96
7	80	96	100	96	88
Set III					
1	100	100	100	100	100
2	100	100	100	100	100
3	100	100	92	92	96
4	100	96	92	92	84
5	100	96	96	92	84
6	100	96	92	92	84
7	100	92	100	100	80

Table 4.4. Reach B tracer recovery rates.

Non 100% recovery in both reaches is attributable to a number of factors. Whilst great care was taken with the tracer searching, it was inevitable that tracers would be missed. The following list suggests the main reasons for this: tracers being missed by the operator during the passage of the locator; particles buried too deep for the locator to pick up a signal; non magnetic tracers becoming buried; signal interference where buried particles are close together; tracers situated in pool areas too deep to search; interference of tracer signals by metallic debris and burial of particles containing small magnets.

4.2 Morphological quantification

A sediment budget study must identify the spatial distribution of storage with tracers documenting the linkages between stores. Cross section surveys will be used to quantify the volumes and extent of these stores, changes in which are related to transfer processes. Comparison of the location of stores in relation to the dynamic linkage fluxes will reveal some of the driving factors influencing the transfer of sediment. In addition, volumetric calculations from cross section data may permit identification of sediment waves (e.g. Hoey and Sutherland 1991), construction of within reach sediment budgets (e.g. Griffiths 1979, Ferguson and Ashworth 1992) and calculation of bedload transfer rates (e.g. Carson and Griffiths 1989, Ferguson and Ashworth 1992).

4.2.1 Objective determination of cross section numbers

Cross section numbers should be determined on the basis of study aims (Neill and Galay, 1967, Mosley 1982), in this case, identification of the three dimensional morphological storage characteristics. Lane et al. (1994) compared volumetric change calculations from digital terrain mapping (DTM) with cross sections for the same reach. Assuming that calculations from the DTM were accurate, they suggest that a 2 m cross section spacing is associated with 20 % error of the estimate of volumetric change. This study aims to reduce this figure whilst utilising a manageable number of sections. The method used to select the cross section spacing is based upon bar elevation (and hence volume) and is illustrated with reference to reach B. The six main bars within this reach (see Figure 3.10) were used.

The analysis involves the calculation of the number of points (n) necessary to determine bar surface elevation with a standard error (SE) of 0.02 m. This SE is the approximate D_{50} of the reach and represents the ± 2 cm accuracy afforded by surveying techniques. The number of points, n, was calculated from

$$n = \left(\frac{\sigma}{SE}\right)^2 \tag{4.1}$$

Standard deviation σ was estimated from

$$\sigma = 0.25(Z_{MAX} - Z_{MIN}) \tag{4.2}$$

This calculation of the standard deviation of bar elevation is strictly an estimate since no actual data were available. The values for maximum and minimum bar elevation (Z_{MAX} and Z_{MIN}) were estimated prior to the fieldwork. The results of the first part of this statistical analysis for reach B are presented in Table 4.5.

The value of n varies according to bar elevation, the larger the relative difference in height, the more points are required. All the figures were estimated, however, comparison with real data taken from survey 1 indicates that these estimates were accurate. The interval between points is calculated with reference to the bar area, A. This interval is both the spacing between points along a section and also the spacing between adjacent sections (in most studies lateral interval is less than downstream interval, Lane et al. 1994). The interval is determined from

$$Spacing = \sqrt{A/n} \tag{4.3}$$

For the preliminary estimate, the values of A were crudely determined using a grid square method. The results from Eq. 4.3. derived for each bar are illustrated in Table 4.5.

Bar	Z_{MAX}-Z_{MIN}	σ	n	A (m^2)	$\sqrt{A/n}$
I	0.15	0.037	3.4	5	1.2
II	0.40	0.100	25.0	65	1.6
III	0.25	0.062	9.8	10	1.0
IV	0.45	0.112	31.6	60	1.3
VI	0.50	0.125	39.1	80	2.0
VIII	0.65	0.162	66.0	85	1.1

Table 4.5. Statistics derived for selection of the number of cross sections at Reach B.

The preceding estimates suggest that cross sections should be located 1 m apart. The data also indicates that no more than 1 m should be between survey points taken in the active channel. This procedure gave similar results for reach A with approximately 1.5 m suggested as the maximum survey interval. These results are consistent with Lane et al. (1994) who indicate that a spacing of 1 m between sections was sufficient for correspondence between DTM and cross section based calculations of volumetric change in an active proglacial braided stream.

4.2.2 Surveying methodology

The guidelines developed above resulted in selection of a detailed network of 115 cross sections at reach A (Figure 4.4). All sections were located c1.5 m apart except for 20 1 m spaced sections around the apex of the central bend where coverage close to the right bank was small compared with the left. A full survey yielded approximately 3400 three dimensional co-ordinate values.

Reach B cross sections were spaced at 1 m intervals creating 106 sections. In some instances the spacing on the right bank was too great therefore 4 extra sections (labelled 33A, 34A, etc.) were added to compensate. A full survey of this dense network (Figure 4.5) yielded approximately 2300 points.

The cross sections were laid out in the summer of 1991 using painted and numbered cross section markers. Once installed, these markers were mapped and their co-ordinates form the basis for the tracer mapping. The first few surveys were carried out using an automatic level, and x,y,z co-ordinates were calculated from trigonometry. For later surveys, the use of a total station EDM and theodolite with an electronic notebook increased efficiency. Where possible, the cross section surveys were carried out at the same time as the tracer searches ensuring comparability between storage changes and movement fluxes.

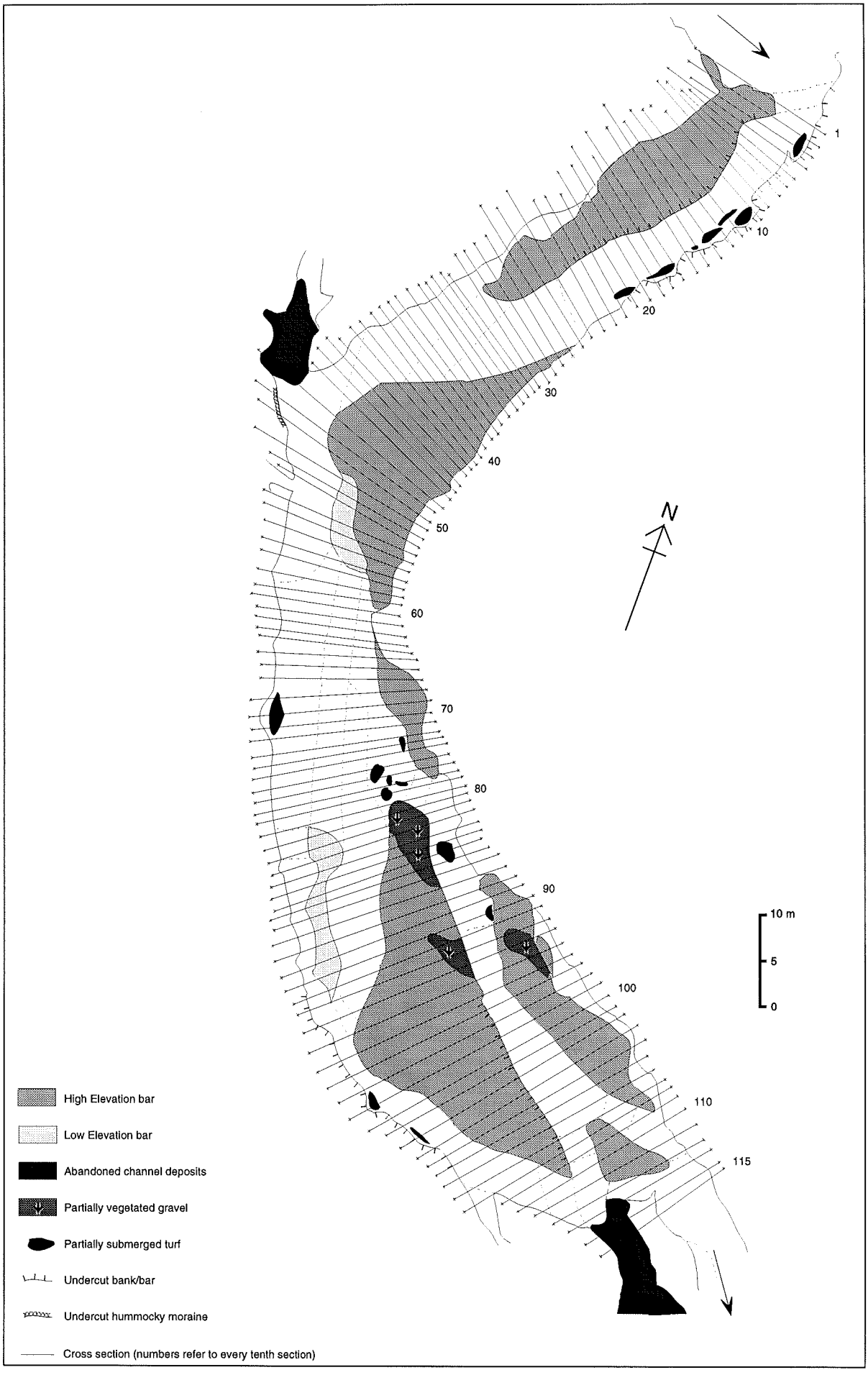

Figure 4.4. Reach A, June 1991. Location of 115 cross sections.

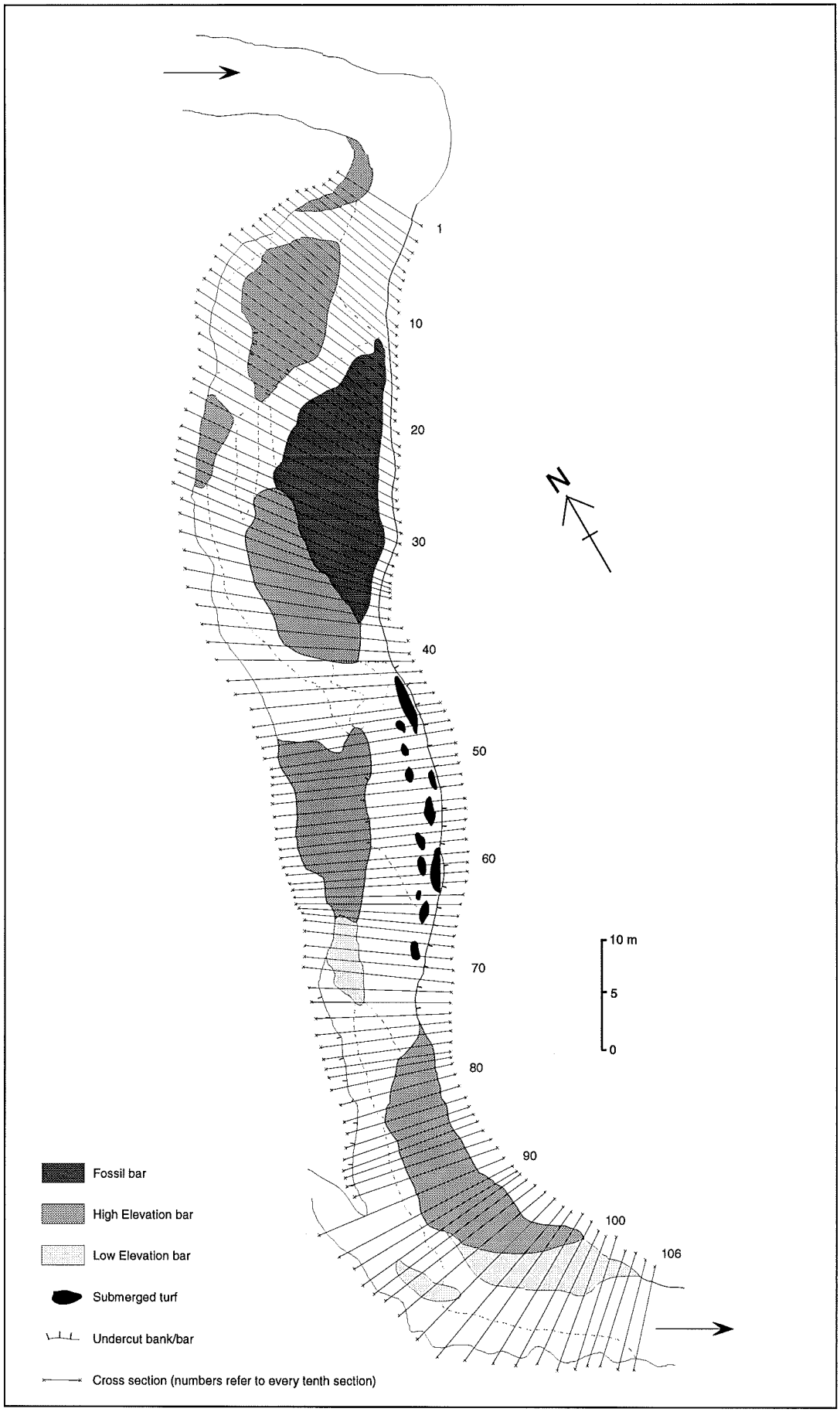

Figure 4.5. Reach B, July 1991. Location of cross sections.

4.2.3 Data availability

A full cross section survey was time consuming, so in some cases it was replaced by a half survey which included every other section. This still resulted in a detailed data set and reduced the risk of flooding curtailing data collection. A total of seven surveys were carried out for reaches A and B (Table 4.6).

Reach A	*Date*	*Type*	*No. XS*	*Reach B*	*Date*	*Type*	*No. XS*
1	21 Sept. 91	Full	115	**1**	20 July 91	Full	110
2	17 Jan. 92	¾	81	**2**	16 Jan. 92	Full	110
3	20 Mar. 92	½	56	**3**	19 Mar. 92	½	55
4	3 Sept. 92	½	54	**4***	4 Sept. 92	Full	110
5	9 Oct. 92	Full	115	**5**	7 Jan. 93	Inc.	27
6	15 Feb. 93	Full	115	**6**	25 Mar 93	Inc.	46
7	18 July 93	Full	115	**7**	17 July 93	Full	110
Total			651				568

Table 4.6. Cross section survey details, Reach A and Reach B. Inc. - Incomplete survey due to flooding. * Incorrect survey.

The data available for reach A are somewhat better than reach B. All surveys were complete and correspond to tracer searches except for search 6 (see Table 4.2). Most of the surveys for reach B also match except for survey 5 which was not carried out at the same time as search 5, flooding causing the abandonment of the survey. The two incomplete surveys (5 and 6) are the result of rising stage preventing completion of the cross sections. Data collected in survey 4, reach B, were erroneous due to an equipment problem. However, very little morphological change was apparent. These data are excluded from the rest of the study.

4.3 Grain size measurements

Measurement of grain size is necessary to allow accurate scaling of tracer data and description of storage characteristics. This section introduces an elevation based storage classification, which is only an approximation of the more accurate storage definition presented in chapter 5. The stores used in this chapter are only used for grain size description and analysis.

4.3.1 Techniques employed

4.3.1.1 Elevation zones

The immediate aim of the grain size work was to quantify the bulk characteristics of the various sediment storage units within each reach. Observation suggested that these sediments were

irregularly distributed in facies (Wolcott and Church 1991), presenting a number of possibilities for sampling. Preliminary measurement using facies mapping identified 25 storage types (providing an unrealistic number of possible stores). As an alternative, elevation was used to define sedimentary zones.

Cross section elevation decreases along the reach due to reach slope so all elevations were calculated relative to a sloping datum set at 7.5 m below the first point. The datum slope was calculated using cross section peg data from the left bank located close to the channel (Figure 4.6). The resultant elevation range at reach A varied from 1.0 m to 3.0 m while at B the range was 1.0 to 2.5 m. The higher activity at A tended to produce bars of greater relative relief. As a result, contrasting storage classifications were adopted for each reach.

Reach A: The aim of the categorisation is to determine a physically distinct set of zones relative to reach morphology. 5 zones were identified, corresponding with well defined morphological units (Table 4.7). The number of individual stores in each zone was visually determined. These represent the specific sites to be sampled (Figure 4.7). Very small sites (less than 5 m^2) were not sampled (except zone $E\alpha$). It is likely that these stores have a minimal effect upon sediment transfer. A total of 21 grain size samples was obtained from reach A.

Elev. Zone	Elevational range	Height (m)	Number	Description
$A\alpha$	2.4 - 3.0	0.60	3	High bar
$B\alpha$	2.2 - 2.4	0.20	7	Low bar
$C\alpha$	2.0 - 2.2	0.20	5	Riffle and shallow submerged channel
$D\alpha$	1.4 - 2.0	0.60	4	Thalweg and deep channel
$E\alpha$	0.8 - 1.4	0.60	2	Pools
Total			21	

Table 4.7. Reach A (subscript α) elevational classifications for grain size sampling. The Number column details the number of separate stores within the elevational zones.

Reach B: Categorisation into stores for reach B was much simpler than reach A. The low relief of the reach allowed division into four 45 cm storage zones (Table 4.8). The location of the 21 units is shown in Figure 4.8.

Elev. Zone	Elevational range	Height (m)	Number	Description
$A\beta$	2.20 - 2.65	0.45	4	High bar
$B\beta$	1.75 - 2.20	0.45	8	Low bar
$C\beta$	1.30 - 1.75	0.45	6	Riffle
$D\beta$	0.85 - 1.30	0.45	3	Pool
Total			21	

Table 4.8. Reach B (subscript β) elevational classifications for grain size sampling.

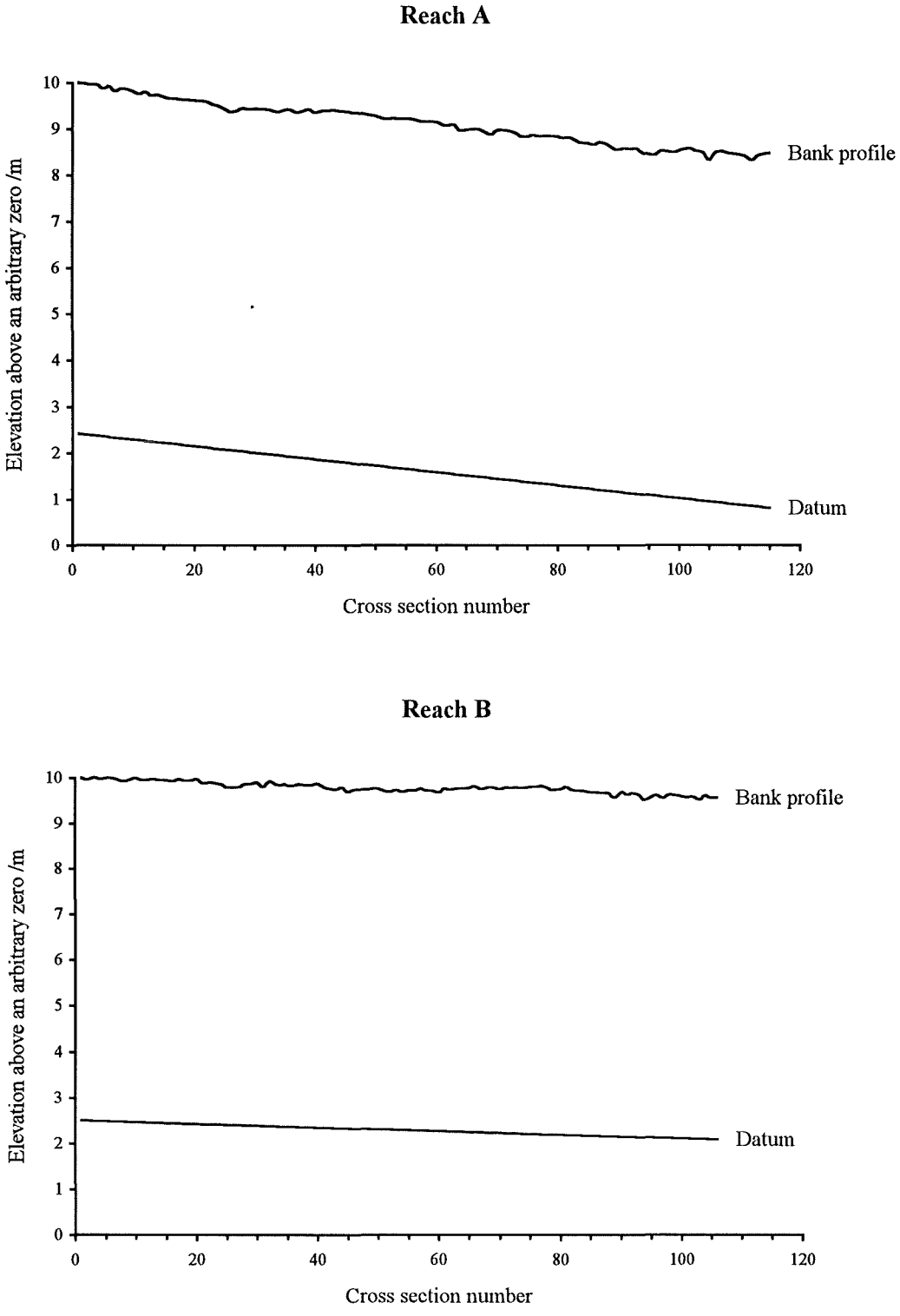

Figure 4.6. Reach A and B datum level. Datum calculated from regression of bank profile and subtraction of 7.5 m. All elevation data is calculated relative to this level. This datum is also used for determination of storage types (see chapter 5). Cross section number is an approximation of distance /m.

Figure 4.7. Reach A, July 1992.
Grain size sample sites.

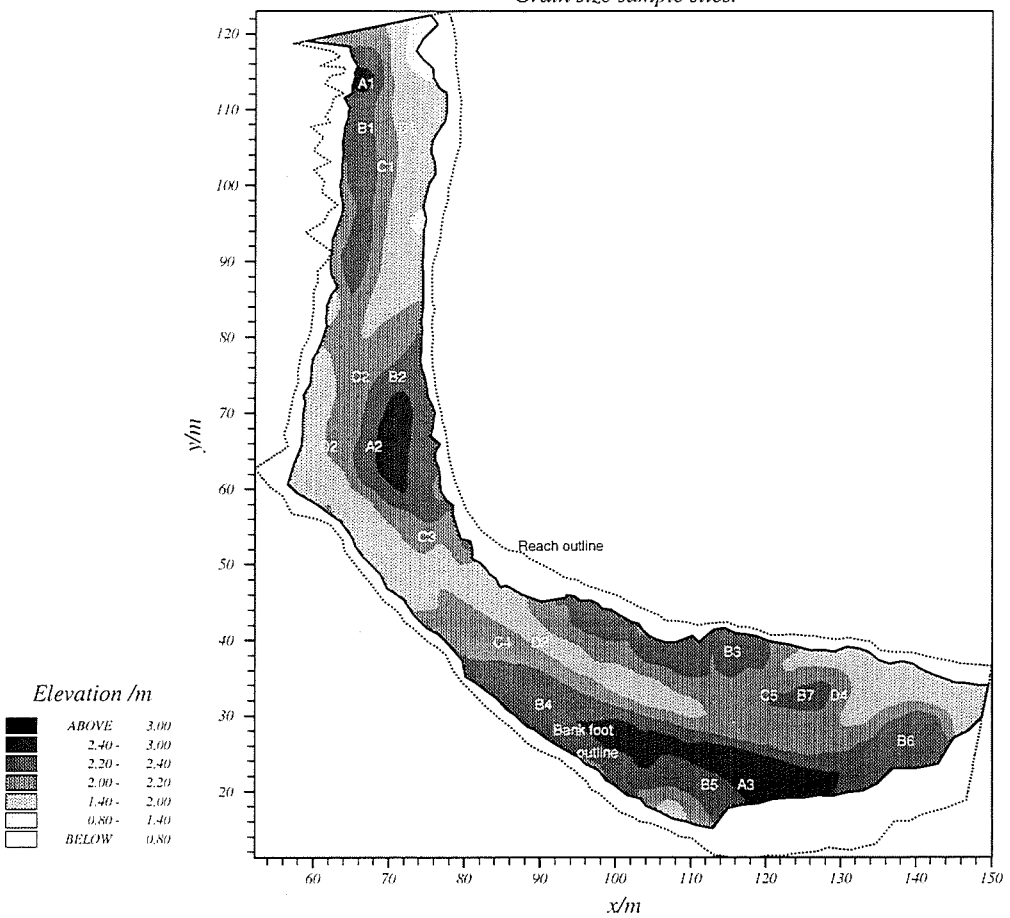

Figure 4.8. Reach B, July 1992.

Grain size sample sites.

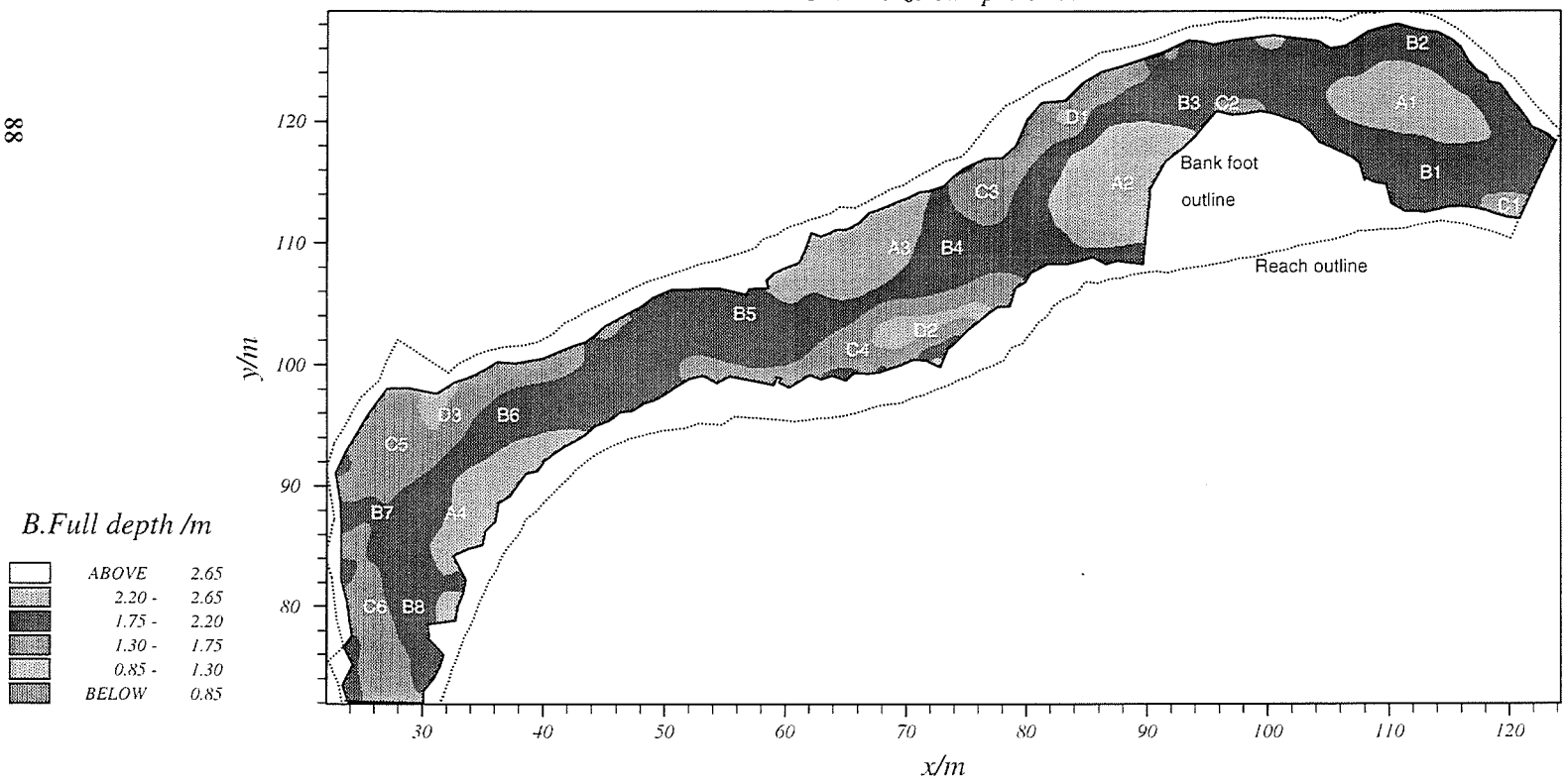

4.3.1.2 Sampling procedure

At reach A, adherence to the Church et al. (1987) criterion where the weight of the largest particle should not exceed 1 % of the sample was not possible; D_{MAX} of the order of 256 mm, indicates a suggested sample size in excess of 500 kg. Collection of 21 samples of this size was not feasible. At reach B, this criterion could be followed as D_{MAX} was invariably less than 90 mm corresponding to a sample mass of less than 100 kg. In addition to bulk sampling, corresponding surface count samples (Wolman 1954) were obtained.

The data of crucial importance in reach A are the grain size distributions between 16 and 180 mm which will be used to scale tracer distributions to bed material. D_{MAX} can therefore be assumed to pertain to the maximum tracer size class and associated geometric mean b axis length, in this case 152.2 mm. Reference to Figure 8b of Church et al. (1987) suggests that if the 5% D_{MAX} criterion is adhered to then a sample size of only 78 kg is necessary. At 2% the sample is 200 kg. For reach A a maximum of 100 kg was a manageable sample size. In exceptional cases, where very coarse particles occupy some zones, a larger sample was taken to ensure that D_{MAX} was within 5% leading to a maximum sample size of 175 kg.

Each store was grid sampled in a similar manner to that described by Wolcott and Church (1991). Facies were not regular within these stores, however, it is the amalgamated mean data which are important. Where definite facies boundaries existed in a store then sampling was altered accordingly. For example, fine sandy gravel sheets overlying coarser sediments were not sampled (e.g. sample $A_{\beta}2$). The surface bulk samples were taken to a depth of D_{MAX}, underlying material formed the subsurface sample.

The zones described herein are approximately similar to the stores defined in chapter 5. The grain size data are not directly comparable, but provide an assessment of within reach variability and the importance of elevation to grain size distributions.

4.3.2 Grain size distributions

Grain size data were collected from all the zones described in Figures 4.7 and 4.8. Deep pools zones E_{α} and D_{β} were not sampled since depth precluded access. A brief description of the relevant characteristics of each sample site is presented in appendix A together with cumulative grain size plots using data truncated at 0.25 mm. For the descriptive purposes of this chapter, summary data (truncated at 0.25 mm) will be commented upon (Table 4.9, reach A and 4.10, reach B).

Zone	Category	% D_{MAX}	D_{84}	Bulk data D_{50}	D_{16}	D_{50} Ratio	Sort Coeff.	Wol. D_{50}
A_α	*A_α1 Sf*	1.5	83.7	47.2	9.7	1.75	2.93	41.6
	A_α1 Sub	2.1	62.7	26.9	2.4		5.11	
	A_α2 Sf	2.6	89.2	56.2	26.3	1.30	1.84	51.7
	A_α2 Sub	1.7	82.8	43.0	13.1		2.51	
	A_α3 Sf	2.5	80.9	39.1	5.2	1.47	3.94	30.7
	A_α3 Sub	3.6	67.5	26.5	3.2		4.59	
B_α	*B_α1 Sf*	1.8	62.6	28.1	3.4	1.32	4.29	37.8
	B_α1 Sub	0.7	51.7	21.2	2.2		4.84	
	B_α2 Sf	2.2	100.2	56.0	19.4	1.32	2.27	46.0
	B_α2 Sub	4.5	81.2	42.4	10.6		2.76	
	B_α3 Sf	1.8	56.4	29.4	5.5	1.18	3.20	37.7
	B_α3 Sub	1.8	54.8	24.8	5.5		3.15	
	B_α4 Sf	4.4	88.2	50.9	24.4	1.31	1.90	49.8
	B_α4 Sub	3.2	78.0	38.7	17.7		2.09	
	B_α5 Sf	2.5	80.9	39.2	5.2	1.47	3.94	30.7
	B_α5 Sub	3.6	67.5	26.6	3.1		4.66	
	B_α6 Sf	1.9	97.9	53.4	19.5	1.93	2.24	47.2
	B_α6 Sub	1.6	56.2	27.6	5.5		3.19	
	B_α7 Sf	1.2	82.3	45.1	19.3	1.39	2.06	40.9
	B_α7 Sub	1.4	62.7	32.3	10.5		2.44	
C_α	*C_α1 Sf*	9.3	135.9	58.7	19.2	1.63	2.66	54.2
	C_α1 Sub	1.4	71.5	36.0	6.1		3.42	
	C_α2 Sf	5.3	125.2	70.6	24.6	2.17	2.25	57.7
	C_α2 Sub	1.8	72.4	32.4	6.1		3.44	
	C_α3 Sf	1.4	60.8	34.8	12.6	1.45	2.19	33.6
	C_α3 Sub	2.2	52.7	24.0	5.0		3.24	
	C_α4 Sf	1.5	106.6	59.4	29.0	1.80	1.91	57.1
	C_α4 Sub	1.7	66.7	32.9	10.5		2.52	
	C_α5 Sf	1.6	96.5	56.3	19.4	1.53	2.23	61.1
	C_α5 Sub	2.8	80.4	36.6	7.5		3.27	
D_α	*D_α1 Sf*	3.4	123.7	78.5	35.9	1.95	1.85	67.6
	D_α1 Sub	3.2	96.3	40.2	12		2.83	
	D_α2 Sf	3.5	119.3	85.2	42.2	1.98	1.68	72.8
	D_α2 Sub	2.4	73.4	43.0	12.7		2.40	
	D_α3 Sf	3.9	120.7	74.9	32.9	1.74	1.91	64.0
	D_α3 Sub	6.3	85.0	42.9	9.2		3.03	
	D_α4 Sf	3.3	121.8	71.1	28.6	2.24	2.06	62.8
	D_α4 Sub	2.2	62.5	31.7	7.0		2.98	

Table 4.9. Reach A summary grain size data. Sf - Surface samples, Sub - Subsurface samples, % D_{MAX} - % of total by mass occupied by D_{MAX}, D_{50} ratio - ratio of surface to subsurface D_{50}, sort. coeff - $(D_{84}/D_{16})^{½}$. Wol. D_{50} - D_{50} derived from surface pebble counts. All data calculated using bulk samples. Wolman data truncated at 8 mm. All grain sizes in mm.

Zone	Category	% D_{MAX}	D_{84}	Bulk data D_{50}	D_{16}	D_{50} Ratio	Sort. Coeff.	Wol. D_{50}
A_β	*A_β1 Sf*	0.5	34.7	21.2	7.6	1.17	2.13	25.6
	A_β1 Sub	0.9	31.1	18.0	1.7		4.27	
	A_β2 Sf	0.9	44.7	27.7	11.4	1.27	1.98	28.5
	A_β2 Sub	0.8	37.4	21.7	3.1		3.47	
	A_β3 Sf	0.7	41.8	27.4	12.7	1.37	1.81	33.7
	A_β3 Sub	0.9	37.9	20.0	3.3		3.38	
	A_β4 Sf	0.9	40.1	21.8	3.9	1.60	3.20	27.0
	A_β4 Sub	0.8	30.4	13.6	1.7		4.22	
B_β	*B_β1 Sf*	0.8	50.4	34.5	19.6	1.25	1.60	38.2
	B_β1 Sub	0.5	43.1	27.4	12.1		1.88	
	B_β2 Sf	0.2	34.3	19.7	7.2	1.21	2.18	22.1
	B_β2 Sub	0.3	29.4	16.2	2.6		3.36	
	B_β3 Sf	0.9	50.6	30.0	10.8	1.56	2.16	34.9
	B_β3 Sub	1.0	39.5	19.2	2.7		3.82	
	B_β4 Sf	0.5	39.3	24.0	9.0	1.10	2.08	26.2
	B_β4 Sub	0.9	38.0	21.8	4.5		2.90	
	B_β5 Sf	0.5	37.0	20.6	4.3	1.23	2.93	28.7
	B_β5 Sub	0.8	31.2	16.7	1.8		4.16	
	B_β6 Sf	0.8	43.1	21.9	4.7	1.27	3.02	31.2
	B_β6 Sub	0.7	34.6	17.2	2.4		3.79	
	B_β7 Sf	0.7	41.4	28.2	17.4	1.21	1.54	33.7
	B_β7 Sub	0.5	33.8	23.2	6.6		2.26	
	B_β8 Sf	0.8	26.7	13.2	2.1	0.98	3.56	23.0
	B_β8 Sub	0.5	26.2	13.4	2.1		3.53	
C_β	*C_β1 Sf*	0.5	53.7	37.6	25.0	1.18	1.46	39.4
	C_β1 Sub	0.7	43.9	31.7	21.3		1.43	
	C_β2 Sf	1.1	52.2	33.9	20.6	1.16	1.59	37.3
	C_β2 Sub	1.2	45.1	29.2	12.0		1.93	
	C_β3 Sf	0.9	49.4	28.2	8.6	1.54	2.39	38.1
	C_β3 Sub	0.7	37.5	18.3	3.6		3.22	
	C_β4 Sf	1.0	45.6	27.8	9.8	1.17	2.15	37.7
	C_β4 Sub	0.6	38.7	23.6	5.9		2.56	
	C_β5 Sf	0.4	51.3	29.9	8.9	1.80	2.40	37.4
	C_β5 Sub	0.4	38.3	16.6	2.2		4.17	
	C_β6 Sf	0.5	41.5	28.0	16.7	1.08	1.57	34.3
	C_β6 Sub	0.8	40.3	25.7	11.8		1.84	

Table 4.10. Reach B summary grain size data. Notation is the same as Table 4.9.

Surface D_{50} ranges from 28.1 mm to 85.2 mm at A and from 13.2 to 37.6 mm at B. In addition, sorting is slightly better at B due to the narrower range of grain sizes available for transfer, illustrating the effect of selective transfer dominated downstream sorting upon local grain size distributions. In general, the degree of bed armouring at A, while not particularly great, tends to exceed that of reach B. A better defined coarse surface layer at A suggests increased bed stability. However, this is offset by the greater shear stress and frequent mobilisation of material from this layer. Wolman samples derived from reaches A and B support the general grain size trends identified from the bulk samples.

4.3.3 The role of elevation upon grain size distributions

One notable trend in the bulk data at both sites is the decrease in D_{50} as elevation increases. In addition, sorting improves and armouring increases as elevation declines (Table 4.11). These trends are less pronounced at reach B, due to the narrow range of grain sizes. The importance of elevation at reach A is a direct indication of the influence of depth of flow and frequency of

Reach A				**Reach B**			
Zone	**Mean D_{50}**	**Mean D_{50} r**	**Mean sorting**	**Zone**	**Mean D_{50}**	**Mean D_{50} r**	**Mean sorting**
AαSf	47.5	1.5	2.90	*AβSf*	24.5	1.4	2.28
AαSub	32.2		4.07	*AβSub*	18.3		3.83
BαSf	43.2	1.4	2.84	*BβSf*	24.0	1.2	2.38
BαSub	30.5		3.30	*BβSub*	19.4		3.21
CαSf	56.0	1.7	2.24	*CβSf*	30.9	1.3	1.92
CαSub	32.4		3.17	*CβSub*	24.2		2.52
DαSf	77.4	2.0	1.87				
DαSub	39.4		2.81				

Table 4.11. Reach A and B, summary grain size data. Mean data calculated for each elevation zone. Mean D_{50} r - mean D_{50} ratio, all other symbols are the same as Table 4.9.

inundation upon grain size distributions and transfer (e.g. Williams and Rust 1969, Laronne and Duncan 1992, Lekach et al. 1992). Poor sorting at high elevations reflect bar formation mechanisms. Sediment is deposited at flood stages with subsequent events sufficient to rework and sort the material being relatively infrequent compared with submerged channel zones. The pool sites are better sorted where bed material reflects the higher competence and associated entrainment probabilities for finer particles.

The importance of elevation can be illustrated using normalised data which permits visual comparison within and between sites (Figure 4.9, 4.10). Surface and subsurface data were divided by overall surface and subsurface D_{50} of the reach (see Chapter 3). The D_{50} ratio is not normalised

since this is already a dimensionless variable. At reach A, pronounced differences are apparent for zones C_α and D_α. Bar zones A_α and B_α are more consistent, indicative of the lack of sorting of bar deposits at high elevations. A similar pattern is apparent in reach B, although trends are less pronounced since only three elevational zones were used.

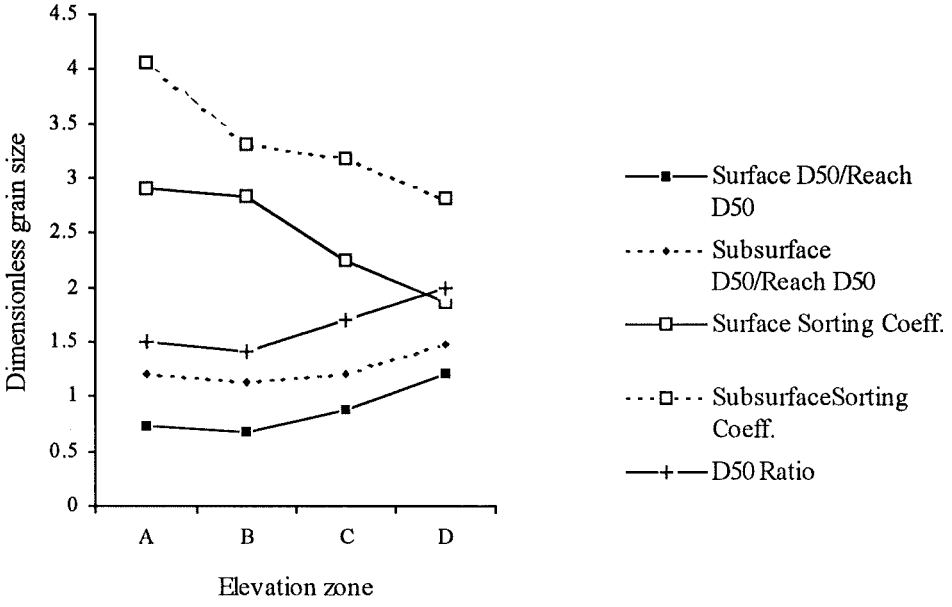

Figure 4.9. Reach A, dimensionless grain size data as a function of elevation. Surface based data was normalised using the reach mean D_{50} of 66.4 mm with subsurface using D_{50} of 26.7 mm.

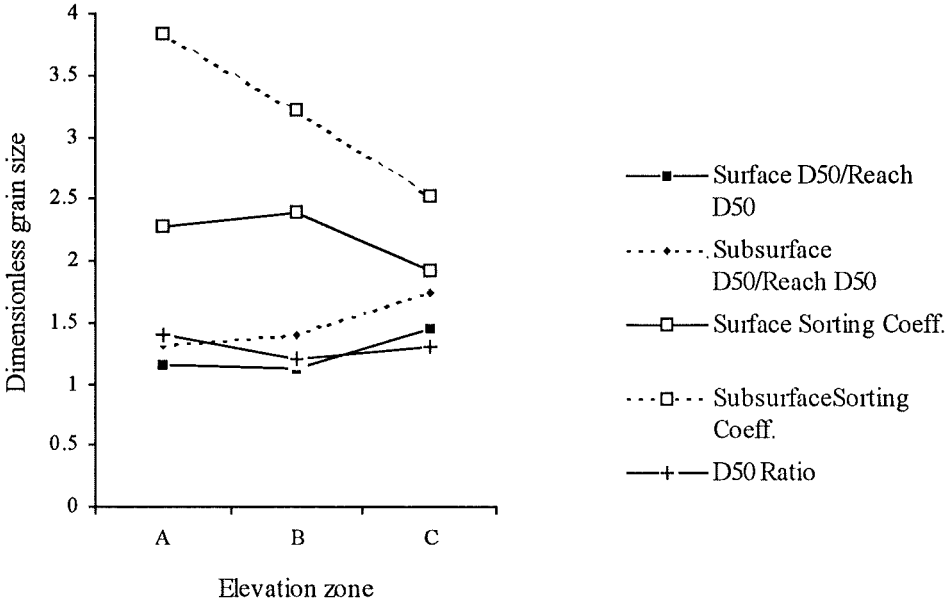

Figure 4.10. Reach B, dimensionless grain size data as function of elevation. Normalisation used reach mean surface D_{50} of 21.3 mm and subsurface D_{50} of 13.9 mm.

There are exceptions, in reach A, C3, B3 and B5 are unusually fine low elevation facies which probably evolved due to flow separation processes. This suggests that elevation is not the only governing factor upon grain size, other important processes include secondary circulation, bar migration and local water surface slope (Markham and Thorne 1992).

The trends in grain size according to elevation at A and B suggest that within the channel, submergence is important. Zones A and B at both sites generally refer to emergent bar zones. C onwards refers to permanently submerged channel zones where the role of elevation becomes most pronounced. Pool and thalweg facies are more armoured and better sorted compared with less active storage zones. These trends tend to be much less pronounced for the subsurface possibly suggesting that sediment sorting processes induced by elevation are confined to a layer a few grains thick.

Linear regression can be used to quantify the effect of elevation upon grain size. Mean storage elevation was calculated per store and regressed against various grain size indices (Table 4.12). The significance of these relationships is greater at reach A than reach B, demonstrating the effect

Reach A				
Y (Dependant variable)	**Gradient**	**Intercept**	**r^2**	**p**
D_{50} ratio	-0.81	3.40	0.40	0.006*
Surface D_{50}	-49.8	164	0.62	0.000*
Surface Sorting coefficient	+1.5	-0.83	0.26	0.036*
Subsurface D_{50}	-12.1	60.1	0.19	0.078
Subsurface Sorting coefficient	+1.42	0.15	0.17	0.096
Reach B				
D_{50} ratio	-0.016	1.32	0.001	0.928
Surface D_{50}	-8.91	43.4	0.20	0.057
Surface Sorting coefficient	+0.51	1.23	0.06	0.306
Subsurface D_{50}	-7.38	34.8	0.18	0.072
Subsurface Sorting coefficient	+1.56	0.15	0.27	0.028*

Table 4.12. Regression analysis of grain size data against elevation, summary statistics. Asterix is indicative of a significant relationship at $p < 0.05$.

of the narrow distribution of grain sizes. In reach A, the surface D_{50} is more strongly related to elevation than the subsurface. Armouring at reach A is much better correlated with elevation than at B. The lower range of elevations and smaller slope and grain sizes at reach B suggest that the processes governing sediment sorting at the reach scale contrast with those at reach A. This characteristic will be examined in chapter 6.

The preceding discussion demonstrates that elevation can be used as a method of categorisation where a wide range of grain sizes are present. The grain size distribution of the stores which were

not sampled (E_α and D_β) can be reconstructed using the derived relationships. This method will be particularly applicable to deep areas such as E_α where elevational effects tend to dominate. The trends thus far presented suggest that the deepest pools contain the coarsest facies. This is consistent with observations of coarse pool bed surfaces made by a number of authors (e.g. Keller and Florsheim 1993) representing areas of maximum competence. The conversion will be more accurate for reach A since the relationship between elevation and grain size is better developed. In order to improve the definition of the relationships, data from zone A_α will be removed since elevational effects between these zones and B_α tend to be constant. The conversion of grain size is presented fully in appendix A.

4.4 Hydrological monitoring

A detailed record of flow during the study period was necessary to relate bedload transfer and morphological change to hydraulics on a consistent temporal scale. Increasing transfer rates have been documented with rising shear stress in both field and flume experiments (Wilcock 1992b, Kuhnle 1992, 1993) and intense bedload transfer is associated with a greater probability of morphological change (Ashmore and Goff 1994). However, Laronne and Duncan (1992) noted bar reworking during relatively small events. Such an apparent anomaly will be examined with reference to flow data during the course of this study.

4.4.1 Stream flow data collection

A gauging station was located close to or within the confines of each reach. Reach A will be correlated with data from gauging station Q3, located downstream of the main bend (see Figure 3.6). The record relevant to reach B was derived from station Q5 (Plate 4.11) situated 10 m downstream of the final cross section.

Stage at each site was measured using a pressure transducer system housed in a gauging station (Plate 4.12). The transducer (Druck model PCDR 830), contained in a stilling well, measured water pressure. The apparatus was powered by a single 12V dry cell battery with output converted to a constant 10V by a regulator. The pressure range of the transducer was 175 mbar (c.1780 mm H_2O) with an output voltage of 0 - 20 mV. This mV data was recorded every 15 minutes and stored within a logger (Grant model MQW8) with a total storage capacity of 8K. The data were stored as 250 incremental units of 0.08 mV (20 mV/250 units = 0.08), each unit corresponding with a water depth of 0.7 mm. The stored data were downloaded in the field every 3 weeks using a Toshiba T1000SE portable computer and Grant software.

Stage - mV rating relationships for each site were:

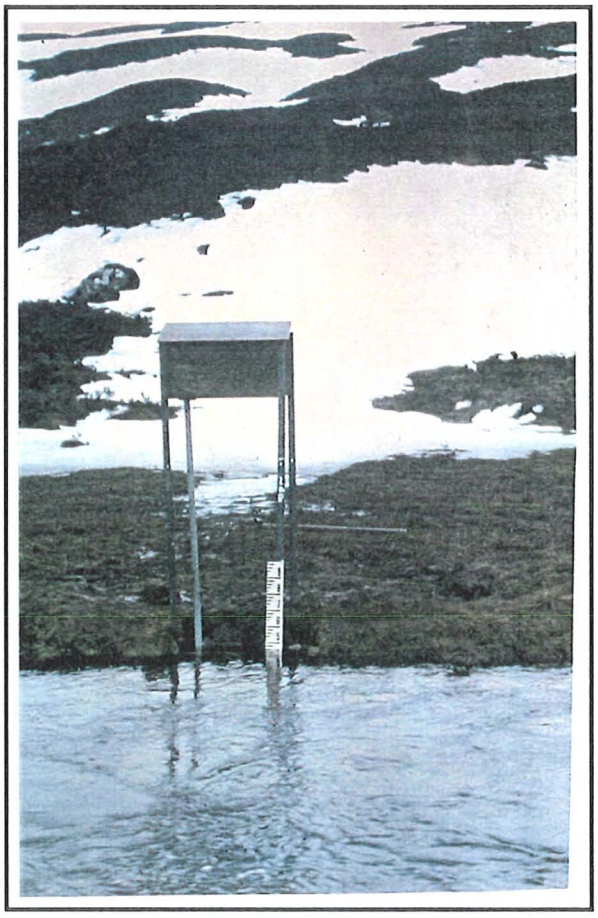

Plate 4.11. Gauging station Q5 located 20 m downstream of reach B.

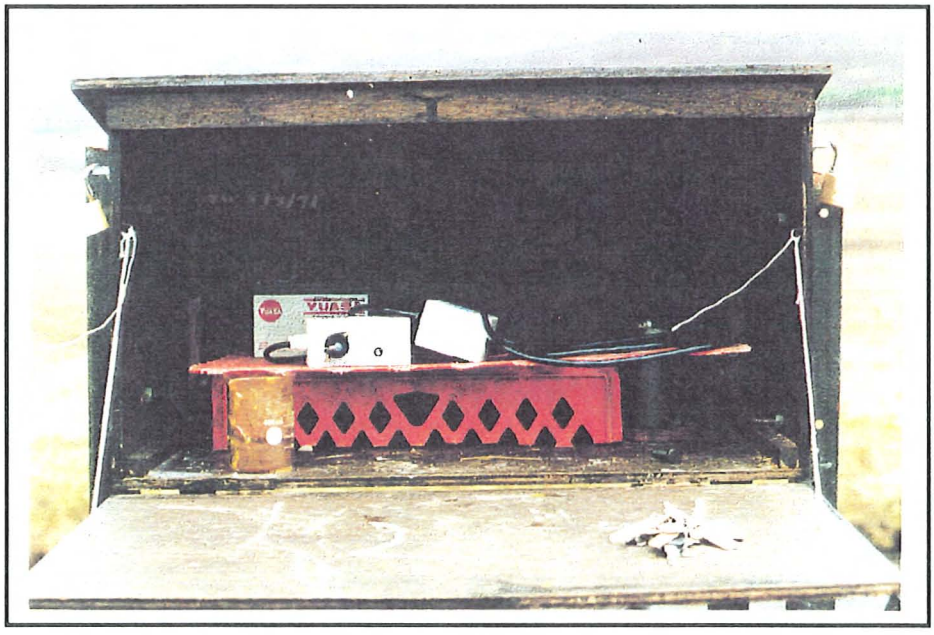

Plate 4.12. Stage recording equipment housed at Q5. Logger, 12V battery and voltage regulator are visible.

Q3	Stage = (-1.61 + 7.2*mV)/100	$r^2 = 99.2\%$ $p < 0.01$	(4.4)
Q5	Stage = (-3.58 + 7.2*mV)/100	$r^2 = 99.5\%$ $p < 0.01$	(4.5)

Stage discharge ratings were also developed. Initial discharge measurements were made using dilution gauging (e.g. Elder et al. 1990) which proved difficult to administer due to inadequate mixing lengths and channel bifurcation. A programme of current metering was therefore undertaken as a replacement. However, the derived rating curves were poorly defined due to two factors: (1), inadequate measurement of high flows, usually for safety reasons; (2) morphological change altered the cross section at or immediately upstream of the gauging stations. All flow data will therefore be based upon stage rather than discharge measurements. An accurate estimate of stage at a point provides a surrogate which can be meaningfully related to shear stress.

4.4.2 Flow record during the study period

A record of stage was built up at Q3 and Q5 from June 1991 until the present day. The data used for this study extends from June 19th 1991 until August 11th 1993, a total of 72000 measurements at each site. The complete stage hydrographs for Q3 are presented in Appendix B, B1 to B6 and for Q5 in B7 to B12. Also illustrated is the threshold stage above which bedload transfer takes place. This will be addressed in more detail in section 4.4.3.

The original mV data for Q3 and Q5 were incomplete. In some cases the 12V cells declined to an output voltage less than 10, insufficient to power the transducer. This problem usually occurred during periods of extreme cold. Where possible, the record has been "repaired" using data from an upstream station, Q1 (Figure 3.1) corrected to Q3 and Q5 mV values. At both stations, there are no data available from 19/2/93 to 18/3/93 and 18/6/93 to 25/7/93. No floods took place during these times so this is not an important loss. In addition, there is an error in the Q5 record between 10/3/92 and 12/3/92, again, no floods were missed. The two records at Q3 and Q5 include all the significant floods which occurred during the study and represent accurate estimates of stage.

Considerable disparity between the Q3 and Q5 record only occurred for January 1993 and was caused by 3 possible effects: (1) ice in the stilling wells may have created a greater pressure (hence apparent depth) than water alone; (2) saturated snow levees increase the bank height and therefore facilitate a greater depth of flow; (3) snow and ice in the channel decreased the channel capacity increasing depth at the recording site. The disparity between the records does suggest that the aforementioned factors tended to act on a localised scale inducing inaccurate measurements. In order to rectify this, data from Q1 (which was not excessively snowbound) was used to reconstruct the records at Q3 and Q5 (Appendix B13 and B14). The actual stage is assumed to be the median

between the extremes presented by the recorded and corrected data and flow duration is calculated on this basis.

4.4.3 Threshold for bedload transfer

Calculation of the time and magnitude above a threshold bedload stage is instructive, allowing temporal explanation of morphological changes and sediment fluxes. A single threshold will be defined. The threshold term used here is based upon the definitions of Bull (1980) and McKercher (1980) where it is the point after which a response would be possible. It represents a consistent basis for defining duration, above which, entrainment is progressive (Newson 1992). Factors such as bed configuration (Church 1978), particle exposure (Fenton and Abbot 1977) and friction angle (Komar and Li 1986, Kirchner et al. 1990) cause entrainment at variable excess shear stresses. Fractional bedload transfer is not possible below the threshold; above it bedload transfer is not assumed to be linearly related to excess shear stress.

Wathen et al. (in prep) observed that bedload transfer did not occur at a site 100 m downstream of reach B at stages below 0.495 m at Q5 (Figure 4.11). This stage value represents a threshold

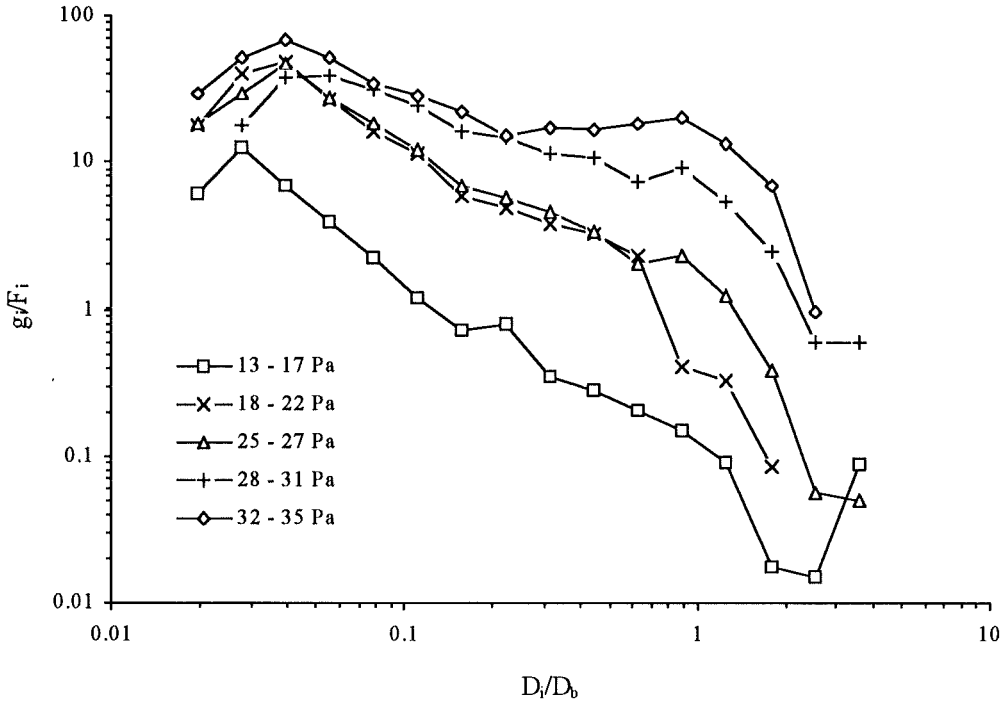

Figure 4.11. Ratio of fractional transfer rate g_i, to fraction in bed surface, F_i, against relative grain size. Data derived from Allt Dubhaig bedload traps, September 1991 to April 1993 and is truncated at 0.25 mm. Minimum shear stress for transfer was 9.53 Nm^{-2}, stage at Q5 = 0.49 m.

which can be used for reach B. Local variation in transfer will occur within pools and riffles as stage rises (e.g. Hassan 1990), however, such variations were not recorded by the traps and are therefore only likely once the threshold is exceeded.

The threshold derived from Q5 was converted to a Q3 stage (0.3605 m) using a rating between Q3 and Q5. This figure is less since the Q3 stage board is set above bed level and the site has a wider cross section than Q5. The threshold is roughly consistent with samples taken by Ashworth (1987) where transfer was reported at discharges > 2.9 m^3s^{-1}, approximately 35 cm at Q3. The increased slope at A compared with B may be cancelled out by the higher grain size; thus, relating a downstream threshold to an upstream site is valid.

The concept of a bedload threshold can be further refined with reference to the transferred grain sizes. Figure 4.11 demonstrates how transfer progresses from marginal (Andrews and Smith 1992) through size selectivity and finally towards equal mobility at the highest flows (Wathen et al. in prep). The threshold thus far used is for all grain sizes although it is unlikely that gravel would be entrained until higher stages. In subsequent chapters, the threshold will be broken down to account for different size fractions.

4.4.4 Duration over the bedload threshold

The stage data presented in Appendix B were edited such that only recordings above the bedload threshold were retained. The data were then used to examine the magnitude, duration and distribution of stages capable of bedload transfer during the study. The record was divided up for corresponding survey and tracer searches. In some cases the timing was not coincident, therefore separate curves are presented. In these situations, the survey and tracer search data are hydraulically incomparable; presentation of the curves allowing assessment of the extent of this (Figures 4.12 and 4.13). The axes are not displayed at the same scale to allow the details of stage distributions at each interval to be fully illustrated. Summary data are presented in Table 4.13.

The steep duration curves indicate that the Allt Dubhaig is extremely flashy with a rapid response to rainfall. The overall record based upon 26 months of data suggests that stage levels are sufficient to transfer bedload approximately 6% of the time. The exact figures differ for Q3 and Q5. This apparent inconsistency is a result of ponding and overbank flow at Q5 (lower slope) maintaining higher stage than Q3, and less importantly, use of Q1 for some corrections (flow conditions at Q1 tend to differ from Q5 and to a lesser extent with Q3).

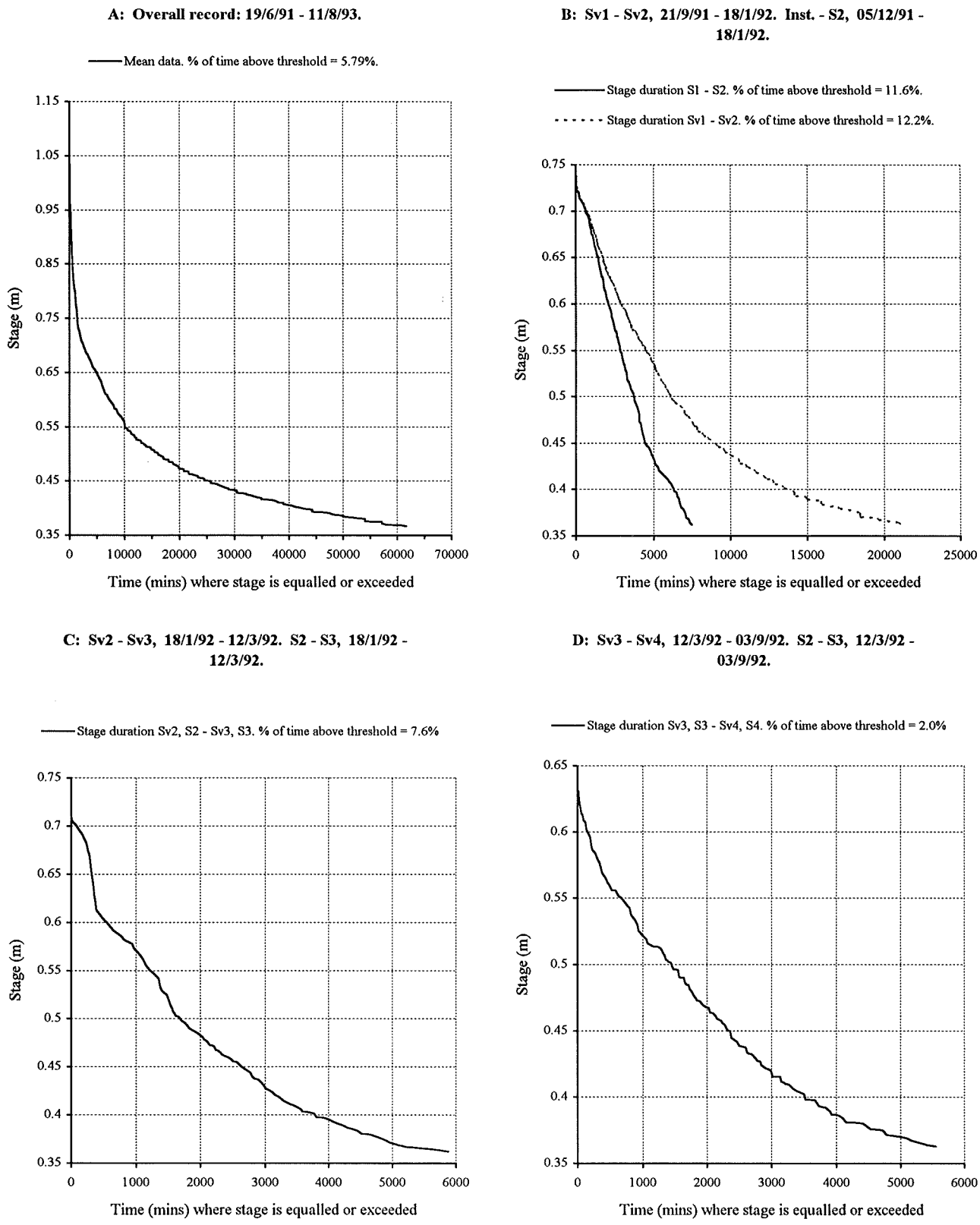

Figure 4.12a - d. Reach A duration above the bedload threshold curves. Overall record, surveys 1 - 4 (Sv1 - Sv4), searches 1 - 4 (Inst. - S4)

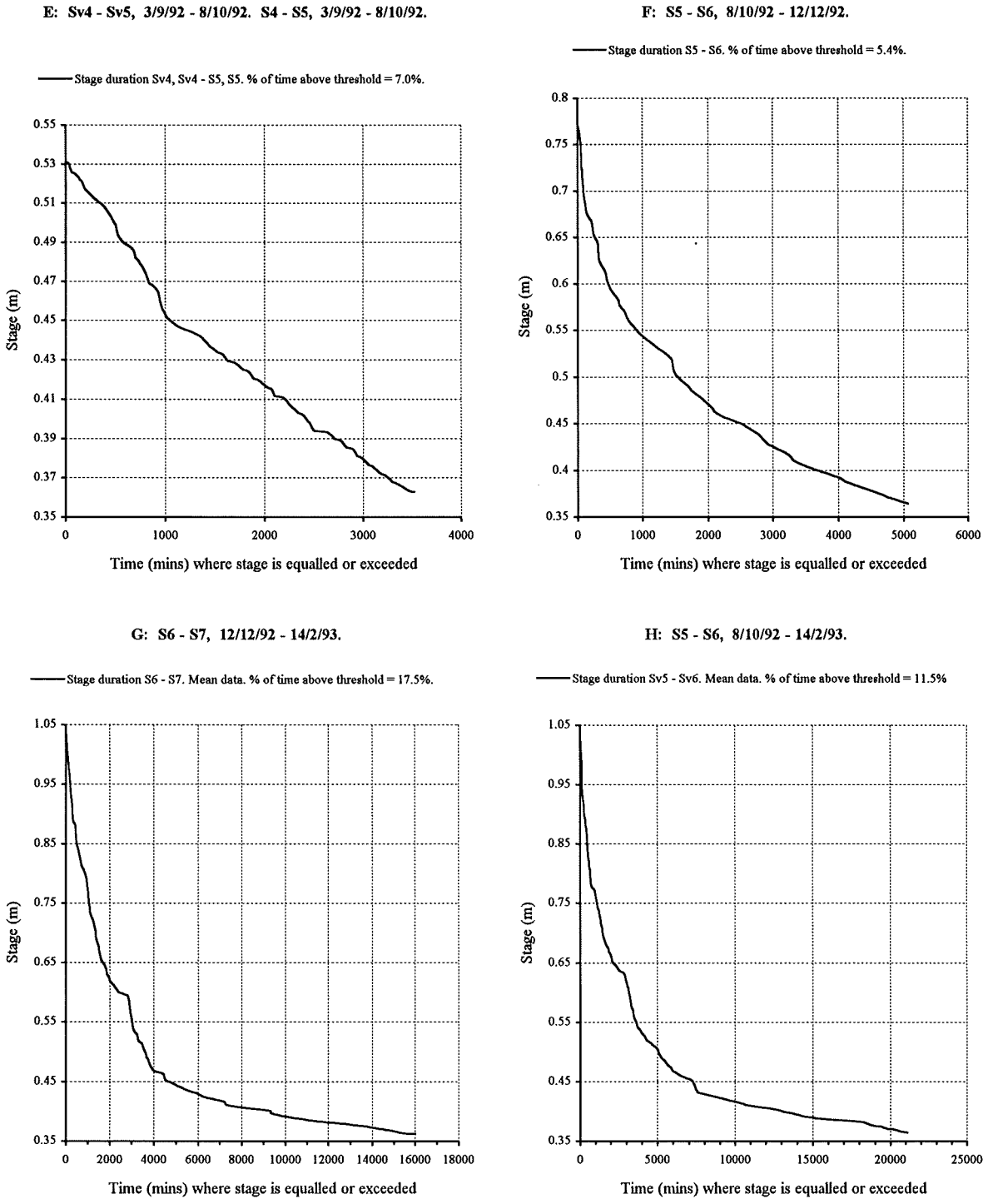

Figure 4.12e - h. Reach A duration above the bedload threshold curves. Surveys 4 - 6 (Sv4 - Sv6), searches 4 - 7 (S4 - S7).

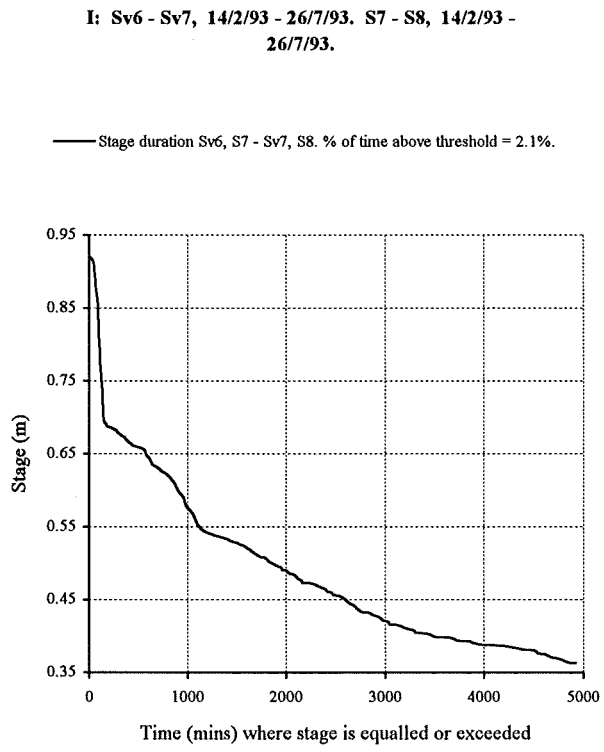

Figure 4.12i. Reach A duration above the bedload threshold curves. Surveys 6 - 7 (Sv6 - Sv7), searches 7 - 8 (S7 - S8).

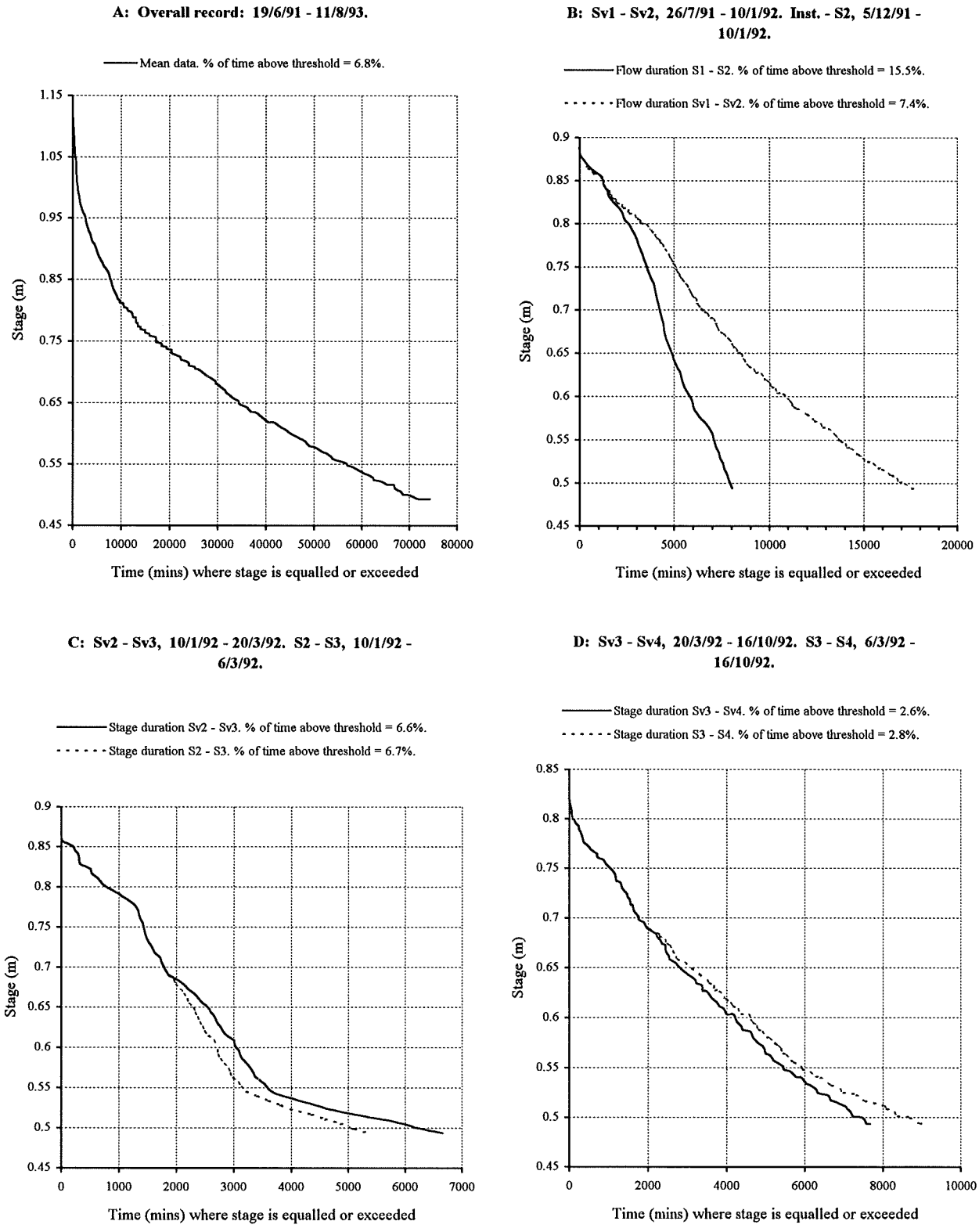

Figure 4.13a - d. Reach B duration above the bedload threshold curves. Overall record, surveys 1 - 4 (Sv1 - Sv4), searches 1 - 4 (Inst. - S4)

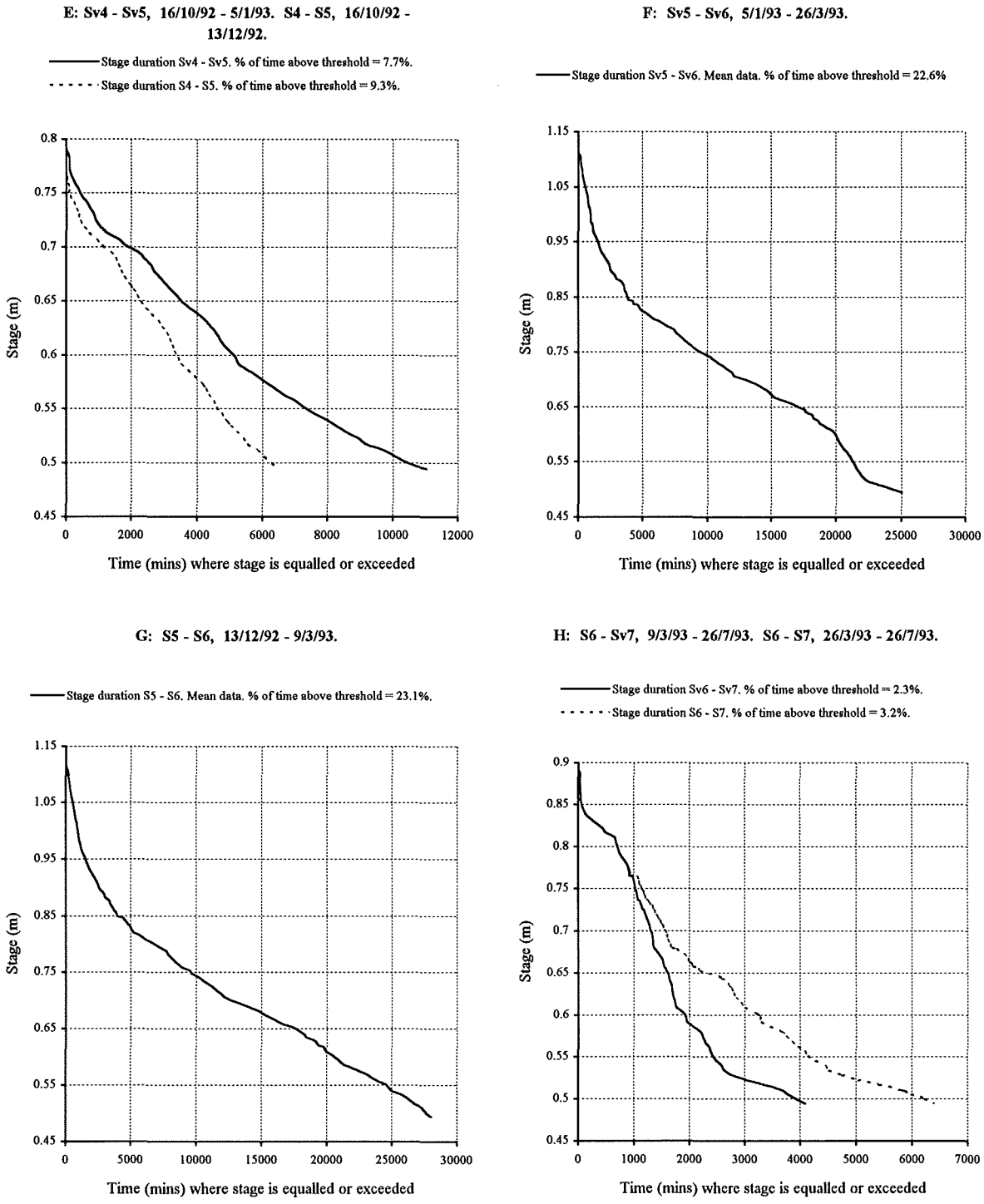

Figure 4.13e - h. Reach B duration above the bedload threshold curves. Surveys 4 - 7 (Sv1 - Sv4), searches 4 - 7 (S4 - S7).

The duration of stage above a threshold at reach A is fairly consistent for successive intervals. The most notable exceptions to this are surveys 3 - 4 and 4 - 5 where the magnitude of stage was much lower (see Table 4.13, 20% values). These lower stages will allow comparison of the magnitude of morphological activity according to stage.

Reach A	*Time above threshold (minutes)*	*% of total*	*Peak stage /m*	*Stage (m)* *20%*	*40%*	*60%*	*80%*
Overall (Mn)	62010	5.8	1.03	0.54	0.45	0.41	0.37
Sv1 - Sv2	21000	12.0	0.74	0.57	0.46	0.43	0.37
Inst. - S2	7400	11.5	0.74	0.70	0.54	0.47	0.42
Sv2 - Sv3, S2 - S3	5900	7.60	0.71	0.57	0.47	0.42	0.38
Sv3 - Sv4, S3 - S4	5550	2.0	0.63	0.53	0.45	0.42	0.38
Sv4 - Sv5, S4 - S5	3550	7.0	0.53	0.49	0.44	0.41	0.39
S5 - S6	5060	5.4	0.79	0.53	0.47	0.43	0.38
S6 - S7	12900	14.0	1.19	0.70	0.43	0.41	0.39
S6 - S7 (Mn)	16040	18.5	1.03	0.60	0.43	0.41	0.39
Sv5 - Sv6	17990	9.7	1.19	0.65	0.44	0.43	0.39
Sv5 - Sv6 (Mn)	21110	11.5	1.03	0.57	0.45	0.43	0.39
Sv6 - Sv7, S7 - S8	4900	2.1	0.92	0.59	0.51	0.43	0.39
Reach B							
Overall (Mn)	74250	6.8	1.12	0.79	0.68	0.61	0.52
Sv1 - Sv2	17900	7.4	0.87	0.80	0.68	0.60	0.54
Inst - S2	8000	15.5	0.87	0.83	0.76	0.65	0.58
Sv2 - Sv3	6700	6.6	0.87	0.83	0.67	0.54	0.52
S2 - S3	5200	6.7	0.87	0.79	0.68	0.54	0.53
Sv3 - Sv4	7700	2.8	0.82	0.73	0.64	0.57	0.53
S3 - S4	9000	2.6	0.82	0.69	0.64	0.57	0.53
Sv4 - Sv5	11050	7.7	0.78	0.70	0.63	0.57	0.53
S4 - S5	6300	9.3	0.78	0.70	0.64	0.58	0.53
Sv5 - Sv6 (Mn)	25520	22.5	1.12	0.81	0.72	0.67	0.6
S5 - S6 (Mn)	28050	22.7	1.12	0.82	0.74	0.65	0.58
Sv6 - Sv7	4080	2.3	0.88	0.81	0.68	0.53	0.52
S6 - S7	6300	3.2	0.88	0.75	0.62	0.58	0.52

Table 4.13. Duration above bedload threshold, summary data. Inst. - tracer installation, Sv - Cross section survey, S - tracer search, Mn - Mean of the data corrected due to snow. % of total column is the proportion of the time stage exceeds the threshold. Stage percentage values refer to the stage above the threshold which is equalled or exceeded for a particular % of the time.

Section 4.4.2 demonstrated the importance of snow at Q3 and Q5 and the need for correction. The disparity between corrected and uncorrected data from January 1993 was much greater at Q5 than at Q3. However, snow and ice did increase shear stresses above normal flood levels at both sites and must be accounted for. A mean of the corrected and uncorrected duration curves was used to represent the period when snow dominated (curves A, G, H at reach A and A, F, G at reach B). Extrapolation was used where the two extremes did not represent the same time period.

The pronounced stage peak in May 1993 represents the largest flood on record. The event took place on 17/5/93 and was caused by cyclonic rainfall. The flood was extremely flashy and will allow evaluation of the relative influences of duration and stage upon reach activity (section 7.2.1).

With the exception of surveys 1 - 2 and search 1 - 2 (Figure 4.13), the non coincidence of cross section and tracer searches in reach B seems to have made only minor differences to the duration curves. This is encouraging allowing almost direct comparison between the relevant data. Most of the data collection at reach B corresponded to similar conditions of peak stage, only the duration of the minor flows varied. The only exception to this is survey 4 - 5 and search 4 - 5. Cumulative duration statistics are illustrated in Table 4.14. D_A data is used in chapter 5 where storage characteristics are expressed relative to absolute time in storage, D_C data is used in chapters 6 and 7 where volumetric fluxes are compared with tracer data.

Reach A					**Reach B**				
Survey	**D**	**Search**	**D_A**	**D_C**	**Survey**	**D**	**Search**	**D_A**	**D_C**
1	0	**Inst.**	0	13600	**1**	0	**Inst.**	0	9900
2	21000	**2**	7400	21000	**2**	17900	**2**	8000	17900
3	26900	**3**	13100	26900	**3**	24400	**3**	13200	23100
4	32450	**4**	19150	32450	**4**	32100	**4**	23700	32100
5	36000	**5**	22700	36000	**5**	43150	**5**	30000	38400
6	57110	**6**	27760	41060	**6**	68670	**6**	58050	66450
		7	43450	57110	7	72750	7	64350	72750
7	62010	**8**	48350	62010					

Table 4.14. Cumulative duration above bedload threshold (minutes). D - cumulative duration after each survey, D_A - cumulative duration relative to installation (Inst.) of tracers, D_C - cumulative duration relative to the start of the study.

5. The reach scale sediment budget: A quantitative framework

Basin scale sediment budget studies, both conceptual and empirical, usually disregard or oversimplify the complex internal interactions within the alluvial channel (Lekach et al. 1992). This chapter presents a framework within which sediment redistribution in the channel can be analysed in quantitative terms. Implicit to this objective is determination of sediment stores and derivation of transit time distribution functions describing the transfer of sediment between these stores.

5.1 Sediment storage type definition

Stores defined in basin scale studies are usually macro scale features with clearly recognisable boundaries. Church and Jones (1982) defined megaforms as channel reaches, on this basis, an example of a macro scale feature would be the whole channel store (including floodplain). Dietrich and Dunne (1978) defined channel, soil and lithology stores with transfer processes including weathering, soil creep and bedload transfer. At a more detailed scale, the alluvial store has been sub-divided according to activity (e.g. Nakamura 1986, Kelsey et al. 1987) with the active channel representing the most active store. Subdivision of the active channel store (as defined by reach boundaries) is the immediate aim of the present section. Field based classification of this type has not been attempted before although Lisle and Madej (1992) and Collins (map of Wildcat Creek presented in Buffington et al. 1992, Figure 2) have defined and analysed different facies representing different levels of activity. Hoey and Sutherland (1991) categorised storage within an active laboratory channel on the basis of direct observation of the intensity of bedload transfer which is not directly repeatable in the field situation.

5.1.1 Criteria for storage definition

It is usual to define alluvial storage in terms of relative sediment mobility; most variables used to do this are proportional to dimensionless shear stress (Eq. 2.2). A store is hereafter defined *as a volume or area of sediment bordered by numerically defined boundaries representing a specific range of potential transfer conditions.* A brief evaluation of the variables which may be used to categorise storage is made below.

a. Elevation: Bed elevation is, in general, inversely correlated with activity (Williams and Rust 1969, Hoey 1989). For example, material stored on high elevation bars is less likely to move than material on lower elevation features (Laronne and Duncan 1992, Lekach et al. 1992).

b. Grain size. Usage of grain size to define storage assumes that facies with similar size distributions are the result of comparable hydraulic processes. However, spatial lag in the transfer process often ensures that facies are representative of upstream rather than point conditions. Field determination of sedimentary units usually involves facies mapping (e.g. Lisle and Madej 1992). However, this method is subjective and time consuming and works best where a small number of discrete facies can be identified.

c. Water surface slope. The variation in water surface slope at high stage provides a useful representation of potential activity. However, the dynamic changes in water slope during and between floods often prevents accurate data collection.

An initial aim of this project was comprehensive categorisation of storage utilising a combination of all the criteria mentioned above. However, if each criterion had, for example, 5 sub classes then an unmanageable number of storage types (5*5*5 = 125) would be defined. In practice, many of these types would be duplicated by others with similar conditions; what is required is a means of producing a classification which produces broader classes.

The variables available to this study for defining storage are either surrogates of activity (b) or more direct measures of shear stress (a,c), combination of all three would be proportional to dimensionless shear stress, τ^*. Insufficient data are available to derive the latter, however, a and c may be combined (by multiplication) as an index proportional to shear stress, which can be used to define sediment storage. Whilst not as accurate as an index of τ^*, grain size effects are included since there is correlation between elevation and grain size in each reach, although less so in reach B. Elevation is readily converted to bankfull depth using cross section survey information. No water surface slope information is available, so bed slope (derived from cross section data) will be used assuming that relative energy gradients at the bed are the same as at the water surface (Richards 1982). Use of this shear stress index (SSI) ensures that storage is defined according to potential for bedload transfer.

5.1.2 Data selection and processing

Elevation was calculated from cross section points converted (relative to a sloping datum, section 4.2.1.1) to xyz co-ordinates. This data was then transferred into UNIMAP 2000, a contouring and data analysis package, input as an irregular grid fashioned by the location of the original cross section points. Bilinear interpolation was used to calculate elevation at nodes on a regular user defined grid. Selection of the interpolation grid size was crucial to the accuracy of the resultant elevation dataset. Reach detail was balanced against demands upon computing resources. An interval of 1 m (101 * 112 grid at A and 102 * 57 at B) was selected for both reaches, no

advantages were offered by a more detailed grid and accuracy is reduced for coarser grids (> 1 m). This resolution compares favourably with the lateral and downstream data interval of 1 m necessary to accurately determine volumetric change (Lane et al. 1994).

The interpolated data were transformed to bankfull depth by subtracting the elevation from 2.74 m at reach A and 2.7 m at B, this figure pertaining to the maximum bank elevation. Local bed slope was computed in two orthogonal directions, perpendicular and parallel to flow. Slope normal to flow was calculated between adjacent cross section points on the assumption that the section was perpendicular to flow at bankfull stage (see Figure 4.4). Slope parallel to flow was calculated at a particular point, $x_iy_iz_i$, on a cross section. The nearest corresponding point $x_jy_jz_j$ on the cross section immediately downstream was identified. A line was then constructed between these two points and the mid point x_ky_k determined. The slope between points i and j was calculated and assigned to point k. The resultant data was in xyz' form, z' representing local bed slope ($z' = dz/dx$). All cross sections were assumed to be normal to flow, and the line joining the nearest points on adjacent cross sections was assumed to be parallel to flow.

The distribution of slope perpendicular to flow interpolated on a 1 m grid illustrates cut bars and steep pool faces (Appendix C, C1 - C13). Both reaches are dominated by a low cross channel gradient with steep lateral bar faces usually less than 1 m wide. These are small areas, so perpendicular slope is not used to categorise storage, but it does provide a partial explanation of storage dynamics.

5.1.3 Storage definition methodology

Changes in bankfull depth per survey are illustrated in Appendix C (C14 - C26). An irregular interval is used to unambiguously define morphological features. The changes in the distribution of depths illustrates the morphological changes discussed in sections 3.3.4 and 3.4.4. Half surveys (section 4.2.3) have a negligible effect upon the accuracy of the estimation of reach depths.

Slope parallel to flow is highly irregular in both reaches. Three annotated plots illustrating the distribution of parallel bed slope are presented in Appendix C, C27 and C28 for reach A and C29 for reach B. Slope alternates between positive and negative values, particularly upon bar tops, as a consequence of two factors. Firstly, detailed bar surface topography is uneven (e.g. Laronne and Carson 1976) due to irregular entrainment and deposition, particularly of small clusters of material (e.g. Brayshaw et. al 1983). Secondly, slope data are accurate to within ± 0.066 m at A and ± 0.021 m at B (i.e. surface D_{50}). Despite the irregularity, major morphological features can be identified from slope data providing a reasonable representation of potential activity at the local scale.

The SSI was calculated as the product of slope and depth at each node on a 1 m grid. Preliminary plots of this outlined a number of irregularly defined areas, which did not always represent observed reach morphology. The data needed adjusting to reduce the variability in defined stores resulting from the presence of negative bed slope values. Multiplication of bankfull depth by a negative slope resulted in a negative SSI, unrepresentative of the relative activity between the stores. The dominant effect of depth was converted to a negative value due to the bed slope. For example, in most cases, a pool face and tail are not equally active but, by virtue of depth the tail maintains an important influence upon transfer. This was not accounted for with negative slopes.

The storage categorisation method is based upon a relative scale, distinguishing stores according to relative activity through the use of a shear stress index. SSI at point j can be conceptualised as

$$SSI_j = f(h_j . s) \tag{5.1}$$

$$SSI_j = f(h_j . (s_r + s_{jl} + s_c)) \tag{5.2}$$

where h_j is bankfull depth at point j and s is slope made up of three components, s_r, reach slope, s_{jl}, local slope at point j and s_c, a slope correction factor. The correction factor removes the negative slopes as its magnitude was determined such that the maximum negative slope, usually at a bank, becomes zero. The correction factors are 0.3 and 0.35 for reaches A and B respectively. This correction factor is additive in stress terms with the resultant SSI depending upon the magnitude of the bankfull depth. This would be problematic if depth and slope were correlated, but this is not the case as no correlation exists between depth and slope (r^2 = 1.4%, p = 0.000 at A and B). Corrected data place increased emphasis upon original positive slopes, the magnitude of the negative slopes being lower. The crucial assumption within this procedure is that a positive slope, i.e. in the same direction as flow, is deemed more important to potential for activity than a negative slope against the flow. This conditions the effects of depth upon activity where a symmetrical pool is considered more active at the head than the tail due to the contrast in slope. Depth remains as the dominant variable by virtue of its magnitude. This method provides a meaningful relative representation of slope which is then multiplied by bankfull depth to provide a relative measure of potential store activity.

Planimetric plots of SSI calculated on a 1 m grid (11312 and 5814 points for A and B respectively) corresponded with the overall morphology of both reaches. Data ranged from 0 to 0.36 m at reach A and 0 to 0.48 m at B, the maxima being indicative of the high magnitude of local bed slopes relative to reach slope. The disparity between reaches is an indication of the contrast in correction values applied to the slope and larger positive local bed slopes in reach B (Appendix C29).

Storage categorisation was undertaken within the limits of the data range. Six zones were defined using an interval of 0.36/6 at reach A and 0.48/6 at B (Figure 5.1a a,b). The tails of the distribution whilst containing a small proportion of the data are potentially very important representing extremes in terms of potential for activity. The three least active stores in each reach correspond to major bar features (Table 5.1). The general morphological terminology presented is fairly arbitrary since boundaries between features cannot be objectively identified. These labels are intended as a rough guideline to the numerically defined stores.

Data range (m)		**General morphology**
Reach A	***Reach B***	
0.000 - 0.06	0.000 - 0.08	Rarely submerged high bar
0.061 - 0.12	0.081 - 0.16	High elevation bar
0.121 - 0.18	0.161 - 0.24	Low elevation bar
0.181 - 0.21	0.241 - 0.28	Riffle and shallow undifferentiated channel
0.211 - 0.30	0.281 - 0.40	Active undifferentiated channel
0.301 - 0.36	0.401 - 0.48	Pool

Table 5.1. Shear stress index (SSI) data intervals and corresponding morphological classification.

The situation within the permanently submerged channel (i.e. the final c40% of the data for each reach) is more complex . Use of a constant interval did not identify stores corresponding with pool and riffle features. The in-channel elements were picked out more accurately by dividing two of the regular scale intervals into quarters: 0.18 - 0.30 reach A, 0.24 - 0.40 reach B (Table 5.1), the first quarter representing riffle zones with the remainder corresponding to undifferentiated channel. The narrow range indicates the lack of a contrast, in terms of broad hydraulics, between submerged features.

The frequency distribution of the SSI data per defined storage type differs between reaches (Figure 5.1a c, d). In each case the riffle area contains a small proportion of the data reflecting the small area occupied by such features. These small areas must be accounted for as they are significant parts of the sediment transfer system (Keller and Florsheim 1993). The exact distribution of the data reflects the dominant morphology in the reach rather than inconsistency in the method of storage definition. Reach A is characterised by an almost normal distribution where intermediate low elevation bar and undifferentiated channel dominate. In reach B, no single morphology dominates.

It is impossible to affix definite morphological labels to these numerically defined stores, so the nomenclature is based upon relative activity, particularly the potential for bedload transfer. The six stores represent a shear stress progression commensurate with a shift from storage dominance to transfer dominance. The terminology to be used hereafter is illustrated overleaf together with explanatory comments. Figures in brackets indicate the value of the SSI for reaches A and B.

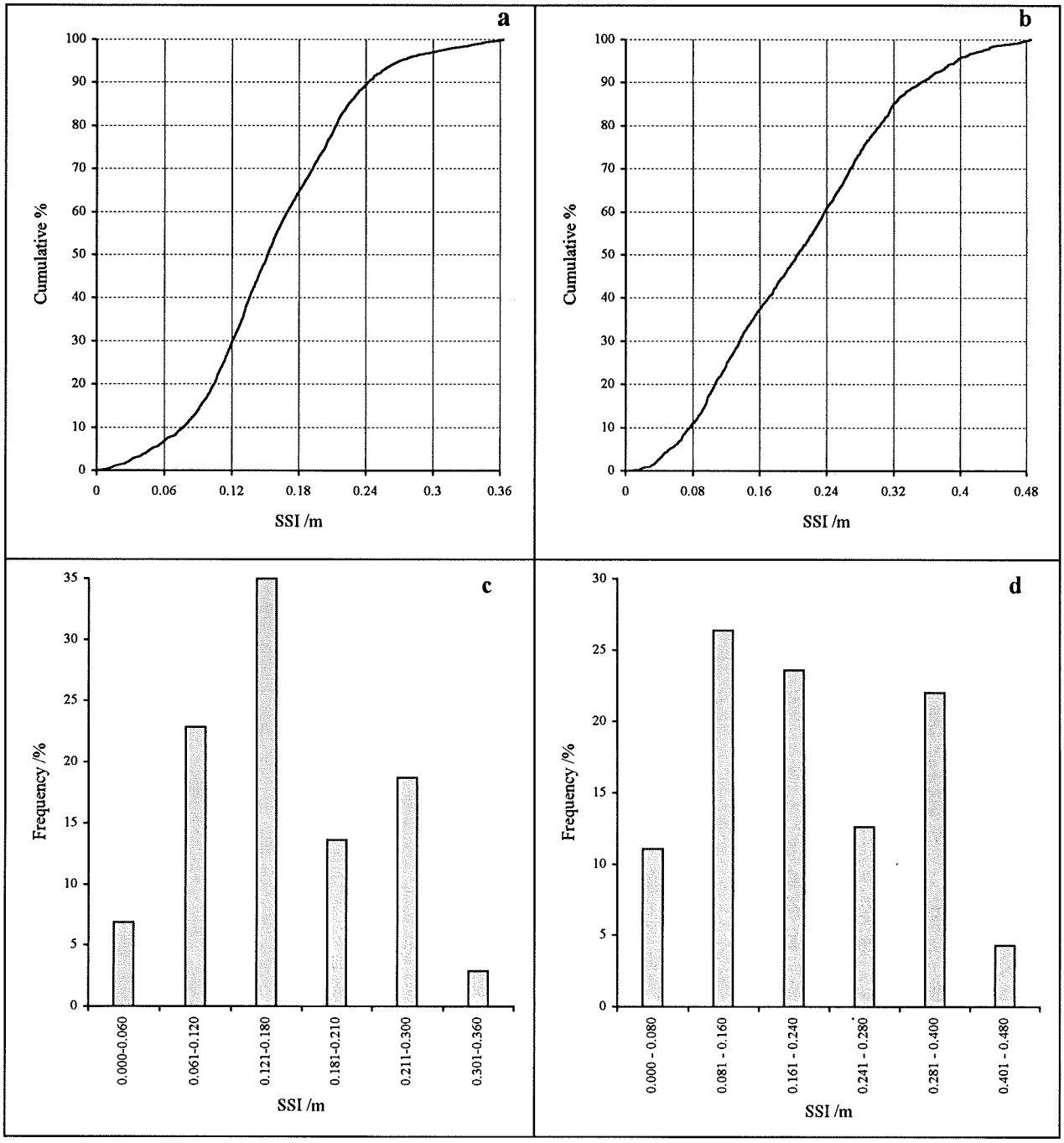

Figure 5.1a. Distribution of SSI data relative to defined storage types. a, b - Reach A and B cumulative curves divided by a regular interval. c, d - Reach A and B histograms of the % data in each storage category.

Very active VA *(>0.3 A, >0.4 B):* Sediment stored within areas of the bed potentially exposed to the maximum shear stress with maximum potential for transfer activity.

Active A *(0.21 - 0.3 A, 0.28 - 0.40 B):* Sediment stored within submerged zones exposed to high shear stresses with potential for frequent transfer activity.

Semi-active SA *(0.18 - 0.21 A, 0.24 - 0.28 B):* Sediment stored within shallow submerged zones frequently exposed to moderate shear stresses conducive to potential transfer activity.

Stable S *(0.12 - 0.18 A, 0.16 - 0.24 B):* Sediment stored within low relief emergent zones infrequently exposed to moderate shear stresses with an associated low potential transfer activity

Inactive IA *(0.06 - 0.12 A, 0.08 - 0.16 B):* Sediment stored within high relief emergent zones rarely exposed to shear stresses of sufficient magnitude for transfer.

Dormant D *(0 - 0.06 A, 0 - 0.08 B):* Sediment stored in areas of the bed rarely submerged with insufficient shear stress for transfer to occur.

Unconstrained sediment redistribution is assumed to take place between all storage types. Conceptualising the reaches according to input, output and within channel redistribution (Figure 5.1b) provides a framework for illustrating possible transfers. Sediment may be input or output from any storage type. Additionally, within the reach boundaries sediment may redistribute between storage types through either erosion or deposition. The physical movement of sediment from one store to another is termed 'dynamic' transfer. Sediment may also 'move' from one store type to another through 'static' transfer (Hoey 1989, Hoey in press, 1995). This occurs to sediment volume i where overlying material is eroded or deposited. For example, in the former case, i may transfer from active to very active storage, the latter case, transfer may be from stable to inactive. The relative proportions of sediment undergoing dynamic and static transfers is very sensitive to the datum used to calculate elevation and the method of storage definition. The significance of static transfer is discussed in chapter 6.

5.1.4 The spatial distribution of sediment storage

5.1.4.1 Storage types

The distribution of sediment storage during this study is illustrated by contour plots of the SSI at reach A (Figures 5.2 - 5.8) and reach B (Figure 5.9 - 5.14). Text labels refer to individual stores

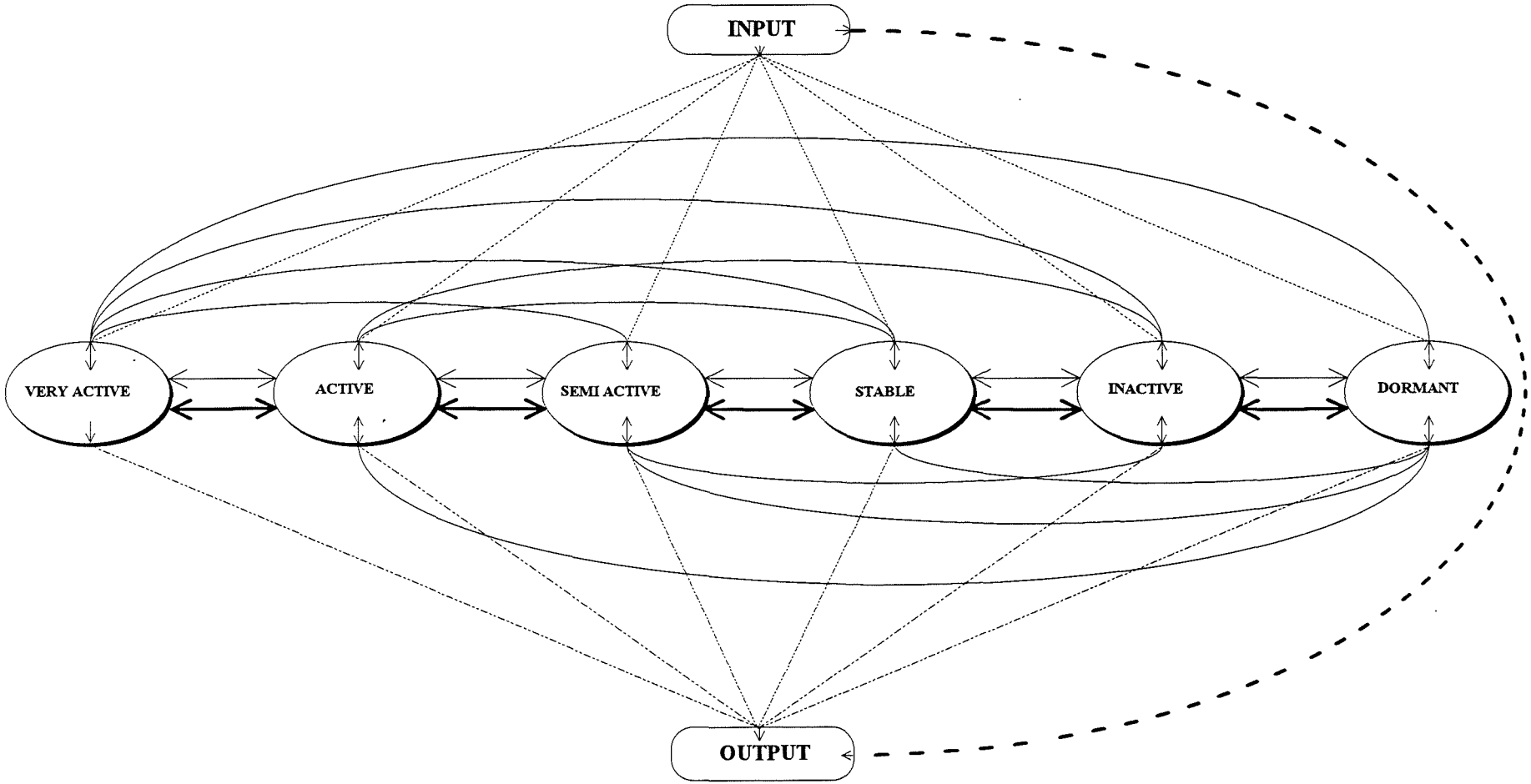

Figure 5.1b. Potential sediment flux pathways. Dotted lines indicate gains of sediment, semi dashed lines detail possible losses. The bold dashed line represents throughput of sediment without entering storage. Solid lines describe possible bi-directional within reach transfers including dynamic transfers (non bold lines) and potential static transfers between stores (bold lines). Double headed arrows in each store represent inputs and outputs of sediment from various sources.

Figure 5.2. Reach A storage types and individual stores. t= 0.

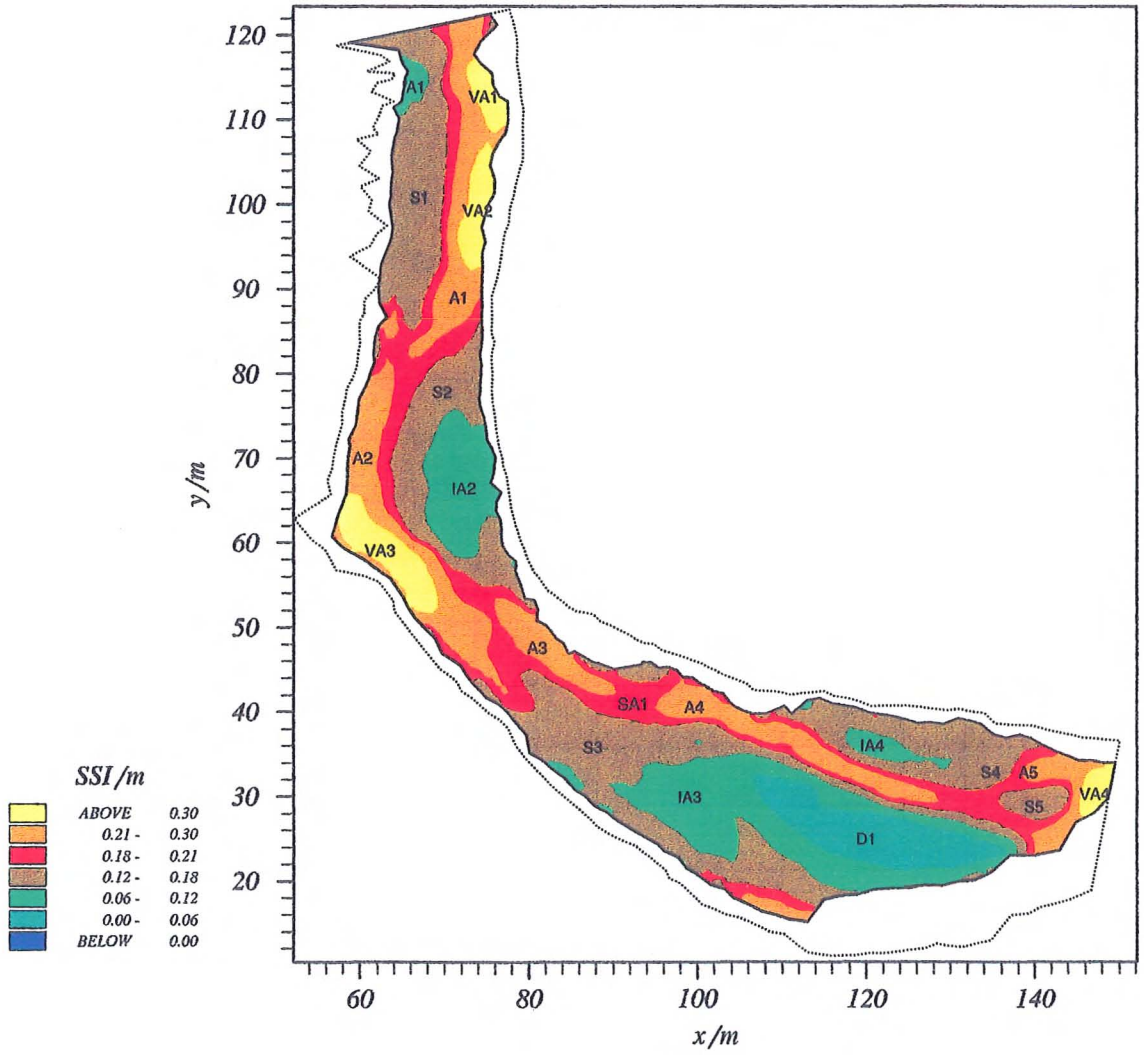

Figure 5.3. Reach A storage types and individual stores. t = 21000.

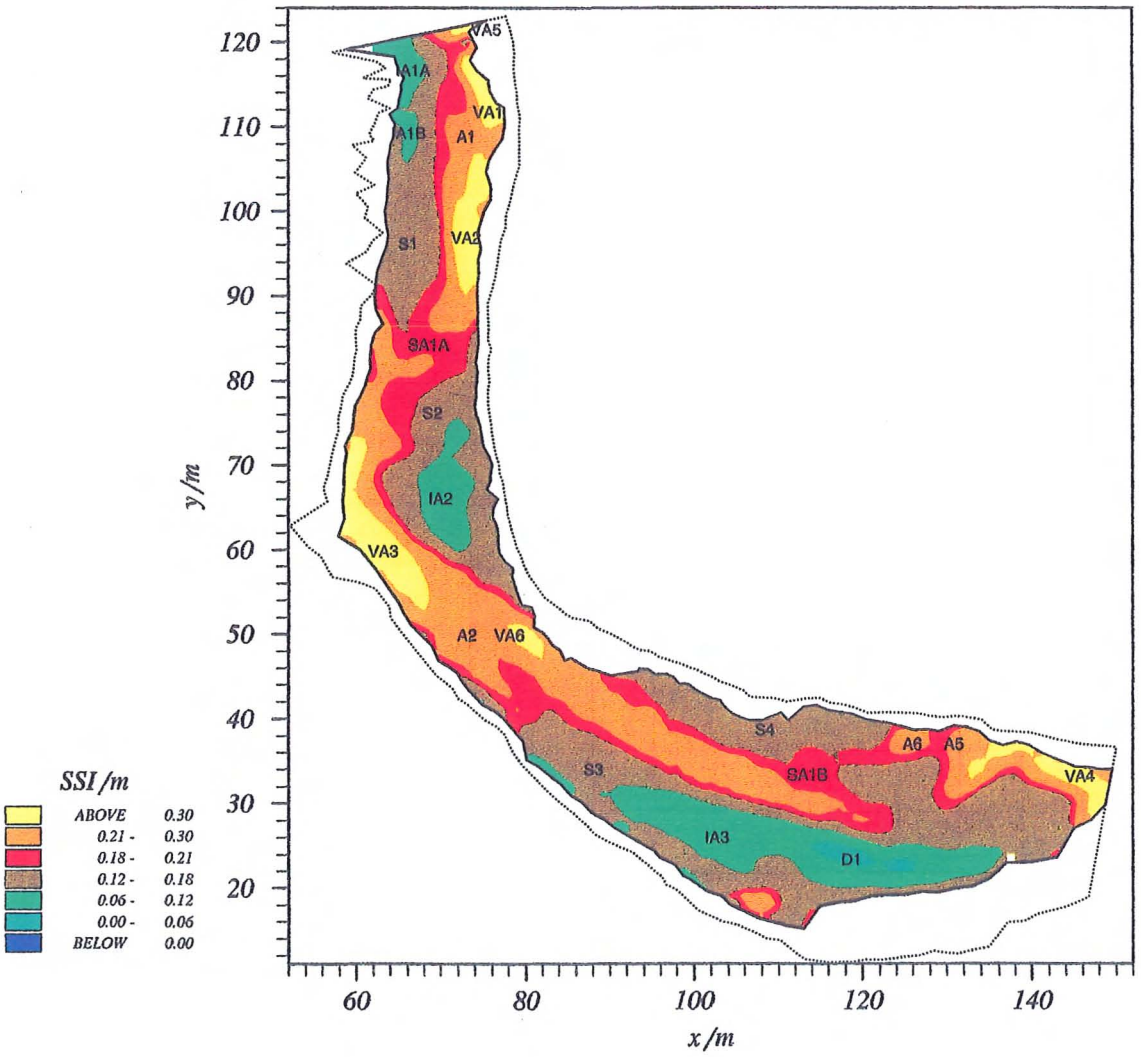

Figure 5.4. Reach A storage types and individual stores. t = 26900.

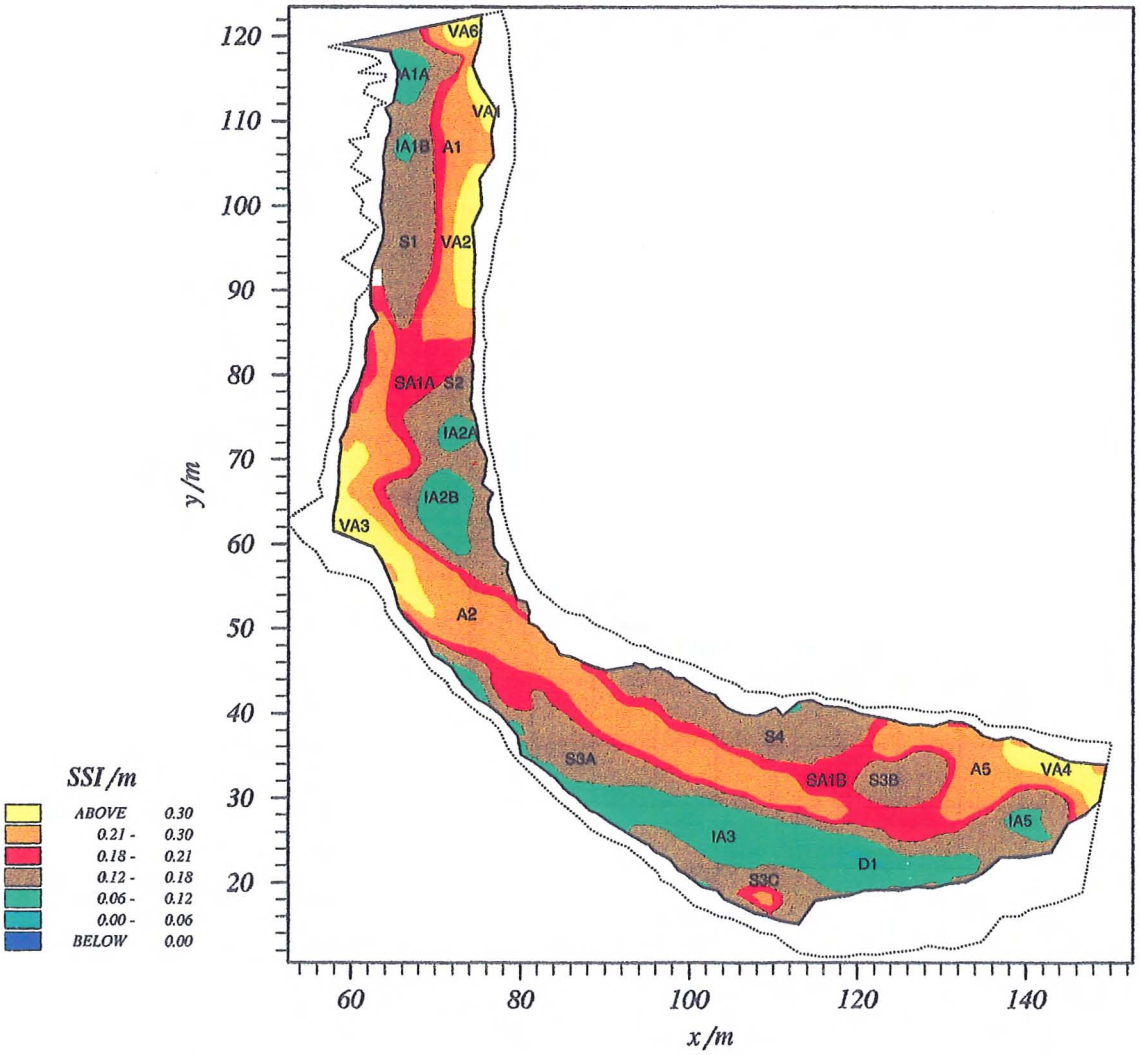

Figure 5.5. Reach A storage types and individual stores. t = 32450.

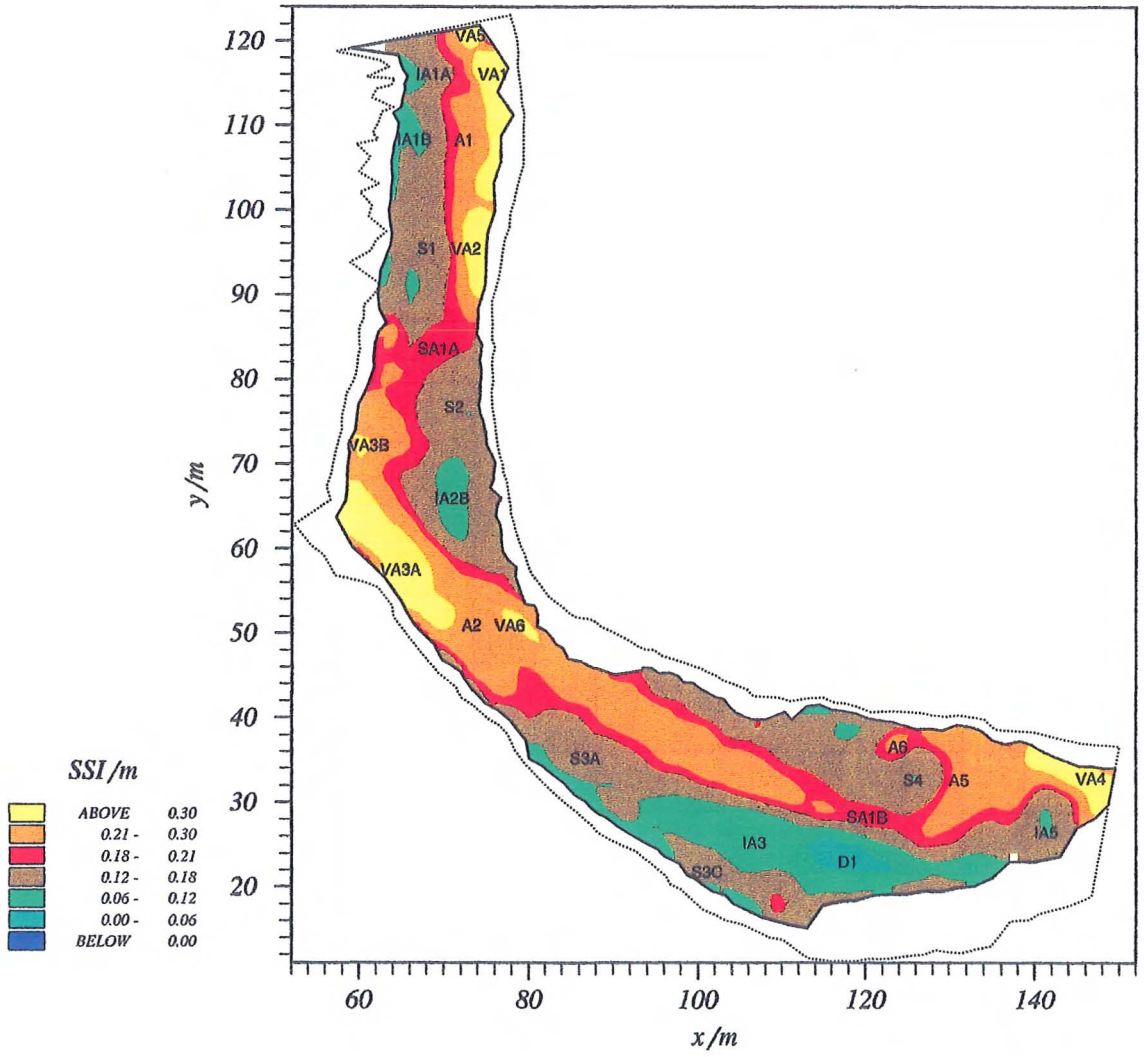

Figure 5.6. Reach A storage types and individual stores. t = 36000.

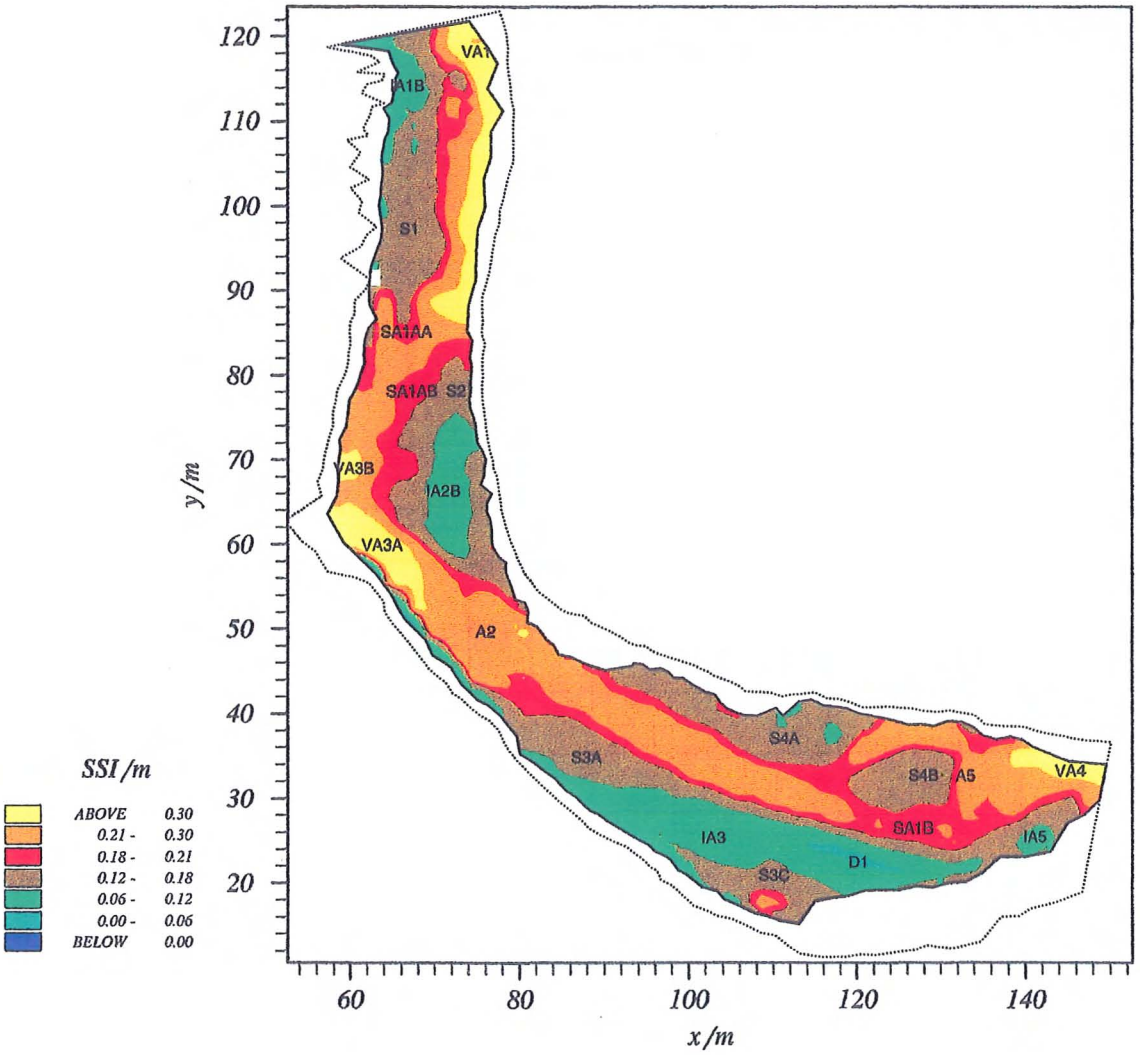

Figure 5.7. Reach A storage types and individual stores. t = 57110.

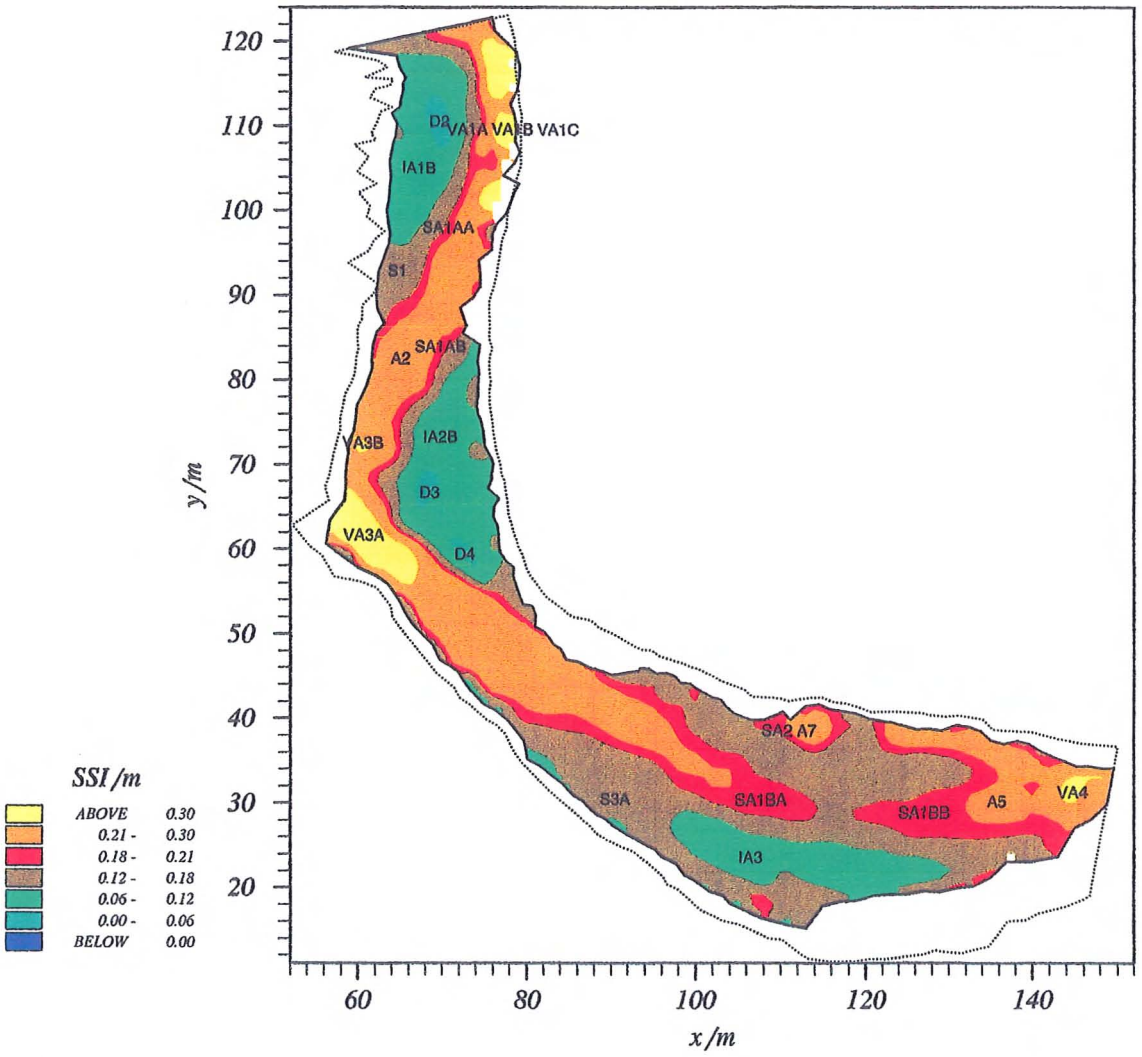

Figure 5.8. Reach A storage types and individual stores. t = 62010.

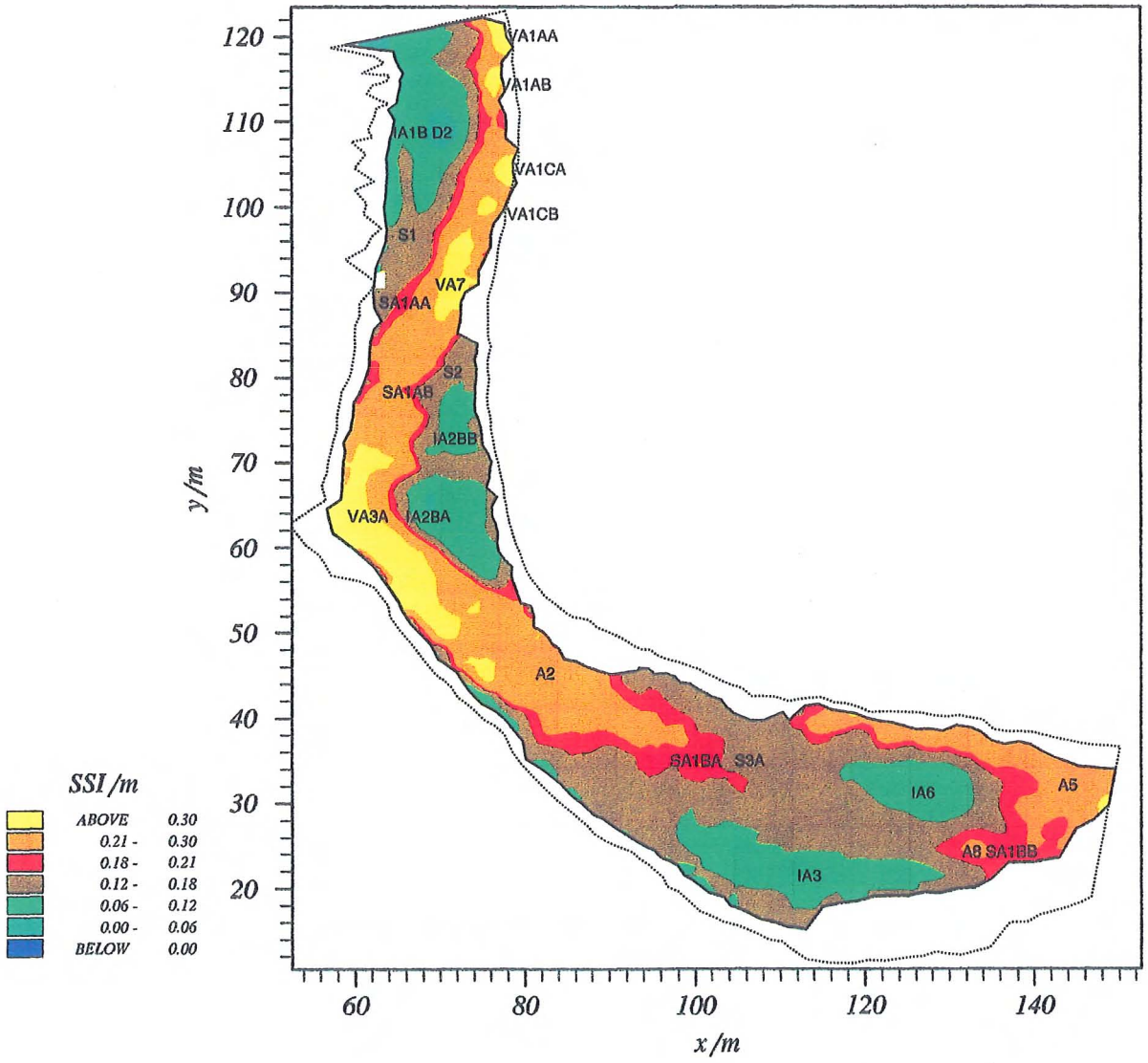

Figure 5.9. Reach B storage types and individual stores. $t = 0$.

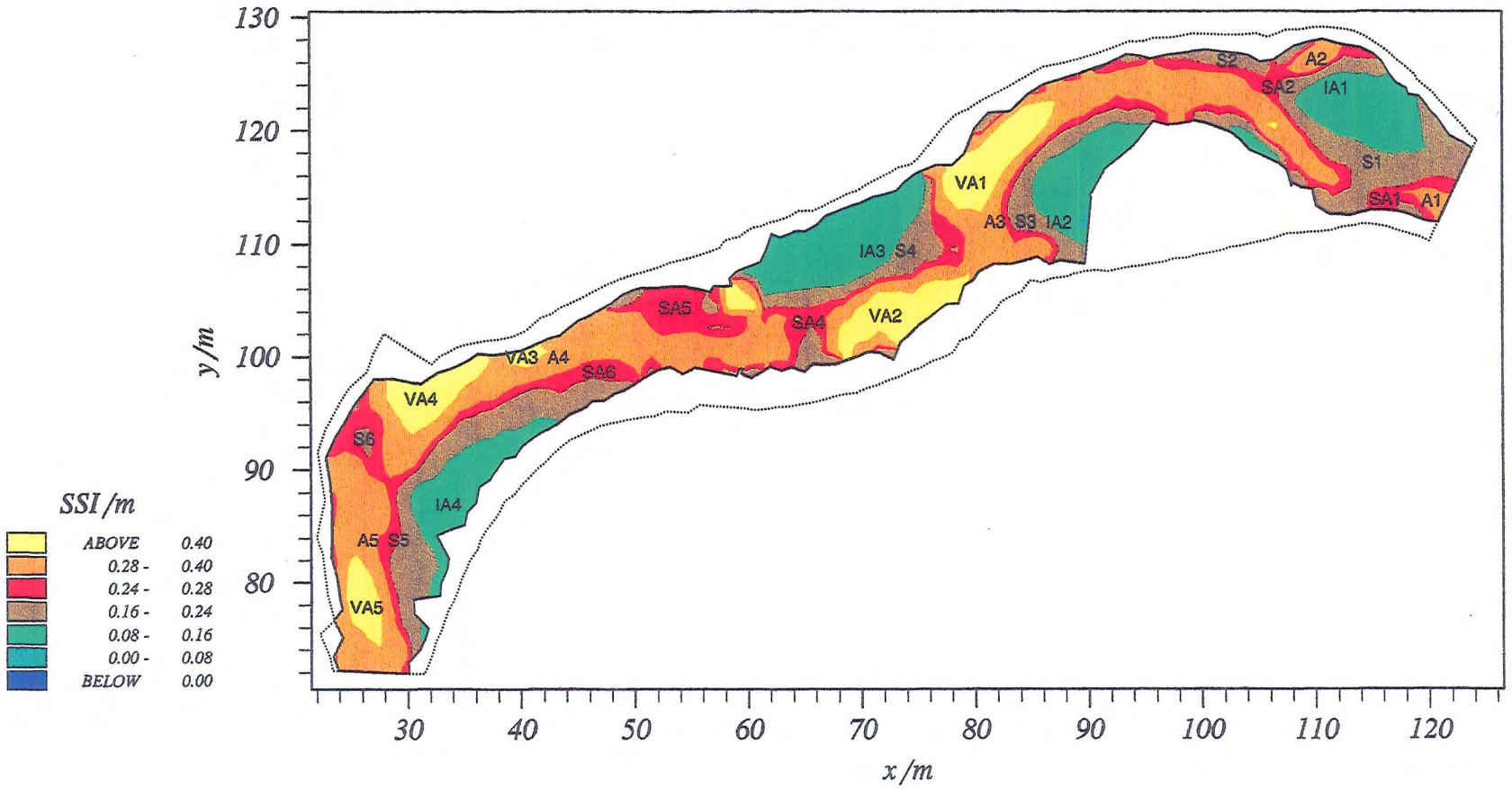

Figure 5.10. Reach B storage types and individual stores. t = 17900.

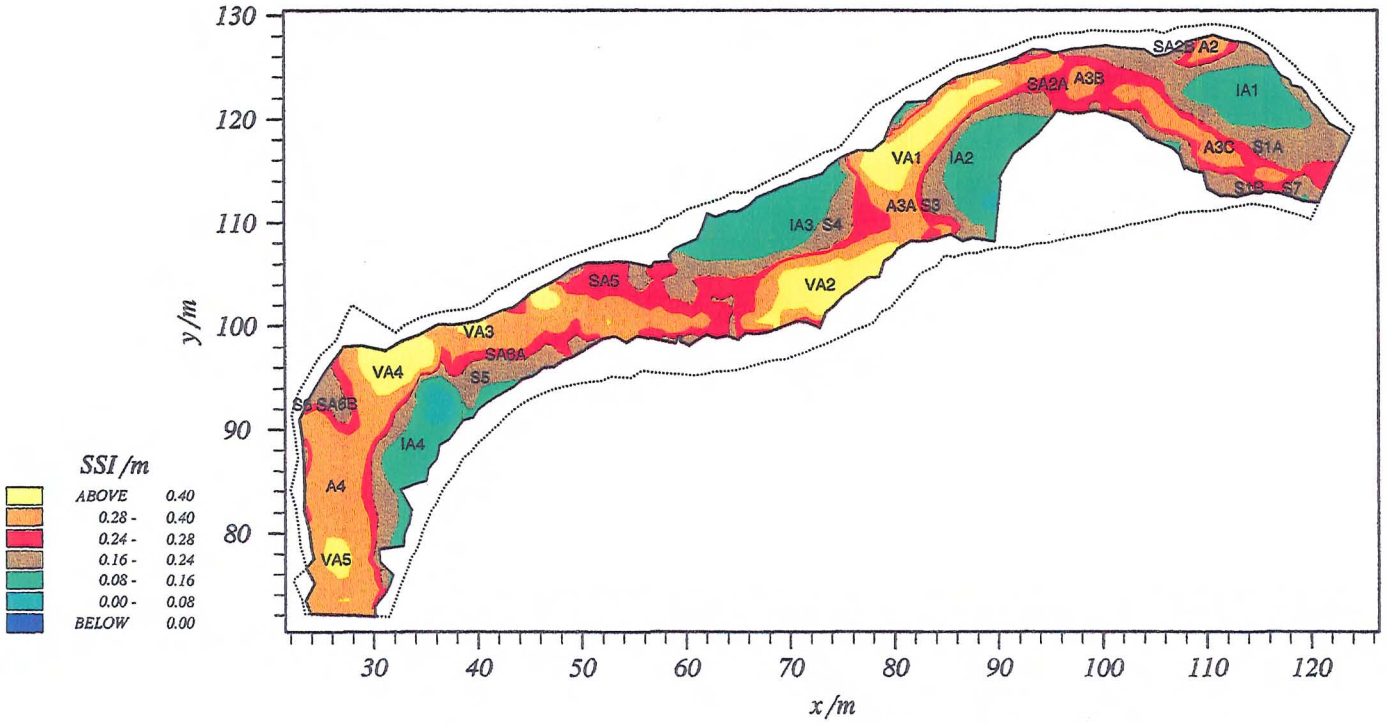

Figure 5.11. Reach B storage types and individual stores. t = 24400.

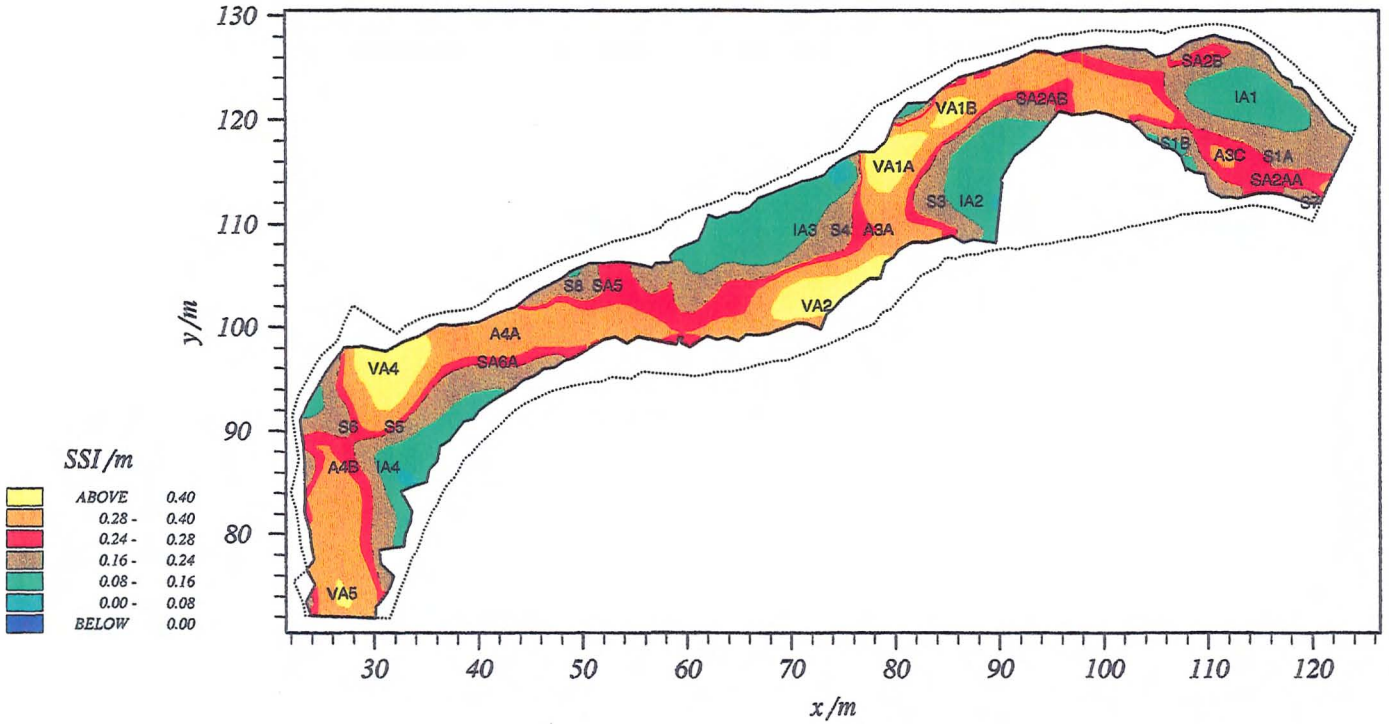

Figure 5.12. Reach B storage types and individual stores. t = 43150.

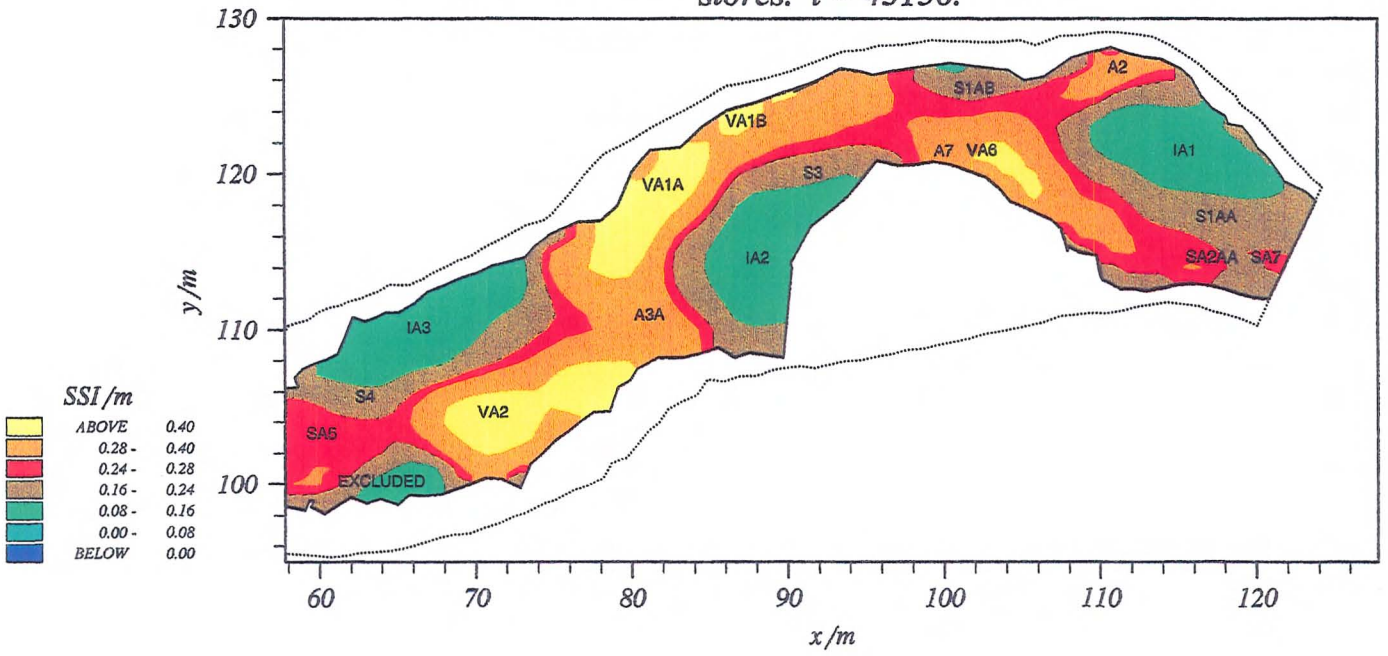

Figure 5.13. Reach B storage types and individual stores. t = 68670.

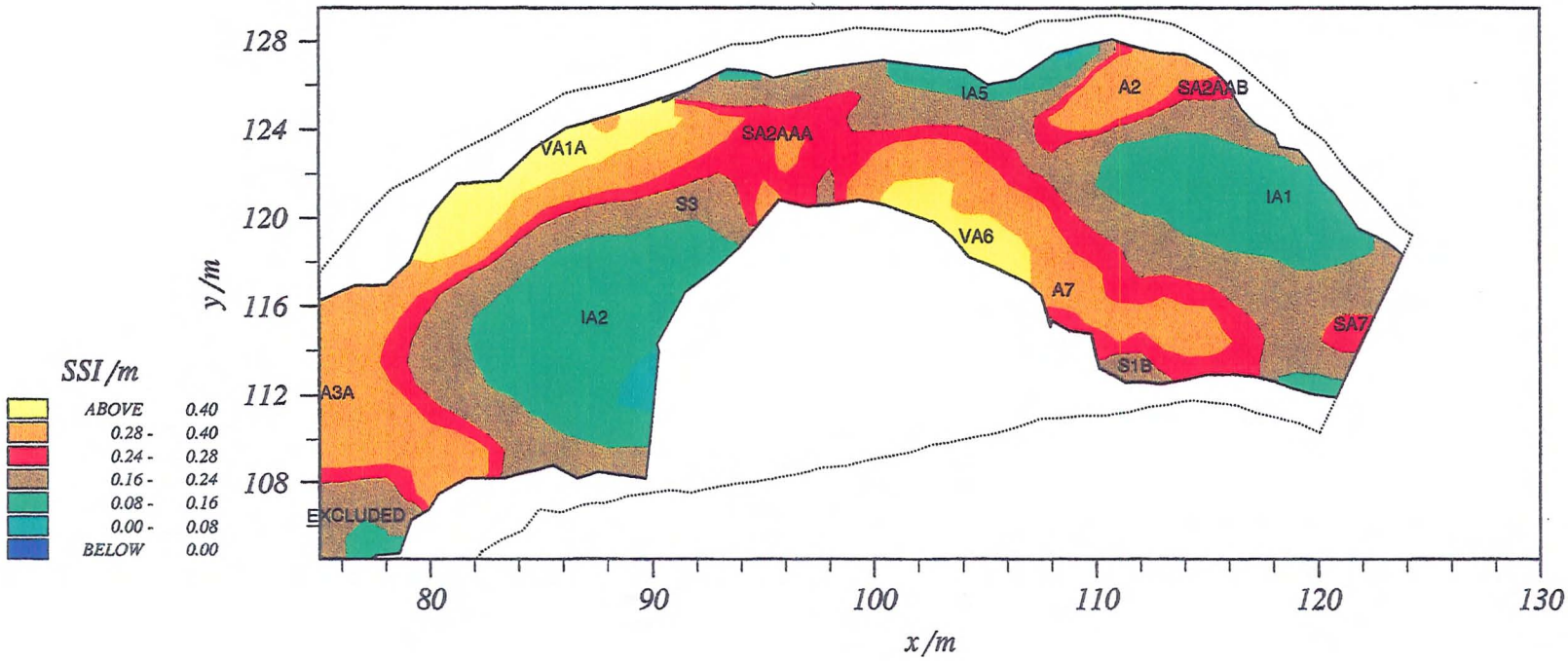

Figure 5.14. Reach B storage types and individual stores. t = 72750.

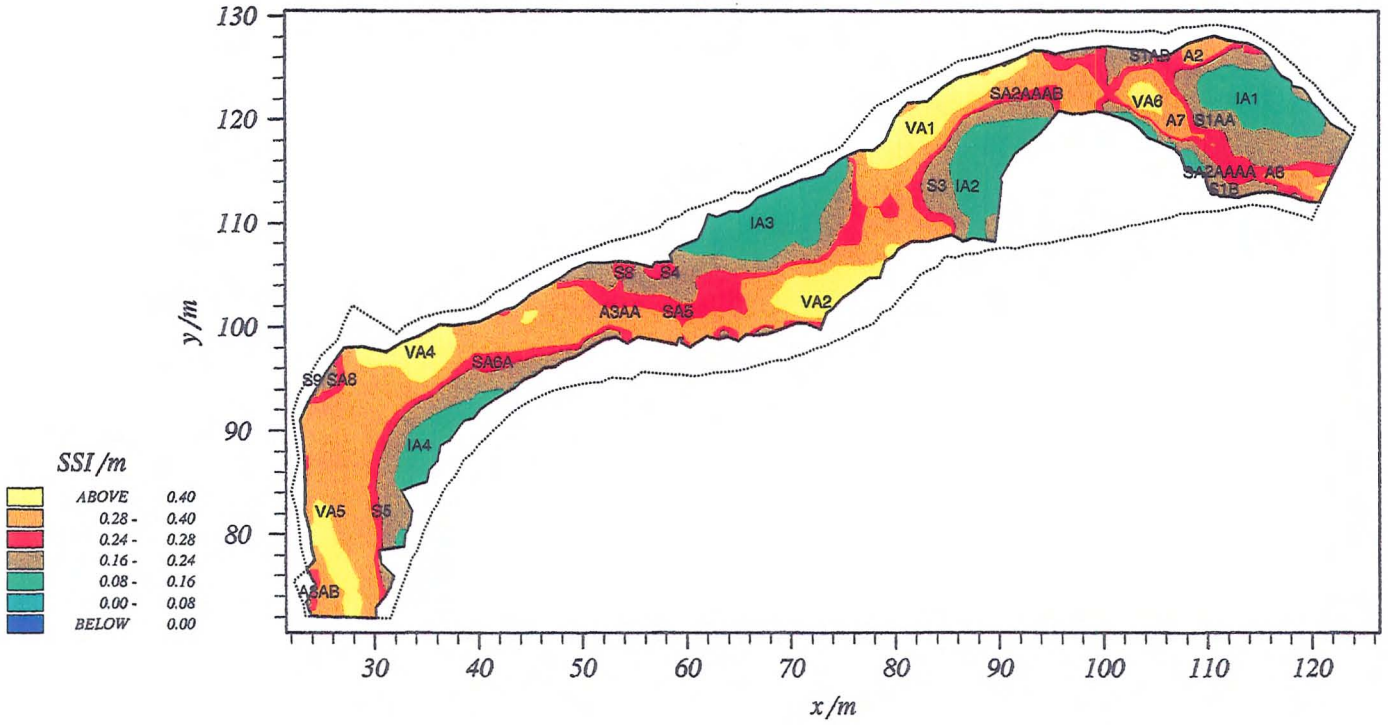

(subsection 5.1.4.2). The channel boundaries are defined to exclude all material between the bank foot and the cross section peg. Additionally, the abandoned backwater area beyond the cut bar (III) in reach A and the fossil bar (V) in reach B are excluded. Reduction of the reach boundary provides a consistent framework for calculating sediment storage volumes. Exclusion of banks, backwaters, coarse hummocky drift material (reach A only) and cantilever failed material ensures that storage volumes contain only gravel.

	Reach A		Reach B	
Survey	Time /min.	Area /m^2	Time /min.	Area /m^2
1	0	2357	0	1181
2	21000	2333	17900	1181
3	26900	2346	24400	1181
4	32450	2383		
5	36000	2372	43150	741
6	57110	2426	68670	502
7	62010	2384	72750	1181

Table 5.2. Extent of the active alluvial channel area during this study. Reach B survey 4 is omitted, surveys 5 and 6 were incomplete.

The area bounded by the region defined above, hereafter referred to as the active alluvial channel, changed progressively at reach A whilst remaining constant at reach B (Table 5.2), reflecting the frequency and magnitude of bank erosion at each site. Apparently cohesive banks, low shear stresses and shallow angle of incidence of flow to the banks at reach B precluded significant erosion. The banks at reach A are less stable by virtue of the high shear stresses and composite nature of the sediments (Thorne and Tovey 1981). There are two major areas of erosion where the angle of flow incidence approaches 90°: the left bank between cross sections 1 and 20 and the right bank (exposed moraine) between sections 47 and 51 (Figure 4.4). Previous erosion has also taken place adjacent to the backwater beyond bar III. The dominance of erosion in this reach is highlighted by the rise in the active alluvial area from 21000 to 57110 minutes above threshold mainly due to the removal of bank foot turf masses and/or renewed erosion of the bank. Bank erosion was highlighted between 36000 and 57110 min. where the banks retreated up to 1.5 m in response to prolonged snow melt flooding in January 1993 (see Appendix B). Anomalous decreases in the active alluvial area are a result of bank collapse and deposition of coarse angular debris (b axis >1 m) at the foot of the moraine (Figure 3.6). In such circumstances erosion may still take place, but most eroded material is deposited at the bank foot reducing the area of exposed gravel within the reach.

Sediment fluxes will be evaluated by analysis of the changing distributions of tracers according to storage type. It is therefore instructive to briefly discuss the areal distribution of storage types (Figure 5.15). There are minor differences in the relative magnitude of storage type extents (Figure

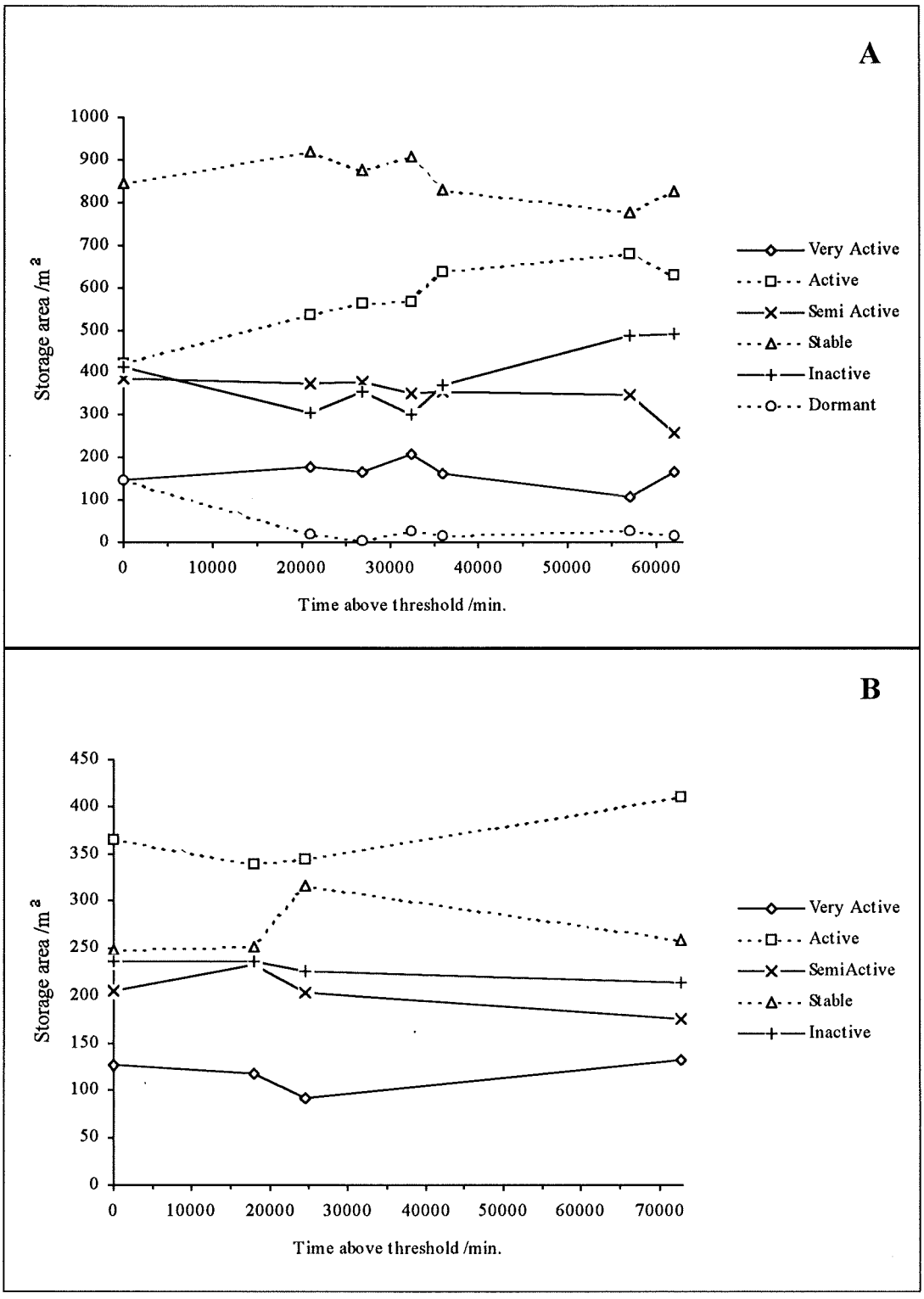

Figure 5.15. Areal distributions of storage types in reaches A and B. Non synchronous time scales result from different survey start points in 1991.

5.15) and those given in Figure 5.1a. The latter is a frequency distribution of SSI in $1m^2$ grid cells whilst the former data is based upon a more accurate contoured area calculated at a higher level of resolution using smooth rather than cellular storage boundaries. Stable and active stores dominate at both reaches (Figure 5.15), the relative magnitude of this dominance fluctuating through time. The relative areal magnitudes of the stores represent the transfer and deposition characteristics of the reaches. Dormant, inactive and stable stores are deposition dominated; semi-active is transitional; active and very active are erosion dominated. Widespread active (transfer dominated by definition) and stable (deposition dominated) storage indicates that within channel fluxes are important and there is neither erosion nor deposition dominance at the reach scale.

5.1.4.2 Individual stores

For any one survey there are a number of separate areas of sediment of the same storage type. The location and number of these stores changes between surveys. A series of criteria for the division and tracing of stores through time was developed (Appendix D). These emphasise the need to be consistent and systematic when dividing up reach-scale storage into individual stores. Most previous studies discount the spatial distribution and non continuity of storage types, instead, concentrating on the role of storage type at the reach scale (e.g. Hoey 1989). The current dataset allows examination of the effect of storage type and individual stores upon sediment dynamics.

The number and labels of each store per survey (see Figures 5.2 to 5.14 for spatial extents) is illustrated schematically in Figures 5.16 and 5.17 demonstrating storage evolution and between survey changes. For example, store IA2 in reach A (Figure 5.16) remains until 21000 min., by 26900 min. it is divided into two due to erosion becoming IA2A and IA2B. These stores remain until 57110 min., subsequently, IA2B is further divided by erosion to become IA2BA and IA2BB, IA2A remains unaltered. Throughout such a progression, storage extent is free to alter as long as the store remains according to the definition criteria outlined in Appendix D.

5.1.5 Areal storage dynamics

Prior to 57110 min. the major morphological changes in reach A took place in the downstream part of the reach. Erosion of bar III (Figure 3.6) resulted in the progressive decline of D1 and increased dominance of S3 (Figure 5.3). This initial erosional phase up to 21000 min. was associated with the removal of S5 and erosion of D1 and IA3. Additionally, IA4 and the lower half of S4 were eroded with aggradation occurring at the bar head. Upstream storage remained virtually unchanged, although aggradation at S3 and S4 indicates that sediment was delivered from upstream. Minimal erosion of IA3 and D1 occurred between 21000 and 26900 min. (Figure 5.4). Upstream migration of A5 via head cut erosion separated the temporary accumulation of sediment

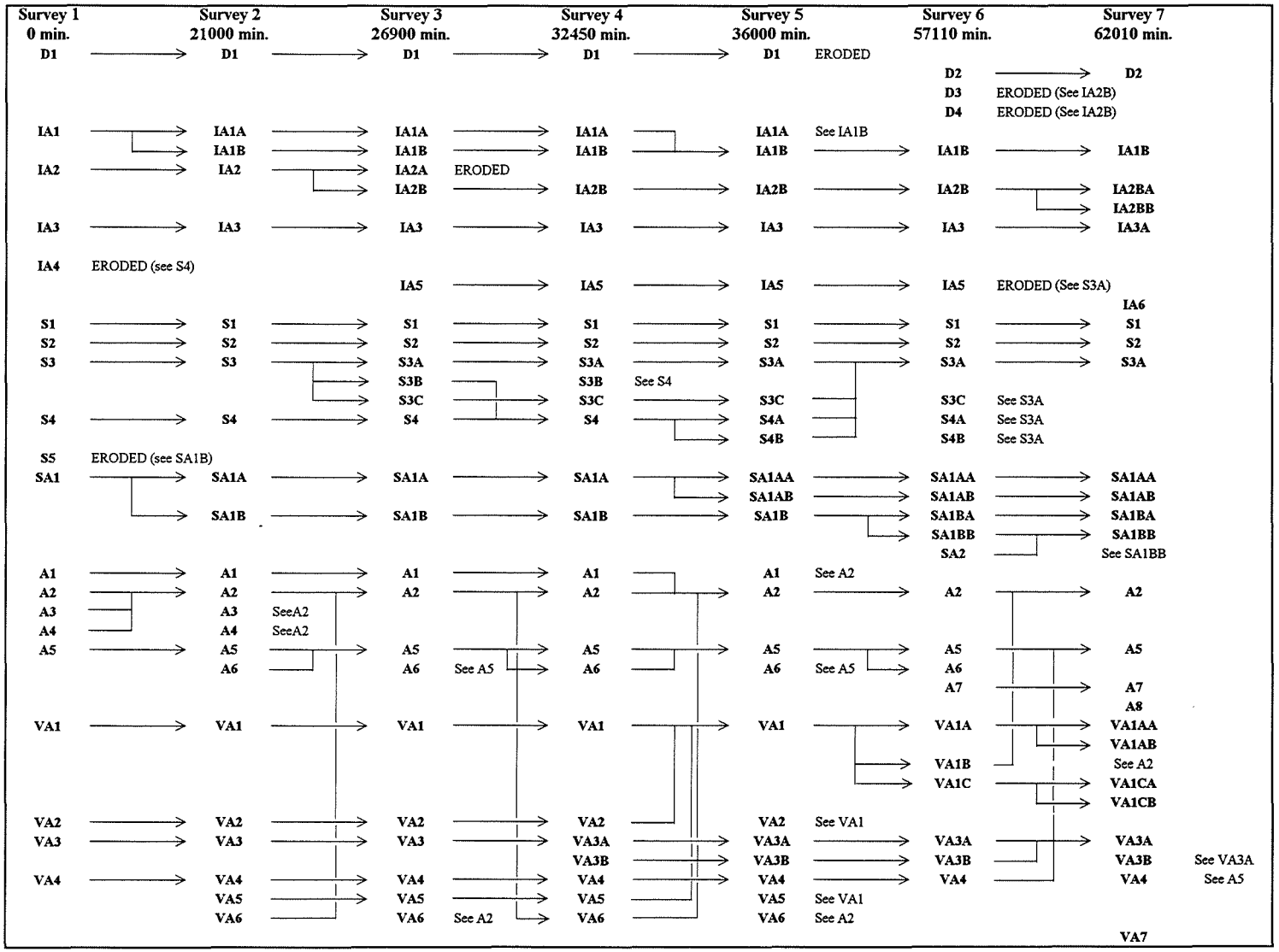

Figure 5.16: Schematic diagram of store formation and erosion in reach A during the study period.

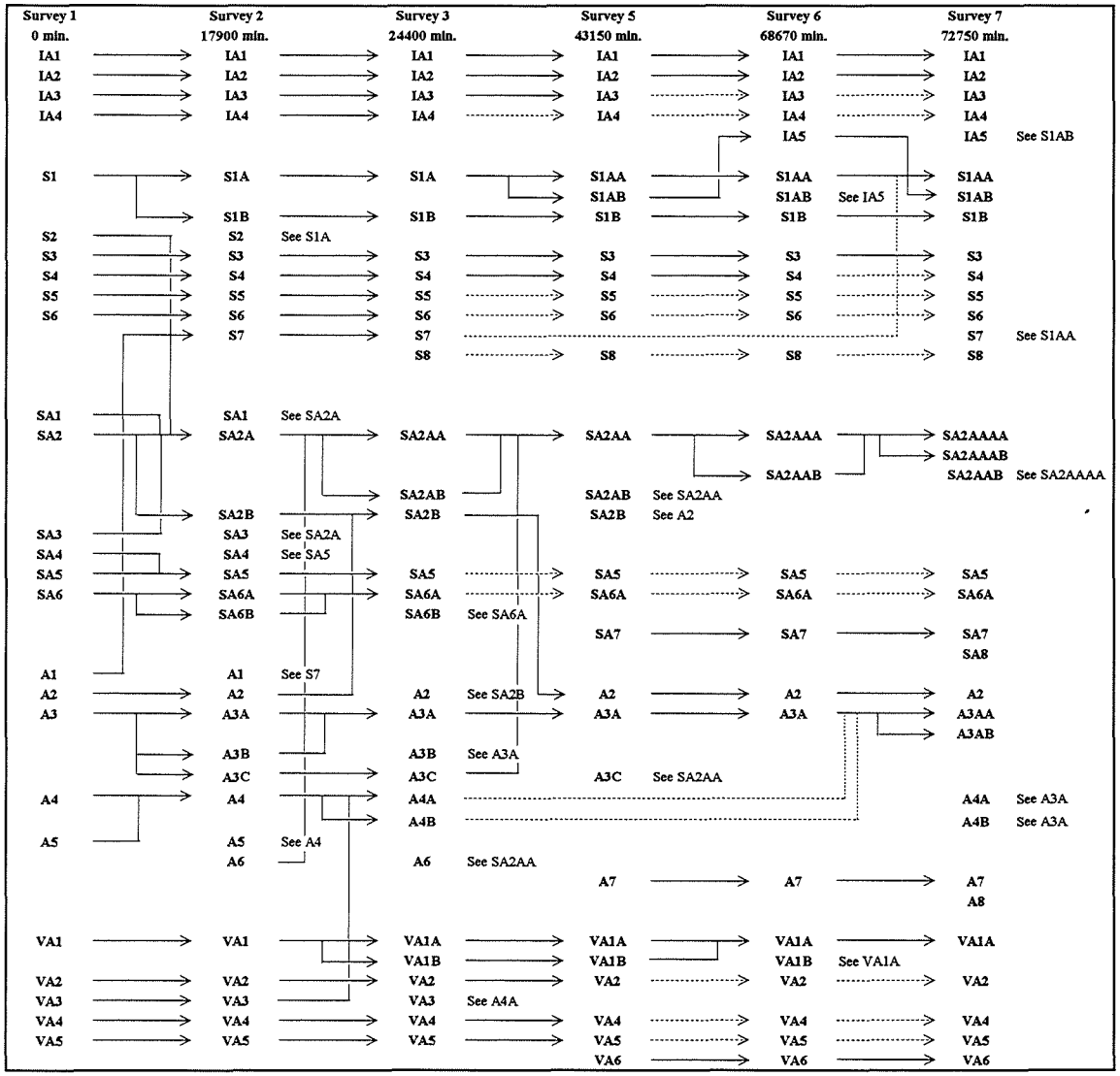

Figure 5.17: Schematic diagram of store formation and erosion in reach B during the study period. Dashed arrows are inferred due to incomplete surveys.

at the tail of S3, resulting in division into S3A and S3B. Again, minimal changes occurred upstream of VA3. The situation was very similar after 32450 min. (Figure 5.5). D1 had aggraded slightly as a result of deposition of fine material on the high bar surface. Headcut erosion at A5 continued in the right anabranch around S3B; the left branch filled with S3B becoming incorporated with S4. No major changes were visible upstream except for alteration to the extent of IA1A, IA2A and IA2B. These bar head locations were very susceptible to turf block accumulation and fine gravel deposition. After 36000 min. A5 had reopened the left anabranch around the now S4B and VA1, VA2 and VA5 had merged (Figure 5.6).

The snow melt floods prior to 57110 min. resulted in large scale changes to storage patterns in reach A. D1, IA5 and most of S4 were eroded (Figure 5.7). The dominance of S3A in the lower region of the reach reflected the reduced depth and increased width of the submerged channel. Upstream, aggradation of bars I and II increased IA1B and IA2B at the expense of S1 and S2 respectively (static transfer). Additionally, VA1 divided into a number of smaller pools, probably in response to the instability caused by the erosion of the left bank. The channel became much less differentiated, and riffles associated with semi active storage eroded to become part of A2. After 62010 min. the extent of S3A had increased due to continued aggradation. In addition, the temporary accumulation of sediment at the tail of S3 after 21000 min. became the more permanent IA6 (Figure 5.8).

In summary, there has been a gradual simplification in storage at reach A, the upstream half characterised by bar aggradation and reduced submerged storage differentiation. Downstream, the channel has aggraded with an associated reduction in the width:depth ratio. More detail will be presented in the discussion of storage volumes in chapter 6.

Reach B presents a contrast to the results from reach A. Data from between 24400 and 72750 min. is incomplete but, changes prior to this period were minimal and it is assumed that this continued throughout the study. Between 0 and 24400 min. reach morphology did not significantly alter (Figure 5.9, 5.10, 5.11) but there were minor differences in storage. Most changes occurred near riffles, while the extent of pool and bar stores remained approximately constant. The incomplete data collected at 43150 and 68670 min. indicate upstream migration of VA1A and the development of a new pool, VA6 (Figure 5.12, 5.13). This feature developed in response to scour behind a partially submerged turf block. By 72750 min., a number of minor changes to the submerged channel had taken place (Figure 5.14). VA4 and VA1 had migrated upstream, and the riffle represented by A3A between SA2AAAB and SA5 had narrowed. Consistent patterns of storage demonstrate that no major morphological change occurred in this reach during the study.

5.2 Transit time development

The transit time distribution from a particular store describes the length of time spent in the store by the output material (Eriksson 1971). At any point in time this is dependant upon local hydraulics and local bed conditions. A sediment budget study should describe sediment storage and mobility with reference to the transit time distribution function (Dietrich et al. 1982). This is possible at the reach scale with single input and output points, ensuring that sediment of different ages cannot mix. At a more detailed scale such as an individual store, sediment is input into storage at different times, and is assigned an age of 0 when input. Plotting of material output against age would disguise the true hydraulic effects responsible for transfer. Flow conditions prior to time t cause output of sediment of age $\leq$ t. It is therefore impossible to calculate meaningful transit times at scales where input is possible at time $t > 0$. In order to describe storage and within reach activity, reference will be made to sediment fluxes and descriptive statistics. These data will provide an insight into areas of the channel which tend to be either storage or transfer dominated. Overall trends in sediment transfer and storage will be examined at four scales: the overall reach; the sub-reach (see section 5.3.2. for a definition); storage type; and, storage type within sub-reaches.

5.2.1 Scaling of tracer results

As tracer grain size distributions differ from those for bed material, some form of scaling is required. Direct comparison between tracer and bed grain size distributions is particularly difficult in any tracing study due to the dynamic nature of fluvial sediments. Tracers occupy different parts of the bed characterised by differing and changing grain size distributions. The number of tracers in any one area is often low thus precluding accurate scaling between tracers and local grain size distributions. However, scaling is possible at the point of installation where sample size is a maximum. Bed grain size distributions can be converted from size by mass samples to particle by number samples, which are directly comparable with the tracer grain size distributions. The number of particles in the half phi class *i* in the bed represented by a single tracer in class *i* can then be determined.

The tracers were installed on the surface of elevation zone E in reach A and zone D in reach B (Figure 4.2, 4.3). The elevation of installation varied across each pool site, so the mean distributions from zones E1 - E2 and D1 - D3 are used for scaling tracer size distributions. Conversion of the tracer data using installation site grain size distributions effectively tracks the movement of a slug of material exported from 3 pool sites in each reach.

Burial depths indicate that tracers were rapidly incorporated within the bed subsurface. After the first hop, 43 % of tracers in A and 62.2% in B were buried (although many tracers at B were buried at the site of installation without transfer). These results suggest that the active layer grain size distribution would be of more use than the surface alone. Surface and subsurface data were combined into an active layer grain size distribution by assuming that the active layer depth, L_a, was $2*D_{84a}$, where D_{84a} is the active layer D_{84} (Hoey and Ferguson 1994). L_a is made up of two components, surface depth, L_s, and subsurface depth, L_{sub}. L_s was assumed to equal the c-axis of the largest clast present at the surface, D_{max}. In the absence of any data, this was taken to be the lower limit of the half phi class containing surface D_{max}. The active layer grain size percentages for the half phi class *i* ($\%Act_i$), were calculated using surface and subsurface percentiles as follows

$$\%Act_i = (L_s.\%Surf_i) + (L_{sub}.\%Sub_i) \tag{5.3}$$

This iterative calculation changed L_{sub} until $L_a=2*D_{84a}$. The resultant active layer depths of 294 mm and 75 mm at reaches A and B respectively are consistent with tracer burial depths in these reaches (see Chapter 7). Minimum tracer diameter was 16 mm so the active layer data were truncated at 16 mm (Figure 5.18). These grain size distributions are covered by the whole range of tracer sizes at B and all at A, except for particles >180 mm (the number of which in the bed was usually small, see Appendix A).

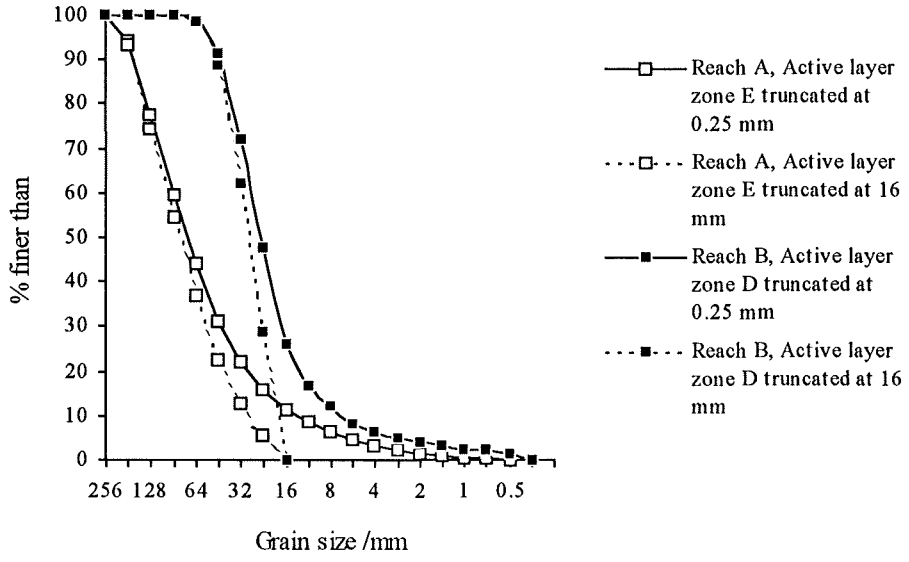

Figure 5.18. Active layer grain size distributions at zones E and D. D_{50} zone E (truncated at 16 mm) = 73.2 mm, zone D (truncated at 16 mm) = 28.2 mm.

The truncated grain size distributions were expressed as a proportion and converted to mass by using total tracer mass for each set, I to III, thus ensuring that both tracer and bed numbers were

derived from the same initial mass of sediment. The number of particles in the bed was determined by division of the mass in half phi class *i* by the mean mass of tracers in class *i*. The proportions of bed material represented by the tracers together with particle numbers are illustrated in Table 5.3. The coarse tracers tend to over-represent the corresponding size fractions in the bed whilst fine material is under-represented. This under-representation of fine fractions is more acute at reach B where grain sizes are finer, and conversely the coarser tracers tend to be in excess of the proportions in the bed. The method of scaling allows determination of the number of bed particles associated with tracer movement. For example, the movement of a < 23 mm particle in set I, reach A is associated with the transfer of 16.8 particles. Whilst it is unlikely that all this material would be derived from one location and deposited at another, it provides a consistent framework to predict sediment fluxes in proportion to the bed. Tracer fluxes will be scaled by multiplying the number of tracers in class *i* within or output from a particular store by the appropriate figure of K_i (Table 5.3). The resultant number of particles is termed the bed tracer equivalent (BTEQ).

Reach A									
Fraction *i*	**Set I**			**Set II**			**Set III**		
mm	**I_i**	**J_i**	**K_i**	**I_i**	**J_i**	**K_i**	**I_i**	**J_i**	**K_i**
<256	0	1.0	N/A	0	1.1	N/A	0	0.6	N/A
<180	20	7.6	0.4	20	6.8	0.3	10	3.5	0.4
<128	32	20.1	0.6	32	21.6	0.7	16	10.0	0.6
<90	32	49.3	1.5	32	45.2	1.4	16	31.5	2.0
<64	32	102.0	3.2	32	110.9	3.5	16	71.6	4.5
<45	32	169.4	5.3	32	191.6	6.0	16	105.1	6.6
<32	32	281.2	8.8	32	278.5	8.7	16	166.8	10.4
<23	32	539.2	16.8	32	573.7	18.0	16	323.1	20.2
Reach B									
<90	30	1.0	0.0	15	0.4	0.0	15	0.4	0.0
<64	50	19.4	0.4	25	7.0	0.3	25	8.3	0.3
<45	50	121.9	2.4	25	53.3	2.1	25	55.5	2.2
<32	50	455.3	9.1	25	201.8	8.0	25	166.2	6.5
<23	50	1232.6	24.7	25	547.6	22.0	25	575.6	23.0

Table 5.3. Number of particles in the bed active layer represented by single tracers in the *i*th half phi class. $\mathbf{I_i}$ - number of tracers installed of fraction *i*, $\mathbf{J_i}$ - relative number of particles in the bed in the *i*th class, $\mathbf{K_i}$ - relative number of particles in the bed represented by a single tracer in fraction *i*. This value varies between sets according to total set mass.

5.3 The distribution of sediment fluxes

5.3.1 The reach scale

The term 'hydraulics' is used in this study to refer to the effect of the imposed flow conditions upon sediment transfer. Hydraulics vary both temporally and spatially, the former as described in

section 4.4.4 and the latter operating at the local scale due to morphological effects upon shear stress. The influence of hydraulics is demonstrated by the proportions of sediment output from the reach and in storage. In order to ensure adequate tracer numbers for accurate data analysis, the grain size fractions were amalgamated into 3 classes in each reach: < 180 mm, < 64 mm and < 32 mm classes at reach A; < 90 mm, < 64 mm and < 32 mm at B. The proportion of material of fraction *i* output from the reach between time t-1 and t, $F_{t,i}$, is given by

$$F_{t,i} = \frac{Q_{t,i}}{S_{t-1,i}} \tag{5.4}$$

where $S_{t-1,i}$ is the bed tracer equivalent number (BTEQ) stored in the reach at time t-1 and $Q_{t,i}$ is the output of sediment (BTEQ) between time t-1 and t. Proportions remaining in storage, $M_{t,i}$, were calculated by substituting $Q_{t,i}$ with $S_{t,i}$. With 100% tracer recovery, $M_{t,i} + F_{t,i} = 1$.

$M_{t,i}$ and $F_{t,i}$ plotted according to grain size reveal a bimodal distribution at reach A (Figure 5.19a). The larger peak in output was due to reach reworking in response to the January 1993 flood 57110 min. above threshold after the start of the study (described in section 3.3.4). Tracers were added to reach A 13600 min. after the start of the study thus the equivalent tracer age is 43450 min. (Table 4.14). All times used in this chapter refer to tracer age rather than the time since the start of the study. Evacuation of sediment between 13000 and 30000 min. was minimal, corresponding with the low peak stages and associated flood duration during this phase of the study (Figures 4.12 and 4.13). $F_{t,i}$ curves plot in ascending order according to decreasing grain size, indicative of reduced mobility of the coarser clasts. All grain sizes are mobile in reach A; in reach B mobility is much lower, especially for coarser sizes (Figure 5.19b), a result of reduced transfer distances with fewer clasts leaving the reach. The < 90 mm clasts were immobile indicating the limit of competence at the reach scale. The fraction containing the reach D_{50} was not as active as the reach A counterpart, commensurate with the decreased slope and shear stresses at this site. The peak for the January 1993 flood is missing at reach B (58050 min), a result of the small number of tracers available for transfer towards the end of the reach.

A transit time function, can be calculated for each reach (considered as a 'black box' with one input and one output point). The transit time (or age) of a tracer is the time the particle remains in the reach and illustrates fractional contrasts in reach activity. Comparison between the transit time functions (Figure 5.20), reveals the extent of this contrast between the two reaches. Reach A data demonstrates the two main phases of activity within the reaches. At both reaches, the BTEQ of < 32 mm clasts is over one order of magnitude greater than the next greater class. The transit time functions are approximately exponential of the form $G_i = a_i e^{b_i t}$, where G_i is cumulative output and a_i and b_i are regression coefficients for fraction *i*; summary statistics are presented in Table 5.4. The regressions were carried out in the form $\ln(G_{t,i}) = a_i' + b_i t$, where $a_i' = \ln(a_i)$.

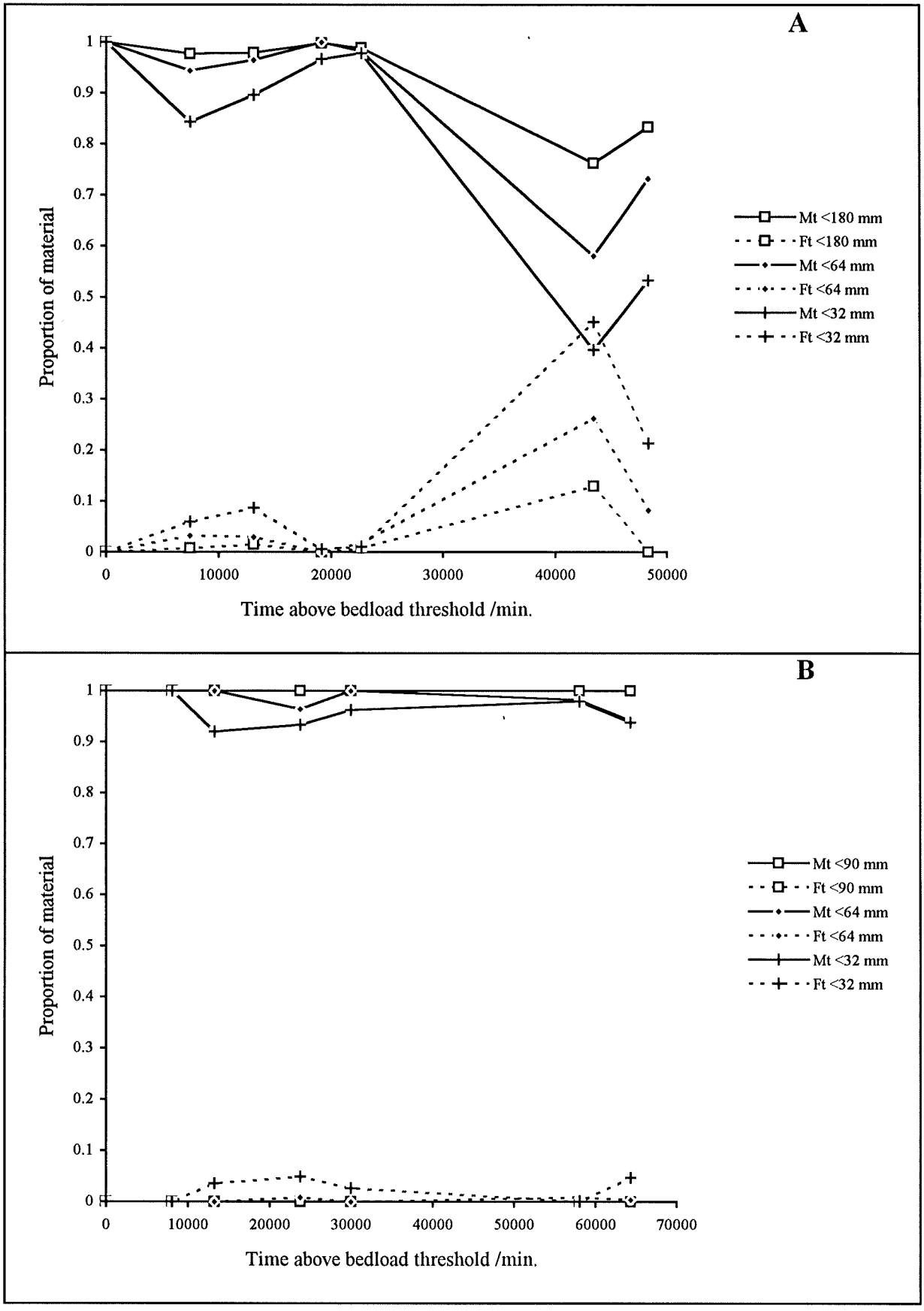

Figure 5.19. Reaches A and B BTEQ output (F_t) and in storage (M_t) at time t expressed as a proportion of storage at t -1. $F_t + M_t < 1$ due to non 100% recovery rates.

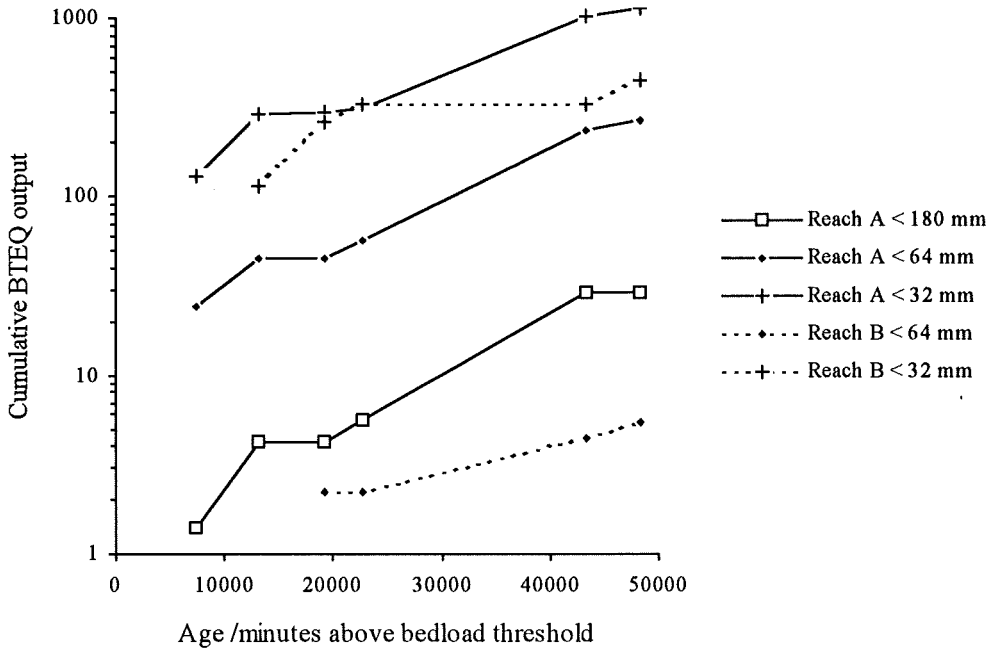

Figure 5.20. Transit time functions for reach A and B tracers according to grain size. Reach B data are plotted at the same time scale as A for illustrative purposes. Semi-log plot is presented to illustrate the fractional contrasts within each reach.

Reach A			**Reach B**	
Size fraction *i*	**b**	**a`**	**b**	**a**
< 180 mm	$7.09*10^{-5}$	0.1	N/A	N/A
< 64 mm	$5.83*10^{-5}$	2.8	$1.90*10^{-5}$	0.1
< 32 mm	$4.94*10^{-5}$	4.7	$2.3*10^{-5}$	4.8

Table 5.4. Transit time distribution summary regression statistics.

The transit time distribution demonstrates within and between reach fractional contrasts. In addition, the form of the distribution may be used to derive inferences about the dominant mode of transfer. If different sizes are equally mobile, then b_i (Table 5.4) should be equal in all cases, whereas if there is size selectivity b_i should decrease with increasing size. In both reaches, b_i increases with size suggesting that coarse fractions eventually overtake the finer clasts. This is unrealistic and it is likely that these results reflect exhaustion in the supply of finer tracers to the reach over time. There is thus no evidence from output that transfer is size selective.

The exhaustion problem is likely to be a function of size selective transfer where finer material is transferred from the reach at a rate in excess of that for coarser sediment, hence fine sediment supply (and thus output) in the reach declines during the study. This problem becomes more acute with time as finer sample sizes decline both due to exhaustion and decreasing recovery rates (Table

4.3). The first tracer hop can be used to test for size selectivity in the absence of tracer exhaustion. If the intercept a_i (BTEQ transfer at t =0) and installed BTEQ (N_i) plotted against D_i are parallel then there is approximate equal mobility (i.e. the bedload transfer grain size distribution mirrors that of the sediment initially available for transfer, Parker et al. 1982a). In fact, the trends are non-parallel in both reaches (Figure 5.21) with a_i falling faster than N_i, therefore transfer is partially selective, consistent with results from other studies on the Allt Dubhaig (Ferguson and Ashworth 1991, Drew 1992, Hoey and Ferguson 1994). The data suggest that size selectivity is present in each reach however, analysis of the distribution of output over time is not useful. The reach scale transit time distribution is an inadequate measure of fractional output fluxes due to exhaustion of finer fractions.

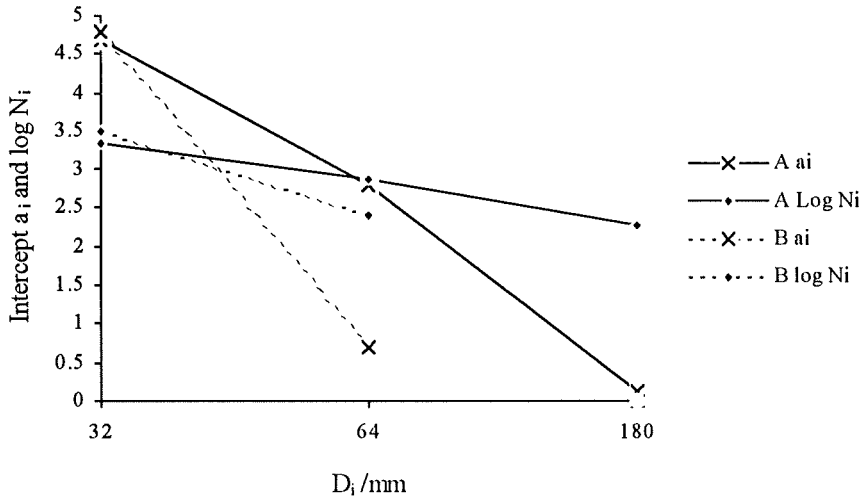

Figure 5.21. Reach A and B relative number of particles, N_i (Column J in Table 5.3) and intercept a_i of the transit time function (Table 5.4). Deviation from parallel lines indicates size selectivity during the first hop.

5.3.1.1 Reach response time

The previous section demonstrated that conclusions drawn from transit times defined on the basis of sediment output are subject to errors due to exhaustion and subsequent reduction of fine tracer samples. In order to overcome such errors the entire tracer sample should be used. The response time Γ_i of a particular reach or store is defined as the time after the initial input of sediment of fraction *i* when the number of stored particles (BTEQ) is exceeded by the cumulative output from the reach/store. This is a function of slope, competence, hydraulics and grain size of the imposed load i.e. the excess stress in the reach over the time period. Response time can therefore be used to accurately identify within and between reach fractional contrasts. The magnitude of Γ_i is subject to possible errors resulting from reduced sample sizes due to exhaustion and tracer recovery rates. The former are unimportant since response time is reached before significant exhaustion.

Response time can be estimated as the point where storage (S_t) and cumulative output (G_t) curves intercept. Regression of these data reduces the variability due to hydraulics and models the general trend in storage and output. $S_{t,i}$ and $G_{t,i}$ characteristically display exponential form, $S_{t,i}$ curves being convex upwards and $G_{t,i}$ concave upwards. The following equations were fitted to the data by ordinary least squares regression;

$$G_{t,i} = ae^{bt} \tag{5.5}$$

$$S_{t,i} = C - ae^{bt} \tag{5.6}$$

a and b being constants obtained from regression and C, a constant representing the asymptote of $S_{t,i}$ as $t \rightarrow \infty$. C was altered iteratively to maximise r^2. The regressions were carried out in the same form as the summary data in Table 5.4. Equation 5.5 is analogous to the transit time regressions discussed in 5.3.1.

	r^2	Intercept a`	Gradient b		r^2	Intercept a`	Gradient b
Reach A				**Reach B**			
<180 mm				*<90 mm*			
Storage	0.98	1.76	$5.35*10^{-5}$	Storage	1.00	1.50	0.00
Output	0.96	0.12	$7.09*10^{-5}$	Output	N/A	N/A	N/A
<64 mm				*<64 mm*			
Storage	0.97	2.61	$3.23*10^{-5}$	Storage	0.88	2.70	$1.51*10^{-5}$
Output	0.95	0.18	$6.71*10^{-5}$	Output	0.98	0.17	$2.30*10^{-5}$
<45 mm				*<32 mm*			
Storage	0.97	2.75	$4.87*10^{-5}$	Storage	0.80	6.79	$9.62*10^{-6}$
Output	0.95	1.66	$6.23*10^{-5}$	Output	0.67	4.88	$1.91*10^{-5}$
<32 mm							
Storage	0.89	4.64	$4.28*10^{-5}$				
Output	0.98	3.95	$4.35*10^{-5}$				
<23 mm							
Storage	0.89	5.65	$3.78*10^{-5}$				
Output	0.91	4.07	$5.43*10^{-5}$				

Table 5.5. Summary regression statistics obtained from fitting exponential models to $S_{t,i}$ and $G_{t,i}$. p - level of significance. All relationships are significant at $p < 0.001$ in reach A and $p < 0.01$ in reach B. Regression of reach B < 90 mm data was not possible due to immobility of these size fractions.

Regression analysis was carried out on logarithmic data broken down according to grain size. Reach A was divided into half phi classes for material < 64 mm and a single class for coarser particles (64 - 180 mm) for which the BTEQ output at discrete time intervals was smaller. This increased number of grain size categories was possible due to the activity of all sediment sizes in reach A and allows more detailed analysis of the fractional trends in Γ_i. In reach B, whole phi classes were used. The exponential models reveal a close fit to the observed data (Table 5.5;

Appendix E1). Regression was not forced through the origin, although $G_{t,i} = 0$ at $t = 0$, as this would reduce the accuracy of the overall prediction. All predictions are significant at $p < 0.01$. The decline in storage is more irregular due to the underestimation of $S_{t,i}$ where tracers are missing. The significance of the relationships at reach B is poorer than that for reach A due to the more sporadic output of very few tracers.

The intersections of the calculated curves, Γ_i, were calculated iteratively until $S_{t,i} = G_{t,i}$ (Table 5.6). This is a more accurate measure of fractional transfer activity than transit time since storage decline and output increases are accounted for. Extrapolation is used where Γ_i was not reached during the experimental period (Figure 5.22a, b). Response time increases with grain size at both reaches, commensurate with the decreased mobility of coarser sediment. The response of reach B to an imposed sediment input was much slower than that of reach A. The half phi class containing the surface D_{50} (truncated at 16 mm) at each reach demonstrates this contrast, $\Gamma_{d50} = 57900$ minutes at A and 117518 minutes at B.

	Response time Γ_i (min)	**Response velocity V_r (ms^{-1})**		**Response time Γ_i (min)**	**Response velocity V_r (ms^{-1})**
A			**B**		
<180	57900	0.00198	*<90*	∞	0
<64	50100	0.00220	*<64*	175000	0.000629
<45	48200	0.00238	*<32*	117500	0.000936
<32	37900	0.00303			
<23	42400	0.00271			

Table 5.6. Response time Γ_i and response velocity V_r for tracer size fractions. Response velocity is defined as reach length divided by response time.

Conceptualising a response sediment velocity, V_r, defined as the reach length divided by Γ_i is useful. Reach length is 115 m at A and 100 m at B. V_r declines with grain size (Table 5.6) and at A is approximately three times greater than B for equivalent size fractions. It is likely that this velocity decreases along the long profile as slope reduces resulting in progressive deposition of coarser sediment. The contrast in velocities provides a mechanism for describing (and possibly predicting) downstream fining along the Allt Dubhaig.

The proportion p_{ri}, where Γ_i is reached should be 0.5 with 100% recovery; actual data are closer to this figure for coarser fractions where recovery rate is relatively high (not 100%) and declines for finer sizes. This error is compounded when extrapolation is used to determine Γ_i since modelled data predict decreasing recovery rates (on the basis of current trends), thus p_r for reach B is considerably lower than at reach A (Figure 5.22). These results may be prone to increased error where the storage decline is considerably overestimated and therefore Γ_i for reach B represents a

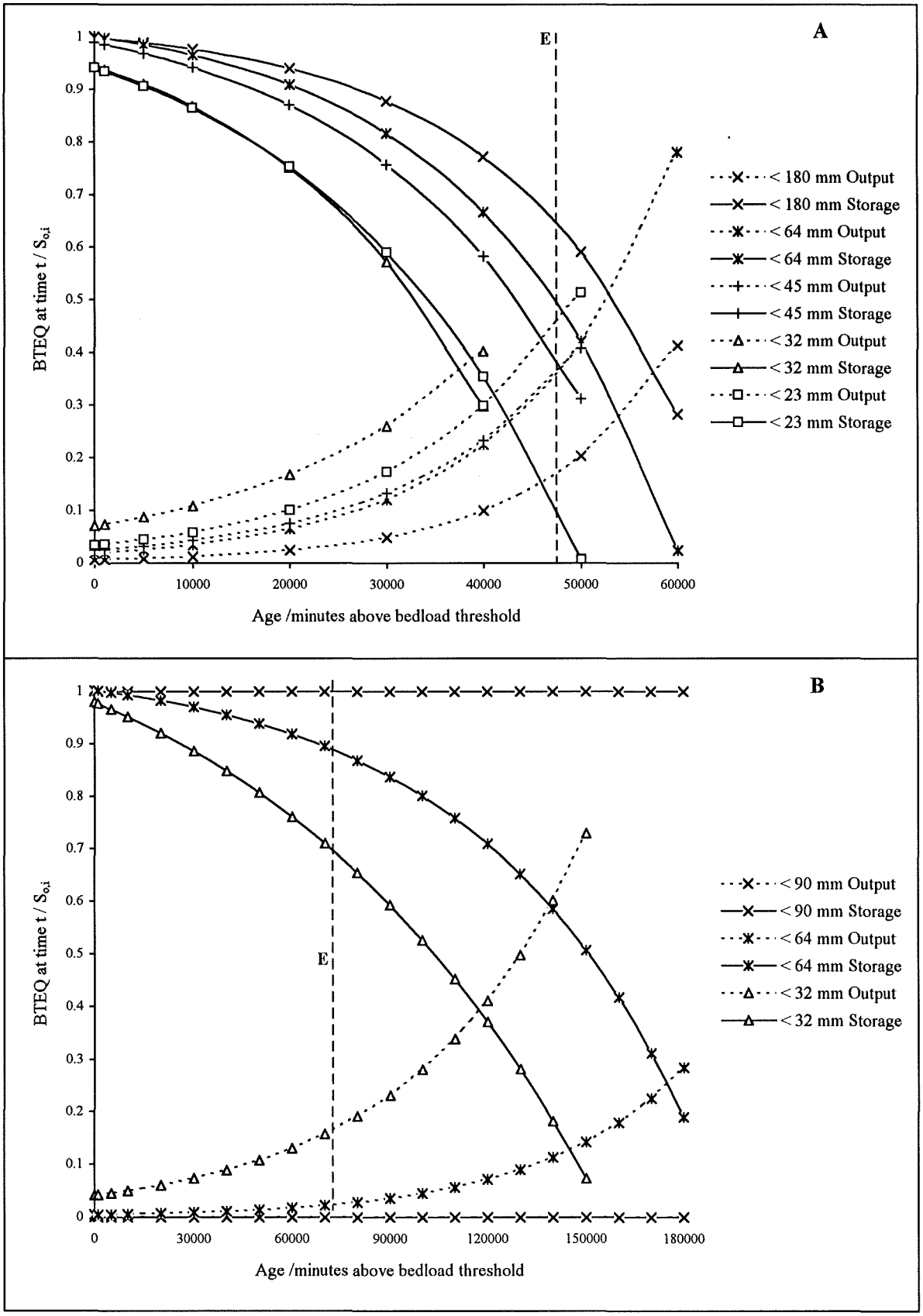

Figure 5.22. Reach A and B predicted decline in storage and increase in transfer according to grain size. Response time is defined by intersection point. Data normalised by BTEQ in storage at t = 0. Dashed line, E, indicates where extrapolation begins.

minimum. The importance of recovery rate may be assessed with reference to the relative proportions of sediment remaining in storage and material output. At the reach scale at time t,

$$S_{0,i} = G_{t,i} + S_{t,i} + e_{t,i} \tag{5.7}$$

where $S_{0,i}$ is the BTEQ in storage at the start of the study or after the first input of material. Error $e_{t,i}$ increases with time. Errors tend to cause overestimation of the decline in $S_{t,i}$ (Eq. 5.6) and underestimation of the increase in $G_{t,i}$ (Eq. 5.5) although the exact magnitude is dependant upon the location of the missing particles. Error in the estimates of the sum of output and stored material at time t can be calculated by rearranging Eq. 5.7 as follows

$$e_{t,i} = (S_{t,i} + G_{t,i}) / S_{o,i} \tag{5.8}$$

This error tends to increase with time and as grain size declines (Figure 5.23), consistent with the trends in recovery rate. These errors are the result of developing predictions based upon incomplete data sets. It is not possible to assign the error to the estimates because the proportion of missing material in storage and output is not known. Previous tracer experiments (e.g. Hassan et al. 1991) suggest that the error is probably closer to being equally distributed than all in $G_{t,i}$. Therefore, the data allow accurate comparison between and within reaches according to grain size.

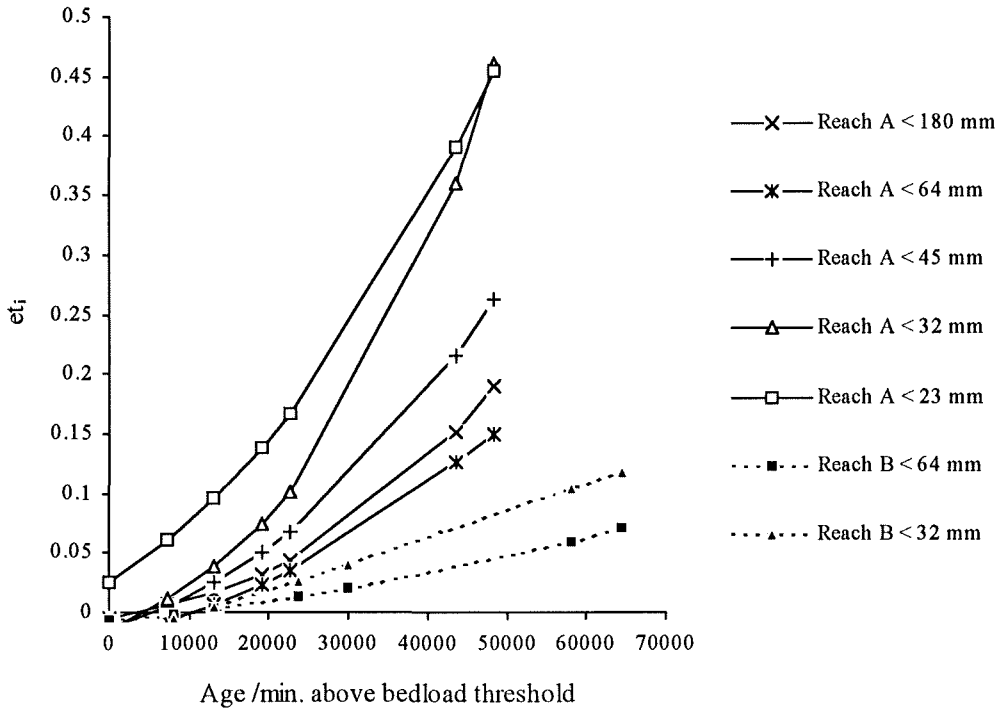

Figure 5.23. Calculated error in the predicted estimates of $S_{t,i}$ and $G_{t,i}$, as a proportion of $S_{o,i}$. Errors below zero arise because the predictive regression relationships (5.5 and 5.6) were not forced through the origin.

Unlike transit time, it is possible to derive an accurate measure of the mode of transfer using response time. This analysis is not possible in reach B due to the small data set. A hiding factor based upon Γ_i has the following form

$$\frac{\Gamma_i}{\Gamma_{d50}} = a\left(\frac{D_i}{D_{50}}\right)^b \tag{5.10}$$

where D_i is the mid point of the classes used. Ordinary least squares regression resulted in coefficients a = 0.94 and b = 0.22 (p = 0.01) indicating a degree of size selectivity. The limited response time data for reach B also suggests this is the case. Unlike transit time, response time is based upon storage and output. Whilst b_i values for output alone (Tables 5.4 and 5.5) are misleading, use of storage together with output allows an accurate assessment of the dominant mode of transfer since response time is determined prior to significant exhaustion of tracers. Deviation away from equal mobility is consistent with other tracer studies where size segregation in transfer has been reported (e.g. Ashworth and Ferguson 1989, Church and Hassan 1992).

5.3.2 Sub-reach sediment fluxes

Each reach was divided into three sub-reaches (hereafter referred to as 1A, 2A, 3A, 1B, 2B, 3B), usually on the basis of riffle locations; effectively, each reach was sub divided into thirds (upstream, midstream and downstream). Each sub-reach is outlined in Appendix F. Sub division is instructive, allowing examination of the spatial distribution of sediment evacuation, particularly the effect of upstream reaches upon downstream storage (e.g. Brewster 1986 (in Ashworth 1987), Saunders 1988). Transit time is only applicable to the reach scale, it is not representative of fluxes in relation to hydraulic conditions where sediment of different ages is allowed to mix (section 5.2). Sub-reach and store characteristics will be assessed using response time since it is based upon time rather than age and also uses both output and storage. Response time is calculated for stores and sub-reaches for < 180 mm, < 64 mm and < 32 mm fractions in reach A and < 90 mm, < 64 mm and < 32 mm in reach B. This reduced number of classes compared with reach scale response times ensures that adequate tracer numbers are located within these smaller storage units.

Sediment fluxes during this study form the basis for all the results presented herein, which are presented for reference purposes in Appendix E2. By definition, reaches 1A and 1B degrade (in terms of tracers) after t = 0 (after which input = 0), most transfer taking place during the first hop. Intermediate reaches 2A and 2B aggraded slightly during the study ($M_{t,i} > 1$), particularly at 2B where decreased transfer distances reduced the amount of sediment passing through from upstream. Particles in 2A passed through fairly rapidly, although this was dependant upon storage type (see

section 5.3.3). The lower sub-reaches acted as temporary sinks of sediment, especially 3A. This reflects the increase in width/depth ratio and associated local volumetric aggradation at this site during the study (see chapter 6) and, to a lesser extent, movement distances of material. Few tracers were stored in 3B due to reduced sediment mobility i.e. not many tracers left 2B.

Response time, Γ_i, can be used to quantitatively demonstrate the sub-reach characteristics. Cumulative output ($G_{t,i}$) and storage ($S_{t,i}$) curves at 1A and 2A indicate rapid output of sediment, whereas 3A displays a wave of tracer movement for < 32 and < 64 mm sizes (Appendix E3). Rather than using regression analysis, Γ_i can be determined directly from the intercept of the curves. In reach B, the response time did not occur during the study therefore the intercept of extrapolated linear regression lines was used for convenience.

Considerable variation in response time is apparent between and within reaches (Table 5.7). Lowest response times were obtained from 1A where tracers did not interact with the bars, but remained exclusively within the submerged channel. At 2A an interesting anomaly is apparent with < 64 mm clasts rapidly removed compared with smaller particles. This is associated with the low recovery rate of < 32 mm clasts from set III (seeded in 2A), pertaining to a 60% deviation away from $M_{t,32} + F_{t,32} = 1$ after the first hop. Response times at 3A are in excess of those at 1A and 2A indicating storage dominance. In addition, Γ_i at 3A is a function of the delivery rate of sediment from upstream where more rapid delivery increases the probability of the response time being reached sooner. 2B is the most active sub-reach in B mainly due to very active pool storage. Data were sparse for 3B due to the lack of material transferred to this sub-reach. A detailed breakdown of these results is presented in section 5.3.5.

			Response time Γ_i (min.)				
Sub-reach	*1A*	*2A*	*3A*		*1B*	*2B*	*3B*
<180	7330	14600	∞	**<90**	∞	∞	0
<64	5400	5580	c.47600	**<64**	209000	180000	∞
<32	5450	12000	36150	**<32**	137730	75040	54380

Table 5.7. Sub-reach response time according to grain size. Reduced grain size classes are used to increase the number of tracers in each class per sub-reach and hence the accuracy of Γ_i.

Movement of sediment from seeding sites in sub-reaches 1 and 2 can be conceptualised for both reaches as waves of sediment transferred through sub-reach 3. Figure 5.24 a,b describe the changes in storage at time t relative to $S_{0,i}$ (t = 0 is 7400 and 8000 min. for reaches A and B respectively). Sediment waves for each tracer fraction propagate downstream with a size related velocity. At reach A, < 32 mm particles peak prior to the < 64 mm wave and the < 180 mm wave did not peak during the study. The < 32 mm wave attains a late peak in 3B whilst the < 64 mm clasts continues to ascend. This contrast with reach A represents a modification in wave behaviour with transfer

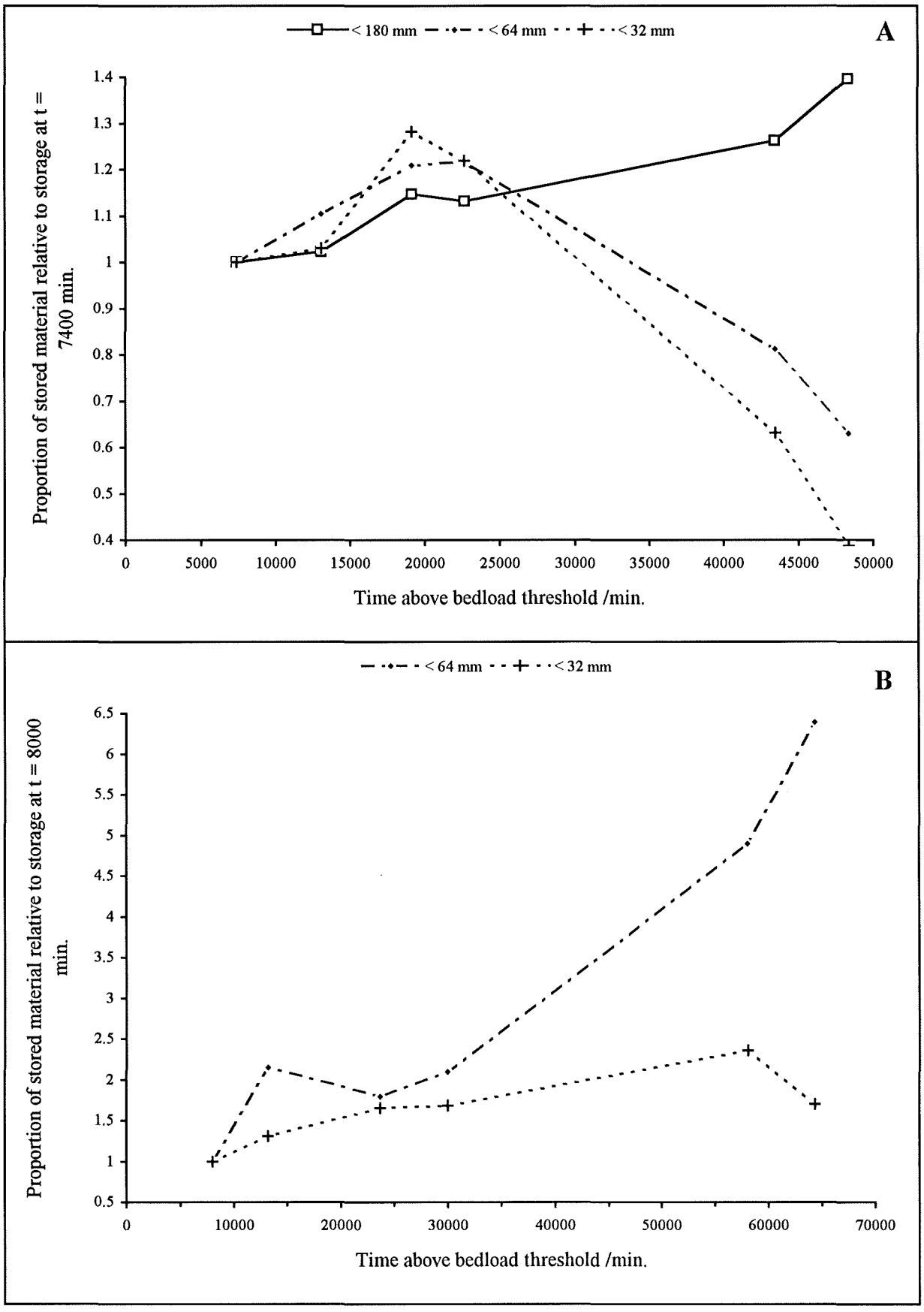

Figure 5.24. Wave-like passage of tracers through sub-reaches 3A and 3B.

downstream. Superimposition of these waves provides potential for modelling downstream fining (chapter 8).

5.3.3 Storage types

Stores defined according to shear stress would be expected to demonstrate contrasting storage and flux trends. This section aims to illustrate the contrasts in storage at the reach scale prior to a more detailed discussion of the stores at the sub-reach scale.

All storage types display contrasting behaviour in terms of tracer flux. In both reaches very active and active storage (where the tracers were seeded) degrade whilst semi active, stable and inactive aggrade (Appendix E4). The exact distributions are dependant upon storage type, hydraulics, storage definition and the number of available tracers. Static output also occurs, defined as a change in storage where a tracer does not move (section 5.1.3). In this case, immobility was defined as movement of < 1 m (the limit of the tracer data accuracy). Static transfer is important to fluxes between stores and will be dealt with in more detail in chapter 6.

Reference to the distribution of stored sediment in reach A during the study (Figure 5.25a) reveals the dominance of stable storage. This reflects both the extent of the storage type and the dominant fluxes within the reach. Most sediment transferred within more active stores is deposited in the relatively accessible low elevation stable bar store. Semi active storage dominated at reach B (Figure 5.25b) reflecting the spatial dominance of this storage type, especially downstream of the seeding sites. The remaining material was stored in the submerged channel divided equally between active and stable storage. The decline in semi active and increase in active storage at 68000 min. is a result of static transfer where the expanse of active storage increased at the expense of semi active between surveys 3 and 7 (Figure 5.13, 5.14).

The output of sediment $Q_{t,i}$ from one store into another store increases with storage activity in both reaches (Figure 5.26, 5.27). This is partly due to seeding of tracers in very active and active storage, although, this material would not have been transferred if the stores were not competent. The decline in transfer with time is a function of progressive sediment evacuation reducing the numbers available for transfer. The dominant transfer store at reach A is active with semi active prominent at B. In general there is a gradual decline in output from active to stable storage in reach A, with a less obvious progression in B.

Most stores transfer more fine particles with exceptions due to small samples in storage. Fitting of monotonic curves (e.g. Bunte 1992) to the output trends is not instructive due to the dependence of $Q_{t,i}$ upon $S_{t-1,i}$. For example, stable storage in reach A contains most sediment and has an

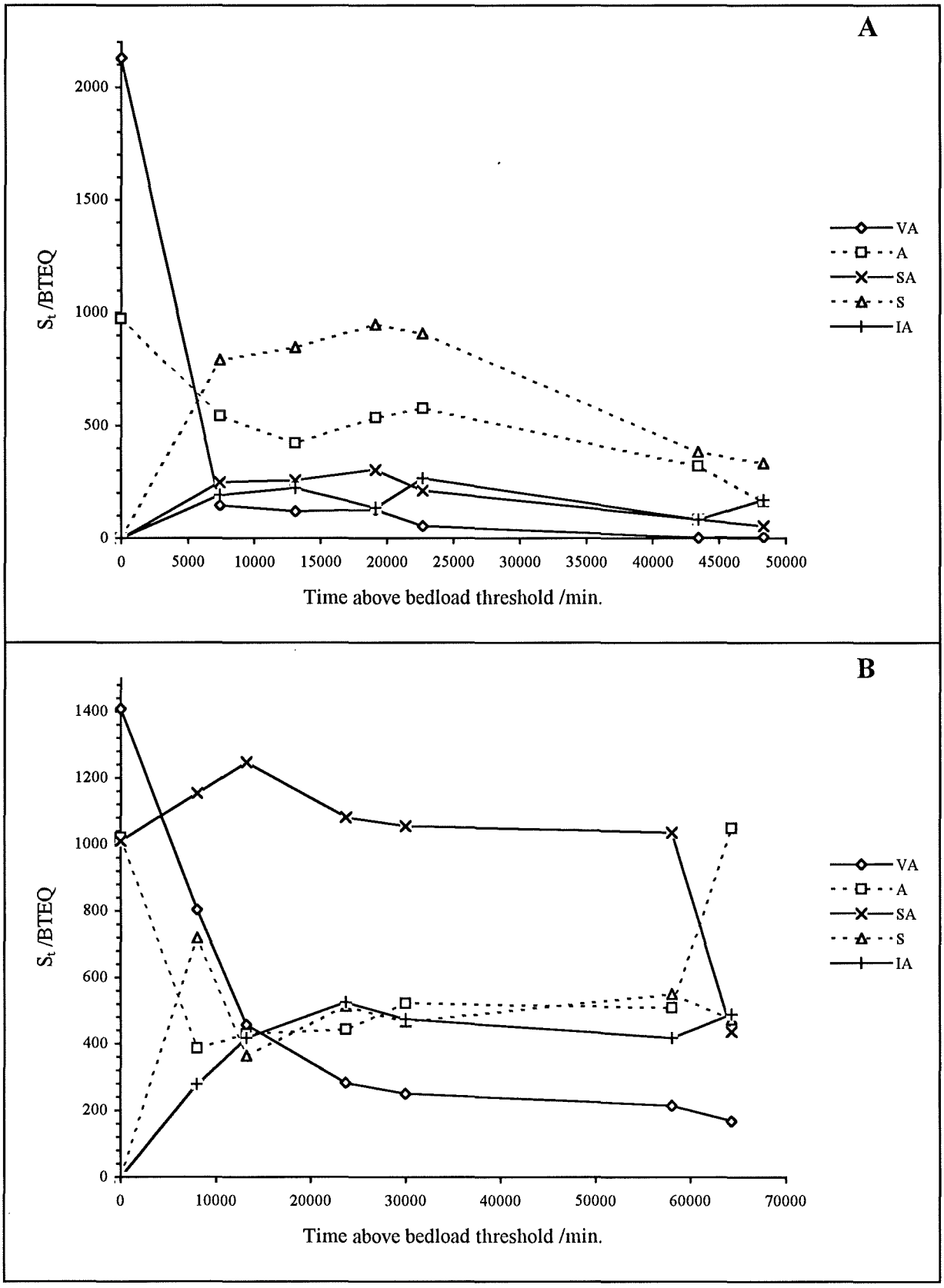

Figure 5.25. Reach distribution of stored sediment S_t according to storage type.

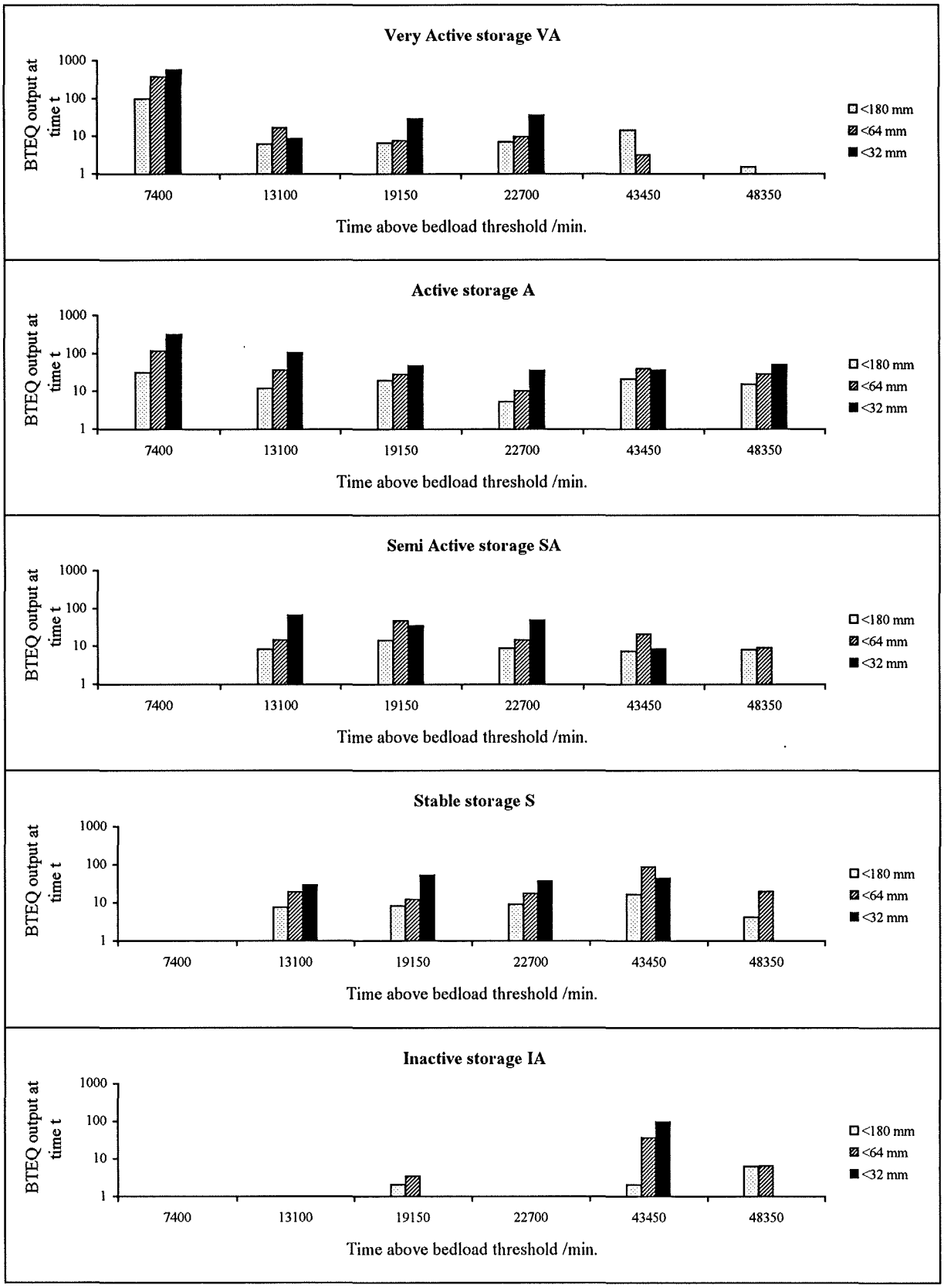

Figure 5.26. Reach A BTEQ output from storage per grain size class. Static output is excluded due to tracer immobility. By definition, static transfer involves transport distances of less than 1 m and is not a direct output flux.

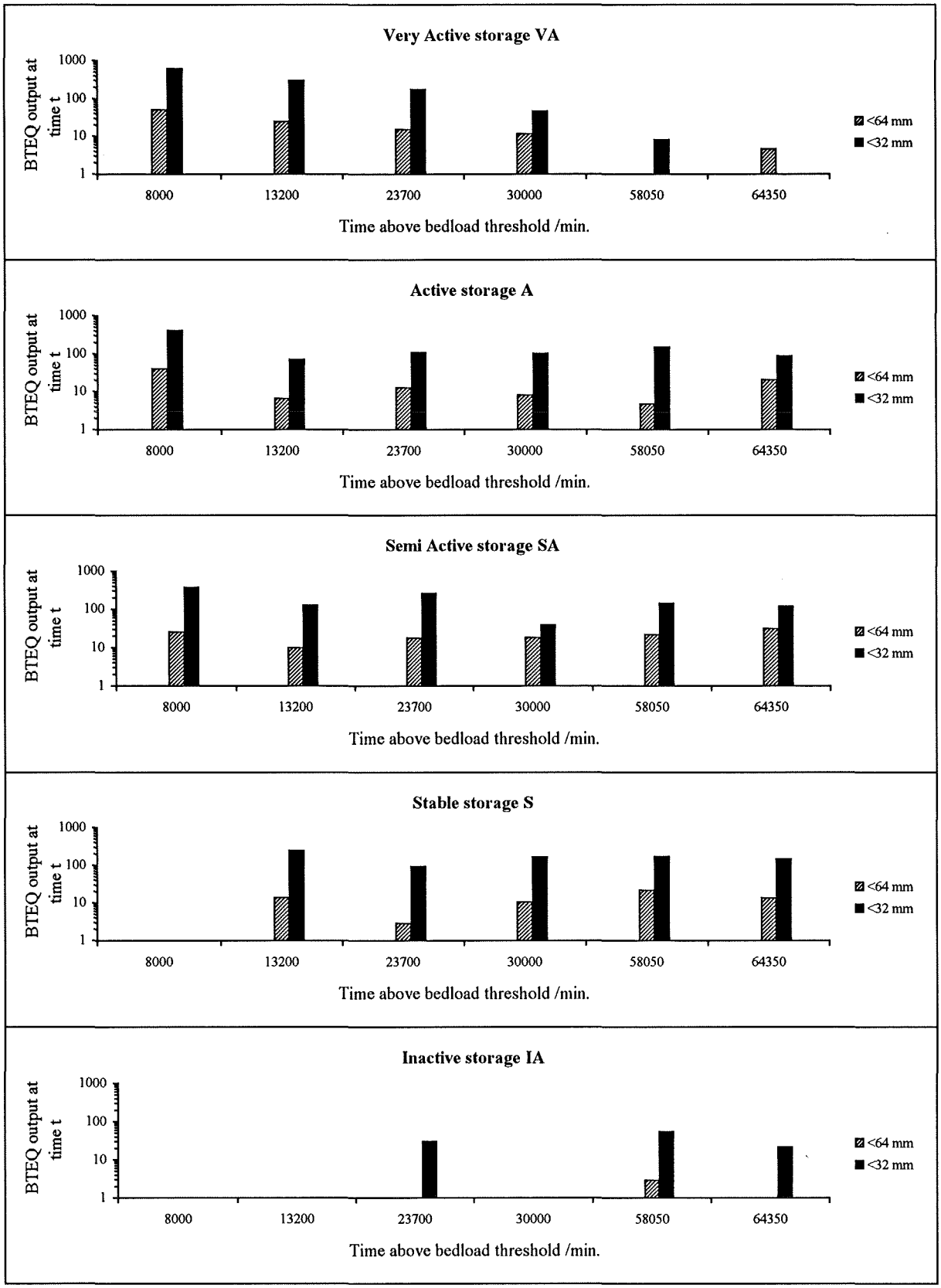

Figure 5.27. Reach B BTEQ output from storage per grain size class, static output is excluded due to tracer immobility.

apparently high output. However, $Q_{t,i}$ expressed as a proportion of $S_{t-1,i}$ does not indicate activity comparable with semi active or active storage. Instead, Γ_i should be used as this utilises both storage and output.

Γ_i is determined from the intercept of $S_{t,i}$ and $G_{t,i}$ curves (Appendix E5). Where two storage peaks occur, especially at reach B, then no value is assigned. The general results indicate that Γ_i decreases with increasing storage activity and smaller grain sizes (Table 5.8). Some anomalies do appear, but are mainly due to recovery rate errors and lower sample sizes (especially inactive storage, reach A). The trends at reach B indicate general activity in most of the storage types with a large amount of data missing due to deviation between storage and input curves. The apparent activity of < 32 mm clasts in stable storage is a function of the nature of the store. These are fine grained moderate elevation stores (see Section 4.3.2) located at the periphery of the submerged channel. As a result there is frequent mobilisation of stored material since τ^*_c is exceeded more frequently than in other stores.

	Response time, Γ_i, (min.).					
	Reach A			Reach B		
	<180	<64	<32	<90	<64	<32
VA	4450	4310	5600	30000	9800	9600
A	17700	9600	7900	NA	NA	NA
SA	20600	39700	22000	62000	47800	58050
S	42450	44800	46350	∞	∞	19600
IA	c.55000	43500	36500	∞	∞	∞

Table 5.8. Reach response time derived according to storage type and grain size. NA indicates a bimodal storage distribution, ∞ indicates divergent $S_{t,i}$ and $G_{t,i}$; Γ_i is estimated where curves intersect outside the study period.

Further analysis of the trends in storage can be carried out using turnover time, $T_{t,i}$ (Bolin and Rohde 1973). This is defined as the ratio of the total sediment in storage divided by the output flux rate. Under steady state conditions (input of sediment to a store equals output) this is equal to residence time. Sediment output rate for the period t-1 to t, $Q_{bt,i}$, was calculated as

$$Q_{bt,i} = \frac{Q_{t,i}}{\Delta t} \tag{5.11}$$

Turnover time was determined in the same way as Bolin and Rohde (1973), where,

$$T_{t,i} = \frac{S_{t-1,i}}{Q_{bt,i}} \tag{5.12}$$

The steady state assumption is invalid for this study due to the constantly changing relative proportions of storage and output per search. Instead, $T_{t,i}$ provides detailed information concerning fluxes of sediment at discrete time intervals within predefined areas of the river. Results derived from $T_{t,i}$ are contradictory. At reach A, $T_{t,180}$ is less than corresponding values for finer sediment, an inconsistent conclusion compared with Γ_i. This was also the case at reach B although the trends were less well defined. These results suggest that $T_{t,i}$ is too sensitive, depending on sample size and recovery rates between time t-1 and t. $T_{t,i}$ was derived on the basis of a steady state, which is not the case in either reach A or B. The results are therefore of little value.

The dominant transfer store in each reach containing significant sediment (so excluding the very active store) can be used to demonstrate the contrast in activity between reach storage. Γ_i is almost five times longer in the semi-active store in reach B than the active store in reach A. The majority of material stored in these riffle zones in B is fairly immobile. Conversely, active stores in reach A tend to transfer a large amount of the imposed material (Figure 5.26). The constantly changing amount of sediment in active storage indicates interaction with other stores, whereas reach B tends to store sediment and slowly release it. Interaction between stores is a reflection of the greater activity and channel morphology at A. This interaction and the effect upon sediment fluxes will be examined at the sub-reach scale in the next sub-section.

5.3.4 Sub-reach storage types

This section presents a spatially disaggregated description of storage type activity and provides explanation of the trends between sub-reaches. The small scale trends make up the overall pattern and must be examined before inferences can be made about reach scale storage characteristics and sediment fluxes. Each sub-reach will be discussed separately with focus concentrated upon the broader trends. More detail is presented in Appendix E6, documenting storage changes during the study and Appendix E7, presenting cumulative output (dynamic output only) and storage curves.

i) Reach A, sub-reach 1. Very active storage transfers most input sediment. Of the seeded tracers, c80% of the < 180 mm and c90% of the < 64 mm clasts were transferred after the first hop. Only 55% of the < 32 mm clasts were evacuated, 5% remained in storage implying a 40% error due to recovery rate as reflected by the high value of Γ_i (Table 5.9). Of the transferred < 32 mm clasts, very few remained in this sub-reach indicating a high sediment velocity with evacuation without further storage.

In general this is a transfer based sub-reach, by the end of the study period most of the input sediment had been evacuated. Γ_i increases with grain size and decreases with storage activity. Sediment is largely confined to the submerged channel; stable and inactive stores receive very little

sediment, the latter none. This suggests that two factors characterise sediment storage and transfer: firstly, sediment for bar development derived from upstream of the sub-reach; secondly, sediment transfer takes place in the submerged channel in response to the location of these bars.

ii) Reach A, sub-reach 2. Like reach 1A, most sediment was immediately expelled from very active storage, although a low recovery rate caused higher than expected Γ_i for < 32 mm clasts (Table 5.9). Response time for active storage is unusually high resulting from the detailed morphology within this storage type in sub-reach 2A. Active storage is made up in part by pool head and tails and avalanche faces. Sediment activity is reduced in these zones where deep burial is likely, hence the long Γ_i value. Semi active and stable stores aggrade (in terms of sediment in total, see Appendix F), gradually releasing sediment during the study. The inactive storage also aggrades but does not release much sediment.

The overall pattern of increasing Γ_i with storage type is consistent with the rest of this study. However, morphology within the storage types complicates these trends. This reach is less transfer based than sub-reach 1, a result of the zero input to the latter after t > 0. Response times are significantly shorter than the study period suggesting a significant, yet gradual (after hop 1), input of material into sub-reach 3.

	Response time Γ_i						
	Reach A				**Reach B**		
Sub 1A	**<180**	**<64**	**<32**	***Sub 1B***	**<90**	**<64**	**<32**
VA	4080	3950	4900		0	27200	21000
A	6400	5100	4400		NA	NA	NA
SA	21100	26500	0		60900	46500	60000
S	NA	34000	0		>70000	62300	28800
IA	0	0	0		0	0	>70000
Sub 2A				***Sub 2B***			
VA	4280	4350	5600		30500	10300	9100
A	26500	31000	32300		NA	48200	14100
SA	20100	16500	19700		∞	52000	44500
S	17900	24700	18200		∞	58200	59000
IA	∞	48350	43450		∞	∞	∞
Sub 3A				***Sub 3B***			
VA	0	21000	10100		0	NA	17100
A	45900	33600	27900		0	NA	NA
SA	18400	22300	29100		0	NA	63500
S	>50000	40080	39200		0	NA	NA
IA	>50000	41600	35200		0	0	0

Table 5.9. Sub-reach response time (in mins.) according to storage type and grain size. NA values indicate two peaks in storage, 0 values refer to stores into which no sediment of fraction i was input. Approximate data are presented where response time is likely to be attained after the study period.

iii) Reach A, sub-reach 3. This was a storage dominated reach. All material input to the very active store was rapidly transferred by the unstable pool complex at the tail of the reach. Active and semi active stores aggraded with a moderate output consistent with the general aggradational nature of this sub-reach; consequently, Γ_i (Table 5.9) was higher than sub-reaches 1 or 2. Stable storage aggraded until 43450 min. after which, S4 was reworked and a large amount of material (particularly < 32 mm) was output from the reach. Inactive storage accounted for a significant proportion of the sediment input to 3A, the majority being > 32 mm, a consequence of flood duration and source area characteristics (see chapter 7).

Sub-reach 3A displays the greatest interaction between tracers and inactive and stable storage. Whereas 1A and 2A contain fixed bars, formed in response to flow, the bars in 3 are free, tending to migrate and undergo regular reworking. Whilst remaining an important supply of sediment, morphology in 1A and 2A did not change suggesting that alteration to 3A (section 3.4.4) was in response to sediment supply from an upstream throughput load. This will be discussed in relation to volumetric changes in the following chapter.

iv) Reach B, sub-reach 1. All reach B sub-reaches display less activity than the corresponding reach A sub-reaches. Very little sediment was input to very active storage in 1B, hence Γ_i (Table 5.9) is not reliable. No data were available for active storage due to the occurrence of two storage peaks. Semi-active storage at this scale, as for the whole reach, tended to aggrade (in terms of tracers) with a moderate output rate. The high Γ_i for < 32 mm clasts is due to vertical winnowing. The semi-active riffles in this sub-reach have coarse surfaces and no fine matrix (sample B1, section 4.3.2.) allowing incorporation of finer clasts within, rather than on the surface. The apparent mobility of < 32 m clasts in stable storage is due to contrasting morphology. Fine particles are deposited as scour accumulations downstream of shallow pools whilst coarser particles were associated with low elevation bar peripheries. The fine grained stable accumulations were temporary giving rise to low Γ_i value for < 32 mm clasts. Bar II (Figure 3.10) comprised the only inactive storage in 1B, any particles deposited here were not released.

v) Reach B, sub-reach 2. Storage trends are very similar to those for 1B. There is a gradual increase in Γ_i as storage activity declines and grain size rises. Like 1B, sediment stored in active, semi active and stable stores tends to be closely grouped in terms of activity. This is a result of the narrow range of shear stresses within the active channel. Variations occur mainly as a result of small scale morphology such as the fine shoals of stable sediment. The riffle sites (semi active) are not as coarse and devoid of fines as in 1B so finer material tends to be more active (e.g. B3, section 4.3.2). These are all small scale trends making interpretation of results from the active channel difficult. Generally, apart from very active and inactive storage, intermediate stores in sub-reach 1B and 2B do not contrast. Very active stores have fairly high Γ_i values compared with the pools

from reach A. Many installed tracers were buried in the pool rendering them almost entirely immobile, giving longer response times at such sites. In addition, tracer distributions at reach B were coarser relative to the bed than at reach A (Table 5.3).

vi) Reach B, sub-reach 3. Very few firm conclusions can be made from this site due to the small number of tracers stored. However, it is apparent that all tracers remain in the submerged channel. This is characteristic of the whole of reach B, in which fixed bars dominate. Rather than functioning as active storage features, these bars tend to dictate flow directions in the submerged channel and therefore influence transfer in more active stores. Flow conditions within the submerged channel show very small differences, compared with reach A. As a result, the storage and transfer characteristics are better defined according to storage at reach A than B. However, even within these broader classes in reach A, morphological irregularity has a significant role (e.g. active storage in sub-reach 2A).

5.4 Discussion

This chapter has introduced a framework for description of within reach sediment budgets in gravel-bed rivers. Storage is classified according to shear stress and therefore potential for bedload transfer. The resultant six storage types broadly relate to morphological features allowing an assessment of the factors dominating storage and transfer fluxes. Tracers scaled to match bed grain size distributions were used to assess channel activity at a range of scales. The most useful discriminatory parameter is response time, Γ, which shows the contrast between reaches A and B with sediment up to three times more mobile within the former. Finer sediment was evacuated faster than coarser fractions indicating selective transfer at both sites. The sub-reaches confirmed that these trends were consistent at a reduced scale. Reach A was characterised by two transfer dominated upper sub-reaches and a storage based lower sub-reach where tracer waves propagate through the system with velocity inversely related to grain size. These waves were also apparent in reach B, although the velocity of propagation was considerably lower. This contrast in sediment mobility and wave propagation provides the possibility for explanation and prediction of downstream fining (see chapter 8).

Accurate transit times at sub-reach and storage scales could not be determined due to the difficulties associated with use of sediment age rather than 'real' time; instead, response time was used. This variable has advantages over both transit and turnover times, principally, the use of 'real' time rather than age in a fluvial environment characterised by variable flood magnitudes. In addition, turnover time is based upon an unrealistic steady state assumption and is too sensitive to tracer recovery rate, tracer numbers and relative $G_{t,i}$ and $S_{t,i}$. Calculation of response time utilises both storage ($S_{t,i}$) and output data ($G_{t,i}$), each being implicitly linked to the other. Use of both

variables provides an accurate measure of storage activity and fractional contrast, which use of each variable in isolation would preclude due to exhaustion effects.

Activity in both reaches (defined using Γ_i) declined from very active storage through to inactive, although this was not a regular decline, especially in reach B. Intermediate stores at reach B display very similar patterns of activity, attributable to two factors. Firstly, the narrow range of grain sizes and low range of excess stress (compared with reach A) results in little variation in local τ^*_c within the submerged channel. Secondly, in both reaches, micro-morphology such as fine grained gravel shoals and coarse surface layers tend to decrease the effect of differences in τ (upon which storage is based). Implicit in this is grain size, a dynamic factor very difficult to assess at such small scales. Submerged channel storage requires detailed definition on the basis of the wide range of morphology and narrow range of shear stresses (an irregular SSI interval was used for active, semi active and stable storage). Time averaged data indicate that over a long period the effects of shear stress, grain size and morphology tend to cancel out with resultant equal activity.

Tracer dispersion patterns were dominated by the location of fixed bars. Few particles interacted with these features in reach B or sub-reaches 1A and 2A. This lack of sedimentary integration implies that forced bars are largely inactive semi permanent features only changing in response to extreme flood events. Such features were mobile in the past, not always situated at present day locations (section 3.3.3 and 3.4.3), but on short time scales in the absence of major floods, fixed bars are stable and semi-permanent. Reach 3A was dominated by free bars migrating within the reach, consequently a number of tracers were incorporated within bar frameworks. Free bars tend to store sediment for shorter periods than fixed features. Once formed, fixed bars tend to only activate through lateral erosion or aggradation (static transfer) during extreme floods. In the short term, stored sediment is not returned to the active system, but these bars tend to shape hydraulics in the adjacent channel.

5.5 Conclusions

1. Sediment storage within the confines of reach boundaries can be successfully categorised using a surrogate measure of shear stress. Sediment redistribution between stores was quantified by scaling tracers to a BTEQ proportional to the grain size distribution of the active layer at the installation site.

2. Reach sediment output is a function of grain size and hydraulics. Transfer in reach A was greater than B due to contrasting reach slope and grain size distributions.

3. This chapter has introduced a new analytical tool, the response time Γ defined as the point in time when cumulative output of tracers exceeds the amount remaining in storage. This variable can be used to make an assessment of the speed at which a reach or store can evacuate sediment and provides comparison at various levels of resolution.

4. Tracer transfer at the reach and sub-reach scale is implicitly related to grain size. A hiding factor calculated from response times indicates deviation away from perfect equal mobility in reach A. Errors due to tracer exhaustion (a result of size selectivity) were minimised since response time is based upon 50 % output which was reached fairly rapidly.

5. Fluxes from storage are related to the SSI characteristics of the particular storage type. These trends vary according to local morphology, particularly the location of fixed bars.

6. Tracers move downstream as waves of sediment with velocity of propagation inversely proportional to grain size. Movement of waves of sediment according to grain size may form the basis for modelling and prediction of downstream fining.

7. Sediment transfer patterns are a function of grain size, reach activity, imposed flooding and storage type. Chapters 6 and 7 assess the extent of the relative importance of these variables and the interrelationships between them.

6. Sediment redistribution fluxes

This chapter describes tracer fluxes between stores and assesses causal mechanisms. Volumetric data are used to identify the distribution of morphological change and within reach volumetric flux rates. Comparison between the distribution of morphological change and tracer fluxes may reveal the relative magnitude of controls upon sediment transfer.

6.1 Calculation of sediment volume

The volume of stored sediment was calculated by interpolation of an irregular xyz grid, defined by cross section data, using UNIMAP. The boundary co-ordinates of the area of interest (either a store, reach or sub-reach) were input, UNIMAP then selected the data within the area and interpolated to a fine resolution. The exact dimensions of the interpolated grid were dependant upon the size of the area of the bed for which a volume was required. The interpolated elevation z1 at each node was then multiplied by the grid resolution (usually 0.1 m * 0.1 m), thereby generating the volume within each grid square, v_g. Summation of v_g resulted in V, the overall volume of sediment stored in the area in question. Net volumetric change was calculated for successive surveys by subtraction. In addition, the spatial distribution of erosion and deposition was determined by subtraction of z2 (elevation interpolated from data at t = 2) from z1 (interpolated at exactly the same grid resolution as z2). The result, Z2, net elevation change at each node, was contoured to reveal the extent of erosion and deposition between surveys (Appendix F).

The UNIMAP method has two main advantages over other methods of volume calculation from cross sections (e.g. the prism formula, Ferguson et al. 1992, Goff and Ashmore 1994). (1) it is computationally faster; (2) it is more accurate as interpolation replicates the bed surface on the basis of all points in the vicinity. However, there are drawbacks, firstly, interpolation is only as good as the data which it is based upon. Micro scale topography between or on a section may affect the accuracy (this applies to all methods of volume calculation from cross sections). Secondly, UNIMAP calculates volume on a square grid. For an irregular area containing incomplete cells the volume algorithm uses a ½ or ¾ of v_g depending upon the proportion of the cell within the area. Sensitivity testing revealed that this error is minimal, although it is a function of the interpolated grid size.

A further analytical unit was necessary to quantify the within reach sediment budget. Reach A was divided into 38 segments and reach B into 37. Segment boundaries were located after every third cross-section (Appendix F); cross section points contained within each segment forming the basis for UNIMAP interpolation. All segments were outlined relative to the reach boundary at t = 0 so that segment area remained constant for subsequent surveys. Three cross sections per segment

were more than adequate to calculate volume. For half surveys (only odd sections were surveyed), every other segment contained data from two sections with the remaining segments containing data from one. Sensitivity analysis compared the results from a full survey (survey 1) and half survey (every other section from survey 1) revealing that accuracy was not compromised, errors being less than 0.75 % and randomly distributed. The volume in each segment was calculated for successive periods allowing tracing of within reach sediment fluxes and calculation of bedload transfer.

6.2 Volumetric fluxes

Morphological change affects sediment redistribution within the confines of the reach and provides partial explanation for the distribution of sediment fluxes. Previous studies suggest that significant volumetric change (and hence tracer transfer) occurs in response to the highest discharges (Ashworth et al. 1992, Goff and Ashmore 1994); it is therefore instructive to evaluate the relationship between the distribution of erosion/deposition and stage. The role of flow duration is evaluated in chapter 7.

6.2.1 Reach scale volumetric change

Reach response to hydraulic conditions and imposed sediment loads is demonstrated by the magnitude of volumetric change. Alternate phases of erosion and deposition occurred in both reaches (Figure 6.1) with larger changes corresponding with the highest flows. These overall fluxes can be used to quantify the effects of hydraulic conditions (measured as peak stage) upon morphological change. As both variables are means sample variance is low. Fitted power functions indicate a significant relationship for reach A between peak stage H (m) and net change ΔS (m^3 - absolute values) where

Reach A:	$\Delta S = 166H^{2.66}$	$n = 6$	$r^2 = 0.69$	$p < 0.05$	(6.1)
Reach B:	$\Delta S = 7.50H^{9.24}$	$n = 3$	$r^2 = 0.79$	$p < 0.05$	(6.2)

The relationship for reach B is not reliable as n is small. The predicted relationships demonstrate that on average, morphological change is proportional to stage and therefore shear stress (Goff and Ashmore 1994).

The pattern of volumetric change in reach A is slightly misleading due to bank erosion. Erosion and bank foot deposition (section 5.1.4.1) increase and reduce ΔS respectively (Figure 6.1). Gravel sized sediment exposed by bank erosion is relatively immobile, a function of reduced shear stresses at the bank (Einstein and Barbarossa 1952, Carling 1983). This material does not immediately interact with sediment elsewhere in the reach (Goff and Ashmore, 1994) and may be excluded from

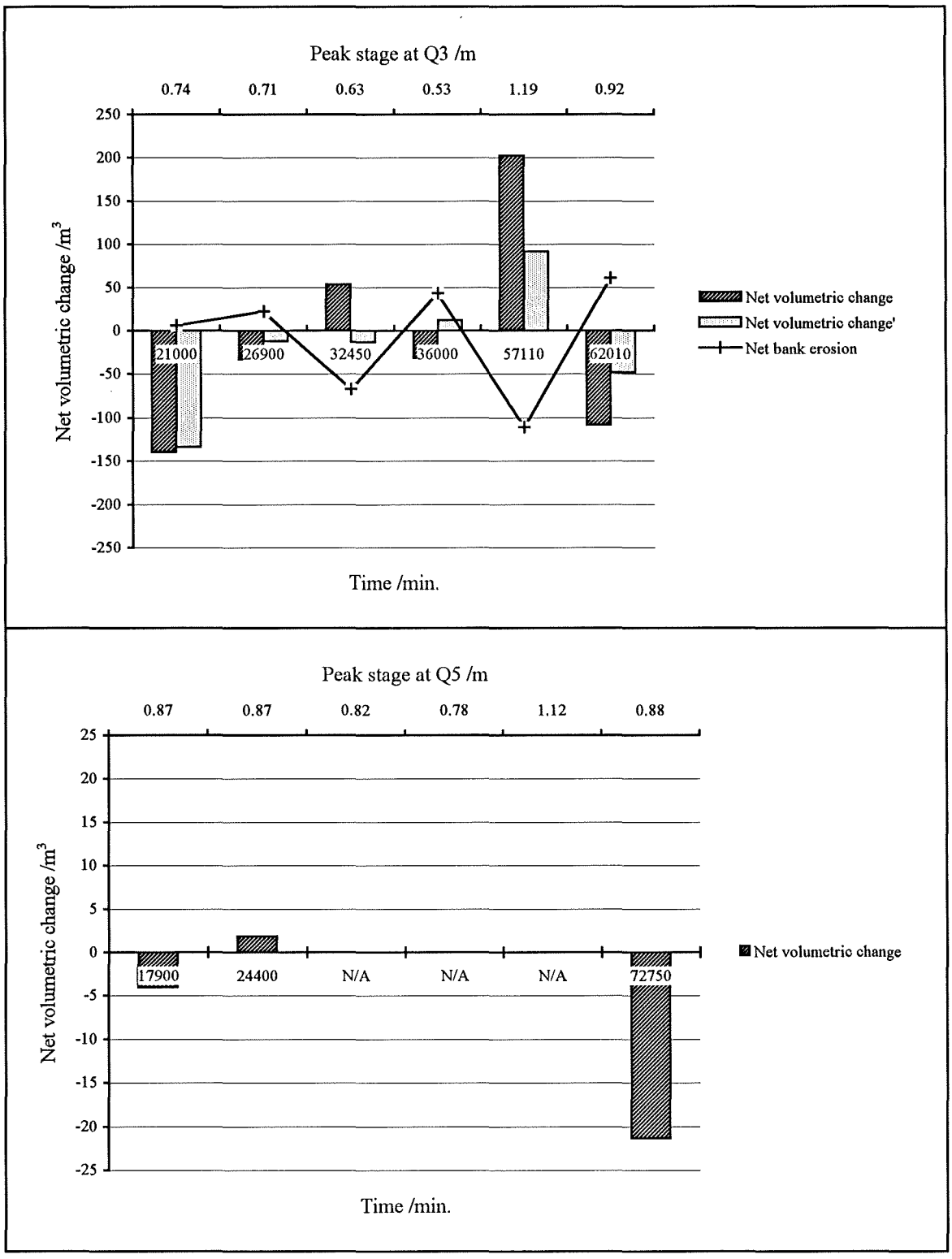

Figure 6.1. Net volumetric change in reaches A and B. Net volumetric change' at reach A excludes bank erosion (Eq. 6.3). No survey data are available for reach B between 24400 and 72750 min.

a short term study of within reach sediment fluxes. The volume of sediment stored for successive time intervals (t = 0 to 7) relative to the active alluvial area boundary at t = 0 (A_o') excludes bank erosion, facilitating meaningful comparison of sediment volumes within the channel and a calculation of the absolute and net volume of bank erosion. The net changes in sediment stored relative to A_o' at time t, $\Delta S_t'$ was calculated from

$$\Delta S_t' = V_t' - V_{t+1}' \tag{6.3}$$

where V_t' is the volume relative to A_o' at time t. The distribution of $\Delta S'$ differs slightly from ΔS (Figure 6.1) although the main erosive and deposition phases remain. The magnitude of net bank erosion ΔB_t (relative to erosion at t -1) is

$$\Delta B_t = (V_t - V_{t+1}) - \Delta S_t' \tag{6.4}$$

where V_t is the volume of sediment stored relative to the reach outline A_t. Two main phases of erosion are apparent (Figure 6.1) usually at the left bank between sections 1 and 20. Erosion is a result of fixed bar I (Figure 3.6) diverting flow towards the bank. Bar I has steadily aggraded since 1984 resulting in progressive erosion of the bank (Ashworth pers. comm. 1991). Aggradation of the bar has increased the angle of incidence and proportion of flow diverted towards the bank. This was exaggerated prior to 57100 min. where the bar prograded into the submerged channel (Figure 6.2), reducing channel width and increasing depth adjacent to the bank. In response the outer bank

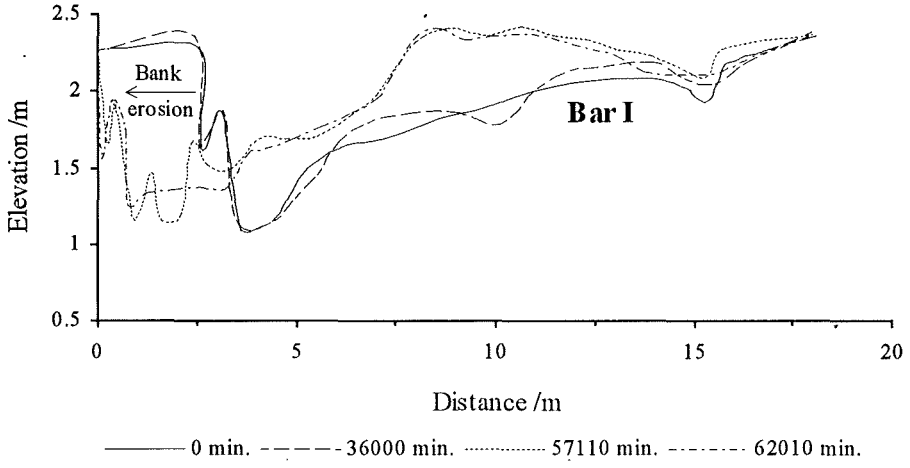

Figure 6.2. Repeated surveys of cross section 13, reach A. View downstream demonstrates erosion of the left bank and aggradation of bar I between 36000 and 57110 min.

eroded up to 2 m between 36000 and 57110 min., a maximum during this study. It is likely that this erosion occurred after deposition of material on bar I; as earlier surveys (Figure 6.2) indicate zero erosion between 0 and 36000 min. and no changes to the morphology of bar I. Bank erosion is

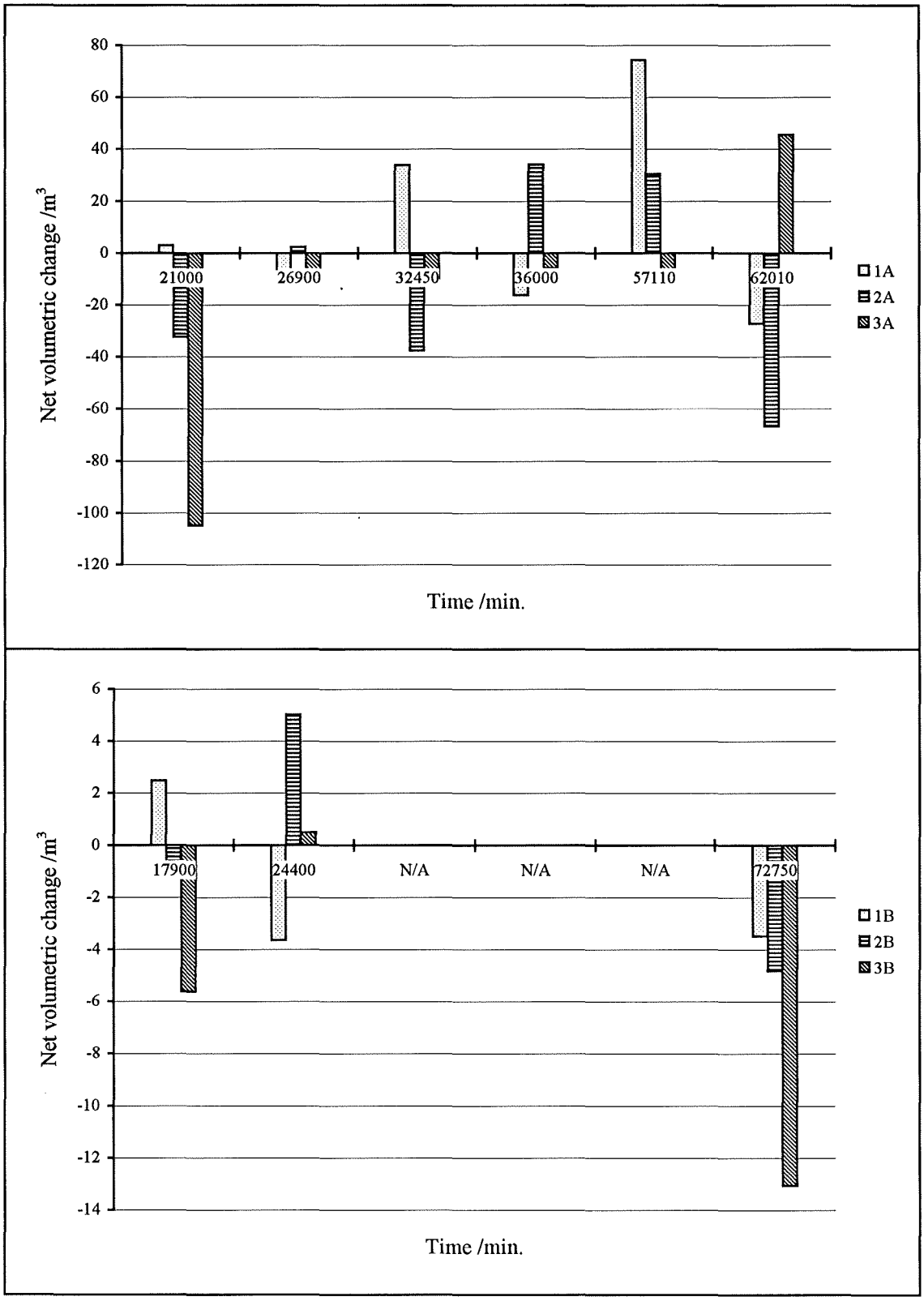

Figure 6.3. Sub-reach volumetric change. Reach A data excludes bank erosion. Note different vertical scales.

frequently reported in associated with bar migration/formation (Ferguson and Werritty 1983, Ashworth et al 1992). Reach A illustrates a mechanism for minor planform alteration based upon semi-permanent non-migratory accumulations of sediment, analogous with processes operating in meander bends (e.g. Thorne and Lewin 1979).

6.2.2 Sub-reach scale volumetric interaction

Net erosion, $\Delta S_t'$, in each sub-reach provides a break down of the fluxes discussed in the previous section. Erosion dominated sub-reach 3A (Figure 6.3), in apparent contradiction to the conclusion of storage dominance derived from the tracers (Chapter 5). The sediment loss was the result of repeated erosion of bar III (Figure 6.4), an area of the reach which did not contain tracers. This dormant store (Figure 5.2) did not receive sediment so the lack of tracers is representative of sediment fluxes during this study. Prior to 22700 min. changes to 1A and 2A were minimal, and confined to local erosion and deposition within the submerged channel. The fixed bars remained unaltered (Appendix F) confirming the conclusion from the tracers that fixed bars dominate flow patterns and hence transfer in the submerged channel. In reach B changes were much less than those at A reflecting the contrast in activity.

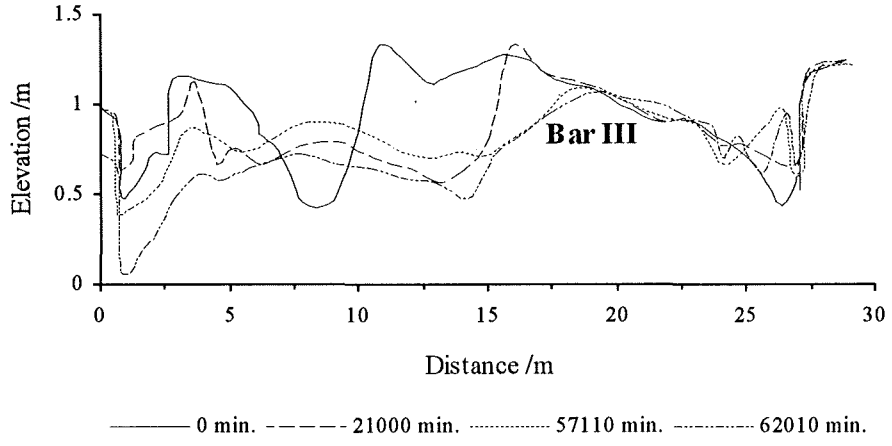

Figure 6.4: Repeated surveys of cross section 95, reach A. View downstream demonstrates erosion of bar III and reworking of channel sediments.

The following description of morphological activity is necessary to explain reach and sub-reach scale fluxes. Reference should be made to Appendix F.

Sub-reach 1A: Prior to 36000 min. morphological change was limited to the submerged channel where pool location changed in response to bank erosion. A more general phase of aggradation occurred between 26900 and 32450 min (Figure 6.3) due to an increase in submerged channel width associated with localised bank erosion (Figure 6.1). Major changes had occurred by 57110 min., material being deposited at the head of the reach as bar I prograded into the channel

(segments 2, 3, 4, 5, Appendix F, F5). After 62010 min., bar I was unaltered and some previously deposited sediment remained in the active channel presumably in response to increased channel width due to bank erosion.

Sub-reach 2A: The changes to morphology in 3A which occurred after 2 years of apparent stability (I. Drew pers. comm. 1991) are a consequence of upstream change in 2A. The riffle linking bars II and III (Figure 3.6, 6) was dissected between 0 and 21000 min. Prior to this, the riffle diverted approximately equal amounts of flow into right and left anabranches around bar III. Incision reduced flow to the right of the riffle allowing aggradation at the head of bar III to block the right anabranch. The left anabranch diverted flow adjacent to bar III resulting in major reworking of in 3A prior to 21000 min.

Further erosion occurred in 2A after 32450 min where the thalweg widened around the apex of the bend resulting in additional deposition at the head of bar III (Appendix F, F15). Widespread channel change occurred during snowmelt flooding in January 1993. The submerged channel widened in response to increased flow depths, a result of aggradation of bar II and subsequent constraint of flow. Initially this sub-reach was characterised by a single fixed bar and associated pool riffle units, but all except the bar disappeared during the study as submerged channel differentiation declined.

Sub-reach 3A: Associated with the upstream channel switch (21000 min.) was removal of a downstream bar complex (segments 36 and 37) and subsequent upstream deposition (store S4, Figure 5.3) probably in response to erosion of bar III. The reach gradually readjusted to the upstream changes prior to further alteration to morphology during the January 1993 flood (57110 min.). Eroded material from the submerged channel in 2A was deposited in the thalweg and S4 was eroded. Channel differentiation was reduced during this period with a decrease in width:depth ratio due to major aggradation (Figure 6.3) and the formation of IA6 (Figure 5.8) by 62010 min.

Morphological changes in 1A do not seem to affect 2A, possibly reflecting rapid transfer of material through this site. However, 3A was very sensitive to upstream changes indicating the transient nature of free bars in wandering systems compared with more stable fixed bars in 1A and 2A (meandering sub-reaches). Fixed bars remained *in situ* even though a major phase of aggradation occurred in 1A and 2A. These bars dominated sediment transfer within the submerged channel and are linked to changes in local and downstream morphology.

Sub-reach 1B: Fixed bars dominate this sub-reach and were unaltered by flood flows. Slight aggradation occurred periodically, field evidence suggesting deposition of gravel sheets a few grains in thickness (too shallow to be differentiated from cross sections). The only other change

during the study period was the evolution of the pool adjacent to bar V (Figure 3.10). This stability is reflected in low ΔS, the only interaction with 2B is a small throughput load which is demonstrated by tracer dispersion.

Sub-reach 2B: Morphological changes were a function of local conditions rather than upstream inputs. Deposition at the head of bar VI is a result of scour from the slowly aggrading pool upstream (plate 4.6). A downstream pool containing set III tracers degraded until 17900 min, with some of the eroded material forming a tail to bar VI.

Sub-reach 3B: The only change to this sub-reach was upstream migration of pool VA3 commencing after 17900 min.

All three sub-reaches in B indicate the importance of localised erosion and deposition. By contrast, volumetric changes at reach A are more widespread and are a response to upstream as well as local conditions. Upstream conditions at reach B operate at such a reduced scale that they are effectively localised. Minimal tracer movement distances confirm this (chapter 7).

6.2.3 Within reach sediment budget

Within reach flux rates between segments can be determined from sediment continuity where

$$Outflow_j = Inflow_j - \Delta S_j \tag{6.5}$$

where ΔS_j is the net volumetric change (erosion is negative) in segment j. The flux rate between segments is calculated relative to an assumed upstream boundary condition, either: (1) zero input to the reach (e.g. McLean 1990), or (2) a minimum value ensuring non zero transfer between all adjacent segments (Griffiths 1979). Segment output was calculated iteratively, input to segment 1 being altered until all outflow values were positive (method 2).

Downstream fluxes reveal the extent and relative magnitude of sediment transfer through each reach. The shallow flux gradient for the upstream part of reach A (Figure 6.5a) indicates that most material delivered into sub-reach 1A is transferred (except between 36000 and 57100 min.), hence the low response time values reported in section 5.3.2. The complex cross over of data at 40 m (bar II) is indicative of alternate phases of erosion and deposition in response to upstream sediment supply and local morphology (Appendix F). Downstream, increased fluxes in 3A result from erosion of bar III and the competence of the flow to transfer the eroded sediment, transfer is therefore locally supply limited. During other periods, reduced fluxes in 3A are a response to aggradation and sediment redistribution particularly at the head of bar III (Appendix F).

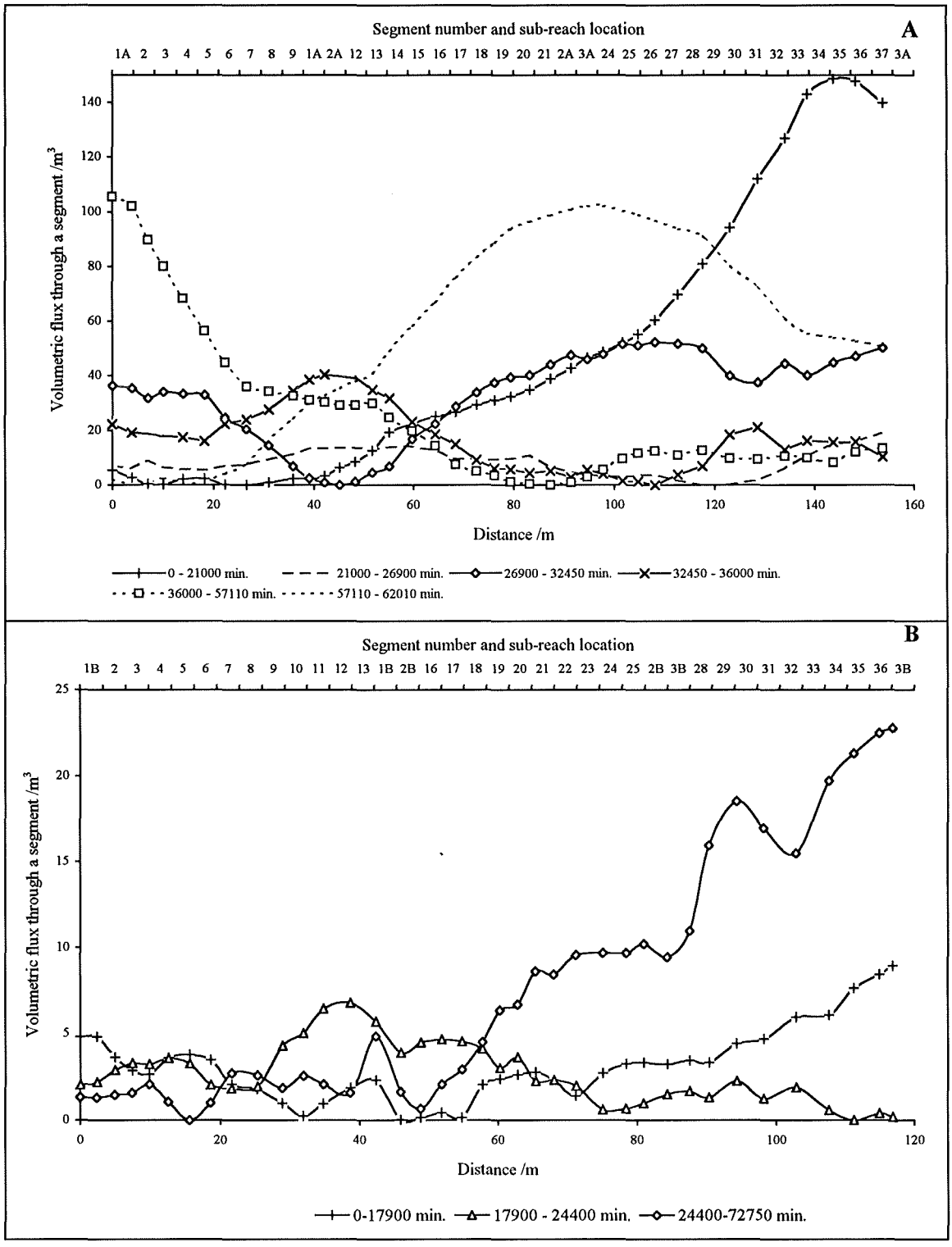

Figure 6.5. Volumetric flux between segments. Upstream boundary condition is set to ensure non negative fluxes (Griffiths 1979).

Fluxes in reach B are small relative to A with a maximum of 20 m^3. These irregular small fluxes reflect the dominance of local conditions upon transfer, rather than upstream influences. The larger flux between 24400 and 72750 min. has a stepped appearance corresponding with migration of two pools in segments 16 (46 m) and 30 (89 m). Flux increases from segment 16 onwards indicate that all the eroded material is transferred from the reach with no deposition. This apparent anomaly is a reflection of the long time scale between the two surveys and reflects the sensitivity of the data to time. Sufficient time was available for transfer of the small volume of sediment released by local erosion out of the reach.

6.2.3.1 Sediment waves

Net changes in segment volume in the downstream direction reveal the longitudinal and temporal form of major phases of within reach sediment transfer (Figure 6.6, 6.7). Reach B fluxes are minimal, with small scale peaks corresponding to pool migration. Volumetric flux in reach A is a function of bedload transfer, upstream supply and aggradational history. For example in reach A, between 26900 and 36000 min. a small scale bed wave can be seen to propagate downstream between segments 5 and 22. The wave was transferred in the active channel, without direct interaction with the fixed bars (Appendix F, F3, F10, F11), so the sediment was rapidly evacuated in subsequent floods (57110 min). Some was deposited in segments 30 and 31 (although the net change is erosive, there was also an area of aggradation, Appendix F17) classified as stable storage and remaining *in situ* until the end of the study. The wave propagated rapidly through 2A in the active channel prior to deposition in 3A where the sediment remained suggesting that wave velocity is a function of both shear stress and recipient morphology.

A larger wave propagated through reach A in the second half of this study with aggradation in 1A and 2A after 57110 min. followed by erosion and re-deposition in 3A, associated with a decrease in wave magnitude and increase in amplitude. Morphological change has been documented as a cause of sediment waves (Ashmore 1991, Young and Davies 1991) and it is probable that the source for this sediment was reactivation and reworking of an abandoned channel 100 m upstream. Two mechanisms can be proposed to explain the decrease in magnitude and increase in wavelength as the wave moved into 3A: (1) deposition of some sediment in fixed bars results in the removal of a proportion of sediment from the wave. Material in these bars remains in storage for longer periods of time (section 5.3.4), corroborating the results from sand tray experiments where the residence time of tracer sediment input as a wave and subsequently stored in less active storage was relatively long (Hoey, in press 1995). In addition, any wave sediment storage in less active stores in 3A will also decrease magnitude. These stores only release sediment in response to intense

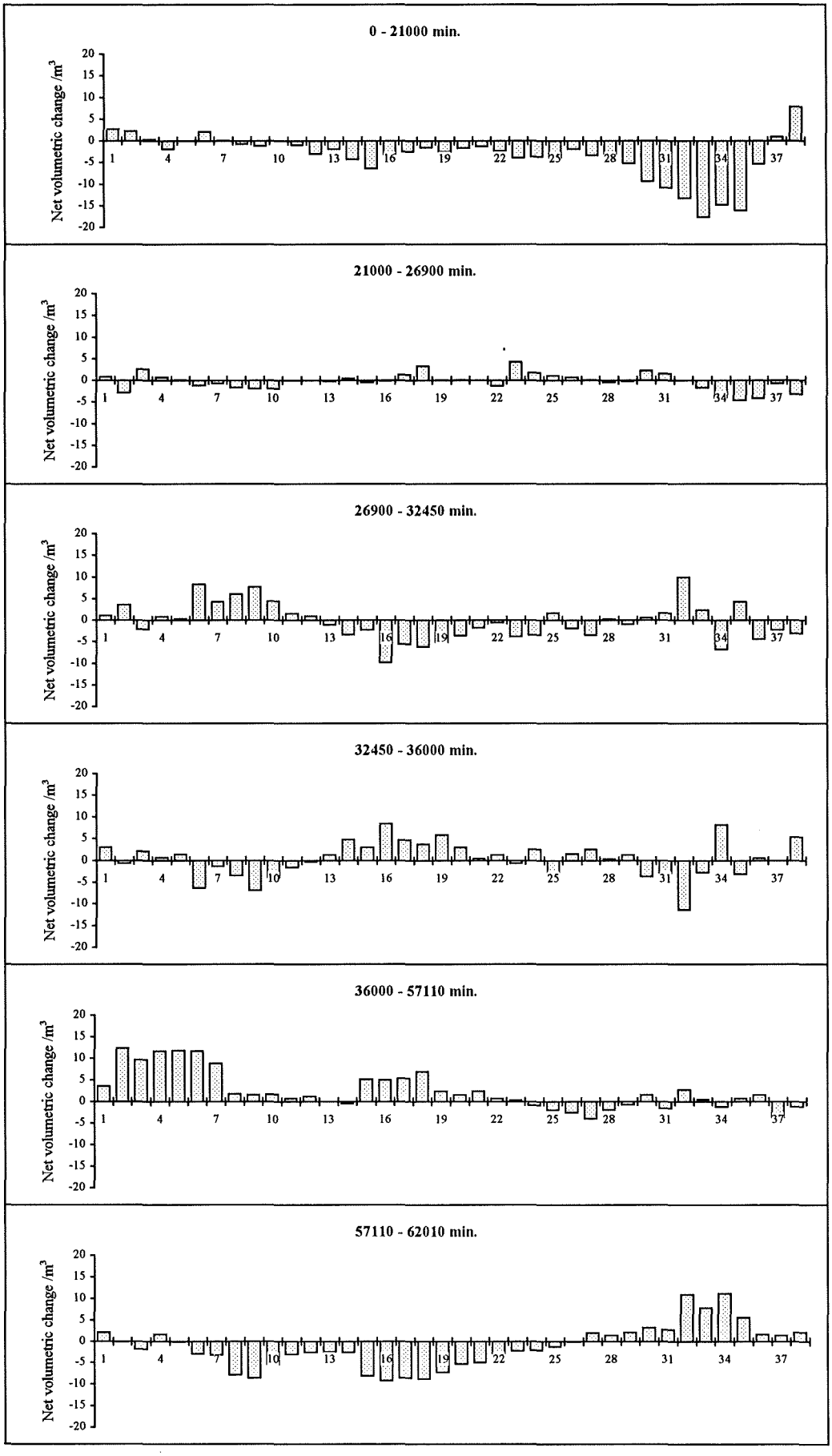

Figure 6.6. Net changes in segment volume, reach A. Segment number is plotted on the abscissa. Refer to Figure 6.5 for corresponding segment distances and sub-reach locations.

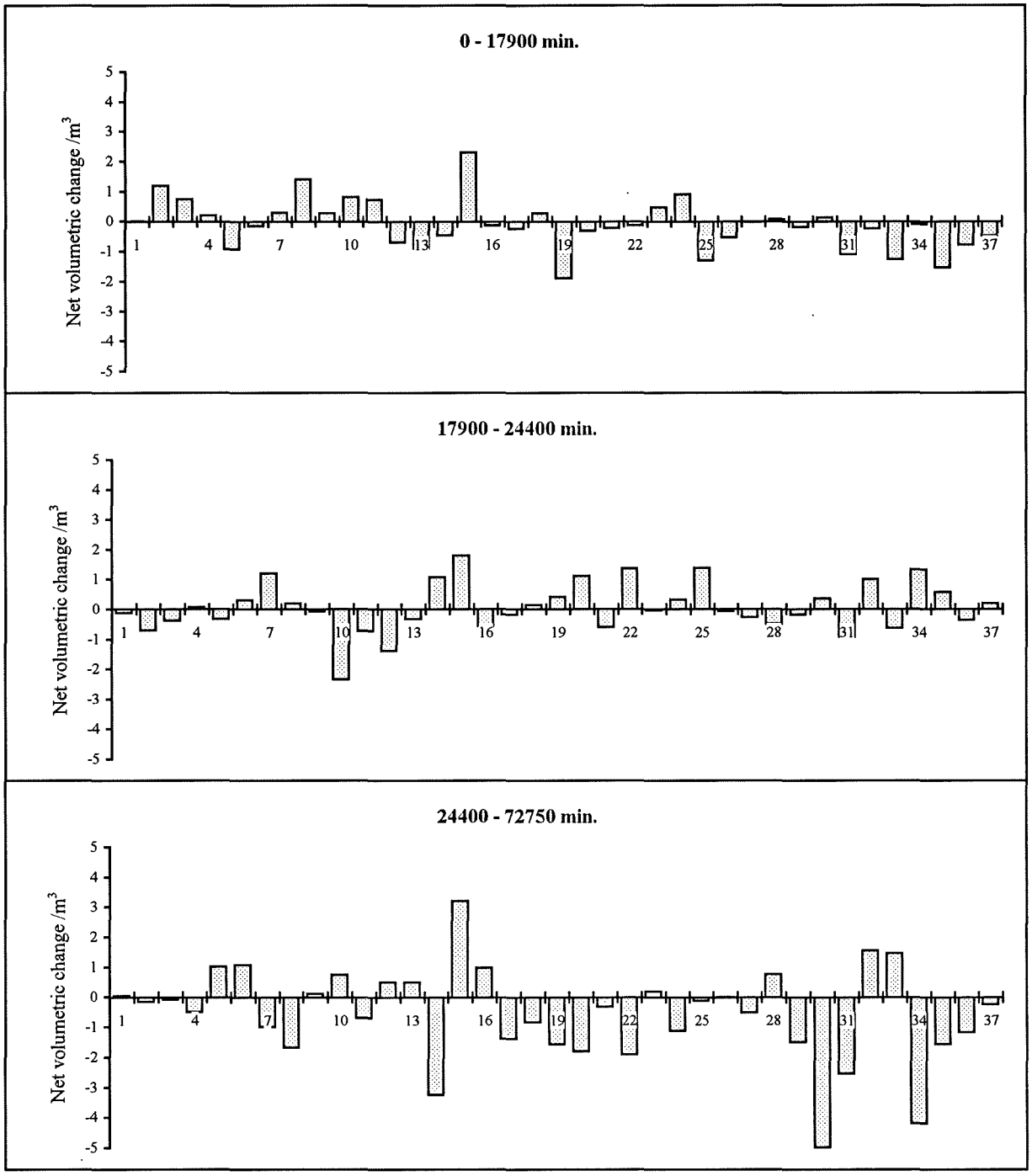

Figure 6.7. Net changes in segment volume, reach B. Segment number is plotted on the abscissa. Refer to Figure 6.5 for corresponding segment distances and sub-reach locations.

flooding; (2) once a wave of mixed size sediment is temporarily deposited, finer material is subsequently re-entrained at a more rapid rate than coarser material.

Reach A can be conceptualised as alternate transfer (meandering 1A and 2A) and storage (braided 3A) zones (e.g. Church and Jones 1982). These definitions are transient as, for example, the submerged channel in 1A and 2A dominates transfer due to the impact of fixed bars upon hydraulic conditions, but, any sediment deposition on fixed bars results in long term storage. Sub-reach 3A is storage based, responsible for increased attenuation of the sediment wave and a possible source area for smaller waves derived from morphological change. The apparent contradiction of a transfer dominated sub-reach containing a fixed bar and a storage dominated reach containing free bars demonstrates the value of a tracer and morphometric study in monitoring detailed sediment interactions.

6.2.3.2 Bedload transfer

Bedload transfer data are available from volumetric information using one of three methods (Goff and Ashmore 1994). The step length approach (e.g. Ferguson and Ashworth 1992, Ferguson et al. 1992) and erosion zones (e.g. Carson and Griffiths 1989, Kussner 1992) both require identification of step lengths and erosion cells. This would be difficult to apply to the Allt Dubhaig where step length is variable and dependant upon discharge (Ashworth 1987), grain size (Drew 1992) and the distribution of scour and fill (e.g. Hassan 1990). Therefore, in the absence of a single representative step length, a sediment budget approach was adopted, where mean bedload transfer was calculated on a spatially averaged scale (e.g. Goff and Ashmore 1994). Output from each segment was converted to mass using sediment bulk density (assumed as 2650 kgm^{-3}) multiplied by $1 - \lambda$, where sediment porosity, λ, was assumed to be 0.3 (Komura 1961). The transferred mass was width averaged and divided by channel length and time, giving a resultant transfer rate (q_b) expressed in $gm^{-1}s^{-1}$.

Downstream variation in transfer rate at both sites (Figure 6.8) reveals considerable scatter, reflecting the sensitivity of the calculation to width and time. Absolute values are comparable to the median of 21 $gm^{-1}s^{-1}$ upstream of A and 2 $gm^{-1}s^{-1}$ upstream of B reported for the Allt Dubhaig by Ferguson and Ashworth (1991). Maximum transfer rates at reach A are associated with the transfer of the previously described sediment wave from 2A to 3A, indicative of the instability which passage of these features produces within the channel. The relative pattern of bedload transfer at each site is a reflection of reach morphology and data sensitivity. Mean transfer rates derived from cross sections are useful in studies where erosion is limited to pool-bar units (e.g. the braided reach of the Sunwapta river used by Goff and Ashmore) or the thalweg (reach B). For

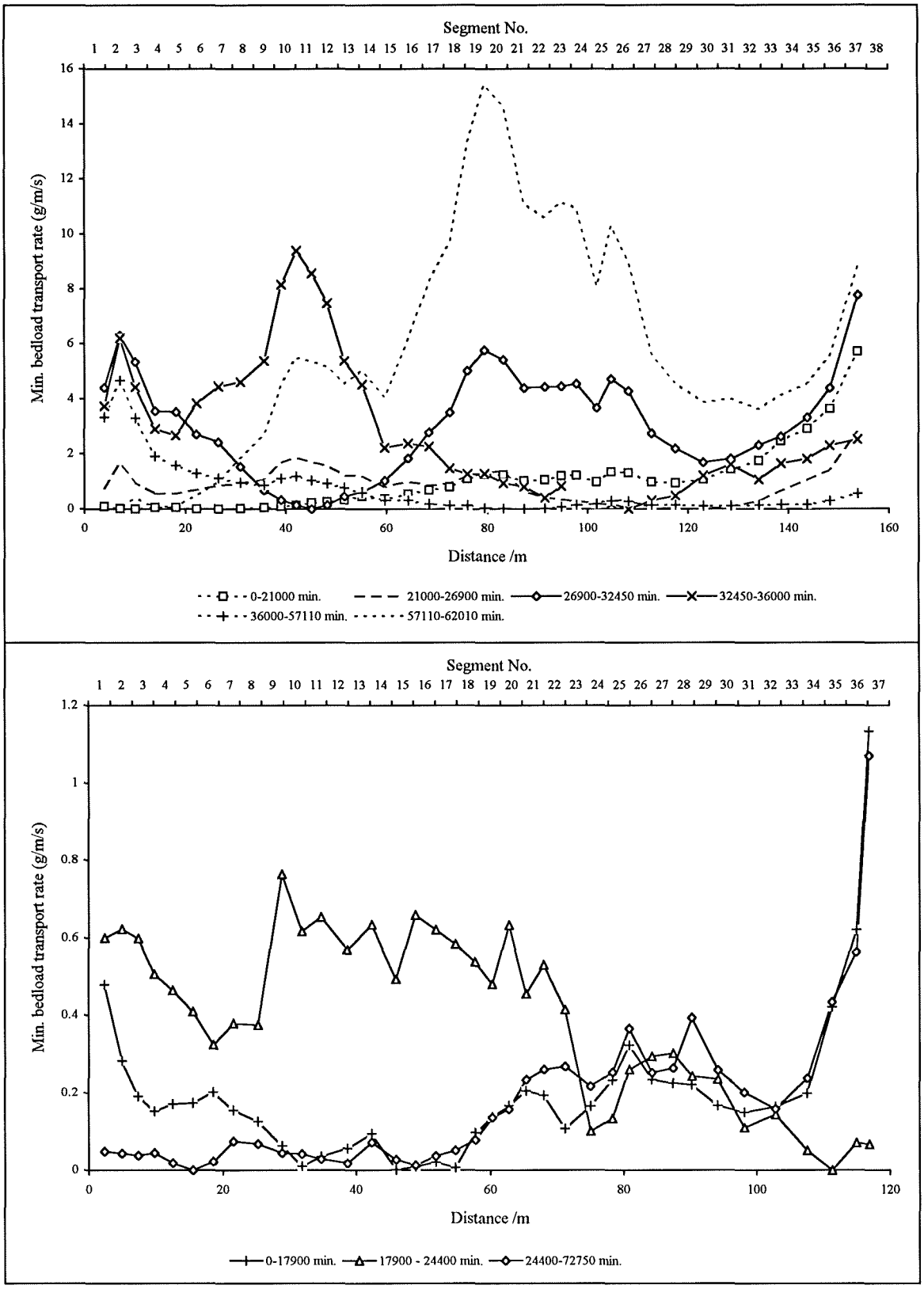

Figure 6.8. Downstream distribution in transfer rates calculated from within reach sediment budget in A and B.

larger more active reaches, coarse temporal resolution between surveys and within reach variability precludes identification of true fluxes.

Transfer rates at reach A were between ten and twenty times greater than reach B, commensurate with the contrast in activity. There is a poor correspondence between rates at B (averaged for each time period) and the bedload traps 100 m downstream (Figure 6.9). The disparity is due to the stability of B compared with the meandering thalweg and submerged shoals of sediment upstream of the traps. In addition, q_b calculated from segments is a minimum value due to the assumed boundary condition.

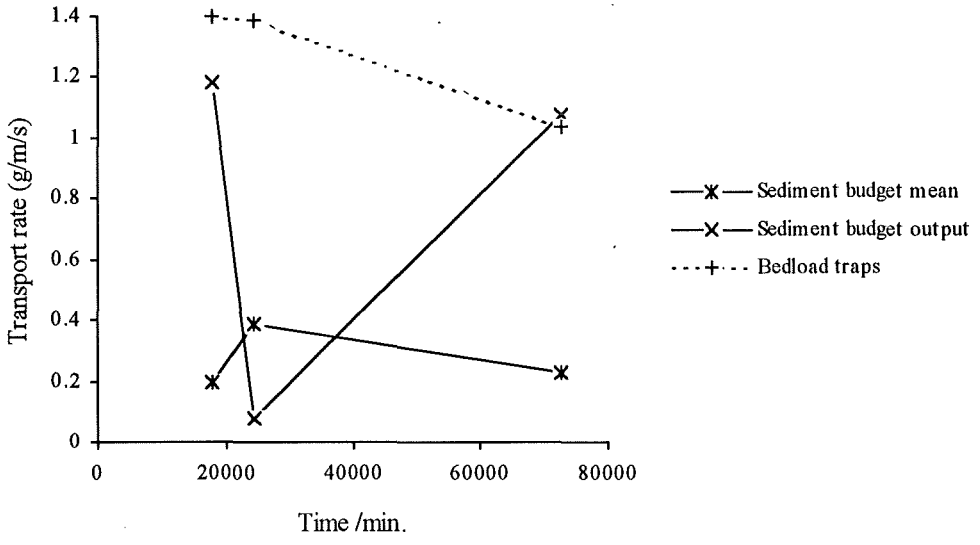

Figure 6.9. Comparison between estimates of transfer rate derived from sediment budget mean and output from section 37 in reach B with mean transfer rate derived from bedload traps during corresponding periods.

6.3 Tracer redistribution fluxes

This section evaluates the dominant sediment fluxes within and between sub-reaches according to flow conditions, storage type and grain size. These fluxes are implicitly related to morphological change and sub-reach activity. The aim of the analysis is to describe the fluxes relative to sub-reach factors and quantify the relative importance of each factor. The data will be presented as a series of matrices detailing the two dimensional transfer of sediment, the third dimension, burial, is assessed in chapter 7. Tracers were installed after the first cross section survey therefore tracer duration above threshold data (as used in chapter 5) are added to a constant (Table 4.14) to ensure the data are comparable with the timescale used for describing volumetric change.

6.3.1 Descriptive matrices

A transition matrix describes the transfer of sediment from one state to a number of possible alternate states. First order Markovian principles have been used to calculate the probabilities of transfer of sediment between storage types (Kelsey et al. 1987, Hoey 1989). In contrast, this study presents descriptive matrices based upon measured tracer fluxes. Data are expressed in BTEQ (section 5.2.1) rather than proportions summing to 1 since absolute fluxes are more representative than relative values. The total flux of tracers of size fraction *i* in sub-reach 1 between time t -1 and t, F_{1it} is thus described by the following row vector,

$$\boldsymbol{F}_{1it} = \begin{pmatrix} \boldsymbol{W}_{1i} & \boldsymbol{O}_{12i} & \boldsymbol{O}_{13i} & \boldsymbol{O}_{1Xi} \end{pmatrix} \tag{6.6}$$

W_{1it}, within sub-reach sediment redistribution of fraction *i* between time t - 1 and t, is given by

$$\boldsymbol{W}_{1it} = \begin{pmatrix} S_{Va_1Va_1} & T_{Va_1A_1} & T_{Va_1Sa_1} & T_{Va_1S_1} & T_{Va_1Ia_1} \\ T_{A_1Va_1} & S_{A_1A_1} & T_{A_1Sa_1} & T_{A_1S_1} & T_{A_1Ia_1} \\ T_{Sa_1Va_1} & T_{Sa_1A_1} & S_{Sa_1Sa_1} & T_{Sa_1S_1} & T_{Sa_1Ia_1} \\ T_{S_1Va_1} & T_{S_1A_1} & T_{S_1Sa_1} & S_{S_1S_1} & T_{S_1Ia_1} \\ T_{Ia_1Va_1} & T_{Ia_1A_1} & T_{Ia_1Sa_1} & T_{Ia_1S_1} & S_{Ia_1Ia_1} \end{pmatrix} \tag{6.7}$$

S is the sediment remaining in the storage type in which it was located at time t, and T refers to sediment redistribution within the sub-reach. Subscripts refer to storage type.

O_{12it} details output of fraction *i* from sub-reach 1 to stores in sub-reach 2 between t - 1 and t where,

$$\boldsymbol{O}_{12it} = \begin{pmatrix} O_{Va_1Va_2} & O_{Va_1A_2} & O_{Va_1Sa_2} & O_{Va_1S_2} & O_{Va_1Ia_2} \\ O_{A_1Va_2} & O_{A_1A_2} & O_{A_1Sa_2} & O_{A_1S_2} & O_{A_1Ia_2} \\ O_{Sa_1Va_2} & O_{Sa_1A_2} & O_{Sa_1Sa_2} & O_{Sa_1S_2} & O_{Sa_1Ia_2} \\ O_{S_1Va_2} & O_{S_1A_2} & O_{S_1Sa_2} & O_{S_1S_2} & O_{S_1Ia_2} \\ O_{Ia_1Va_2} & O_{Ia_1A_2} & O_{Ia_1Sa_2} & O_{Ia_1S_2} & O_{Ia_1Ia_2} \end{pmatrix} \tag{6.8}$$

Each element in the matrix represents the BTEQ of fraction *i* transferred from storage in sub-reach 1 to a store in sub-reach 2.

O_{13it} details output from sub-reach 2 to stores in sub-reach 3 where,

$$\boldsymbol{O}_{13it} = \begin{pmatrix} O_{Va_1Va_3} & O_{Va_1A_3} & O_{Va_1Sa_3} & O_{Va_1S_3} & O_{Va_1Ia_3} \\ O_{A_1Va_3} & O_{A_1A_3} & O_{A_1Sa_3} & O_{A_1S_3} & O_{A_1Ia_3} \\ O_{Sa_1Va_3} & O_{Sa_1A_3} & O_{Sa_1Sa_3} & O_{Sa_1S_3} & O_{Sa_1Ia_3} \\ O_{S_1Va_3} & O_{S_1A_3} & O_{S_1Sa_3} & O_{S_1S_3} & O_{S_1Ia_3} \\ O_{Ia_1Va_3} & O_{Ia_1A_3} & O_{Ia_1Sa_3} & O_{Ia_1S_3} & O_{Ia_1Ia_3} \end{pmatrix} \quad (6.9)$$

Output of fraction *i* from sub-reach 1 to the absorbing state (i.e. output from the reach), O_{1Xit} is given by,

$$\boldsymbol{O}_{1Xit} = \begin{pmatrix} O_{Va_1X} \\ O_{A_1X} \\ O_{Sa_1X} \\ O_{S_1X} \\ O_{Ia_1X} \end{pmatrix} \quad (6.10)$$

Numerical subscripts in Eq. 6.7 to 6.10 denote the source sub-reach and sink sub-reach respectively. Transfer of sediment from sub-reach 2 is given by

$$\boldsymbol{F}_{2_{i\,t}} = \begin{pmatrix} W_{2i} & O_{23i} & O_{2Xi} \end{pmatrix} \quad (6.11)$$

with transfer from sub-reach 3 given by

$$\boldsymbol{F}_{3_{i\,t}} = \begin{pmatrix} W_{3i} & O_{3Xi} \end{pmatrix} \quad (6.12)$$

Matrices were calculated per tracer search for each sub-reach according to grain size. The full matrices are presented in Appendix G as 3 dimensional column charts where the 5 source stores are plotted on the ordinate and the destination stores on the abscissa.

6.3.1.1 Matrix types

Explanation of 210 matrices would involve excessive description, so they were classified into 14 types according to the balance between storage, transfer and output between t -1 and t. These categorisations are flexible and can be broken down for storage types as well as sub-reaches. The matrix types are based upon five flux characteristics of fraction *i* at time t:

ΣS_{ti}, storage in the sub-reach in question (Eq. 6.7);
ΣT_{ti}, redistribution within the sub-reach (Eq. 6.7);
$\Sigma O2_{ti}$, output to sub-reach 2 (Eq. 6.8);

$\Sigma O3_{ti}$, output to sub-reach 3 (Eq. 6.9);
ΣOX_{ti}, output from the reach (Eq. 6.10).

These values represent the sum of the elements in each transition matrix per search. Sample matrices of the major types are illustrated in Figure 6.10. Note in the following definitions that the matrix types have to be defined differently for the different sub-reaches.

Type A: *Sediment Immobility.* Most sediment remains in the sub-reach storage type where it was located at t-1, redistribution and output are minimal, $\Sigma S_t > \Sigma T_t$. The sum of sediment remaining in the sub-reach should be in excess of 85% of the total flux (Eq. 6.6, 6.11, 6.12). The value of 85% was arbitrarily selected to indicate immobility. Conditions:

Sub-reach 1	$(\Sigma S_{ti} + \Sigma T_{ti}) > (\Sigma O2_{ti}+\Sigma O3_{ti}+\Sigma OX_{ti})$	$(\Sigma S_{ti} + \Sigma T_{ti}) > 0.85*F_{ti}$
Sub-reach 2	$(\Sigma S_{ti} + \Sigma T_{ti}) > (\Sigma O3_{ti}+\Sigma OX_{ti})$	$(\Sigma S_{ti} + \Sigma T_{ti}) > 0.85*F_{ti}$
Sub-reach 3	$(\Sigma S_{ti} + \Sigma T_{ti}) > (\Sigma OX_{ti})$	$(\Sigma S_{ti} + \Sigma T_{ti}) > 0.85*F_{ti}$

Type B: *Within sub-reach flux.* Most sediment remains in the sub-reach but is redistributed between storage types, output is minimal, $\Sigma S_{ti} \leq \Sigma T_{ti}$. Other conditions are the same as type A.

Type C: *Local flux and small scale transfer. I.* Most sediment remains in the sub-reach with some local redistribution, a significant amount of sediment is output to the sub-reach immediately downstream. Where $\Sigma S_{ti} > \Sigma T_{ti}$ matrix is type C, if $\Sigma S_{ti} < \Sigma T_{ti}$, matrix is C'. Conditions:

Sub-reach 1	$(\Sigma S_{ti} + \Sigma T_{ti}) > (\Sigma O2_{ti}) >> (\Sigma O3_{ti}+\Sigma OX_{ti})$	$(\Sigma S_{ti} + \Sigma T_{ti}) > 0.85*F_{ti}$
Sub-reach 2	$(\Sigma S_{ti} + \Sigma T_{ti}) > (\Sigma O3_{ti}) >> (\Sigma OX_{ti})$	$(\Sigma S_{ti} + \Sigma T_{ti}) > 0.85*F_{ti}$
Sub-reach 3	$(\Sigma S_{ti} + \Sigma T_{ti}) > (\Sigma OX_{ti})$	$(\Sigma S_{ti} + \Sigma T_{ti}) > 0.85*F_{ti}$

Type D: *Local flux and small scale transfer. II.* Most sediment is transferred to the sub-reach immediately downstream, although some material remains in the sub-reach. Where $\Sigma S_{ti} > \Sigma T_{ti}$ matrix is type D, if $\Sigma S_{ti} < \Sigma T_{ti}$, matrix is D'. Conditions:

Sub-reach 1	$(\Sigma S_{ti} + \Sigma T_{ti}) < (\Sigma O2_{ti}) > (\Sigma O3_{ti}+\Sigma OX_{ti})$	$(\Sigma S_{ti} + \Sigma T_{ti}) < 0.85*F_{ti}$
Sub-reach 2	$(\Sigma S_{ti} + \Sigma T_{ti}) < (\Sigma O3_{ti}) > (\Sigma OX_{ti})$	$(\Sigma S_{ti} + \Sigma T_{ti}) < 0.85*F_{ti}$
Sub-reach 3	$(\Sigma S_{ti} + \Sigma T_{ti}) < (\Sigma OX_{ti})$	$(\Sigma S_{ti} + \Sigma T_{ti}) < 0.85*F_{ti}$

Type E: *Local flux and downstream transfer. I.* Most sediment remains in the sub-reach with some local redistribution, a significant amount of sediment is output to the sub-reach furthest downstream. Conditions:

Sub-reach 1	$(\Sigma S_{ti} + \Sigma T_{ti}) > (\Sigma O3_{ti}+\Sigma OX_{ti}) > (\Sigma O2_{ti})$	$(\Sigma S_{ti} + \Sigma T_{ti}) > 0.85*F_{ti}$
Sub-reach 2	$(\Sigma S_{ti} + \Sigma T_{ti}) > (\Sigma OX_{ti}) > (\Sigma O3_{ti})$	$(\Sigma S_{ti} + \Sigma T_{ti}) > 0.85*F_{ti}$
Sub-reach 3	$(\Sigma S_{ti} + \Sigma T_{ti}) > (\Sigma OX_{ti}) > 0$	$(\Sigma S_{ti} + \Sigma T_{ti}) > 0.85*F_{ti}$

Type A: 2A, < 180 mm, 26900 min.

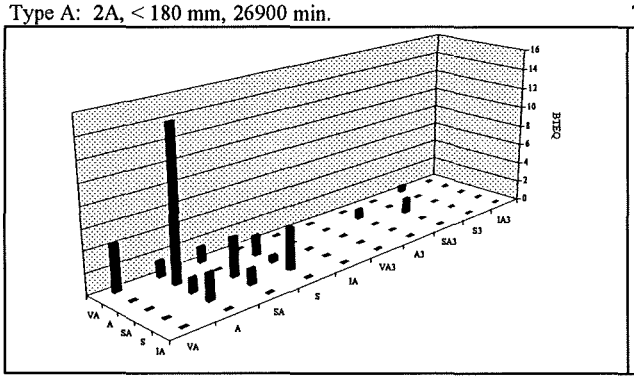

Type B: 1B, < 64 mm, 17900 min.

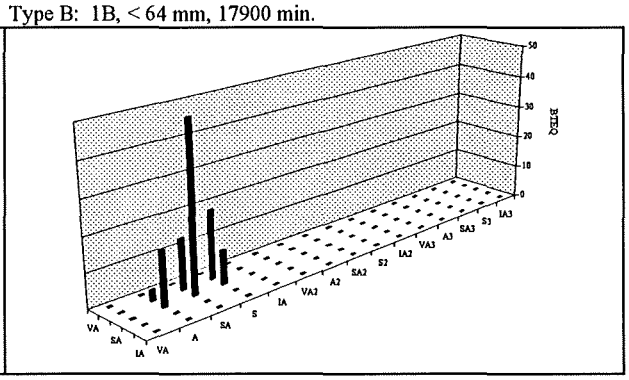

Type C: 2B, < 32 mm, 32100 min.

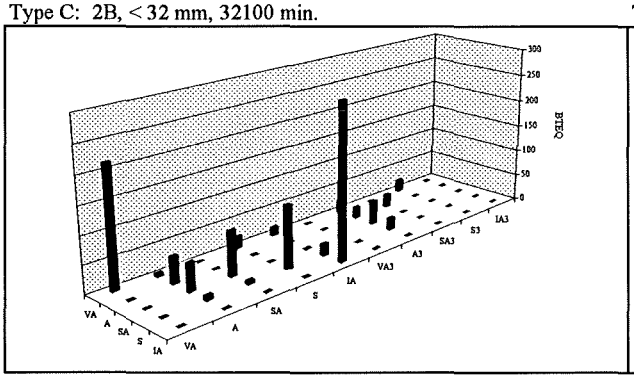

Type D: 1A, < 180 mm, 57110 min.

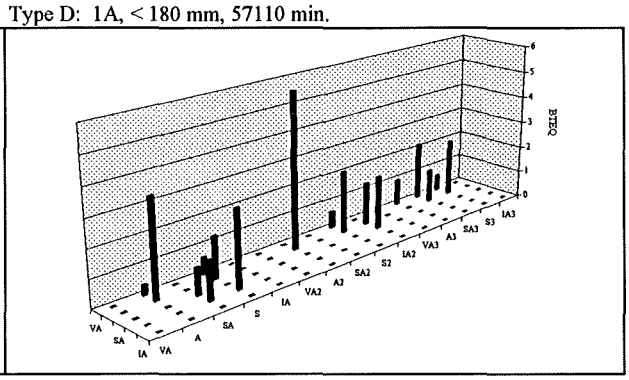

Type E, 1A, < 32 mm, 57110 min.

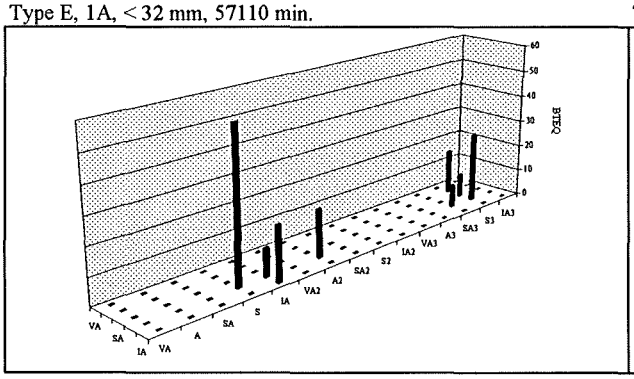

Type F, 1A, < 32 mm, 21000 min.

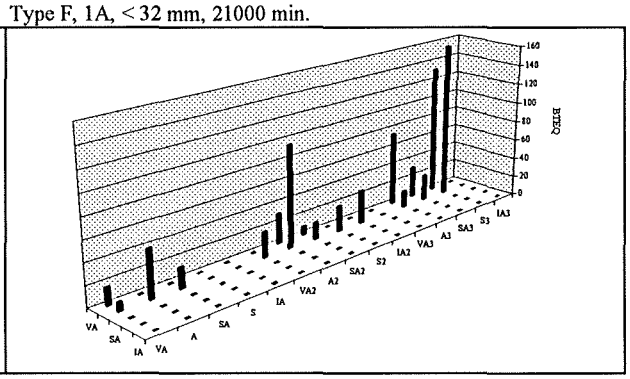

Type I, 2A, < 32 mm, 21000 min.

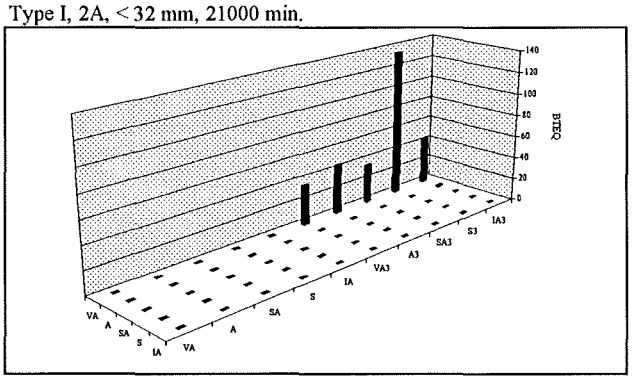

Figure 6.10. Examples of the dominant matrix types. Labels refer to sub-reach, grain size and time. Source store - ordinate destination store - abscissa. Destination stores are numerically labelled according to downstream sub-reaches. Note different vertical scales.

Type F: *Local flux and downstream transfer. II.* Most sediment is transferred to the sub-reach furthest downstream although some material does remain in the sub-reach. Where $\Sigma S_{ti} > \Sigma T_{ti}$, the matrix is type F, if $\Sigma S_{ti} < \Sigma T_{ti}$, matrix is F'. Conditions:

Sub-reach 1	$(\Sigma S_{ti} + \Sigma T_{ti}) < (\Sigma O3_{ti}+\Sigma OX_{ti}) > (\Sigma O2_{ti})$	$(\Sigma S_{ti} + \Sigma T_{ti}) < 0.85*F_{ti}$
Sub-reach 2	$(\Sigma S_{ti} + \Sigma T_{ti}) < (\Sigma OX_{ti}) > (\Sigma O3_{ti})$	$(\Sigma S_{ti} + \Sigma T_{ti}) < 0.85*F_{ti}$
Sub-reach 3	$(\Sigma S_{ti} + \Sigma T_{ti}) < (\Sigma OX_{ti}) > 0$	$(\Sigma S_{ti} + \Sigma T_{ti}) < 0.85*F_{ti}$

Type G: *Storage and reach scale sediment redistribution.* Most material (70 %) remains in the sub-reach, $\Sigma S_{ti} > \Sigma T_{ti}$, output (30 %) is evenly distributed between downstream sub-reaches. This matrix type is only applicable to sub-reaches 1 and 2. Conditions:

Sub-reach 1	$(\Sigma S_{ti} + \Sigma T_{ti}) < (\Sigma O3_{ti}+\Sigma OX_{ti}) \approx (\Sigma O2_{ti})$	$(\Sigma S_{ti} + \Sigma T_{ti}) > 0.70*F_{ti}$
Sub-reach 2	$(\Sigma S_{ti} + \Sigma T_{ti}) < (\Sigma O3_{ti}) \approx (\Sigma OX_{ti})$	$(\Sigma S_{ti} + \Sigma T_{ti}) > 0.70*F_{ti}$

Type H: *Reach scale sediment redistribution.* Sediment is redistributed, stored and output between sub-reaches in approximately equal quantities. Conditions:

Sub-reach 1	$\Sigma S_{ti} \approx \Sigma T_{ti} \approx (\Sigma O2_{ti}+\Sigma O3_{ti}+\Sigma OX_{ti})$
Sub-reach 2	$\Sigma S_{ti} \approx \Sigma T_{ti} \approx (\Sigma O3_{ti}+\Sigma OX_{ti})$
Sub-reach 3	$\Sigma S_{ti} \approx \Sigma T_{ti} \approx (\Sigma OX_{ti})$

Type I: *No storage.* All sediment is output. If any sediment is redistributed within the source sub-reach then the matrix is classified as I'. Conditions:

Sub-reach 1	$(\Sigma O2_{ti}+\Sigma O3_{ti}+\Sigma OX_{ti}) > (\Sigma S_{ti} + \Sigma T_{ti}) \approx 0$
Sub-reach 2	$(\Sigma O3_{ti}+\Sigma OX_{ti}) > (\Sigma S_{ti} + \Sigma T_{ti}) \approx 0$
Sub-reach 3	$(\Sigma OX_{ti}) > (\Sigma S_{ti} + \Sigma T_{ti}) \approx 0$

Type J: *No sediment redistribution.* No tracer sediment is present in fraction *i* in the sub-reach at time t, $\Sigma O2_{ti}=\Sigma O3_{ti}=\Sigma OX_{ti}=\Sigma S_{ti}=\Sigma T_{ti}=0$.

6.3.2 The magnitude and distribution of tracer fluxes

Tracer fluxes in this study are the result of two often independent processes. First, entrainment of individual particles from or close to the bed surface due to random small scale scour and fill processes (Hassan 1990), and second, morphological change, where tracer sediment is entrained as part of an eroding/migrating bar or sediment wave. The magnitudes of these processes are determined by four factors. (1) shear stress - bedload transfer and morphological change are a function of excess shear stress (sub section 6.2.1). Shear stress affects sediment pathways with, in general, small floods restricting tracer movement to the submerged channel (Laronne and Duncan

1992); (2) bed material - the size of the bed sediment relative to tracer D_{50} determines the magnitude of hiding and protrusion of the tracer sediment (Fenton and Abbott 1977), in addition, sediment packing affects relative tracer mobility (Church and Hassan 1992, Hassan and Church 1992); (3) morphology - response time analysis indicated that the transfer potential of sediment is determined by its location in the storage system (Kelsey et al. 1987, Carson and Griffiths 1989), in addition, channel morphology determines the distribution of sediment transfer (Laronne and Duncan 1992), particularly where fixed bars are present; (4) tracer grain size - in general, finer particles are transferred further than coarser clasts (Hassan et al. 1992). The relative importance of these factors upon sediment activity is discussed in the following sections under the headings of hydraulics (shear stress), tracer grain size, sub-reach (general morphology) and storage type (detailed morphology). The role of bed material is considered in chapter 7.

6.3.2.1 Hydraulic effects

The magnitude of bedload transfer and resultant morphological change (and therefore tracer fluxes) is dependant upon the imposed shear stress (Gomez 1989, Hassan and Church 1992). For example, transfer based type C, D, and F matrices dominate between 13601 and 21000 min. and 36001 and 62010 min. in reach A (Table 6.1). Reach B fluxes are small scale and limited to type A

Time /min.	**Grain size /mm**			**Time /min.**	**Grain size /mm**		
Sub-reach 1A	**< 180**	**< 64**	**< 32**	**Sub-reach 1B**	**< 90**	**< 64**	**< 32**
21000	C	F	F	*17900*	A	B	B
26900	A	C	C	*23100*	A	A	C
32450	A	C	G	*32100*	A	C	E
36000	A	A	A	*38400*	A	A	A
57110	D	F	E	*66450*	A	A	A
62010	E	F	F	*72750*	A	A	A
Sub-reach 2A				**2B**			
21000	D'	I	I	*17900*	A	A	A
26900	A	C	C	*23100*	A	A	C
32450	A	A	C	*32100*	A	A	C
36000	A	A	A	*38400*	A	A	C
57110	D	D	D	*66450*	A	C	C
62010	C	H	D	*72750*	A	A	C
Sub-reach 3A				**3B**			
21000	J	J	J	*17900*	J	J	J
26900	A	A	C	*23100*	J	A	C
32450	A	A	A	*32100*	J	C'	C
36000	A	A	A	*38400*	J	A	C
57110	A	C'	C'	*66450*	J	C	C
62010	A	C	C	*72750*	J	A	C

Table 6.1. Sub-reach transition matrix types according to tracer search and grain size.

and a small number of type C matrices. Small tracer fluxes during intermediate flood events in reach A and throughout the study period in B are a response to reduced flows with minor morphological change, most material remaining in storage (Figure 6.11). Tracer entrainment during these periods is confined to the submerged channel (Appendix G), being dependant upon local turbulence, bed position (i.e. storage type) and bed structure (Hassan et al. 1991, Hassan and Church 1992). In general, tracers are not evacuated from less active stores during intermediate floods, and tracer sediment supply is therefore reduced in the absence of significant morphological change.

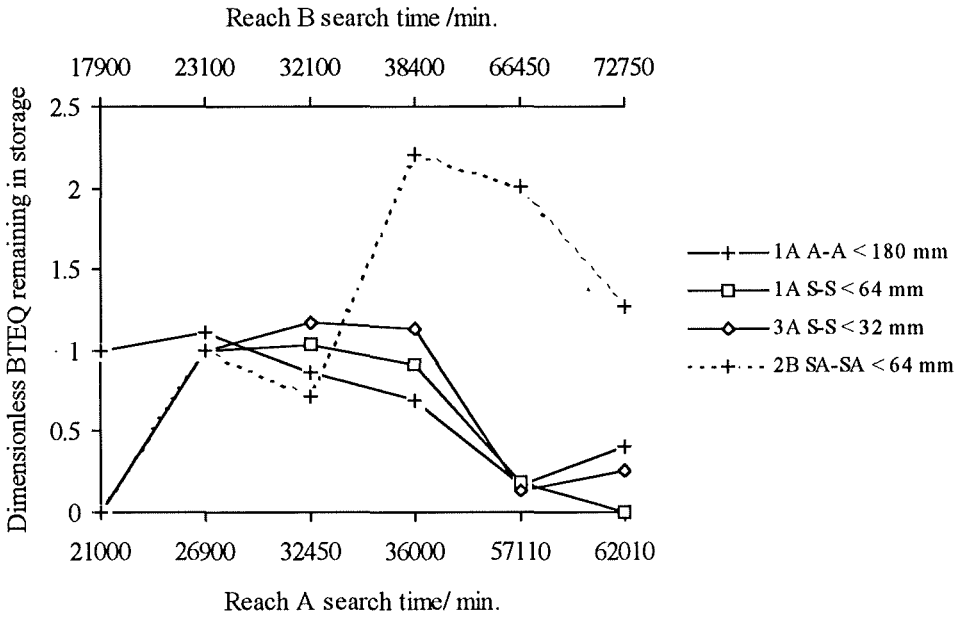

Figure 6.11. BTEQ of sub-reach sediment remaining in selected stores, ΣS_{ti}, normalised by the BTEQ when sediment first entered the store after first hop (selected data). Active storage transfers most sediment during the intermediate searches. The trough in reach A is a result of maximum shear stress and associated morphological change. Reach B data indicates random local entrainment as significant morphological change was absent.

The magnitude of sediment fluxes corresponds with fluctuations in morphological change (Figure 6.12). In reach A, small fluxes correspond with spatially disparate low magnitude volumetric changes (Appendix F), involving few tracers. Between 36001 and 57110 min., tracers were transferred in large quantities due to both entrainment from the bed and transfer associated with morphological change. The scale used in Figure 6.12 is somewhat misleading since morphological change such as bar erosion is not described, rather, a sub-reach average is presented. Isolated areas of morphological change are responsible for the release of a significant number of previously stored tracers, for example, erosion of the head of S4A (Appendix F, F17).

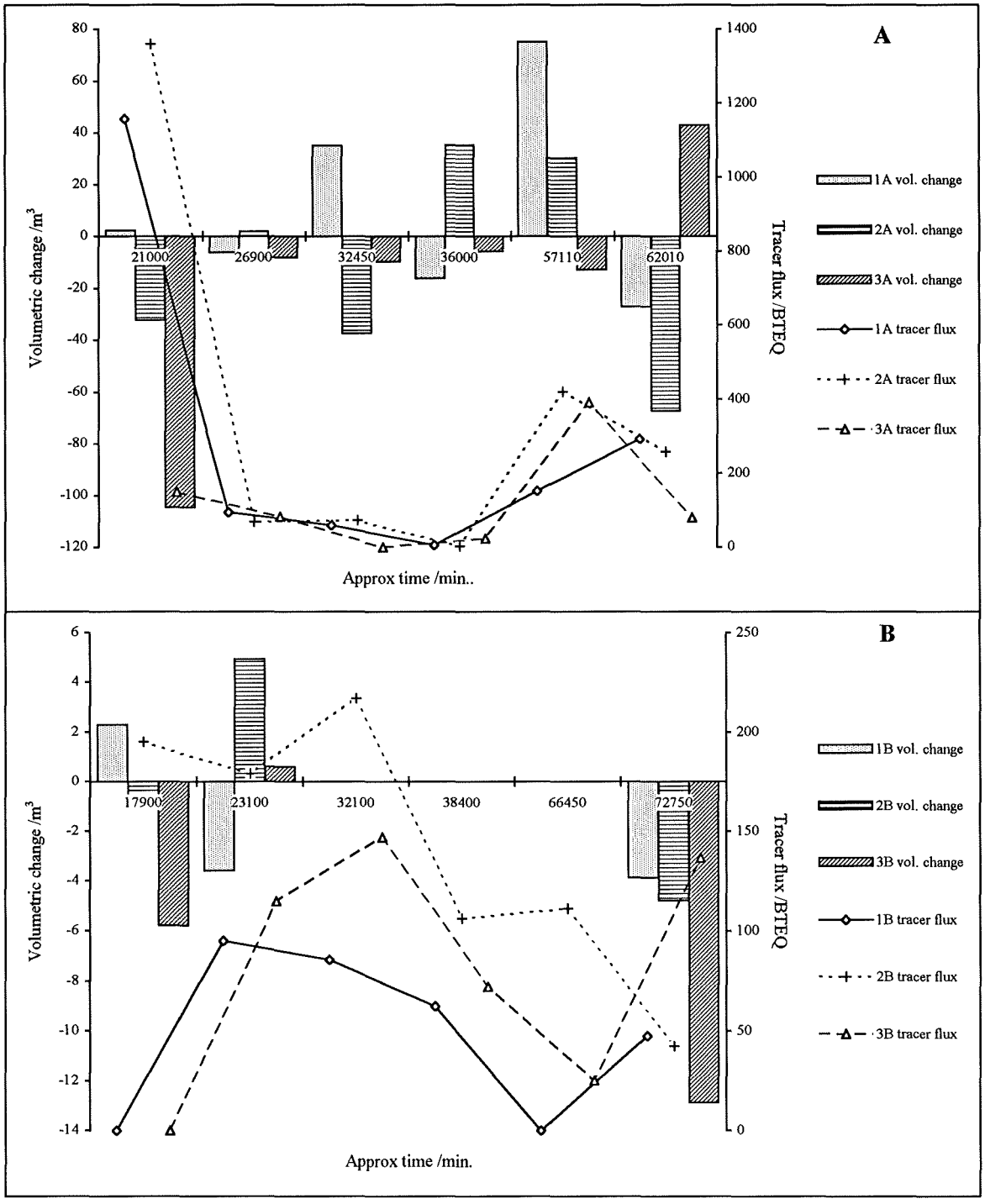

Figure 6.12. Sub-reach tracer fluxes and volumetric change. Time is approximate corresponding to the nearest tracer search and cross section survey.

In summary, tracer transfer during the first hop was a response to pool competence and prolonged shear stress. During intermediate searches in reach A and all searches in B transfer was limited, occurring primarily as a response to relatively high imposed shear stresses in the submerged channel. In reach A, this process was intensified between 36001 and 57110 min. with prolonged high shear stresses with additional tracer sediment added to the transfer system in response to morphological change via reworking of less active stores.

6.3.2.2 Grain size effects

In addition to hydraulic conditions, tracer fluxes can be characterised according to grain size. The size of the tracer sediment determines the distance moved and the pathway taken due to interactions with bed material, secondary flow and morphology. Finer material is transferred further (on average) than coarser sediment (Church and Hassan 1992), the previous chapter identified tracer waves propagating through the reach with a velocity inversely proportional to grain size. At the sub-reach scale, the increased number of D and F type matrices for < 64 mm (reach A only) and < 32 mm clasts (Table 6.1) indicate that finer material is more rapidly transferred downstream. In reach B, type A matrices dominate with the small number of type C matrices restricted to finer particles. These particles are closer to the reach D_{50} and are therefore transferred further in this low energy reach. Transfer of coarser clasts is constrained in the absence of morphological change due to higher critical stress with flow rarely being competent.

6.3.2.3 Sub-reach morphological effects

The number of type A matrices increases from sub-reaches 1A to 3A and decreases according to grain size. This decrease is commensurate with increased transfer of finer tracers and storage dominance of 3A (section 5.3.2). Transfer is dominated by entrainment in response to scour and fill (in the absence of significant morphological change, Appendix F) in 1A and 2A, the submerged channel being competent to transfer most sediment by virtue of fixed bar location. Only a small proportion of the sediment interacts with the fixed bars (section 5.3.2). In 3A, tracer transfer is generally low as the wide shallow submerged channel infrequently attains sufficient shear stress for significant direct entrainment from the bed, although small scale random entrainment does occur (Hassan and Church 1992). Transfer is concentrated during periods of high flows where local shear stresses are sufficient for morphological change and direct entrainment from the bed. This is illustrated by type C matrices first occurring for fine sediment after 36001 min., whereas coarser sediment remained in the reach. Reach B is characterised by type A matrices and significant transfer is restricted to < 32 mm sediment in 2B and 3B. Contrasts in sub-reach activity are a response to morphological differences within the submerged channel producing contrasting patterns of tracer transfer, and no systematic trends are apparent.

6.3.2.4 Storage type and lateral sorting

Tracers are rendered temporarily immobile whilst in less active storage (for example bars, Church and Hassan 1992) with transfer continuing through more active stores. It is therefore instructive to examine the spatial distribution of these small scale trends and evaluate the importance of these in terms of deviations away from equal mobility, and downstream fining.

Tracer fluxes from each sub-reach are a function of entrainment and morphological change according to hydraulic conditions, grain size and local morphology. The shallow depth in 3A restricts sediment transfer to periods of high shear stress and morphological change. These principles may be applied to storage types. Direct transfer from VA, A and to a lesser extent SA storage is due to local scour and fill processes, whereas the majority of sediment released from S and IA storage is associated with morphological change and extreme flood events (hence increased residence times for such stores, Kelsey et al. 1987).

The matrix types introduced in 6.3.3 can be determined for each storage type according to grain size and sub-reach, effectively describing fluxes from individual stores (Table 6.2). At the store scale in reach A, there is a reduction in activity from VA to IA storage (consistent with Γ), indicated by the increasing number of type A or J matrices characterising S and IA stores. In general, stable storage is characterised by type A or B matrices until 57110 min. in reach A, when the number of type C and D matrices increases indicating transfer in response to morphological change (Appendix F). The number of type B and C matrices associated with IA and S storage increases for finer fractions suggesting that this material is released from storage with many coarse particles remaining *in situ*. In reach B, transfer is predominantly confined to < 32 mm tracers. Activity is distributed across A, SA and S storage, confirming that there is very little difference between these storage types in terms of potential for transfer.

Sediment transfer in reach A is size selective in the submerged channel with little interaction with S or IA storage until sub-reach 3A. Tracer wave evidence (section 5.3.1) indicates that finer sediment is supplied to 3A at a faster rate than coarser fractions although all are present in significant quantities. Material passing through 3A is either incorporated within less active storage (S and IA) or transferred out of the reach via more active stores. Periodically, sediment is added to the transfer system (VA, A and to a lesser extend SA) due to morphological change. This addition and the efficiency of the channel to transfer the imposed grain sizes is evaluated below. This analysis is not possible in reach B where transfer of sediment is confined to A, SA and S storage with no interaction with IA sediment (Table 6.2).

Time /min.			<180					<64					<32		
1A	**VA**	**A**	**SA**	**S**	**IA**	**VA**	**A**	**SA**	**S**	**IA**	**VA**	**A**	**SA**	**S**	**IA**
21000	C'	C	J	J	J	F'	F	J	J	J	F	D	J	J	J
26900	A	C	D	B	B	I	C	F'	C	J	C	D	D	A	A
32450	A	A	C	A	J	J	D	A	A	A	A	B	F'	C'	A
36000	A	A	A	A	J	J	A	C	A	J	B	J	B	A	A
57110	F'	D	F	A	J	J	I	I	F	J	J	I	I	F	A
62010	J	C	D'	A	J	J	F	I	J	A	J	F	J	C	A
2A															
21000	D'	A	J	J	J	I	J	J	J	J	I	I	J	J	J
26900	A	A	C	B	J	C	D	A	B	A	A	C	B	A	A
32450	B	C	C'	C'	J	C	A	A	A	B	C	C	C	A	B
36000	A	A	A	A	A	B	C	B	B	A	B	A	B	B	A
57110	I	C	C'	D'	A	I	D	I	D'	J	I	D	F'	I	A
62010	I	D	B	D	A	J	C	J	J	B	J	D	J	B	A
3A															
21000	J	J	J	J	J	J	J	J	J	J	J	J	J	J	J
26900	J	A	C	A	A	J	A	C'	A	A	I	C'	A	A	A
32450	J	A	A	A	A	J	A	B	A	A	J	A	B	A	A
36000	J	A	A	A	A	I	A	B	A	A	I	A	B	A	A
57110	J	C	D	A	A	J	D'	D	C'	B	J	J	D	D	B
62010	J	B	A	A	A	J	C	B	C	A	J	A	J	C	A
			<90					<64					<32		
1B															
17900	J	B	A	J	J	J	B	A	J	J	J	B	A	J	J
23100	J	B	A	J	J	J	A	A	C'	J	J	D	C	C'	A
32100	J	J	A	B	J	I	C	A	B	J	B	H	A	B	A
38400	J	J	A	J	J	J	C	A	C'	J	A	C	D	B	A
66450	J	J	A	B	J	J	A	A	B	J	A	A	A	B	A
72750	J	A	B	J	J	J	B	B	C'	J	A	C	A	B	A
2B															
17900	A	A	J	J	J	C	B	J	J	J	C	B	J	J	J
23100	A	A	A	A	A	A	C	C	A	A	C	C	C	C	A
32100	A	A	A	A	A	A	A	B	A	A	C	D	C	C	A
38400	A	A	A	A	A	A	A	A	A	A	A	C	A	C	A
66450	A	A	A	A	A	A	C	C	A	A	A	C	A	C	A
72750	A	A	A	J	A	A	C	A	C	A	A	C	A	C	A
3B															
17900	J	J	J	J	J	J	J	J	J	J	J	J	J	J	J
23100	J	J	J	J	J	J	J	A	J	J	H	I	A	B	I
32100	J	J	J	J	J	B	A	I	J	J	D'	D	D	C'	A
38400	J	J	J	J	J	J	A	J	B	A	A	C	C	I	A
66450	J	J	J	J	J	J	C	J	J	J	B	C	A	B	A
72750	J	J	J	J	J	A	C	J	J	A	J	A	D	I	A

Table 6.2. Descriptive matrix type characterising fractional transfer characteristics of sub-reach stores during the study period.

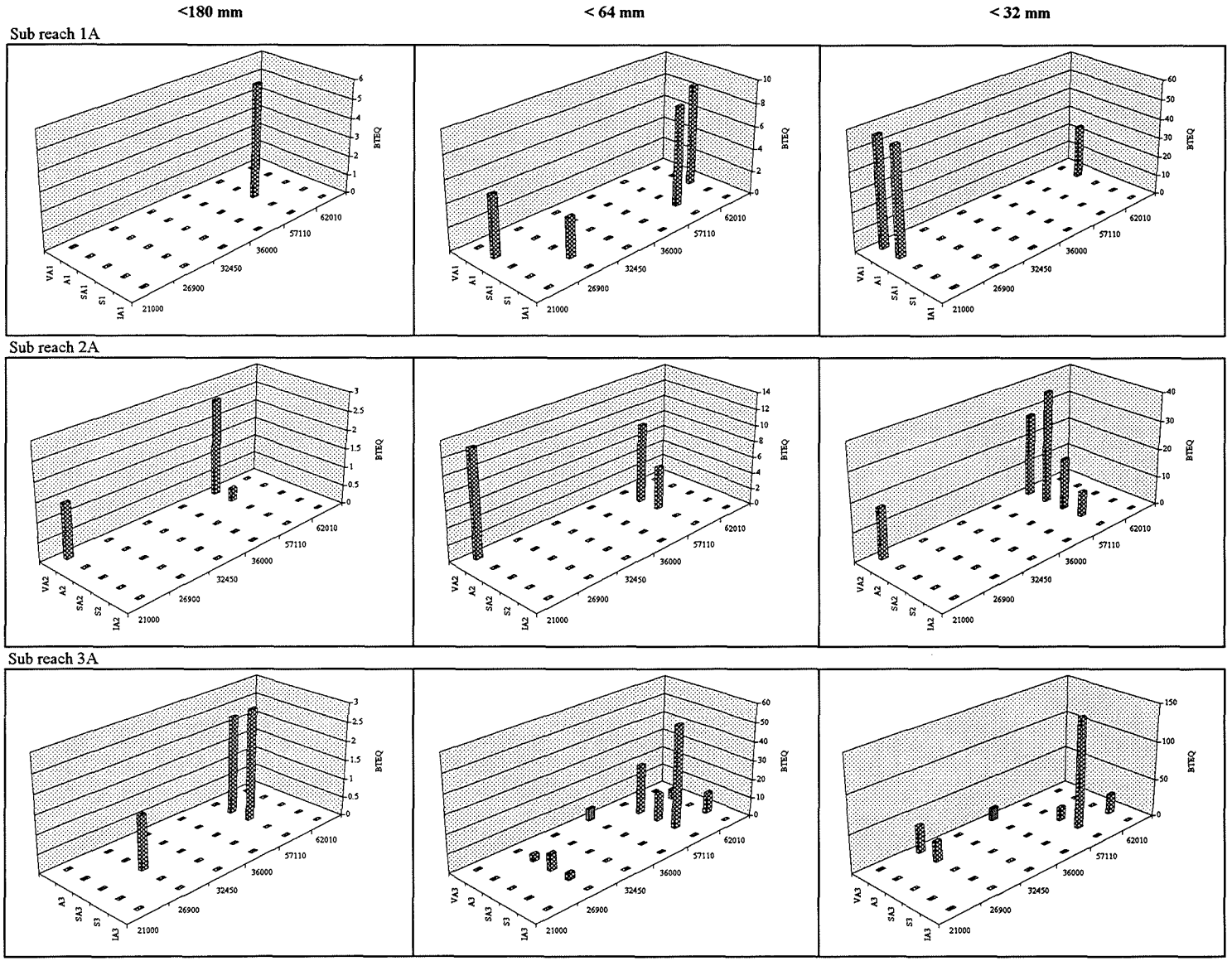

Figure 6.13. Distribution of source area (ordinate) for sediment output from reach A per search (abscissa).

In reach A, the BTEQ of fraction *i* output from storage type s, X_{si} is non zero exclusively in active and very active stores for < 180 mm sediment in sub-reaches 1A and 2A. Some material is transferred from SA storage in 3A where distance to the reach exit is less (Figure 6.13). τ^*_c is reached earlier in more active stores, so material is entrained sooner than elsewhere and (providing the stores through which it passes are competent at that point) transferred further according to grain size and possibly out of the reach. Sediment is entrained from VA storage before, for example, SA storage. Of this entrained material, finer sediment moves further than coarser (Table 6.3, 6.4) as τ^*_c for entrainment is achieved earlier for the fines. This argument is only applicable to transfer based VA, A and SA stores. For the storage based areas, transfer is dominated by morphological change.

Sediment in stable storage in 3A prior to the January 1993 snowmelt floods provides an example of grain size and storage effects, material of all sizes being incorporated into stable stores, S3 and S4. Prior to 57110 min., tracer release from stable storage was minimal (Appendix G and Table 6.4), corresponding with negligible morphological change. After this search, over 50 % of the tracers were removed from storage (Figure 6.14), this proportion increasing with grain size. No coarse particles were output from the reach, but, sediment was transferred within 3A. For the finer

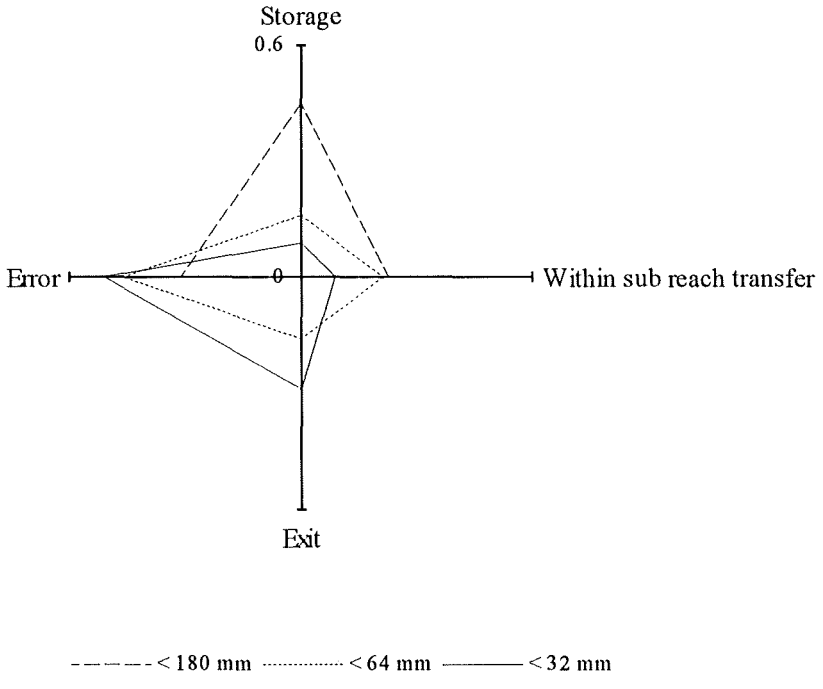

Figure 6.14. Radar diagram illustrating transfer pathways of sediment in stable storage in sub-reach 3A at search 7. Data are expressed as a proportion of sediment stored at t = 57110 min. Error arises due to non 100 % recovery rate. Sum of values on each axis per grain size class equals unity.

sediment, most of the < 32 mm material removed from storage was output, the proportion being slightly larger than for < 64 mm particles. One drawback with this example is the low recovery rate. However, the minimal error for coarse sediment increases the confidence in these observations. The lower recovery rates of finer clasts are a function of burial and transfer distance, with greater dispersal leading to lower recovery rates, especially out of the reach. Whilst not absolute, it is likely that the trends presented are correct in relative terms.

Sediment stored in stable and inactive storage is temporarily removed from the transfer system. Once the store is eroded, the fine material is transferred more rapidly by virtue of its size, leaving the coarser clasts behind. In some instances, flow depth at these locations may be insufficient for coarse sediment transfer. Sediment in less active stores demonstrates the effect of lateral storage rather than lateral sorting (e.g. Seal et al 1993) where coarse particles are rendered less mobile than finer clasts by virtue of storage location within the channel.

6.3.3 Quantitative assessment of within reach sediment fluxes

The preceding section illustrated that the distribution of sediment transfer (as evidenced by matrix types) is a function of dimensionless shear stress. Results indicate that type A matrices are more frequent for less active stores, coarser grain sizes and intermediate events and conversely, type F matrices are associated with more active stores, fine grain sizes and extreme flood events. Using this as a basis, it is possible to analyse the relative magnitude of τ^* required for dominant storage, redistribution and output of sediment. The relative dimensionless shear stress required, can be determined from three variables: hydraulics, storage type and grain size. Hydraulic conditions raise τ^* through increasing τ (Eq. 2.1), storage type affects τ^* through its effect upon depth and hence τ and coarser grain size reduces τ^*.

It will be assumed that conditions at the point of entrainment condition transfer distances. Analysis presented in chapter 7 partially validates this where entrainment is shown to be a more important determinant of transfer distances than transport effects (e.g. hop location). In addition, average hydraulic conditions and tracer grain size do not alter between entrainment and hop locations, the only analytical factor which changes during transport is storage type. This method therefore represents a fairly accurate assessment of the factors determining transfer in each reach.

Storage was divided (on the basis of results presented in chapter 5) into transfer (VA and A), transitional (SA) and storage (S and IA) based classes in reach A. For reach B, VA was transfer based, A, SA and S were transitional and IA was storage. This simplification is necessary to reduce the size of the dataset allowing more general trends to be examined. The aim is to develop a surrogate measure of τ^* describing the potential for transfer of each grain size fraction from each

storage type during each flood period. The matrix type describing transfer patterns from each of these combinations (Table 6.2) can then be determined and a characteristic τ^* for each matrix type calculated. The data available to determine a relative measure of τ^* are 3 storage classes, 3 grain size classes and 6 hydraulic classes. In order to quantify this, the factors were converted to dummy variables using an ordinal scale of 1 to 5 (Table 6.3a), 1 corresponding with highest potential for transfer and 5 the lowest. These combinations are presented as a matrix, M, detailing the possible range of τ^* conditions at entrainment during this study applicable to each sub-reach (Table 6.3b).

a) Scaling of data.					
τ^*	**High**	⇐	⇐	⇐	**Low**
Score	***1***	***2***	***3***	***4***	***5***
Hydraulics:					
Time /min. (A)	57110	62010	21000	26900	32450/36000
Time /min. (B)	66450	72750	17900	23100	32100/38400
Storage:					
Storage class	Transfer		Transitional		Storage
Grain size:					
	< 32 mm		< 64 mm		< 180/90 mm

Table 6.3a. Ranked variables determining the relative magnitude of τ^*. Ranking is inversely proportional to τ^*. These data are used to calculate MSS and matrix M.

b) Matrix M									
				Grain size /mm					
	180	*180*	*180*	*64*	*64*	*64*	*32*	*32*	*32*
Storage class:	*Tr*	*Tns*	*St*	*Tr*	*Tns*	*St*	*Tr*	*Tns*	*St*
Search time. A/B									
21000/17900	9	11	13	7	9	11	5	7	9
26900/23100	10	12	14	8	10	12	6	8	10
32450/32100	11	13	15	9	11	13	7	9	11
36000/38400	11	13	15	9	11	13	7	9	11
57110/66450	7	9	11	5	7	9	3	5	7
62010/72750	8	10	12	6	8	10	4	6	8

Table 6.3b. Tabulated MSS values according to combinations of grain size, hydraulics and storage type. Tr - Transfer based storage, Tns - transitional storage, St - storage based stores. This matrix is applicable to all sub-reaches. Each element may be thought of as a particular entrainment condition during the study.

Each element is a summation combining location characteristics of hydraulic conditions, storage and grain size during this study, hereafter referred to as the matrix type dimensionless shear stress (MSS), where

$$MSS = \sum (Hydraulics + Grainsize + Storage) = f(1/\tau^*) \qquad (6.13)$$

A descriptive matrix, D, was developed for each matrix type (Appendix H). This documented the number of times a matrix type described transfer patterns from the locations detailed in matrix M. D was then multiplied by M and a mean MSS value was calculated describing the τ^* conditions particular to a matrix type. The analysis was carried out for matrix types A, B, C, D and F and provides a framework for analysing within sub-reach and between sub-reach transfers and the circumstances according to which they are likely to dominate.

6.3.3.1 Within sub-reach fluxes: Type A and B matrices

The distribution of type A and B matrices reflect the dominance of within sub-reach storage S and transfer T. Storage dominates (type A matrices) more frequently for intermediate searches, coarser grain sizes and less active stores (Appendix H1). The distribution of within sub-reach transfer dominated matrices (Type B) is less frequent reflecting the importance of output to the next sub-reach during periods of activity (Appendix H2). In reach B, reduced movement distances ensured that a large proportion of sediment remained in the sub-reaches, hence more type B matrices occur.

Matrix type	**A**	**B**
Sub-reach:		
1A	10.9	10.2
2A	10.6	10.5
3A	11.1	9
1B	8.6	8.8
2B	10.0	9
3B	9.1	7.2
Reach average:		
Reach A	10.9	9.9
Reach B	9.2	8.3

Table 6.4: Matrix type A and B mean MSS values.

The contrast between sub-reaches can be demonstrated with reference to the average MSS for each matrix type (Table 6.4). In both reaches type A matrices are characterised by higher MSS than type B indicating that the latter are a response to higher τ^* than type A. Lower MSS values in reach B demonstrate that sediment remains in storage in response to higher relative τ^* (defined in relative rather than absolute terms by increased flow conditions, reduced grain size or IA $\rightarrow$ VA storage types) than reach A. Likewise a higher relative τ^* is required for transfer. These comparisons demonstrate the reduced sediment activity at reach B.

6.3.3.2 Between sub-reach fluxes

Downstream transfer during significant flooding is especially prevalent in reach A. It is pertinent to examine the factors causing this transfer and the contrast with reach B to develop inferences

about the magnitude and frequency of sediment transfer and its importance to within channel morphology. The importance of sediment transfer upon local bar development and sediment storage is a poorly understood process (Ashworth 1987, Ashworth et al. 1992) with little documentary evidence. The scale used in this study is too coarse to examine detailed sediment interaction, however, inferences can be made regarding factors which are likely to cause significant transfer from upstream as indicated by the τ^* characteristics of matrix types C, D, and F.

Type C matrices characterise intermediate events, coarser sediment and less active storage (Appendix H3). Moderate τ^* results in minor transfer to downstream sub-reaches. Type D and F (Appendix H4, H5) matrices are associated with large scale sediment transfers so are confined to higher τ^* associated with more active floods, increased storage activity and reduced grain size. These preliminary results indicate that the magnitude of downstream transfer is a direct function of τ^* conditions at entrainment. These patterns are repeated in reach B where transfer is limited to type C matrices (there are few type D matrices) reflecting the small excess shear stresses compared with reach A.

Matrix Type	**C**	**D**	**E**	**F**
Sub-reach:				
1A	10.5	8.1	0	7.3
2A	9.3	7.7	0	5
3A	8.5	7.2	0	0
1B	8.45	8.5	0	0
2B	7.4	9.0	0	0
3B	7.83	7.8	0	0
Reach average:				
Reach A	9.4	7.7	0	6.1
Reach B	7.9	8.4	0	0

Table 6.5: Matrix type C, D, E and F mean MSS values.

Summary data indicate a progression of matrix types based upon τ^* (Table 6.5). Larger τ^* is required to transfer sediment out of the sub-reach, the magnitude of stress required increasing with transfer distance. Corresponding figures in reach B are lower than in reach A indicating that higher τ^* is required for similar transfer, reflecting the contrast in activity.

Sediment transfer is multivariate in its controls and dependant upon the relative magnitudes of hydraulic conditions, grain size and storage. Most tracer studies dismiss the latter concentrating instead upon the effects of shear stress and grain size upon movement distances (e.g. Church and Hassan 1992). The importance of each variable at the reach and sub-reach scale can, however, be assessed by computation of a reduced MSS by excluding each variable from Eq. 6.11. Plotting full MSS according to matrix type and comparing the trend with the reduced MSS allows separation of the factors dominating sediment transfer (Figure 6.15a, b). The basis for comparison is deviation

away from the gradient of the full MSS displayed by the reduced MSS. Positive deviation where exclusion reduces the difference in relative τ^* characterising each matrix, suggesting that the factor is an important determinant of sediment fluxes. Negative and zero deviation suggests the factor is

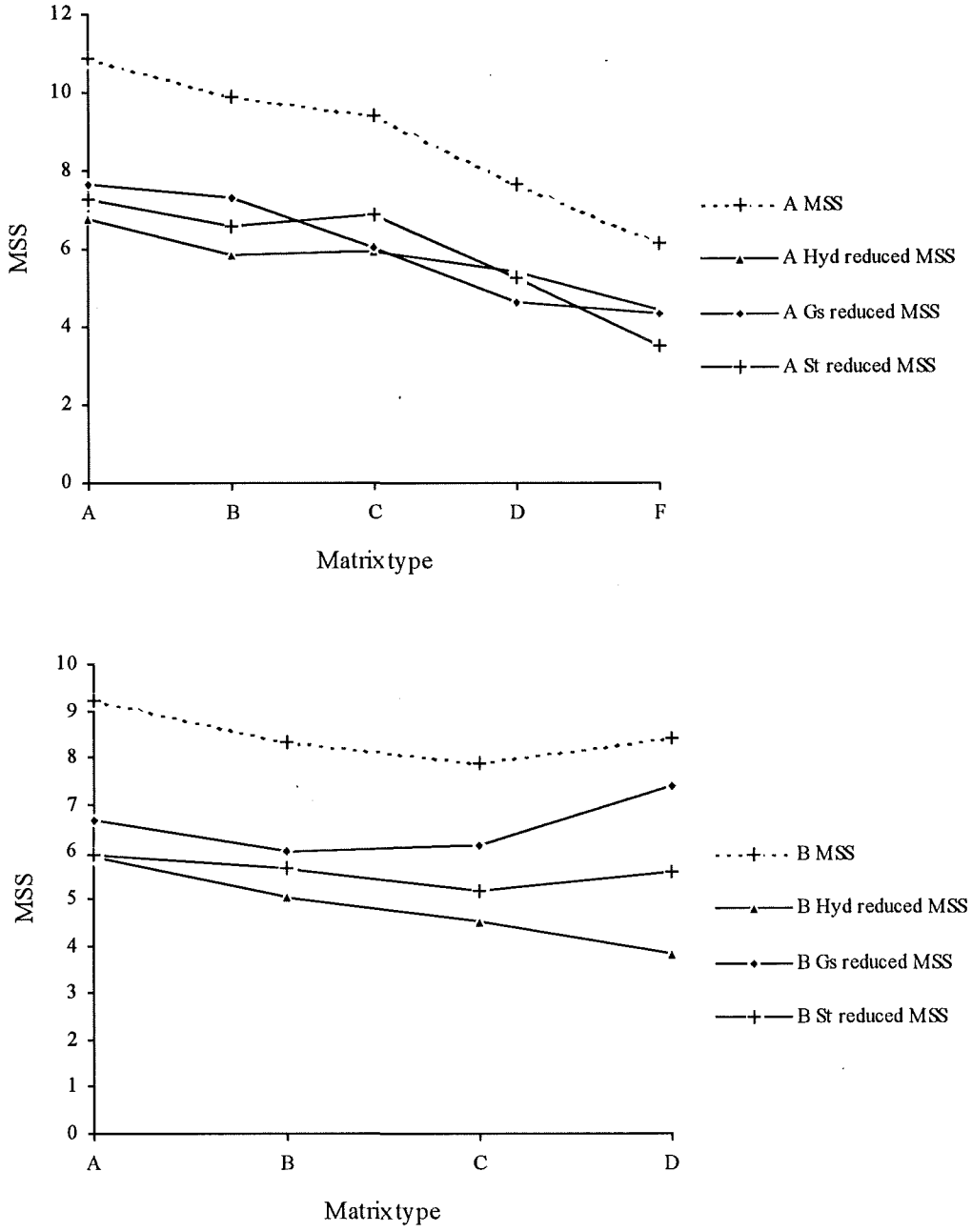

Figure 6.15. Reach scale MSS (A and B) and reduced MSS characterising matrix types. Data are reduced by excluding one of hydraulic conditions (Hyd reduced MSS), grain size (Gs reduced MSS) or storage type (St reduced MSS) from the calculation of MSS.

ineffective. Negative deviation suggests the excluded factor reduces the disparity between matrices. This anomaly is attributable to data scatter (Table 6.2) where some matrix types occur in

accordance with unusual combinations of factors, probably in response to low tracer numbers. The absolute magnitude of the reduced MSS are not comparable due to the simplistic ranking system employed in Table 6.3a.

The situation in reach A is complex as the overall gradient does not significantly alter and there is irregular fluctuation of reduced MSS values. These frequent crossovers indicate that in an active reach sediment transfer is a function of hydraulic conditions, grain size and storage; no single factor dominates. The trends in reach B are more regular indicating a less complex transfer system. Exclusion of hydraulic conditions does not affect the relationship. The effect of hydraulic conditions is minimal probably due to frequent overbank flow maintaining a near constant imposed excess shear stress during higher stage. Sediment fluxes are also independent of storage type confirming observations made in this and the preceding chapter where interaction with inactive storage types is small and differentiation within the submerged channel is low. Removal of grain size produces maximum deviation, particularly for type C and D matrices. This is indicative of pronounced size selectivity in reach B, where finer fractions close to D_{50} are most mobile. Equal mobility (Parker et al. 1982a) would be indicated if tracer fluxes were independent of grain size.

The sub-reach scale provides a revealing break down of these overall trends (Figure 6.16). Generally, grain size is the dominant factor in 1A, exclusion decreasing the τ^* between matrices. Transfer is broadly a function of grain size in this transfer dominated sub-reach where all storage types in the submerged channel are subject to competent shear stresses imposed by the large depths due to the fixed bar. In 2A the situation is more complex. This is a shallower more differentiated less transfer based sub-reach than 1A. The heterogeneity of the sub-reach is reflected in the frequent crossovers where no single factor dominates transfer. In 3A the values are of similar magnitude, possibly a response to the importance of all the factors in this storage based shallow reach where size selectivity dominates. Deviation is greatest due to exclusion of hydraulics for type D matrices, a response to transfer due to morphological change during extreme flows.

Grain size is not a determinant of the contrast between type A and B matrices in reach B possibly reflecting infrequent sediment mobilisation. However, once sediment is mobilised, grain size is the most important factor in each sub-reach reflecting the increased mobility of sediment closer to reach D_{50}. Fluxes are independent of hydraulic conditions in all sub-reaches; sediment transfer not bring a function of excess shear stress in reach B.

6.3.4 Static transfer

This section considers the factors causing net changes to sediment volume in each storage type: dynamic transfer (defined in section 5.1.3), static transfer and data accuracy. Previous studies have

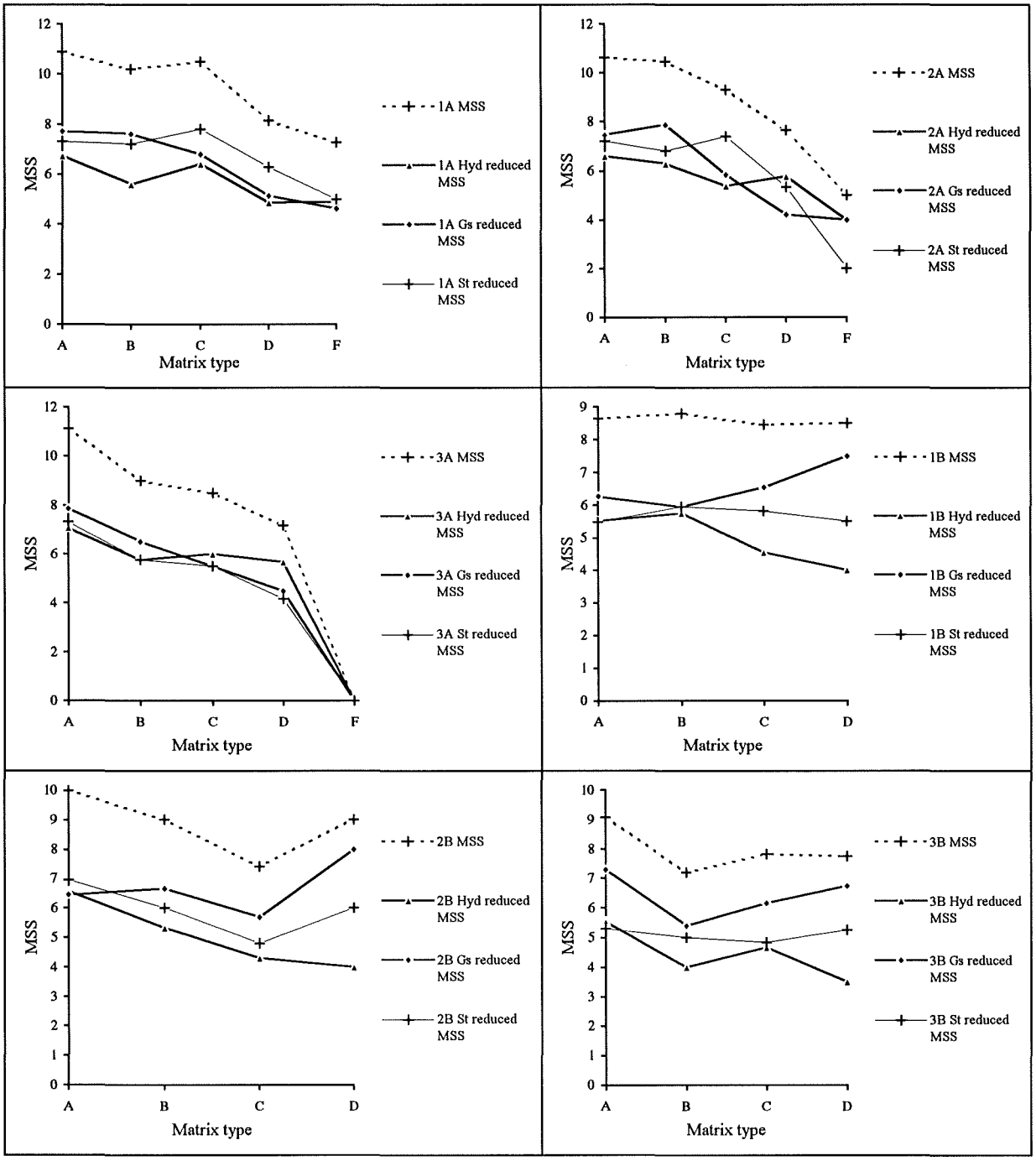

Figure 6.16. Sub-reach scale MSS and reduced MSS characterising matrix types. See Figure 6.15 for key to abbreviations.

separated the transfer processes using volumetric data, where static transfer was readily identifiable due to the method of storage definition (Hoey in press 1995). A definition based upon shear stress precludes such a separation. However, static and dynamic transfer can be separated using tracers. Static tracer transfer may occur in two ways: firstly, dynamic transfer may change the storage type without resident tracers moving; secondly, tracers may exchange between stores where the store boundary shifts in response to data resolution in the absence of morphological activity, the resolution of the survey data being too coarse to repeatedly define the storage boundary in the same location.

Sediment storage relative to storage at t = 0 and reach scale static transfer (defined by tracers which move < 1m yet change store) plotted as a time series indicate the causes of volumetric changes within and between storage types (Figure 6.17). Significant changes to storage in reach A occur in response to floods at the start and end of the study; with minimal changes during the intermediate timed events. Static transfer due to actual volumetric change (based upon field observation) is generally small. There are two exceptions which result from aggradation at the head of bar III after 26900 min. and aggradation of stable storage resulting in IA6 after 62010 min. In general, static transfer is small during major floods due to large scale tracer evacuation. Maximum static transfer during the intermediate searches (reduced tracer mobility) indicates that some of the volumetric changes during this period are a result of survey errors where storage boundaries change in response to data accuracy rather than morphological change. These are small errors (c0.75 m) and do not affect any discussion of storage evolution. The small error is distributed across all storage types and throughout the reach.

Static transfer in reach B is on average almost four times greater than reach A. The distribution of static transfer is a result of data error and to a lesser extent very local morphological change around bar margins (where many tracers were located). The trends in storage volumes according to these surveys are likely to be spurious, however, these errors are non systematic and do not affect the tracer results.

Contrasts in static transfer between A and B reflect the sensitivity of survey data to the method of storage definition. Stores in reach A are defined according to a wider elevational range than in B therefore the effect of survey resolution is minimised. In reach B the storage boundaries are sensitive to data resolution and small errors may cause a shift in the storage boundary. These errors are minor compared with the overall dataset but are worth noting particularly in relation to future storage definition in reaches with differing relative relief.

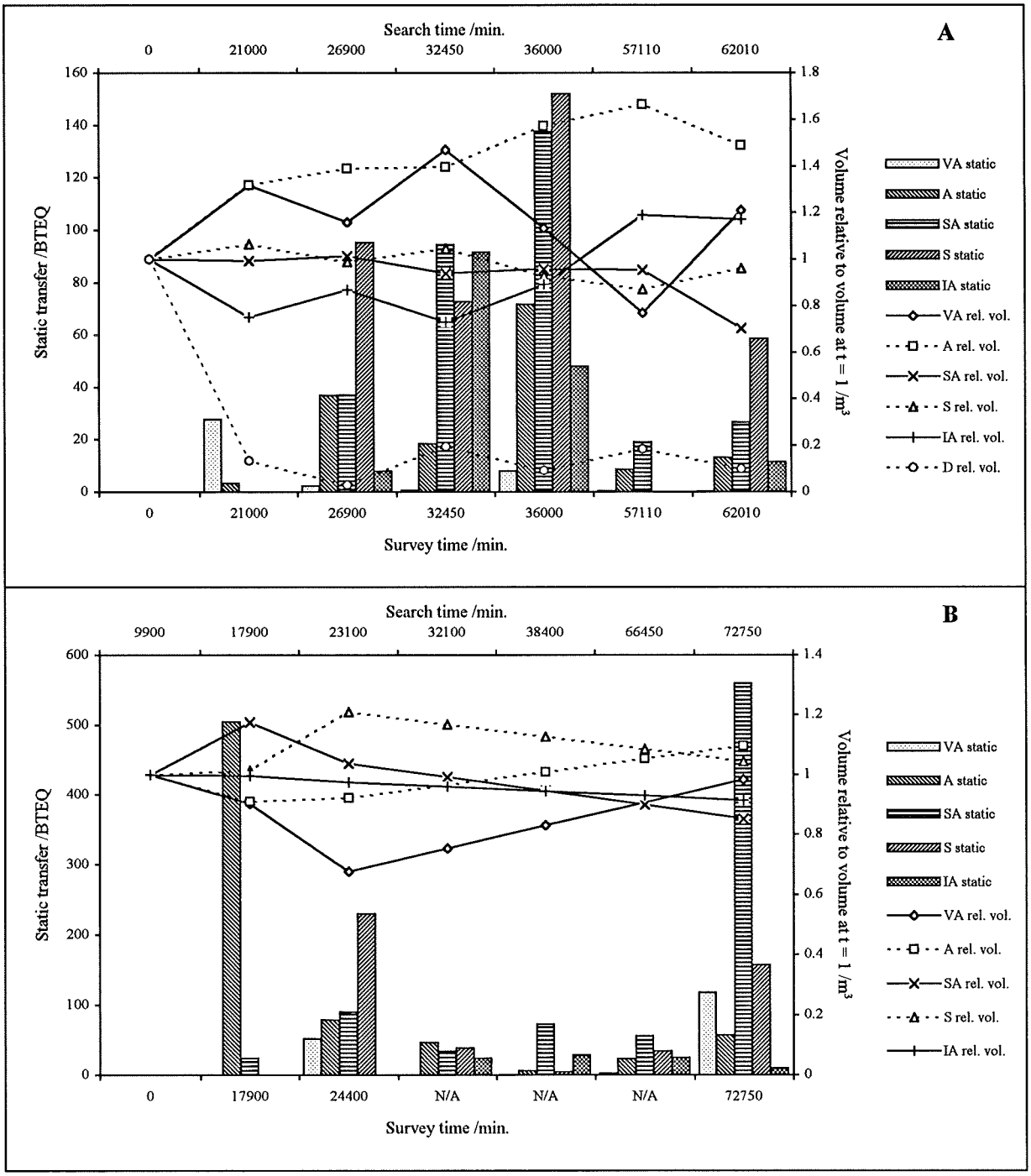

Figure 6.17. Static tracer transfer according to relative volumtric change per storage type.

6.4 Discussion

The preceding analysis has demonstrated the close association between patterns of volumetric change and tracer fluxes. Volumetric change is a response to hydraulic conditions, morphology and upstream supply; morphology conditioning the other two factors, usually as a result of fixed bar location. In this study volumetric change is often associated with increased tracer fluxes in response to extreme flow conditions. Where morphological change is minimal, tracer transfer is confined to more active stores within the submerged channel often in response to the flow fields resulting from the location of fixed bars.

It is a simplification to state that tracer transfer varies according to shear stress and grain size. In reality, tracer fluxes are a function of τ^* where hydraulic conditions and storage type condition shear stress, and grain size determines whether entrainment and transfer is possible; the magnitude of these relationships depending upon local morphology. In reach A tracer fluxes are a function of all three, these complex reach interactions reflecting the heterogeneity of A in terms of processes and morphology. However, at the sub-reach scale, transfer in 1A is largely independent of storage type and hydraulic conditions. Conditions are altered by fixed bar location such that excess stress is available within the submerged channel irrespective of storage type and to a lesser extent, flood intensity, the absolute magnitude of transfer being dependant upon grain size. In reach B transfer is dominated by grain size. It is possible to conceptualise reach B as a largely undifferentiated channel with flow fields dominated by fixed bars. Overbank flow reduces the shear stress variation once the bedload threshold is exceeded so transfer is almost entirely a function of grain size. The importance of relative grain size and burial to these trends is discussed in chapter 7.

Most tracer studies describe transfer as a function of shear stress and grain size, but this study demonstrates the additional importance of storage type. Whilst storage, in particular bar location (Hassan and Church 1992) is acknowledged as a determinant of transfer distances, few attempts have been made to isolate it. Results suggest that in reach A it is an important component of the transfer system, whereas in B, where submerged channel morphology is less distinct, it is not important. The effect of storage type is more important in higher energy systems where sediment interactions between stores are significant (see Figure 5.1b). This study has used a morphological approach to separate the three factors which contribute to the apparently stochastic transfer of sediment (Hassan and Church 1992). As these factors vary according to reach and sub-reach, it is unsurprising that results differ according to the type of channel conditions used (e.g. Hassan et al. 1992).

Tracer movement is often simplified with transfer due to morphological changes overlooked. Sediment storage in bars temporarily excludes sediment from the transfer system and is therefore

not comparable in terms of movement with tracers in more transfer based stores (where size selectivity characterises transfer). Superimposed over these trends of more mobile finer particles is temporally distinct release of sediment from storage based areas of the bed. Sediment of all grain sizes is released selectively, fine particles being transferred further than the coarser sediment which often remains in storage a short distance downstream. Both transfer and storage based stores cause reach coarsening with progressively more coarse sediment left in former storage based area, although time scales may differ. Storage of sediment in bars simply delays the more rapid passage of finer sediment downstream. Tracer transfer due to both entrainment and morphological change contribute to downstream fining on the Allt Dubhaig.

The role of fixed bars in each reach reflects the contrast in activity. In reach A fixed bars induce bank erosion, reduce the magnitude of sediment waves as they propagate downstream and condition sediment transfer in the submerged channel, influencing flow fields and shear stress distributions (Whiting and Dietrich 1991). Reduced activity in reach B confines the influence of fixed bars to transfer only. These bars have steadily aggraded, probably in response to frequent deposition of shallow gravel sheets. Bar location in reach B has steadily evolved (Figure 3.11) indicative of long term stability. The relative elevation of these features ensures no interaction with tracer sediment (except bar VI), the only possible direct influence with the transfer system being through lateral erosion of bar faces.

Sediment and tracer flux data (Figure 6.5, Figure 6.12) indicate that 1A and 2A are transfer based whilst 3A is storage based. These sub-reaches roughly correspond to meandering and wandering channel patterns respectively, the results are therefore somewhat anomalous. However, both meandering sub-reaches contain fixed bars which give the impression of a storage based system when in fact it is transfer based. The occurrence of fixed bars reduces interaction between stores and decreases differentiation in the submerged channel. This is demonstrated by sub-reach 1A and the throughput reach B. These semi-permanent features are crucial factors dominating (directly and indirectly) the distribution of sediment fluxes. These observations confirm the need for classifications within transitional pattern reaches (e.g. Ferguson 1987) based upon sediment activity and interactions between morphology and flow rather than morphology alone.

6.5 Conclusions

1) Volumetric and tracer fluxes are implicitly linked. In the absence of volumetric change, tracers are transferred due to local scale entrainment. During large events tracer transfer is related to morphological change and entrainment. Sediment is released frequently from transfer based stores in response to small scale scour and fill with releases from less active storage confined to periods of morphological change.

2) Descriptive matrices categorised into distinct types according to flux characteristics (storage, transfer and output) are a useful tool for analysis of the factors conditioning sediment transfer. The frequency of occurrence of each type varied according to event magnitude, grain size and storage type. Each type is a surrogate of dispersion and hence proportional to dimensionless shear stress, type A characterises small local τ^* whilst type F refer to high local τ^*.

3) Finer tracers are transferred further from all storage types due to either entrainment or morphological change. These trends are consistent with observed downstream fining on the Allt Dubhaig.

4) Downstream transfer of sediment is proportional to the imposed shear stress. These fluxes influence bar formation in downstream sub-reaches, usually during intense flooding. Sediment remains in storage where flow is less intense. These trends are conditioned by storage type and grain size.

5) The distribution of critical dimensionless stress describes the potential for tracer transfer. A breakdown of this suggests that hydraulic conditions, storage type and grain size combine to determine transfer in reach A with grain size dominating in B. Deviation at the sub-reach scale is a reflection of the effect of local morphology upon the distribution of critical dimensionless shear stress.

6) Flux rates in reach B are less than in reach A. Relatively small morphological change volumes and tracer transfer fluxes reflect the smaller imposed shear stresses and relatively high critical dimensionless stress in reach B.

7) The location of fixed bars dominates activity and transfer within the submerged channel. These semi-permanent sediment accumulations modify flow fields and shear stress distributions in the submerged channel and hence alter fluxes of sediment and the distribution of morphological change.

7. Sediment transfer distances

The preceding chapters document the importance of lateral storage effects to sediment transfer. The role of storage type, grain size and hydraulics upon sediment transfer was quantified with reference to matrix types. Comparison of transfer distances with conditions at entrainment and assessment of the dominant mode of transfer (equal mobility or size selectivity) allows extension of the MSS analysis where the importance of other factors such as relative grain size and flow duration may be determined.

Recent tracer literature focuses upon two main areas: (1) the characteristic displacement of bed material according to grain size and event magnitude (e.g. Hassan and Church 1992, Hassan et al. 1992) and, (2) the distribution of the entire tracer sample after each flow event (e.g. Hassan and Church 1992, Schmidt and Ergenzinger 1992). It has been speculated that local conditions, particularly flow turbulence are responsible for pseudo-random patterns of sediment transfer (Church and Hassan 1992). Adoption of the storage approach described in chapters 5 and 6 where tracer transfer was assessed relative to reach morphology provides a level of resolution at which movement of individual particles ceases to be entirely random (Hassan and Church 1992).

Transfer distance data reflect the combination of: (1) hydraulic conditions, grain size, morphology and storage type at the initial storage location and (2) the distribution of these factors along the transfer pathway regarded as a series of particle hops (transport). MSS analysis is based entirely on the former. In this chapter the effects of entrainment and transport are isolated with reference to transfer distances. In addition, the use of burial data allows analysis of the importance of sediment transfer within the active layer according to storage type.

7.1 Calculation of tracer transfer distances

The transfer distance of each particle between searches was calculated as the total distance parallel to the thalweg between initial and final locations. Thalweg position was identified from cross section data at the time of each search and distance travelled was calculated relative to the thalweg at the end of the time period in cases where the thalweg position changed.

Previous studies have not shown clear relationships between tracer diameter and distance moved (e.g. Ashworth and Ferguson 1989, Hassan and Church 1992), but aggregation into half phi classes, as used here, reveals trends in some cases. All the data, including that from the first hop will be used when comparing the trends in distance moved from a particular storage site. Although installed in unnatural bed positions, the relative distribution of tracer distances is accurate (Hassan et al. 1991). Where absolute distances are compared, the first hop data are excluded.

Tracer transfer distances vary with event magnitude (e.g. Ashworth and Ferguson 1989). Scaling of these data ensures that the distribution of distances moved according to tracer grain size between successive searches is comparable for a particular storage type or sub-reach. It is usual to scale the mean distance moved by phi class *i*, L_i, with the mean distance moved by the half phi class containing either the surface or subsurface D_{50} (Church and Hassan 1992). In this study, L_i is scaled by $L_{D50surf}$, therefore precluding bias introduced by the effects of relative grain size and vertical winnowing (Parker and Klingeman 1992). Particle movement also reflects the size of the particle relative to the bed material (Church and Hassan 1992). In order to compare relative size trends between reaches, the grain size data are also scaled using surface D_{50}. This choice is based upon the dominant interaction between tracer and bed sediment.

In summary, the following sections present scaled distance L_i^* and grain size D_i^* data where $L_i^*=L_i/L_{D50surf}$ and $D_i^*=D_i/D_{50surf}$ (D_i is the geometric mean of the half phi class *i*). Transfer distances are presented at three spatial scales consistent with chapters 5 and 6: reach, sub-reach and storage type. Insufficient data were available for reliable comparison of sub-reach stores.

7.2 The dominant mode of sediment transfer and relative activity

This section extends the MSS analysis by breaking down the hydraulic effects upon transfer into peak stage and duration. In addition, the mode of transfer is used to assess the importance of relative grain size according to flow conditions. Absolute distances of transfer are compared to evaluate the accuracy of the response time data.

7.2.1 The reach scale

This sub-section examines the dominant mode of transfer in each reach and the controlling factors. Both reaches demonstrate size selective transfer where L_i^* is a maximum during any event for minimum D_i^* (Appendix I1). In reach A the amount of selectivity varies according to the magnitude of the flood event. In particular, transfer during smaller intermediate events is less size selective, due to the narrower range of movement distances associated with such events. Standard errors of the estimate of L_i^* are high since a large number of particles do not move. Event duration influences transfer distances as well as peak magnitude (Hassan et al. 1992). Using this as a basis, it is possible to summarise the data into three characteristic distributions (excluding the first hop): (1) transfer during high peak, low duration events displays pronounced size selectivity (26900 and 62010 min.); (2) small peak, low duration events are characterised by weakly defined size selectivity (32450 and 36000 min.); (3) high peak, long duration events display intermediate selectivity with coarser particles more mobile than in the other event types.

The situation in reach A clearly contrasts with B (appendix I1, B) where there is less differentiation in terms of size selectivity between events. This reflects the narrow range of shear stresses and the frequency of overbank flow at this site, broadly consistent with the results from previous chapters. Comparison of L_i^* (per search) with mean L_i^* (calculated from all searches) reveals considerably more scatter at reach A (Figure 7.1) for $D_i^* < 1$. Less variability occurs at reach B reflecting the coarse nature of the tracers relative to the bed (D_i^* ranges from 0.35 to 2.2 and 0.6 to 2.5 in reaches A and B respectively). At grain sizes below the reach D_{50} the probability of tracers being trapped is increased (Church and Hassan 1992) so the distribution of transfer distances is more scattered.

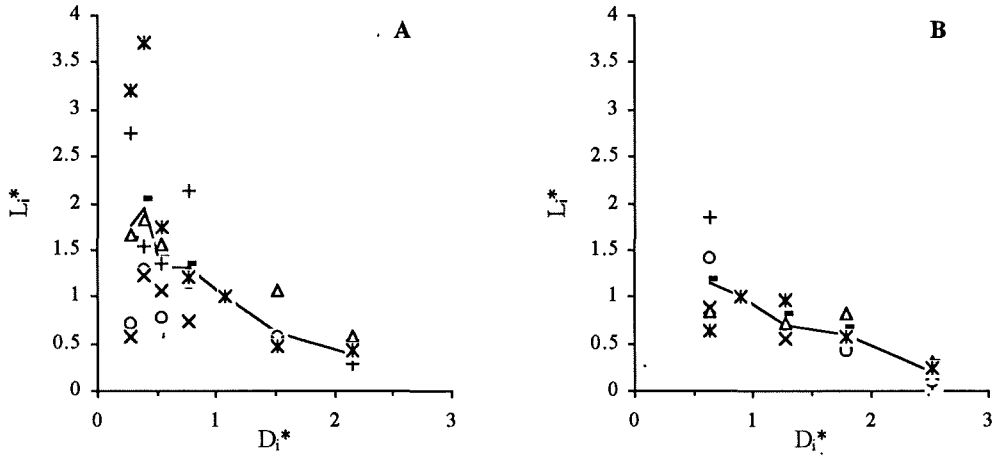

Figure 7.1. Dimensionless plot of fractional movement distances for each tracer search (represented by different symbols). Mean data (solid line) are derived from all six events at each reach.

Data presented in Appendix I1 demonstrate the influence of both reach grain size and hydraulic conditions, hence the need for scaling. The distance a particle moves was related to hydraulic conditions by Hassan et al. (1992) using excess stream power. In this study, it is instructive to assess the importance of peak stage and flow duration upon sediment transfer, previous chapters having demonstrated that tracer and volumetric fluxes are a function of peak stage. This section aims to quantify this for transfer distances and additionally examine whether fractional transfer distances are a function of duration above a bedload threshold. In order to develop functional relationships perpendicular least squares regression (PLS) should be used where error in the dependant and independent variables is apportioned according to standard deviation. However, the small sample size (n = 5) available indicates that PLS offers no advantages in accuracy over the less complex ordinary least squares regression. The aim of this analysis is to assess the relative importance of stage and duration upon fractional transfer distances therefore ordinary least squares multiple regression is an acceptable tool. Regression was carried out of the from $L_i = a + bT + cH$

where H is peak stage (m), T is duration above the bedload threshold and a, b, c are regression constants. Absolute distances are used in the analysis so first hop data were excluded. Summary regression statistics are presented in Table 7.1.

	Predicted relationship	r^2	*p*	*T p*	*H p*
Reach A					
Mean	-42.6+(0.0007*T)+(71.2*H)	97.3	0.03*	0.44	0.07
L_{180}	-11.9+(0.0009*T)+(15.1*H)	97.2	0.03*	0.11	0.23
L_{128}	-16.8+(0.0022*T)+(13.6*H)	98.5	0.02*	0.03	0.39
L_{90}	-23.2+(0.0012*T)+(35.6*H)	97.2	0.03*	0.16	0.14
L_{64}	-28.6+(0.0015*T)+(43.7*H)	99.3	0.01*	0.04	0.04
L_{45}	-47.2+(0.0013*T)+(73.5*H)	97.2	0.03*	0.26	0.10
L_{32}	-90.6-(0.0014*T)+(169*H)	94.3	0.06	0.48	0.07
L_{23}	-80.3-(0.0011*T)+(149*H)	97.4	0.03*	0.38	0.03
Reach B					
Mean	6.35+(0.00004*T)-(3.55*H)	20.0	0.80	0.59	0.55
L_{90}	0.58+(0.00003*T)-(0.05*H)	45.9	0.54	0.67	0.99
L_{64}	4.87+(0.00010*T)-(3.49*H)	83.7	0.16	0.18	0.45
L_{45}	1.61-(0.00002*T)+(2.30*H)	3.80	0.96	0.86	0.82
L_{32}	13.0+(0.00011*T)-(10.2*H)	85.4	0.14	0.10	0.07
L_{23}	11.6-(0.000013*T)-(6.30*H)	12.2	0.87	0.98	0.87

Table 7.1. Relationships between L_i and peak stage (H) and duration (T) derived from multiple regression. Mean L_i is the mean distance moved of fraction *i* during the study (excluding the first hop). Summary regression statistics are also presented. p - level of significance, * - significant at 95% confidence level, T p and H p - level of significance of duration and peak respectively in the predicted relationships.

The relative importance of duration and peak stage in accounting for the variability in fractional transfer distances may be assessed with reference to the distribution of the level of significance of each variable within the multiple regression relationships, T p and H p. The data indicate that duration accounts for a higher proportion of the variability in coarse sediment transfer distances (D_i*>1) although peak stage is important. Most variability in transfer distances of finer clasts (D_i*<1) is accounted for by peak stage with duration being relatively unimportant. Although rarely significant at 95%, these data do indicate the relative importance of peak and duration to fractional transfer distances. The results demonstrate the role of peak stage in early mobilisation of fine sediment which may subsequently be trapped due to downstream pocket geometry (increased scatter in Figure 7.1). Conversely, the probability of entrainment of coarse sediment increases with event duration (usually in association with competent peak stage). Once entrained, this sediment is less likely (relative to fines) to stop, hence duration is the dominant variable. The cross over in T p and H p reflects the non dominance of relative size effects where $D_i^* \approx 1$. These trends provide explanation of the distributions of data presented in Appendix I1. For example, after 57100 min., selectivity is evident but is less pronounced than in other searches. All sediment sizes were mobile,

and finer clasts were entrained earlier and subsequently became increasingly trapped downstream allowing coarser fractions (which were more likely to move later in the event) to start to catch up.

Hydraulic conditions in reach A influence fractional sediment transfer in more than one way. In addition to the effects upon individual particles, morphological change and enhanced sediment transfer are more likely in high peak and long duration events. Transfer in smaller events is restricted to the submerged channel (chapter 6). Once mobile, event characteristics and relative grain size effects condition relative transfer distances. No significant regression relationships were obtained in reach B ($p < 0.05$). This again results from the flow conditions at this site, the narrow range of dimensionless shear stress, and lack of morphological change.

The reach scale results indicate that sediment is transferred size selectively at both sites, consistent with results from other studies on the Allt Dubhaig (e.g. Ferguson and Ashworth 1991, Drew 1992). Comparison between mean L_i^* in reaches A and B and tracer sets T1 - T6 (see Figure 3.1), where mean L_i^* was calculated for each size class over the whole study period, reveals that the mode of sediment transfer in both reaches (Figure 7.2) is consistent with the overall trends in size

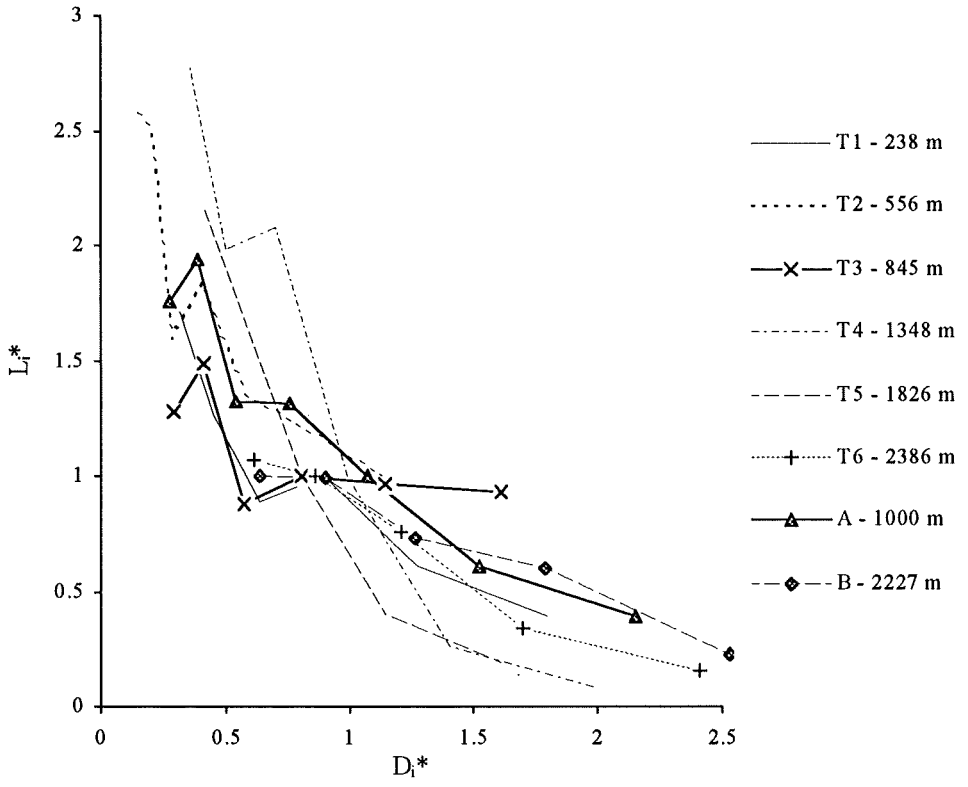

Figure 7.2. Dimensionless plot comparing fractional transfer distances of tracer sets T1 - T6 with reaches A and B. Figures in legend refer to distance from the head of the alluvial reach of the Allt Dubhaig. T3 and reach A are presented as bold lines.

selectivity along the long profile, concordant with observed downstream fining. Reach A demonstrates more pronounced size selectivity than T3, seeded 100 m upstream of A. Rather than a difference in the mode of transfer, this result reflects the contrast in seeding location and downstream morphology. Tracers from T3 were concentrated in a downstream bar and abandoned channel. Tracers located closer to the surface and in more active parts of the bed formed a coarser sub set than the original set giving rise to apparent reduced size selectivity at this site. These results emphasise the need for careful consideration of tracer seeding sites and the importance of morphology upon sediment storage and release at local spatial and temporal scales.

7.2.2 The sub-reach scale

The following section provides a breakdown of reach scale trends in size selectivity isolating the effects of local sub-reach conditions upon the dominant mode of transfer. Movement distances at time t are calculated relative to the tracer location at t-1, for example, if a tracer was in sub-reach 1 at t-1 and sub-reach 2 at t then the distance moved represents activity of sediment in sub-reach 1 (the same condition is also applied to storage type data presented in the following sub-section).

Mean L_i* for the duration of the study indicates that 1A and 2A display approximately the same degree of size selectivity while 3A (where morphology differs from 1A and 2A) contrasts (Figure 7.3). Maximum variability in L_i* occurs at D_i*<1 for all sub-reaches. Pronounced size selectivity

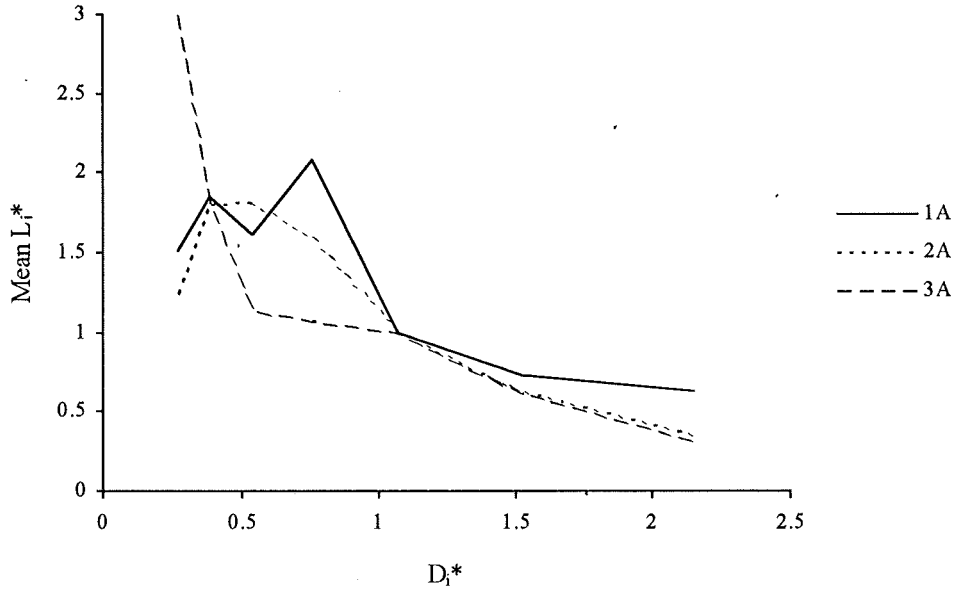

Figure 7.3. Reach A, sub-reach distribution of mean dimensionless distance moved averaged over the whole study.

is apparent in sub-reaches 1A and 2A where the majority of tracers were restricted to the submerged channel. Tracers are subject to potentially high shear stress so the probability of transfer, particularly of the finer fractions, is enhanced. In 3A most tracers are located in storage based S and IA stores requiring morphological change in association with high magnitude, long duration events for appreciable transfer. This type of entrainment reduces the relative mobility difference between grain sizes (except for < 32 mm clasts), as evidenced by reach scale trends, although transfer remains size selective.

Presenting the data per event reveals irregular distributions for the intermediate flood events (Appendix I2) resulting from small numbers of mobile tracers. The majority of tracers in 1A and 2A did not move except for isolated particles travelling considerable distances producing large standard errors of the estimate of the mean. Mobility in 3A was low due to shallow depths. Scour during such events was minor so direct entrainment from the bed was dominated by hiding and protrusion reducing absolute size effects (e.g. Andrews 1983) and the degree of size selectivity compared with upstream sub-reaches. Overall, the dominant mode of transfer in each sub-reach reflects the effect of morphology upon local stage and duration above threshold distributions.

Trends in mean L_i^* in reach B suggest size selectivity is dominant in characterising sediment transfer except for sediment finer than surface D_{50} in sub-reach 1B (Figure 7.4). Sub-reaches 1B and 2B (Appendix I2) indicate decreasing size selectivity with time and no apparent relation to

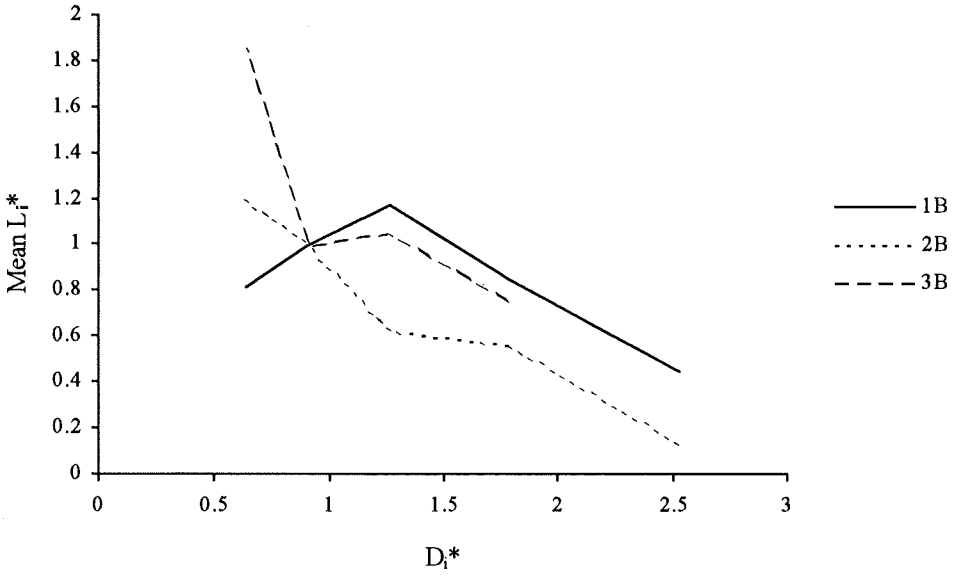

Figure 7.4. Reach B, sub-reach distribution of mean dimensionless distance moved averaged according to event.

contrasting peak stage and duration. The decrease in size selectivity probably reflects the increased incorporation of (more mobile) fine tracers into the subsurface (Schick et al. 1987a). This is

attributable to both vertical winnowing (probably into coarse riffles e.g. sample B1, see section 4.3.2) and local aggradation due to thin gravel sheets scoured from pool sites. Scour in this reach was local, preventing release of previously buried sediment in the short term. The importance of burial is discussed in section 7.4. Results from sub-reach 3B are less reliable due to decreased sample size but indicate a wider range of L_i* values than 1B and 2B suggesting increased activity, particularly for finer fractions.

Assessment of sub-reach activity can be made by normalising fractional transfer distance L_i for each sub-reach by the transfer distance at the reach scale, L_{ir}, for the corresponding fraction *i*. The resultant variable, L_i'* can be used to assess the validity of the response time results from chapter 5. Data for each sub-reach per event are too noisy to derive general trends (Appendix I3) so a mean was taken across the five searches, excluding the first hop. In general, sub-reach 3A is the least active (Figure 7.5a) with activity in 1A slightly greater than 2A, consistent with trends in Γ_i (Table 5.7). The mean L_i'* across all grain size classes, L'*, indicates the mean proportion of total transfer distances accounted for by each sub-reach. Results in reach A indicate a decline in this figure from 1.15 at 1A, 1.09 at 2A to 0.84 at 3A. Mean L'* declines from 2.33 at 3B to 0.99 and 0.81 at 2B and 1B respectively indicative of the higher activity in 3B compared with upstream sub-reaches, although, sample sizes are small. Reduced activity at 1B may result from vertical winnowing of finer sediment into the riffles.

The trends in transfer distance are consistent with response time in all sub-reaches (section 5.3.2). Γ_i and tracer activity are attributable to the combined effects of storage type, hydraulic conditions, and grain size. In addition, this section has demonstrated that relative grain size is important. The interaction of all these variables at the local scale are responsible for the results discussed herein. A more complete comparison between distance and response time data is presented in section 7.2.5.

7.2.3 Storage type.

Too few tracers are located in individual stores to allow comparison in as much detail as in previous chapters, but sufficient data exist to compare the mode of sediment transfer and relative activity of storage types. This information provides a breakdown of reach scale trends relative to storage type.

Data are presented as L_i* per event for each storage type in both reaches (Appendix I4). In reach A, sediment transfer from each storage type is generally size selective, particularly for finer fractions and intermediate events (as shown by L_i*>4). Generalising this data into mean L_i* over the whole study (Figure 7.6) reveals that transfer of sediment from all stores is size selective although the relative trends contrast. The data are scattered for D_i* < 1 and storage based S and IA

Whiting, P. S., Dietrich, W. E., Leopold, L. B., Shreve, R. L. and Drake, T. G. (1988) 'Bedload sheets in heterogeneous sediments', *Geology,* **16**, 105 - 108.

Wiberg, P. L. and Smith, J. D. (1987) 'Calculation of the critical shear stress for motion of uniform and heterogeneous sediments', *Wat. Resour. Res.*, **23**, 1471 - 1480.

Wilcock, P. J. (1988) 'Methods for calculating the critical shear stress of individual fractions in mixed sized sediment', *Wat. Resour. Res.*, **24**, 1127 - 1135.

Wilcock, P. J. and Southard, J. B. (1988) 'Experimental study of incipient motion in mixed size sediment', *Wat. Resour. Res.*, **24**, 1137 - 1151.

Wilcock, P. J. (1992a) 'Flow competence: A criticism of a classic concept', *Earth Surface Processes and Landforms*, **17**, 289 -298.

Wilcock, P. J. (1992b) 'Experimental investigation of the effect of mixture properties on transport dynamics' in Billi, P., Hey, R. D., Thorne, C. R. and Tacconi, P. (Eds.), *Dynamics of Gravel Bed Rivers*, Wiley, Chichester, England, 109 - 139.

Wilkin, D. C. and Hebel, S. J. (1982) 'Erosion, redeposition and delivery of sediment to midwestern streams', *Wat. Resour. Res.*, **18**, 1278 - 1282.

Williams, P. F. and Rust, B. R. (1969) 'The sedimentology of a braided river', *Jnl. of Sedimentary Petrology*, **39**, 649 - 679.

Wolcott, J. and Church, M. (1991) 'Strategies for sampling spatially heterogeneous phenomena: The example of river gravels', *Jnl. of Sedimentary Petrology*, **61**, 534 - 543.

Wolman, M. G. (1954) 'A method of sampling coarse river bed material', *Trans. Am. Geophys. Union*, **35**, 951 - 956.

Wolman, M. G. and Gerson, R. (1978) 'Relative scales of time and effectiveness in watershed geomorphology', *Earth Surface Processes*, **3**, 189 - 208.

Yalin, M. S. and Karahan, E. (1979) 'Inception of sediment transport', *Jnl. of Hydraulics Division, ASCE*, **105**, 1433 - 1444.

Sternberg, H. (1875) 'Untersuchungen uber Langen-und Querprofil Geschiebefuhrende Flusse', *Zeischrift fur Bauwesen*, **25**, 483 - 506.

Stott, T. A., Ferguson, R. I., Johnson, R. C. and Newson, M. D. (1986) 'Sediment budgets in forested and unforested basins in upland Scotland', in Hadley, R. F. (Ed), *Drainage Basin Sediment Delivery*, IAHS Publication, No. 159, 57 -68.

Sutherland. A. J. (1987) 'Static armour layers by selective erosion' in Thorne, C. R. Bathurst, J. C. and Hey, R. D. (Eds.), *Sediment Transport in Gravel Bed Rivers*, Wiley, Chichester, England, 243 - 267.

Takayama, S. (1965), 'Bedload movement in torrential mountain streams' *Tokyo Geographical Paper*, **9**, 169 - 188.

Thorne, C. R. and Lewin, J. (1979) 'Bank processes, bed material movement and planform development in a meandering river', in Rhodes and Williams (Eds.), *Adjustments of the Fluvial System*, Kendall/Hunt, Dubuque, Iowa, USA, 117 - 137.

Thorne, C. R. and Tovey, N. K. (1981) 'Stability of composite river banks', *Earth Surface Processes and Landforms*, **6**, 469 - 484.

Thorne, C. R., Zeuenbergen, L. W., Pitlick, J. C., Rais, S., Bradley, J. B. and Julien, P. Y. (1985) 'Direct measurements of secondary currents in a meandering sand bend river', *Nature*, **316**, 746 - 747.

Trimble, S. W. (1981) 'Changes in sediment storage in the Coon Creek basin, Driftless area, Wisconsin, 1853 to 1975', *Science*, **214**, 181 - 183.

Wathen, S. J., Ferguson, R. I., Hoey, T. B. And Werritty, A. (in prep.) 'Unequal mobility of sand and gravel in weakly bimodal sediment'.

Werritty, A. (1992) 'Downstream fining in a gravel bed river in S. Poland: Lithologic controls and the role of abrasion', in Billi, P., Hey, R. D., Thorne, C. R. and Tacconi P. (Eds.), *Dynamics of Gravel Bed Rivers*, Wiley, Chichester, 333 - 350.

Whiting, P. J. and Dietrich, W. E. (1991) 'Convective accelerations and boundary shear stress over a channel bar', *Wat. Resour. Res.*, **27**, 783 - 796.

Schmidt, K. M. and Ergenzinger, P. (1992) 'Bedload entrainment, travel lengths, step lengths, rest periods - Studied with passive (iron, magnetic) and active (radio) tracer techniques', *Earth Surface Processes and Landforms*, **17**, 147 - 165.

Schumm, S. A. and Khan, H. R. (1972) 'Experimental study of channel patterns', *Geol. Soc. of Am. Bull.*, **83**, 1755 - 1770.

Schumm, S. A. and Stevens, M. A. (1973) 'Abrasion in a place: a mechanism for rounding and size reduction of coarse sediments in rivers', *Geology*, **1**, 37 - 40.

Seal, R., Parker, G. And Paola, C. (1993) 'The effect of local patchiness of gravel grain size distributions on bed load transport in braided rivers, paper presented at International Conference on Hydroscience and Engineering, ASCE, Washington, D. C.

Sear, D. (1992) 'Impact of Hydroelectric Power releases on sediment transport processes in pool riffle sequences', in Billi, P., Hey, R. D., Thorne, C. R. and Tacconi, P. (Eds.), *Dynamics of Gravel Bed Rivers*, Wiley, Chichester, 629 - 650.

Seminara, G. and Tubino, M. (1989) 'Alternate bars and meandering', in Ikeda, S. and Parker, G. (Eds.), *River Meandering*, Water Resource Mangr. Ser., Vol 12, AGU, Washington DC, 267 - 320.

Shields, A. (1936) 'Anwendung der Aehnlichkeitsmechanik und der turbulenzforschung auf die gescheibebewegung', *Mitteilung der Praussischen versuchsanstadlt fuer Wasserbau und Schiffbau*, **Heft 26**, Berlin.

Shih, S. M. and Komar, P. D. (1990a) 'Hydraulic controls of grain size distributions of bedload gravels in Oak Creek, Oregon, USA', *Sedimentology*, **37**, 367 - 376.

Shih, S. M. and Komar, P. D. (1990b) 'Differential bedload transport rates in a gravel bed stream: A grainsize distribution approach', *Earth Surface Processes and Landforms*, **15**, 539 -552.

Singh, V.P., Krstanovic, P. F. and Lane, L. J. (1988) 'Stochastic models of sediment yield', in Anderson, M. G. (Ed), *Modelling Geomorphological Systems*, Wiley, Chichester, 259 - 285.

Smith, R. (1991) 'The application of cellular automata to the erosion of landforms', *Earth Surface Processes and Landforms*, **16**, 273 - 281.

Pickup, G., Higgings, R. J. and Grant, I. (1983) 'Modelling sediment transport as a moving wave - transfer and deposition of mining waste', *Jnl. of Hydrology*, **60**, 281 - 301.

Prestegaard, K. L. (1983) 'Variables influencing water surface slopes in gravel bed streams at bankfull stage', *Geol. Soc. of Am. Bull.*, **94**, 673 - 678.

Reid, I., Frostick, L. E. and Brayshaw, A. C. (1992) 'Microform roughness elements and the selective entrainment and entrapment of particles in gravel bed rivers', in Billi, P., Hey, R. D., Thorne, C. R. and Tacconi, P. (Eds.), *Dynamics of Gravel Bed Rivers*, Wiley, Chichester, 253 - 275.

Richards, K. S. (1982) '*Rivers. Form and Process in Alluvial Channels*', Methuen, London.

Ritchie, J. C., Hawks, P. and McLeary, R. J. (1975) 'Deposition rates in valleys determined using fallout Caesium - 137', *Geol. Soc. of Am. Bull*, **86**, 1128 - 1130.

Robinson, M. and Blythe, K. (1982) 'The effect of forestry drainage operations upon upland sediment yields', *Earth Surface Processes and Landforms*, **7**, 85 - 90.

Rundle, A. (1985) 'The mechanisms of braiding', *Z. Geomorph., Suppl. Bl.*, **55**, 15 - 37.

Rust, B. (1972) 'Pebble orientation in fluvial sediments', *Jnl. of Sedimentary Petrology*, **42**, 384 - 388.

Sambrook-Smith, G. and Ferguson, R. I. (in press) 'The gravel sand transition along river channels', *Jnl. of Sedimentary Research*.

Saunders, D. (1988) 'Bedload transport in a riffle pool bar sequence of the R. Feshie, Scotland', *unpublish. Honours Dissertation*, St. Andrews University, No. 76.

Schick, A. P., Hassan, M. A. and Lekach, J. (1987a) 'A vertical exchange model for coarse bedload movement: numerical consideration', in Ahnert, F (Ed.), *Geomorphological Models - Theoretical and Empirical Aspects*, Catena Suppl. 10, 73 - 83.

Schick, A. P., Hassan, M. A. and Lekach, J. (1987b) 'Vertical exchange of coarse bedload in desert streams' in Frostick, L. E. and Reid, I. (Eds.), *Desert sediments: Ancient and Modern*, Geological Soc. Of London, Spec. Publ., 7 - 16.

Newson, M. (1992) 'Geomorphic thresholds in gravel-bed rivers - Refinement for an era of environmental change', in Billi, P., Hey, R. D., Thorne, C. R. and Tacconi, P. (Eds.), *Dynamics of Gravel Bed Rivers*, Wiley, Chichester, England, 3 - 15.

Oldfield, P., Thompson, F. R. and Dickson, D. P. E. (1981), 'Artificial enhancement of stream bedload: a hydrological application of superparamagnetism', *Physics of Earth and Planetary Systems*, **26**, 107 - 124.

Paola, C. and Wilcock, P. J. (1989) 'Downstream fining in gravel bed rivers', *EOS*, Sept. 19.

Parker, G. (1979) 'Hydraulic geometry of active gravel rivers', *Jnl. of Hydraulics Division, ASCE,* **105**, 1185 - 1201.

Parker, G. (1990) 'A surface based bedload transport relation for gravel bed rivers', *Jnl. of Hydraulic Research,* **28**, 417 - 436.

Parker, G. (1991a) 'Selective sorting and abrasion of river gravels. I. Theory', *Jnl. of Hydraulic Engineering*, **117**, 131 - 149.

Parker, G. (1991b) 'Selective sorting and abrasion of river gravels. II. Applications', *Jnl. of Hydraulic Engineering*, **117**, 150 - 171.

Parker, G. and Klingeman, P. C. (1982) 'On why gravel bed streams are paved', *Wat. Resour. Res.*, **18**, 1409 - 1423.

Parker, G. and Sutherland, A. J. (1990) 'Fluvial Armour', *Jnl. of Hydraulic. Research.*, **28**, 529 - 544.

Parker, G., Klingeman, P. C. and McLean, D. C. (1982a) 'Bedload and size distribution in paved gravel-bed streams', *Jnl. of Hydraulics Division, ASCE*, **108**, 544 - 571.

Parker, G., Dhamotharan, S. and Stefan, H. (1982b) 'Model experiments on mobile paved gravel-bed streams', *Wat. Resour. Res.*, **18**, 1395 - 1408.

Pickup, G. (1988) 'Hydrology and Sediment models', in Anderson, M. G. (Ed.), *Modelling Geomorphological Systems*, Wiley, Chichester, 153 - 216.

Meland, N. and Norrman, J. O. (1966) 'Transport velocities of single particles in bed load motion', *Geografiska Annalar*, **48A**, 165 - 182.

Meland, N. and Norrman, J. O. (1969) 'Transport velocities of individual size fractions in heterogeneous bedload', *Geografiska Annalar*, **51A**, 127 - 144.

Meyer-Peter, E. and Müller, R. (1948) 'Formulas for bedload transport', *Proc. of the International Assc. of Hydraulic Research*, 3rd Annual Conference, Stockholm, 39 - 64.

Miall, A. D. (1977) 'A review of the braided river depositional environment', *Earth Science Reviews*, **13**, 1 - 62.

Milhous, R. T. (1973) 'Sediment transport in a gravel bottomed stream', *Unpublish. Ph.D. thesis*, Oregon State University, Corvallis.

Miller, J. P. (1958) 'High mountain streams; effects of geology on channel characteristics and bed material', *New Mexico State Bureau of Mines and Mineral Resources*, **Memoir 4**.

Mosley, M. P. (1978) 'Bed material transport in the Tamaki River near Dannevirke, North Island, New Zealand', *New Zealand Journal of Science*, **21**, 165 - 184.

Mosley, M. P. (1982) 'A procedure for classifying river channels', *Water and Soil Science Miscellaneous Publ. 32*, Wellington, National water and soil conservation organisation, NZ, 68pp.

Murray, A. B. and Paola, C. (1994) 'A cellular model of braided rivers', *Nature*, **371**, 54 - 57.

Nakamura, F. (1986) 'Analysis of storage and transport processes based on age distribution of sediment', *Trans. Jap. Geomorph. Union*, **7-3**, 165 - 184.

Nakamura, F., Araya, T. and Higashi, S. (1987) 'Influence of river channel morphology and sediment production on residence time and transport distance', *Erosion and Sedimentation in the Pacific Rim (Proc. of the Corvallis Symposium, August, 1987)*, IAHS Publication, No. 165.

Neill, C. R. and Galay, V. J. (1967) 'Systematic evaluation of river regime', *Jnl. of waterways and Harbours Divn., ASCE*, **WW1**, 25 - 63.

Leopold, L. B, Emmett, W. W and Myrick, R. M. (1966), 'Channel and hillslope processes in a semi arid area, New Mexico', *USGS Prof. Paper*, **352-G**.

Lewin, J. (1976) 'Interaction of bedforms and meanders in coarse grained sediment', *Geol. Soc. of Am. Bull.*, **87**, 281 - 285.

Lewin, J. (1989) 'Sediment reduction processes in natural rivers', *Interim Report on NERC GR3/6340*, 10pp.

Lewin, J., Davies, B. E. and Wolfenden, P. J. (1977) 'Interactions between channel change and historic mining sediments', in Gregory, K. J. (Ed.), *River channel changes*, Wiley, Chichester, 353 - 367.

Li, Z. and Komar, P. D. (1986) 'Laboratory measurements of pivoting angles for applications to selective entrainment of gravel in a current, *Sedimentology*, **33**, 413 - 423.

Lisle, T and Madej, M. (1992) 'Spatial variation in armouring in a channel with high supply', in Billi, P., Hey, R. D., Thorne, C. R. and Tacconi, P. (Eds.), *Dynamics of Gravel Bed Rivers*, Wiley, Chichester, 277 - 293.

Little, W. C. and Meyer, P. C. (1976) 'Stability of channel beds by armoring', *Jnl. of Hydraulics Division, ASCE*, **102**, 1647 - 1661.

Markham, A. and Thorne, C. R. (1992) 'Geomorphology of gravel bed river bends', in Billi, P., Hey, R. D., Thorne, C. R. and Tacconi, P. (Eds.), *Dynamics of Gravel Bed Rivers*, Wiley, Chichester, 433 - 456.

McKercher, A. I. (1980) 'Thresholds in deterministic models of the rainfall-runoff process', in Coates, E. R. and Vitek, J. D. (Eds.), *Thresholds in Geomorphology*, George Allen and Unwin, London, 171 - 177.

McLean, D. G. (1990) 'The relation between channel instability and sediment transport on Lower Fraser River', *unpublish. Ph.D. thesis*, Univ. of British Columbia.

Meade, R. H. (1982) 'Sources, sinks and storage of river sediment in the Atlantic drainage of the US', *Jnl. of Geology.*, **90**, 235 - 252.

Kuhnle, R. A. (1992) 'Fractional transport rates of bedload on Goodwin Creek', in Billi, P., Hey, R. D., Thorne, C. R. and Tacconi, P. (Eds.), *Dynamics of Gravel Bed Rivers*, Wiley, Chichester, England, 141 - 155.

Kuhnle, R. A. (1993) 'Fluvial transport of sand and gravel mixtures with bimodal size distributions', *Jnl. Hydraul. Eng.*, **118**, 1443 - 1446.

Kussner, B. (1992) 'Morphological measurement of bedload transport rate in braided streams', *B.Sc. thesis*, The University of Western Ontario, 83pp.

Lane, S. N., Richards, K. S. and Chandler, J. H. (1994) 'Developments in monitoring and modelling small-scale river bed topography', *Earth Surface Processes and Landforms*, **19**, 349 - 369.

Lane, S. N., Richards, K. S. and Chandler, J. H. (in prep) 'Discharge and sediment supply controls on erosion and deposition in a dynamic alluvial channel'.

Laronne, J. B. (1987) 'Recommended bed material discharge techniques for NSW rivers', *Report to the NSW Dept. of Water Resources*, 25pp.

Laronne, J. B. and Carson, M. A. (1976), 'Interrelationships between bed morphology and bed material transport for a small gravel bed channel', *Sedimentology*, **23**, 67 - 85.

Laronne, J. B. and Duncan, M. J. (1992), 'Bedload transport path and gravel bar formation, in Billi, P., Hey, R. D., Thorne, C. R. and Tacconi, P. (Eds.), *Dynamics of gravel bed rivers*, Wiley, Chichester, 177 - 200.

Leeder, M. R. (1982) *Sedimentology: Process and Product*, Allen and Unwin, London.

Lekach, J., Schick, A. P. and Shlesinger (1992) 'Bedload yield and in channel provenance in a flash flood fluvial system', in Billi, P., Hey, R. D., Thorne, C. R. and Tacconi, P. (Eds.), *Dynamics of Gravel Bed Rivers*, Wiley, Chichester, 537 - 554.

Leopold, L. B. and Wolman, M. G. (1957) 'River channel patterns - braided, meandering and straight', *USGS Prof. Paper*, **282A**.

Leopold, L. B, Wolman, M. G and Miller, J. P. (1964), *Fluvial processes in geomorphology*, Freeman, San Francisco.

Kelsey, H. M., Lamberson, R. and Madej, M. A. (1987) 'Stochastic model for the long term transport of stored sediment in a river channel', *Wat. Resour. Res.*, **23**, 1738 - 1750.

Kirchner, J. W., Dietrich, W. E., Iseya, F. and Ikeda, H. (1990) 'The variability of critical shear stress, friction angle, and grain protrusion in water worked sediments', *Sedimentology*, **37**, 647 - 672.

Kodama, Y. (1992) 'Effect of abrasion on downstream gravel-size reduction in the Watarase River, Japan: Field work and laboratory experiment', *University of Tsukba Environmental Research Center Paper*, **15**, 88pp.

Komar, P. D. (1987) 'Selective grain entrainment by a current from a bed of mixed sizes: a reanalysis', *Jnl. of Sedimentary Petrology*, **57**, 203 - 211.

Komar, P. D. and Li, Z. (1986) 'Pivoting angle analysis of the selective entrainment of sediment by shape and size with application to gravel thresholds', *Sedimentology*, **33**, 425 - 436.

Komar, P. D. and Shih, S. M. (1992) 'Equal mobility versus changing bedload grainsizes in gravel bed streams', in Billi, P., Hey, R. D., Thorne, C. R. and Tacconi, P. (Eds.), *Dynamics of Gravel Bed Rivers*, Wiley, Chichester, 73 - 106.

Komura, S. (1961) 'Bulk properties of river bed sediments, its application to sediment hydraulics', *Proc. 11th Japan Nat. Congr. Appl. Mechs.*, 227 - 231.

Krigstrom, A. (1962) 'Geomorphological studies of sandur plains and their braided rivers in Iceland', *Geografiska. Annalar.*, **44**, 328 - 346.

Krumbein, W. C. (1941) 'The effects of abrasion on the size and shape of rock fragments', *Jnl. of Geology*, **49**, 482 - 500.

Kuenen, P. H. (1956) 'Experimental abrasion of pebbles. 2. Rolling by current', *Jnl. of Geology*, **64**, 336 - 368.

Kuhlne, R. A. and Southard, J. B. (1988) 'Bedload transport fluctuations in a gravel bed laboratory channel', *Wat. Resour. Res.*, **24**, 247 - 260.

Hjulström, F. (1935) 'Studies of the morphological activity of rivers as illustrated by the River Fyris', *Bulletin of the Geological Institute, University of Uppsala*, **25**, 221 - 527.

Hoey, T. B. (1989) 'An examination of the forms and processes associated with bed waves in gravel bed rivers, with special reference to the braided river type', *unpublish. Ph.D. Thesis*, University of Canterbury, Christchurch, 287pp.

Hoey, T. B. (in press 1995) 'Sediment dispersion and duration of storage in model braided river beds', *Jnl. of Hydrology (New Zealand)*.

Hoey, T. B. and Sutherland, A. J. (1991) 'Channel morphology and bedload pulses in braided river: A laboratory study', *Earth Surface Processes and Landforms*, **16**, 447 - 462.

Hoey, T. B. and Ferguson, R. I. (1994) 'Numerical simulation of downstream fining by selective transport in gravel bed rivers: Model development and illustration', *Wat. Resour. Res.*, **30**, 2251 - 2260.

Hooke, R. L. (1975) 'Distribution of sediment transport and shear stress in a meander bend', *Jnl.of Geology*, **83**, 543 - 565.

Hubbell, D. W. and Sayre, W. (1964) 'Sand transport studies with radioactive tracers', *Jnl. of Hydraulics Division, ASCE*, **90**, 36 - 98.

Iseya, F. and Ikeda, H. (1987) 'Pulsations in bedload transport rates induced by longitudinal sediment sorting: a flume study using sand and gravel mixtures', *Geografiska. Annalar*, **69A**, 15 - 27.

Keller, E. A. (1971) 'Areal sorting of bedload material; the hypothesis of velocity reversal', *Geol. Soc. of Am. Bull.*, **82**, 753 - 756.

Keller, E. A. and Florsheim, J. L. (1993) 'Velocity-reversal hypothesis: A model approach', *Earth Surface Processes and Landforms*, **18**, 733 - 741.

Kellerhals, R. and Bray, D. I. (1971) 'Sampling procedures for coarse fluvial sediments', *Jnl. of Hyraulics Division, ASCE*, **97**, 1165 - 1180.

Kelsey, H. M. (1980) 'A sediment budget and an analysis of geomorphic process in the Van Duzen River basin, N. coastal California 1941 - 1975', *Geol. Soc. of Am. Bull.*, **91**, 1119 - 1216.

Goff, J. R. and Ashmore, P. (1994) 'Gravel transport and morphological change in braided Sunwapta river, Alberta, Canada', *Earth Surface Processes and Landforms*, **19**, 195 - 213.

Gomez, B. (1991) 'Bedload transport', *Earth Science Reviews*, **31**, 89 - 132.

Gomez, B. and Church, M. (1989) 'An assessment of bedload sediment transport formulae for gravel bed rivers', *Wat. Resour. Res.*, **25**, 1161 - 1186.

Gomez, B., Naff, R. L. and Hubbell, D. W. (1989) 'Temporal variations in bedload transport rates', *Earth Surface Processes and Landforms*, **14**, 135 - 156.

Griffiths, G. A. (1979) 'Recent sedimentation history of the Waimakariri River, New Zealand', *Jnl. of. Hydrology (New Zealand)*, **18**, 6 - 28.

Grigg, N. S. (1970) 'Motion of single particles in alluvial channels', *Jnl. of the Hydraulics Division, ASCE*, **96**, 2501 - 2518.

Hassan, M. A. (1990) 'Scour, fill and burial depth of coarse material', *Earth Surface Processes and Landforms*, **15**, 341 - 356.

Hassan, M. A. and Church, M. (1992) 'The movement of individual grains on the streambed', in Billi, P., Hey, R. D., Thorne, C. R. and Tacconi, P. (Eds.), *Dynamics of Gravel Bed Rivers*, Wiley, Chichester, 159 - 175.

Hassan, M. A. and Church, M. (1994) 'Vertical mixing of coarse particles in gravel bed rivers: A kinematic model', *Wat. Resour. Res.*, **30**, 1173 - 1185.

Hassan, M. A., Schick, A. P. and Laronne, J. B. (1984) 'The recovery of flood dispersed coarse sediment particles, a 3-D magnetic tracing method', in Schick, A. P. (Ed.), *Channel Processes - Water, Sediment and Catchment Controls*, Catena Suppl. 5, 153 - 162.

Hassan, M. A., Church, M. and Schick, A. P. (1991) 'Distance of movement of coarse particles in gravel bed streams', *Wat. Resour. Res.*, **27**, 503 - 511.

Hein, F. J. and Walker, R. G. (1977) 'Bar evolution and development of stratification in the gravely, braided, Kicking Horse River, British Colombia', *Canadian Jnl. of Earth Sciences*, **14**, 562 - 570.

Eriksson, E. (1971) 'Compartment models and reservoir theory', *Annu. Rev. Ecol. and System*, **2**, 67 - 84.

Everitt, B. L. (1968) 'Use of cottonwood in an investigation of the recent history of a floodplain', *Am. Jnl. of Science*, **266**, 417 - 439.

Fenton, J. D. and Abbott, J. E. (1977) 'Initial movement of grains on a streambed: the effect of relative protrusion', *Proc. of the Royal Society London Ser. A*, **352A**, 523 - 527.

Ferguson, R. I. (1987) 'Hydraulic and sedimentary controls of channel pattern', in Richards, K. S. (Ed.), *River Channels: Environment and Process*, Blackwell, 125 - 158.

Ferguson, R. I. and Werritty, A. (1983) 'Bar development and channel changes in the gravely River Feshie, Scotland', in Collinson, C. D. and Lewin, J. (Eds.), *Modern and Ancient Fluvial Systems*, Special Publn. of the Assc. of Sedimentologists, **6**, 181 - 193.

Ferguson, R. I. and Ashworth, P. J. (1991) 'Slope-induced changes in channel character along a gravel-bed stream: The Allt Dubhaig, Scotland', *Earth Surface Processes and Landforms*, **16**, 65 - 82.

Ferguson, R. I. and Ashworth, P. J. (1992) 'Spatial patterns of bedload transport and channel change in braided and near braided rivers', in Billi, P., Hey, R. D., Thorne, C. R. and Tacconi, P (Eds.), *Dynamics of Gravel Bed Rivers*, Wiley, Chichester, 477 - 496.

Ferguson, R. I., Prestegaard, K. L. and Ashworth, P. J. (1989) 'Influence of sand on hydraulics and gravel transport in a braided gravel bed river', *Wat. Resour. Res.*, **25**, 635 - 643.

Frostick, L. E. and Reid, I. (1980) 'Sorting mechanisms in coarse grained alluvial sediments: Fresh evidence from a basalt plateau, Kenya', *Jnl. of Geological Society of London*, **129**, 431 - 441.

Frostick, L. E., Lucas, P. M. and Reid, I. (1984) 'The infiltration of fine matrices into coarse-grained alluvial sediment and its implications for stratigraphic interpretation', *Jnl. of Geological Society of London*, **141**, 955 - 965.

Gilbert, G. K. (1914) 'Transport of debris by running water', *USGS Prof. Paper*, **86**.

Diplas, P. and Parker, G. (1992) 'Deposition and removal of fines in gravel bed streams', In Billi, P., Hey, R. D., Thorne, C. R. and Tacconi, P (Eds.), *Dynamics of Gravel Bed Rivers*, Wiley, Chichester, 313 - 329.

Drew, I. B. (1992) 'Bedload transport, vertical exchange and sediment storage in two Scottish Highland gravel bed streams', *unpublish. Ph.D. thesis*, St. Andrews University.

du Boys, M. P. (1879) 'Etudes du régime et l'action exercé par les eaux sur un lit à fond de graviers indéfiniment affouiable', *Ann. Ponts Chaussees*, **5**, 141 - 195.

Egiazaroff, I. V. (1965) 'Calculation of non uniform sediment concentrations', *Jnl. of Hydraulics. Division, ASCE.*, **91**, 225 - 247.

Einstein, H. A. (1937) 'Bedload transport as a probability problem' (in German), *Ph.D. dissertation*, Eidgenoess. Tech. Hochsch, Zurich, Switzerland.

Einstein, H. A. (1942) 'Formulas for the transportation of bedload', *Trans. of the American Society of Civil Engineers*, **107**, 561 - 597.

Einstein, H. A. (1950) 'The bedload function for sediment transportation in open channel flows', *Technical Bulletin, USDA*, **1026**.

Einstein, H. A. and Barbarossa, N. L. (1952) 'River channel roughness', *Trans. of the American Society of Civil Engineers*, **117**, 1121 - 1146.

Elder, K., Kattelmann, R. and Ferguson, R. I. (1990) 'Refinements in dilution gauging for mountain streams', *Int. Assoc. Hydrol., Proc. Mountain Hydrology Symposium*, Lausanne.

Ergenzinger, P. (1992) 'Riverbed adjustments in a step pool system: Lainbach, Upper Bavaria', in Billi, P., Hey, R. D., Thorne, C. R. and Tacconi, P. (Eds.), *Dynamics of Gravel Bed Rivers*, Wiley, Chichester, 415 - 430.

Ergenzinger P. and Custer (1983) 'Determination of bedload transport using naturally magnetic tracers', *Wat. Resour. Res.*, **19**, 187 - 193.

Ergenzinger P., Schmidt, K-H and Busskamp, R. (1989) 'The pebble transmitter system (PETS): first results of a technique for studying coarse material erosion, transport and deposition', *Zeitschrift für Geomorpologie N. F.*, **33**, 503 - 508.

Church, M. and Kellerhals, R. (1978) 'On the statistics of grain size variation along a gravel river', *Canadian Jnl. of Earth Sciences*, **15**, 1151 - 1160.

Church, M. and Jones, D. (1982) 'Channel bars in gravel bed rivers', in Hey, R. D., Bathurst, J. C. and Thorne, C. R. (Eds.), *Gravel Bed Rivers. Fluvial process, Engineering and Management*, Wiley, Chichester, England, 291 - 339.

Church, M. and Hassan, M. A. (1992) 'Size and distance of unconstrained clasts on a streambed', *Wat. Resour. Res.*, **28**, 299 - 303.

Church, M., McLean, D. G. and Wolcott, J. F. (1987) 'River bed gravels: Sampling and analysis', in Thorne, C. R. Bathurst, J. C. and Hey, R. D. (Eds.), *Sediment Transport in Gravel Bed Rivers*, Wiley, Chichester, England, 43 - 79.

Dawson, M. (1988) 'Sediment size variation in a braided reach of the Sunwapta River, Alberta, Canada' *Earth Surface Processes and Landforms*, **13**, 599 - 618.

Dietrich, W. E. and Dunne, T. (1978) 'Sediment budget for a small catchment in mountainous terrain', *Z. Geomorph.*, **29**, 191 - 206.

Dietrich, W. E. and Smith, J. D. (1983) 'Influence of the point bar on flow through curved channels', *Wat. Resour. Res.*, **19**, 1173 - 1192.

Dietrich, W. E. and Smith, J. D. (1984) 'Bedload transport in a river meander', *Wat. Resour. Res.*, **20**, 1355 - 1380.

Dietrich, W. E., Dunne, T., Humphrey, N. F. and Reid, L. M. (1982) 'Construction of sediment budgets for drainage basins', in Swanson, F. J., Janden, R. J., Dunne, T. and Swanston, D. N. (Eds.) *'Sediment budgets and routing in forested drainage basins'*, USDA Forest Service, Pacific NW forest and range experiment station, General Technical Report PNW-141, 165pp.

Dietrich, W. E., Kirchner, J. W, Iseya, H. and Ikeda, F. (1989) 'Sediment supply and the development of the coarse surfaced layer in gravel bedded rivers', *Nature*, **340**, 215 - 217.

Diplas, P. (1987) 'Bedload transport in gravel-bed streams', *Jnl. of Hyd. Engineering., ASCE*, **113**, 277 - 292.

Carling, P. A. (1987) 'Bed stability in gravel streams, with reference to stream regulation and ecology', in Richards, K. S. (Ed.), *River Channels: Environment and Process, Spec. Publ. 17*, Institute of British Geographers, London.

Carling, P. A. (1991) 'An appraisal of the velocity-reversal hypothesis for stable pool-riffle sequences in the River Severn, England', *Earth Surface Processes and Landforms*, **16**, 19 - 31.

Carling, P. A. and McMahon, C. P. (1987) 'Natural siltation of brown trout (Salmo Trutto) spawning gravels during low flow conditions', in Craig, J. F. and Kemper, J. B. (Eds.), *Regulated Streams*, Plenum.

Carling, P. A. and Wood, N. (1994) 'Simulation of flow over pool-riffle topography: A consideration of the velocity reversal hypothesis', *Earth Surface Processes and Landforms*, **19**, 312 - 332.

Carling, P. A., Kelsey, A. and Glaister, M. S. (1992) 'Effects of bed roughness, particle shape and orientation on inertial motion criteria', in Billi, P., Hey, R. D., Thorne, C. R. and Tacconi, P. (Eds.), *Dynamics of Gravel Bed Rivers*, Wiley, Chichester, 23 - 39.

Carson, M. A. (1986) 'Characteristics of high energy meandering rivers: The Canterbury Plains, NZ', *Geol. Soc. of Am. Bull.*, **97**, 886 - 895.

Carson, M. A. and Griffiths, G. A. (1985) 'Tractive stress and the onset of bed particle motion in gravel stream channels', *Jnl. of Hydrology*, **79**, 375 - 388.

Carson, M. A. and Griffiths, G. A. (1987) 'Bedload transport in gravel channels', *Jnl. of Hydrology (New Zealand)*, **26**, 1 - 151.

Carson, M. A. and Griffiths, G. A. (1989) 'Gravel transport in the braided Waimakariri River: Mechanisms, measurements and predictions', *Jnl. of Hydrology*, **109**, 201 - 220.

Church, M. (1972) 'Baffin Island sandurs: a study of arctic fluvial processes', *Bull. of the Geol. Survey of Canada*, **216**, 208pp.

Church, M. (1978) 'Palaeohydrological reconstructions from a Holocene valley fill', in Miall, A. D. (Ed.), *Fluvial Sedimentology*, Canadian Soc. Pet. Geol., Calgary, 743 - 772.

Brewer, P. A., Leeks, G. J. L. and Lewin, J. (1992) 'Direct measurement of in-channel abrasion processes', In Bogen, J., Walling, D. and Day, T. J. (Eds.), *Erosion and Sediment Transport Monitoring Programmes in River Basins*, IASH Publication, **210**, 21 - 30.

Bridge, J. S. and Jarvis, J. (1982) 'The dynamics of a river bend, a study in flow and sedimentary processes', *Sedimentology*, **29**, 499 - 541.

Bridge, J. S. and Dominic, D. F. (1984) 'Bedload grain velocities and sediment transport rates', *Wat. Resour. Res.*, **20**, 476 - 490.

Brierley, G. J. (1989) 'River planform facies models: The sedimentology of braided, wandering and meandering reaches of the Squarmish River, British Colombia', *Sedimentary Geology*, **61**, 17 - 35.

Brierley, G. J. and Hickin, E. J. (1985) 'The downstream gradation of particle sizes in the Squarmish River, British Colombia', *Earth Surface Processes and Landforms*, **10**, 597 - 606.

Brown, C. B. (1950) 'Sediment transportation', in Rouse, H. (Ed.) *Engineering Hydraulics*, Wiley, New York, 769 - 857.

Brunsden, D. and Thrones, J. B. (1979) 'Landscape sensitivity and change', *Transactions of the Institute of British Geographers*, **4**, 485 - 515.

Buffington, J. M., Dietrich, W. E. and Kirchner, J. W. (1992) 'Friction angle measurements on a naturally formed gravel streambed: implications for critical boundary shear stress', *Wat. Resour. Res.*, **28**, 411 - 425.

Bull, W. B. (1980) 'Geomorphic thresholds as defined by ratios', in Coates, E. R. and Vitek, J. D. (Eds.), *Thresholds in Geomorphology*, George Allen and Unwin, London, 259 - 263.

Bunte, K. (1992) 'Particle number grain-size composition of bedload in a mountain stream', in Billi, P., Hey, R. D., Thorne, C. R. and Tacconi, P. (Eds.), *Dynamics of Gravel Bed Rivers*, Wiley, Chichester, England, 55 - 72.

Butler, R. P. (1977) 'Movement of cobbles in a gravel bed stream during a flood season', *Geol. Soc. Am. Bull.*, **88**, 1072 - 1074.

Carling, P. A. (1983) 'Threshold of coarse sediment transport in broad and narrow streams', *Earth Surface Processes and Landforms*, **8**, 1 - 18.

Ashworth, P. J. and Ferguson, R. I. (1989), 'Size selective entrainment of bedload in gravel bed streams', *Wat. Resour. Res.*, **25**, 627 - 634.

Ashworth, P. J., Ferguson, R. I., Ashmore, P. E., Paola, C., Powell, D. M. and Prestegaard, K. J. (1992) 'Measurements in a braided river chute and lobe (2). Sorting of bedload during entrainment, transport and deposition', *Wat. Resour. Res.*, **28**, 1887 - 1896.

Baker, V. R. and Ritter, D. F. (1975) 'Competence of rivers to transport coarse bedload material', *Geol. Soc. of Am. Bull.*, **86**, 975 - 978.

Bhomik, N. G. and Demissie, M. (1982) 'Bed material sorting in pools and riffles', *Jnl. of Hydraulics Division, ASCE*, **108**, 1227 - 1231.

Bluck, B. J. (1979) 'Structure of coarse grained braided stream alluvium', *Transactions of the Royal Society of Edinburgh*, **70**, 181 - 221.

Bluck, B. J. (1982) 'Texture of gravel bars in braided streams', in Hey, R. D., Bathurst, J. C. and Thorne, C. R. (Eds.), *Gravel Bed Rivers. Fluvial process, Engineering and Management*, Wiley, Chichester, England, 339 - 357.

Bolin, B. and Rodhe, H. (1973) 'A note on the concept of age distribution and transit time in natural reservoirs', *Tellus*, **25**, 58 - 62.

Borah, D. K., Alonso, C. V. and Prasad, S. N. (1982) 'Routed graded sediments in streams: formulations', *Jnl. of Hyraulics Division, ASCE*, **108**, 1486 - 1503.

Bradley, W. C. (1970) 'Effects of weathering on abrasion of granitic gravel, Colorado River, Texas', *Geol. Soc. of Am. Bull.*, **81**, 61 - 80.

Bradley, W. C., Fahnestock, R. K. and Rowekamp, E. T. (1972) 'Coarse sediment transport by flood flows on Knik River, Alaska', *Geol. Soc. of Am. Bull.*, **83**, 1261 - 1284.

Brayshaw, A. C., Frostick, L. E. and Reid, I. (1983) 'The hydrodynamics of particle clusters and sediment entrainment in coarse alluvial channels', *Sedimentology*, **30**, 137 - 143.

References

Abbott, J. E. and Francis, F. R. D. (1977) 'Saltation and suspension trajectories of solid grains in a water stream', *Philosophical Transactions of the Royal Society*, **284A**, 225 - 253.

Adams, J. (1979) 'Wear of unsound pebbles in headwaters', *Science*, **203**, 171 - 172.

Allen, J. R. L. (1965) 'A review of the origin and characteristics of recent alluvial sediments', *Sedimentology*, **5**, 89 - 191.

Andrews, E. D. (1979) 'Scour and Fill in a stream channel, E. Fork River, W. Wyoming', *USGS Prof. Paper*, **1147**.

Andrews, E. D. (1983) 'Entrainment of gravel from naturally sorted river bed material', *Geol. Soc. of Am. Bull.*, **94**, 1225 - 1231.

Andrews, E. D. and Erman, D. C. (1986) 'Persistence in the size distribution of surficial bed material during an extreme snow melt flood', *Wat. Resour. Res.*, **22**, 191 - 197.

Andrews, E. D. and Parker, G. (1987) 'The coarse surface layer as a response to gravel mobility', in Thorne, C. R., Bathurst, J. C. and Hey, R. D. (Eds.), *Sediment Transport in Gravel Bed Rivers*, Wiley, Chichester, 269 - 325.

Andrews, E. D. and Smith, J. D. (1992) 'A theoretical model for calculating marginal bedload transport rates of gravel', in Billi, P., Hey, R. D., Thorne, C. R. and Tacconi, P. (Eds.), *Dynamics of Gravel Bed Rivers*, Wiley, Chichester, England, 41 - 52.

Anderson, M. G. and Calver, A. (1977) 'On the persistence of landscape features formed by a large flood', , *Transactions of the Institute of British Geographers*, **2**, 243 - 255.

Ashmore, P. E. (1991) 'Channel morphology and bedload pulses in braided, gravel-bed streams', *Geografiska Annaler*, **73A**, 37 - 52.

Ashworth, P. J. (1987), 'Bedload transport and channel change in gravel bed streams', *unpublish. Ph.D. Thesis*, Stirling University.

Ashworth, P. J. and Ferguson, R. I. (1986) 'Interrelationships of channel processes, changes and sediments in a proglacial braided river', *Geografiska Annaler,* **68A**, 361 - 371.

patterns in other rivers, particularly the role of upstream supply to downstream stability and channel change.

(2) Sediment routing. Conventional routing models ignore or generalise local scale effects. The cellular model demonstrates that detailed resolution is required to understand transfer processes. Many of the probabilities were arbitrarily defined and further field and laboratory study is necessary to accurately parameterise this model. Sensitivity analysis of this model may reveal the relative importance of the factors described during this study. It is unlikely that this model will be used for predictive purposes due to the detailed level of resolution precluding volumetric predictions.

(3) Downstream fining models. Seal et al. (1993) provide a two dimensional treatment of sediment sorting based upon downstream fluxes and the occurrence of patches across the channel width. This model may be extended to include a third elevational dimension where sediment storage is described relative to an arbitrary datum. Storage may promote fractional mobility and must be accounted for within a downstream fining model. At a reduced level of complexity, it may also be possible to predict downstream fining through description of tracer wave propagation (section 8.4.1).

This study demonstrates that sediment transfer is more structured than previously noted. Adoption of a three dimensional description of each reach has allowed identification of factors which combine to condition sediment transfer fluxes. Implicit to this is sediment storage type. This factor provides explanation for the non exponential distance distributions obtained by previous workers. In addition, the somewhat contradictory evidence regarding burial effects may also be re-evaluated with reference to storage type behaviour and flood type. Previous tracer studies crucially exclude this lateral (and vertical) dimension when describing tracer distributions but this study has demonstrated that this is implicit to understanding the sediment transfer system. Lateral effects are included in the cellular model which may eventually provide a quantitative assessment of the factors dominating the transfer system.

7. The factors affecting sediment transfer may be categorised as promoting motion or particle inertia, hence conditioning the absolute magnitude of τ^*. Factors which alter the imposed shear stress at the bed are peak stage, duration, storage type and morphology (local and sub-reach). Peak stage and duration increase transfer fluxes whilst storage type may alter local depth and hence shear stress. Morphology determines shear stress distributions through confinement of flow within relatively narrow deep areas. Inertial factors promote resistance to imposed shear stress and include grain size (absolute and relative) and burial. All these factors are linked, for example the importance of burial varies according to storage type and peak stage. In addition, the relative magnitude and importance of each factor varies per event and between reaches. The latter reflects the effectiveness of the imposed flooding and in response, the stability of the reach/sub-reach to imposed changes. Isolation of the conditions at entrainment provided an accurate estimate of the relative importance of hydraulics, storage type and grain size. Data describing the other factors were insufficient in isolation but each factor is implicitly linked to the three main factors studied. In reach A, no single factor dominated sediment transfer, although trends were somewhat better defined within sub-reaches due to fixed bar effects. In reach B, grain size effects dominated as the bedload threshold was frequently exceeded but morphology prevented a wide range of excess shear stress values. Contrasting controls upon the same process demonstrate the need for numerous study sites and the problem of deriving general conclusions from site specific observations.

8. Semi-quantitative description of all the factors controlling sediment transfer was possible by conceptualising each reach as a cellular type model (Smith 1991, Murray and Paola 1994)). Routing of discharge between cells accounts for fixed bar effects upon submerged channel shear stresses. The probability of transfer from each cell was described according to cell characteristics and the factors affecting τ^* discussed herein. At present this model is purely conceptual and in order to provide quantitative explanation and prediction sensitivity analysis and increased process information would be necessary. For example, the effect of relative grain size varies according to stage and storage type (assuming it is a significant factor); however this factor was only afforded semi-quantitative treatment in this study. No field based studies have addressed relative grain size controls which have only been analysed in laboratory studies of pivot angles (e.g. Buffington et al. 1992). A future study may extend such methods to simulate flow conditions and storage characteristics.

This study raises numerous possibilities for future analysis and research. These may be summarised by three objectives:

(1) Sediment transfer and flood effectiveness. This study has illustrated the importance of position in conditioning flood effectiveness and transfer characteristics. At present these results are somewhat site specific and a useful extension would be to study transfer within other channel

surface entrainment (Hassan 1990) whilst sediment in storage based stores remained immobile. The reach B transfer system was characterised by these processes irrespective of flood magnitude. In reach A, rising stage increases the probability of morphological change providing a mechanism for release of sediment from less active stores (significant morphological change was not evident in reach B). The probability of morphological change and hence transfer from storage zones increases with stage and event duration (Goff and Ashmore 1994). This rather simplistic view of reach scale transfer systems varies spatially according to local morphology, particularly in response to the effect of fixed bars upon submerged channel shear stresses where surface based entrainment rates may be increased.

4. Hassan and Church (1992) advocated a morphological approach to explain the non systematic distribution of transferred sediment. The importance of storage types was demonstrated by Hassan et al. (1991) where irregular peaks in exponential distributions of normalised distance corresponded with temporary sinks of sediment. Sediment entrainment, burial and storage duration are implicitly related to storage type and the associated mechanisms responsible for sediment release. Material is rapidly transferred from (and within) more active stores, and providing it remains in such storage types is rapidly evacuated from a reach. Once material enters less active storage, passage through a reach is inevitably delayed, often requiring morphological change and extreme flood events for release. This lateral storage effect reduces mobility of stored coarse sediment relative to fines which are released at a more rapid rate.

5. The mobility of buried sediment cannot be adequately studied using two dimensional analysis (e.g. Hassan and Church 1994). The significance of burial varies across the channel according to the distribution of storage types. Sediment in storage based stores is less active than submerged channel counterparts until intense flooding and morphological change. Burial is not simply related to flood activity (increasing depth of scour), but is also a function of morphological change inducing scour and deposition during bar formation and migration. The probability of this being a significant process is storage type dependant.

6. Morphology and dominant sediment release mechanisms determine the mode of transfer. During intense flooding, release of previously buried sediment from less active stores reduces overall reach size selectivity (this reduction is also a result of duration and relative grain size effects). When considered in isolation, the degree of selectivity of transfer from transfer based stores is more pronounced than storage based stores which are closer to an approximation of equal mobility. The overall reach mode is dependant upon the distribution of stores and the effectiveness of flooding at local scales. These effects may provide explanation for the apparent approach towards equal mobility at high stage (Kuhnle 1993).

9. Conclusions

Sediment transfer fluxes are usually attributed to reach averaged hydraulic conditions and grain size (e.g. Schmidt and Ergenzinger 1992, Hassan et al. 1992). This study provides the increased level of resolution necessary to explain the frequently noted pseudo stochastic patterns of sediment transfer (Hassan et al. 1991). Detailed volumetric survey and large tracer samples applied to pre-determined small scale reach systems allow evaluation of all factors responsible for these trends (summarised as dimensionless shear stress, τ^*). This study provides a comprehensive three dimensional review of the sediment transfer process detailing entrainment, transport and depositional influences. The main conclusions may be summarised as follows:

1. Two reaches of contrasting morphology and activity were divided into six numerically defined storage types using a shear stress index (SSI). Interpolated bankfull depth and bed slope data were used to determine SSI at 1m spaced grid nodes. This provides the least subjective method of storage classification used to date, but requires intensive measurement. Digital terrain mapping (Lane et al. 1994) provides potential for less intensive data collection whilst retaining definition accuracy. The method used in this study is vindicated by storage specific tracer flux rates. A progression of activity across the spectrum of stores was apparent within each reach, being more clearly defined in reach A than B. In addition, sediment in less active stores in reach A was only mobilised significantly in response to morphological change and direct entrainment of non surface material was rarely documented. The definition procedure may be applied to other sites irrespective of channel pattern, but flood effectiveness must be accounted for. In less active reaches a more detailed definition procedure may be required reflecting within channel shear stress gradients and the importance of local scale processes.

2. Storage type characteristics were inadequately described by transit times. Although more useful than turnover time (where an unrealistic steady state is assumed, Bolin and Rohde 1973), transit time distributions do not make allowance for hydraulic variation where contrasting ages of sediment may be output from storage during the same flood event. In addition, transit times are also subject to errors arising from sediment exhaustion (non attainment of a steady state). As a consequence, response time (the time at which cumulative tracer output exceeds that remaining in storage) was introduced providing a measure of storage activity in real time. Exclusion of sediment age and use of output and storage is crucial to accurate determination of storage characteristics where imposed flooding varies. On this basis, response time has distinct advantages over transit, turnover and residence times.

3. Storage activity was a function of the dominant transfer process for that storage type. Sediment within more active stores was transferred during intermediate flood events due to small scale

pattern stability and propensity for change. The morphological approach may be applied to active braided channels where monitoring of tracer and sediment fluxes may be used to assess mechanisms and causes of channel migration. Extension of a study area upstream would permit evaluation of upstream effects upon downstream fluxes and braided activity. A similar study has been carried out by Lane et al. (in prep) using only volumetric data, additional use of tracers would permit monitoring of these fluxes and assessment of their important to channel change. Similarly such a morphological approach may be applied to analyse the flux patterns (upstream and local) associated with meander stability/migration. Once the role of upstream supply and local morphology is more completely understood, then models such as the cellular type may be developed to predict the effect of upstream changes such as channelisation upon downstream reaches.

Rather than forming a predictive tool, this model describes detailed process interaction effect upon sediment transfer. Utilisation of detailed data is crucial to such process understanding, but such a resolution is not necessary for predictive purposes. On this basis, existing approaches to sediment routing prediction (e.g. Pickup et al. 1983, Kelsey et al. 1987) developed at broad scales are more instructive. However, this detailed study has demonstrated the importance of morphology and local grain size effects, factors which must be paramaterised within predictive models.

8.5 The morphological approach

Sediment transfer studies which relate fluxes to reach and flood averaged conditions, whilst instructive, are somewhat generalised. A morphological approach provides a more detailed analytical framework to explain sediment transfer with reference to three dimensional storage characteristics (Hassan and Church 1992). A tracer study must consider the effect of storage upon sediment redistribution together with recognition of the importance of contrasting flood types (e.g. Hassan et al. 1992). Morphology and storage type may promote (e.g. fixed bars) or reduce (e.g. lateral storage) mobility in time and space, dependant upon flood type (levels 1a - 2b) and the associated incidence of morphological change. These factors are responsible for the apparent stochastic distributions of tracer fluxes previously reported (e.g. Hassan et al. 1991). This study has improved existing understanding of sediment transfer by adopting a detailed level of data collection. However, whilst suitable for process studies, this resolution is not necessary for predictive purposes.

8.6 Broader applicability of the approach

The morphological approach has identified storage controls upon sediment fluxes and ultimately channel pattern. In reach A, fixed bars in upstream sub-reaches were responsible for maintaining a high rate of supply (demonstrated by tracer and volumetric fluxes) to downstream sub-reach 3A. Fixed bars in 1A and 2A (defined as transfer reaches, adopting the terminology of Church and Jones, 1982) are stable in the short term and maintain a meandering pattern where aggradation within the submerged channel was rapidly evacuated and fixed bars maintained. Increased downstream supply into 3A results in an over aggraded (Lane et al. in prep.) storage based (Church and Jones 1982) braided pattern with frequent channel migration in response to the instability imposed from upstream. Reach B is analogous to the transfer sub-reaches 1A and 2A where fixed bars restrict activity to the submerged channel. Channel pattern is maintained by the semi permanence of these bars in such a low activity reach.

Although some of the conclusions above are site specific, dependant upon local morphology and pattern, it is likely that morphology induced sediment supply is a major determinant of channel

deposited, the probability of deposition increasing linearly as D_i* declines below unity. These assumptions indicate that hop length is a function of absolute and relative grain size rather than a stochastic processes.

Once a particle is deposited in a cell there is a discrete probability of burial depending upon the number of other tracers entering. Mobile sediment is buried by material also in motion (Hassan 1990) so the probability of burial is high if a large number of tracers enter a cell. Conversion of tracers into BTEQ may be used to provide an approximation of burial depth. The accuracy of any predicted distributions (for the reach as a whole) may be tested with reference to the distribution of buried sediment detailed in section 7.4.

Once immobile, a particle is subject to the same re-entrainment factors as described in 8.4.2.2. Once the temporal iterations during a flood period are completed, the final deposition locations may be compared with field data providing the possibility for sensitivity analysis. It is likely that such analysis will indicate the importance of contrasting factors at A and B. Cellular morphology is adjusted to reach conditions after each model run. At present, it is difficult to convert particle fluxes to volumetric changes at each cell, and this presents a problem for future research to address.

8.4.2.5 Model evaluation

The model described in the preceding subsection represents a useful tool for understanding local controls upon transfer but has limited predictive value. Initially, the model should aim to replicate the fluxes reported in this study. A principle aim should be accurate calibration of the probability values. Initial sensitivity analysis may be used to assess the significance of some parameters, particularly the importance of D_i* during contrasting floods. In addition, it may be necessary to carry out additional experiments to accurately quantify some variables, particularly the role of relative grain size once the bedload threshold is exceeded (Table 8.6) and the probability of lateral rather than downstream movement directions according to cell orientation.

A major problem with the model is the invariance of morphology. This study has demonstrated that morphology and morphological change are major determinants of transfer fluxes. The data used to verify this model often cover several floods hence maximising the morphology induced errors. Ideally, the model should be verified with reference to tracer and volumetric data collected after a single flood. Digital terrain mapping (Lane et al. 1994) may allow accurate volumetric quantification per flood providing more time to monitor tracers.

Morphological changes during a model run may be incorporated by conversion of fluxes to BTEQ rather than tracers. However, this is unlikely to be successful due to the detailed resolution used.

8.4.2.3 Sediment transfer pathways

Once mobile, a particle undergoes a series of hops (Einstein 1937). Non-perfect correspondence between response time and distance moved suggests that hop location is a determinant of transfer distances (Schmidt and Ergenzinger 1992). The distribution of transfer is a function of dimensionless shear stress conditions at entrainment and at each subsequent hop location. Once a particle is entrained it moves to the next downstream cell. The direction of movement is dependant upon cell orientation. If the source cell is horizontal then the probability of transfer to the cell immediately downstream, p_d, is 1, transfer to adjacent left and right cells, p_l and p_r, is zero. For every 10° increase in horizontal slope, p_d declines by a factor of 1.5, thus p_l increases since $p_l = 1-p_d$, $p_r = 0$, if the cell slopes to the right then $p_r = 1-p_d$ (Figure 8.10). The figure of 1.5 is arbitrary reflecting the importance of lateral movement in this study. No detailed data are available to test the accuracy of this figure, but laboratory experiments may be carried out for verification purposes. The relationship between sediment direction and cell slope reflects gravitational effects and accounts for lateral erosion detailed in Appendix C where sediment may be transferred non parallel to flow. Lateral transfer due to secondary flow currents is not accounted for due to its relative insignificance compared with other factors (section 7.3.1).

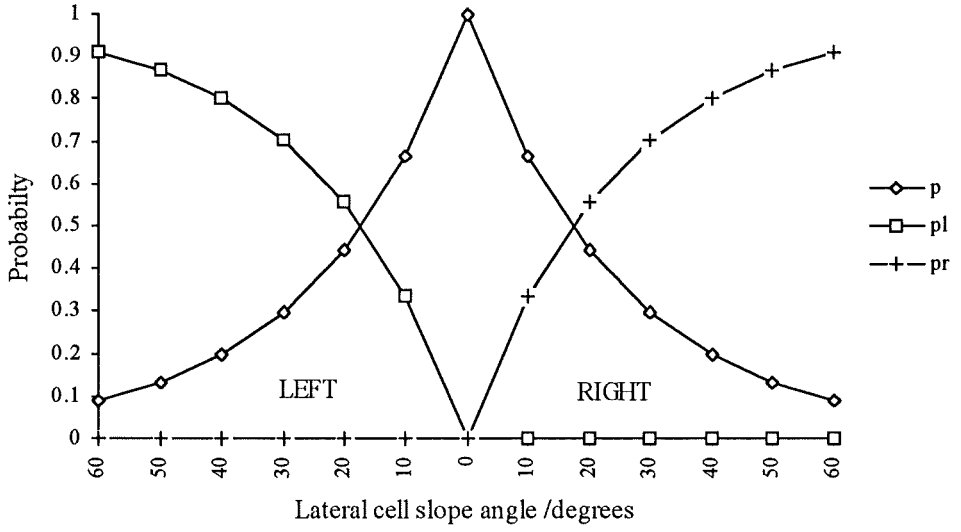

Figure 8.10. Probability of lateral transfer according to cell angle perpendicular to flow.

8.4.2.4 Sediment deposition

Once a particle enters a neighbouring cell the probability of deposition is a function of local shear stress relative to the fractional threshold, relative grain size (conditioned by absolute shear stress) and burial. If shear stress is below the threshold then the particle is deposited. If in excess of the threshold, the probability of deposition is dependant upon D_i^*. Where $D_i^* > 1$ the particle is not

		Percentage mobile					
	Threshold at Q3 /m	*2*	*3*	*4*	*5*	*7*	*8*
Peak stage:		**0.74**	**0.71**	**0.63**	**0.53**	**1.03**	**0.92**
Grain size							
< 180	0.80	81.9	35.5	88.4	22.4	98.0	83.0
< 90	0.65	95.6	61.2	93.8	31.2	98.8	81.9
< 45	0.59	95.6	61.2	94.4	45.0	98.8	88.7
< 23	0.56	97.9	75.0	97.9	50.0	95.9	95.9

Table. 8.7. Percentage of sediment mobile according to tracer search in reach A. Peak stage data are not of sufficient resolution to determine sediment mobility relative to fractional thresholds.

The model should consider entrainment of buried sediment, again probabilistically. Section 7.4 demonstrated the sensitivity of the active layer to storage type and peak shear stress. The probability of entrainment of buried sediment during an intermediate event is a maximum in a VA store and a minimum for an IA store. During small scale events, buried sediment is only mobilised due to random scour processes (Hassan 1990). As stage rises, the depth of scour increases (Figure 7.15) so releasing progressively deeper buried sediment. This probability of entrainment of a particle buried at depth b during an intermediate event is a function of shear stress (and hence active layer depth). Once shear stress is sufficient to provide scour to the depth of particle burial then the probability of entrainment is assumed to be random reflecting the nature of scour during such events. No distinction is made between surface, within (material locked within the bed surface matrix rather than resting on top) and buried sediment (e.g. Church et al. 1991). Material locked within surface pocket geometry ($D_i^*<1$) is therefore classified as buried and subject to the conditions described.

During intense flooding, local scour continues in the active stores with increased probability of entrainment as the depth of potential scour rises. The probability of release of sediment from storage based cells (S and IA) increases disproportionately compared with more active stores as the probability of morphological change increases. This probability is enhanced by increased shear stress (Goff and Ashmore 1994) and duration at a cell (this process is precluded in reach B). In addition to hydraulic conditions, morphological change is also a function of cell stability (defined from sub-reach stability) and sediment delivery (Lane et al. in prep). Maximum probability of morphological change is associated with high shear stress and duration together with increased sediment delivery from upstream (as documented by modelled dispersion of tracers converted to BTEQ) and recipient cell instability (semi-quantitatively defined from volumetric information). Where a cell undergoes morphological change, all stored sediment is released to the transfer system to a depth of scour proportional to imposed shear stress. Further volumetric study is required to ascertain the probability of morphological change in response to sediment delivery, possibly using detailed data derived from other sites (e.g. Lane et al. in prep).

more accurate to determine grain size parameters directly from the plotted data. The latter point reflects the narrow range of grain sizes in B. A sediment sorting parameter should also be included since it is implicit to the distribution of friction angles (Komar and Li 1987, Kirchner et al. 1990, Buffington et al. 1992), but this proved difficult to predict so relative grain size is utilised.

At low excess shear stress, an increase in relative grain size increases the probability of entrainment as friction angle is reduced (Kirchner et al. 1990). Coarser particles have narrower distributions due to limited protrusion (and the absence of hiding) with finer clasts having a wider distribution as relative grain size is reduced. Buffington et al. (1992) report that critical shear stress reflects friction angle, although this partly reflects experimental conditions where the effect of bed packing constraints upon coarser sediment was not replicated. Relative grain size effects are a maximum at low excess shear stress; as stage rises relative size effects decline in importance. The probability of entrainment of finer clasts is always greater than coarse sediment reflecting progression in the threshold. Once the threshold for entrainment of coarse sediment is exceeded, relative size effects for fine clasts are unimportant. A probability scale can therefore be calculated for each size fraction according to excess shear stress and relative grain size (Table 8.6). The probabilities presented are entirely arbitrary. No exact values can be determined since the range of floods studied was too narrow to separate out the effects of fractional thresholds upon transfer distances. Data derived from reach A indicate that the relative proportion of coarse sediment in transfer declines with stage (Table 8.7), consistent with the probabilities presented in Table 8.6. Accurate quantification of these probabilities and the role of relative grain size effects as excess stress rises presents the possibility for future combined laboratory and field based study. It may be necessary to define a simpler model in reach B where the grain sizes in transfer are restricted.

	Threshold exceeded				*Significant D_i**			
	<180	<90	<45	<23	<180	<90	<45	<23
Grain size	***Probability of entrainment***							
< 180	0.7	0	0	0	✓			
< 90	0.8	0.7	0	0	✓	✓		
< 45	1	0.8	0.7	0	x	✓	✓	
< 23	1	1	0.8	0.7	x	x	✓	✓

Table 8.6. Probability of surficial entrainment from a cell according to absolute and relative grain size effects. Results are based upon the occurrence of increased mobilisation of coarser tracers as shear stress increases. Hiding of fine tracers is restricted to a small number of surficial clasts. Probability values are arbitrary illustrating the progressive decline in the importance of D_i* as stage rises.

and burial effects upon entrainment. The threshold is a mean of these local factors. However, this problem is also a drawback for other methods of determining the threshold. These include partitioning excess shear stress according to response time and use of hiding functions developed from bedload traps (Wathen et al. in prep). Both methods are averages for the reach and are more complex and arbitrary offering no advantage over the measured thresholds described above. Ideally, thresholds should be determined for each store, but data resolution precludes such analysis. The significance of these thresholds can be tested during sensitivity analysis of the model. Future field study may accurately calculate these fractional thresholds by seeding specific stores and comparing fractional mobility with peak stage estimates from crest stage recorders.

Once a threshold for a tracer of size fraction *i* resident in a cell is exceeded, the probability of entrainment, p_{ei}, from the surface is determined from

$$p_{ei} = f(\textit{excess shear stress, relative grain size, friction angle, sediment sorting}) \quad (8.4)$$

All these factors need to be combined for each cell in order to determine the probability of entrainment. As excess shear stress increases over the threshold for fraction *i*, the probability of entrainment increases and the importance of the other factors is progressively reduced (see level 2a, section 8.2.2). An initial study should predict entrainment for each grain size on the basis of shear stress with the other factors being introduced as required during sensitivity analysis. Exclusion is not important during intense flooding in reach A where process levels are sufficient to hide the effect of local grain scale factors. However, at low excess shear stresses (during intermediate floods in A and all floods in B), local factors are more important. Incorporation of such variables requires a greater level of analytical resolution (section 8.3.4) and hence predictive resolution.

Relative grain size for each cell may be predicted from cell elevation. Cell D_{50} in reach A may be obtained from regression results presented in section 4.3.3 (Figure 8.9), whereas in reach B it is

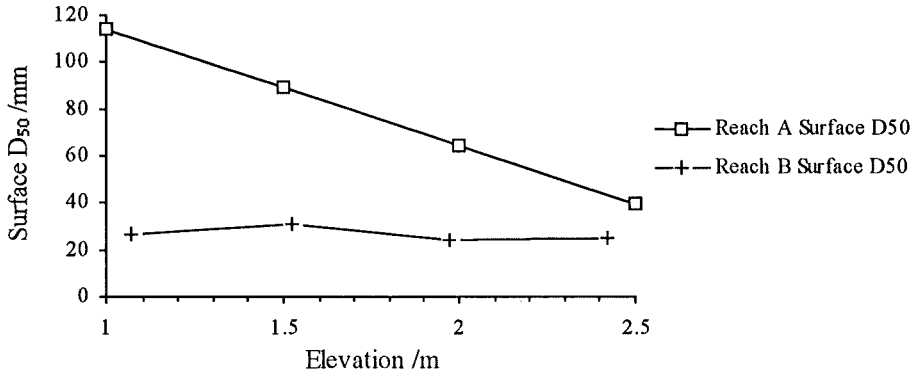

Figure 8.9. The relationship between grain size and cell elevation.

8.4.2.2 The probability of entrainment

As transfer in each reach is size selective, fine material is mobilised before coarse particles and fractional thresholds are required, above which transfer of a particular size fraction from a cell is possible. A threshold for fraction *i* is defined as the shear stress value below which entrainment is not possible. The threshold stage for transfer of tracers in class *i*, calculated in the absence of duration, is defined by an exponential relationship at reach A (Figure 8.8), derived from the best fit line presented in Figure 8.3, 2. A threshold discharge is determined for each tracer fraction from the Q3 rating curve and is input to the reach A lattice. The threshold for fraction *i* is the shear stress attained in the deepest cell. It is assumed that the bedload threshold refers to the discharge at which initial entrainment is possible, so transfer is most likely from the most active (deepest) part of the channel with the remainder inactive.

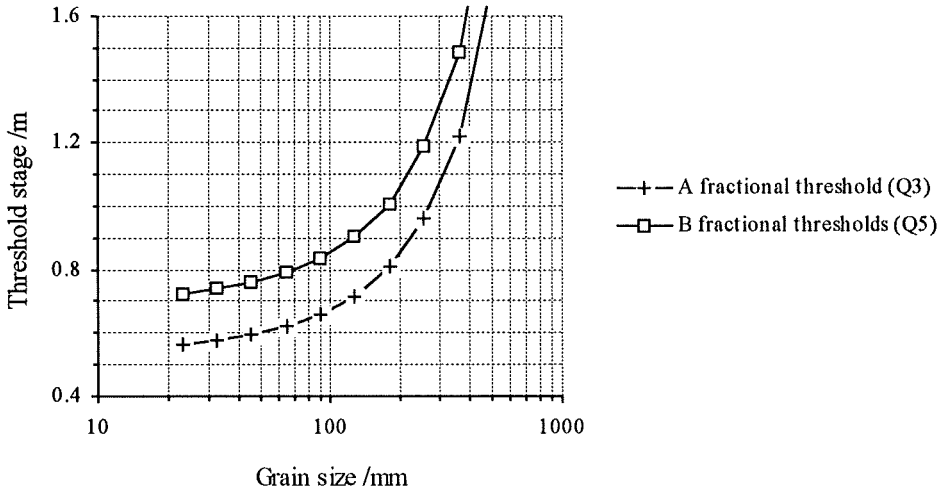

Figure 8.8. Fractional threshold stage predicted from the exponential regression relationship for reach A presented in Figure 8.3 and reach B.

No significant relationships exist at reach B between grain size and peak stage due to the narrow range of channel shear stresses. However, MSS analysis revealed grain size to be a major factor determining fluxes. Fractional thresholds, although not entirely applicable to this reach where factors conditioning particle inertia dominate, may be determined from conversion of Q3 stage thresholds to Q5 using regression (r^2 = 98%, $p < 0.001$). The resultant thresholds (Figure 8.8) are somewhat high and correspond to overbank flow. However, thresholds during overbank conditions provide support for the non importance of peak stage and duration upon sediment transfer.

The preceding analysis is flawed since average process conditions expressed as a threshold discharge are only poorly related to point thresholds as there is exclusion of local relative grain size

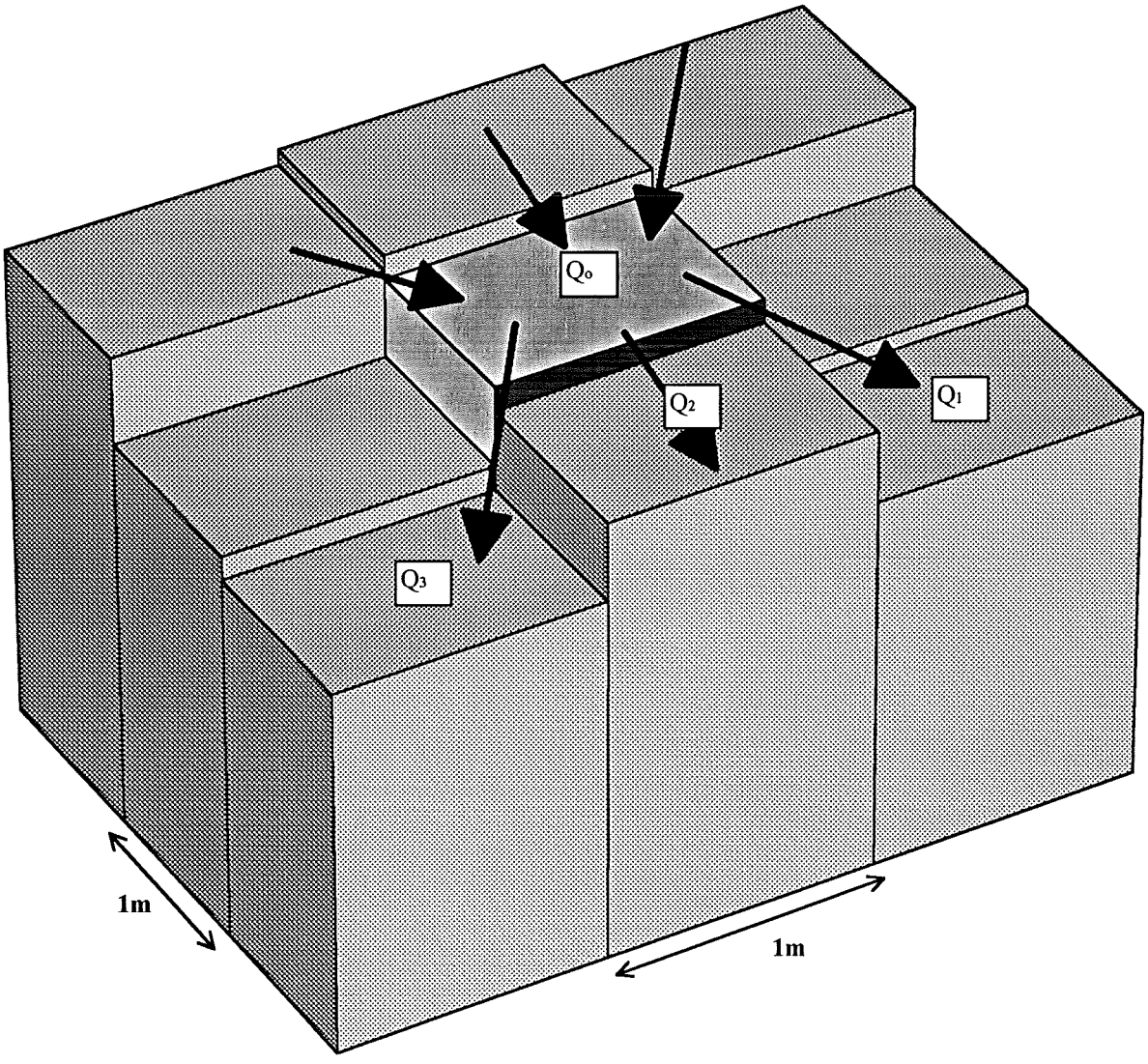

Figure 8.7. Discharge routing between cells. (Based upon Murray and Paola 1994).

Paola (1994) where braided morphology was successfully developed from a simulated homogeneous cellular bed. The aim of the conceptual model is to describe fractional sediment dispersion at the grain scale utilising the process information collected during this study. No numerical simulation was carried out.

Each reach is divided into a regular lattice entirely enclosed by peripheral banks. The latter assumption is valid for most flows in reach A, but is invalid in B where overbank flow is frequent during even moderate events. To counter this, the banks are assumed to constrain all flow and a maximum attainable cellular depth is set. This value is calculated as the bankfull depth according to the cell location; any excess depth is removed from the model. In effect, a bankfull datum is set constraining water depth and preventing attainment of unrealistic shear stresses.

8.4.2.1 Routing of water

Sediment transfer from a cell is a function of shear stress determined from cellular discharge and hence depth. Discharge is routed downstream through each cell according to elevation and relative slope (Murray and Paola 1994). An example of the lattice together with potential flow pathways is demonstrated in Figure 8.7. Output discharge, Q_o from a cell is routed into the three downstream cells Q_1, Q_2 and Q_3 according to relative slope. Slope S_i between the output cell and downstream cell i (where i = 1 to 3, 1 - left cell, 2 - centre cell, 3 - right cell) is calculated as the elevation difference. S_3 and S_1 are afforded less importance to discharge routing and are weighted by $\sqrt{2}$ (Murray and Paola 1994). In this conceptualisation, cells slope both parallel and perpendicular to flow (unlike the original model) so mean elevation should be used. Where slope is positive into at least one cell then Murray and Paola routed discharge according to

$$Q_i = Q_o S_i^n / \sum S_i^n \tag{8.3}$$

where Q_i is the input discharge and n is a constant derived from flow equations (e.g. Mannings roughness equation) assumed to be 0.5. Normalisation by the sum of slopes ensures that all water is routed downstream. Where all slopes are negative, discharge is routed according to the relative magnitude of slopes (see Murray and Paola 1994). Routing water using this method ensures continual flow either up or down slope and replicates fixed bar effects upon submerged channel hydraulics with flow constrained within the deepest cells for a specified discharge. The routed discharge in a cell at any point in time is converted to shear stress using du Boys formula (Eq. 2.2) averaged for a cell.

consistent with response times. If sediment was deposited in stable or inactive stores (e.g. the sediment wave, between 36000 - 57110 min.) then wave form would become more attenuated. In addition, wave form is dependant upon the effect of incident flooding upon sorting processes. In 1A and 2A, sediment remained in S and IA stores during intermediate floods, but material in the submerged channel was more mobile. Fractional wave attenuation is dependant upon the distribution of sediment in storage (lateral storage effects, section 6.3.2.4).

This idealised proposal represents a possibility for future research. The data presented in this study are of insufficient quality to facilitate such analysis for three reasons: (1) tracers were located in three sets rather than a single input point; (2) timescales were insufficient for all grain size waves to peak; (3) study reach length precluded the use of more than 2 segments (in this case sub-reaches). Assuming that a concave long profile such as the Allt Dubhaig is used, this study may be repeated or carried out simultaneously in upstream or downstream locations to assess wave characteristics and the magnitude of downstream fining according to contrasting slope and channel pattern. Interpolation between study sites (assuming wave form varies systematically downstream) would provide a basis for modelling sediment transfer along a whole river. Addition of sediment along the long profile (not accounted for by tracer waves) due to surficial entrainment or morphological change may then be incorporated providing a process based representation of sediment transfer in a size selective system.

Division into segments is similar to the idealised study for determination of transit times advocated by Dietrich et al. (1982). Although the aims differ, the suggested study would provide transit time data which may be compared to local morphology and the incidence of morphological change. This method of prediction of downstream fining incorporates the importance of lateral effects and morphology along the long profile into a 2-D model of sediment dispersion. Usage of this additional dimension has considerable advantages in accuracy over existing 1-D approaches (e.g. Hoey and Ferguson 1994) whilst not representing an unnecessary increase in complexity.

8.4.2 Within reach sediment transfer

The factors governing sediment transfer vary in magnitude according to peak stage, duration and local morphology (section 8.2). This section combines the results from the whole study into a single reach scale conceptualisation of sediment transfer based upon the schematic diagram presented in Figure 8.2 and the levels of resolution in section 8.2. Each reach is divided up into 1 m^2 cells with discharge in each cell determining the magnitude of the linkages between factors operating at a local scale. Cellular models may be used to describe dynamic systems whose behaviour is determined by local conditions and factors (Smith 1991), in this case the probability of sediment transfer. Such an approach has already been applied to gravel-bed rivers by Murray and

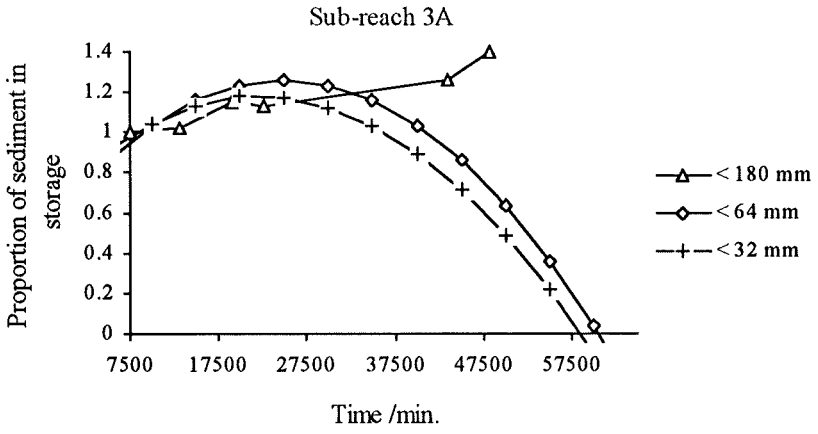

Figure 8.5. Sub-reach 3A, propagation of tracers as downstream waves. Proportion is calculated relative to the first input of sediment at t = 7400.

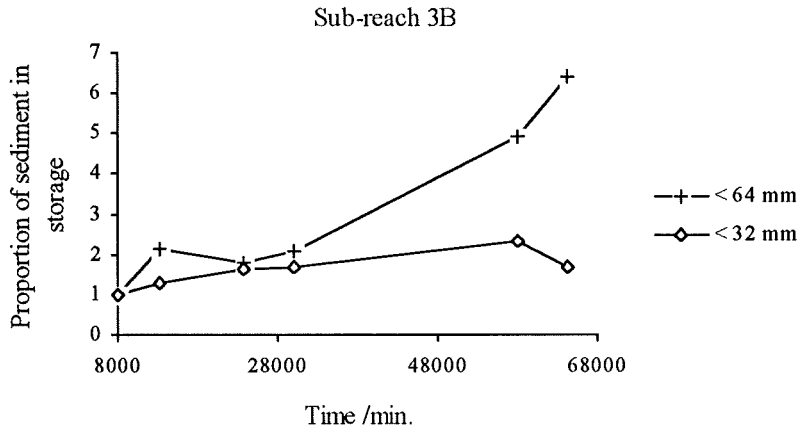

Figure 8.6. Sub-reach 3B. Proportion of sediment in 3B relative to the storage at t = 8000. Waves are less well defined due to low activity and do not attain a definite peak during the timescale of the study.

Downstream sediment transfer may thus be conceptualised as waves of particles moving downstream from various input points with a grain size related velocity. Velocity at any point is a function of the downstream decrease in slope. Isolation of these waves can be achieved from tracer studies where dispersion of sediment from a single input point is monitored through downstream segments (Mosley 1978). Each segment should contain at least two pool riffle units (hence of the order of 10 - 15 channel widths long) thus accounting for sub-reach morphology and providing a realistic level of resolution. The output of tracers across the downstream boundary may be used to determine fractional wave form, magnitude and velocity. Wave characteristics describe sediment dispersion and the magnitude of active sorting processes contributing to downstream fining. For example, waves passing through 1A and 2A would be high magnitude with minimal attenuation,

factors are less important to system behaviour where increased activity enhances the relative importance of other factors. These conclusions are based upon the aims of the data collection programme particular to this project. For other studies, if detailed process information is not required, an inactive system may be deemed less important and thus not worth intense measurement.

8.4 Conceptualisation and prediction of sediment transfer

This section combines the results from this study into two conceptual models: (1) Description of the processes contributing to downstream fining, providing an example of the use of tracers for process prediction; (2) Detailed breakdown of within reach local sediment transfer using a cellular type model (Murray and Paola 1994). The two scales are linked with detailed reach scale processes responsible for variations in downstream trends. The two models presented are purely conceptual, describing and summarising rather than simulating the processes responsible for downstream and lateral transfer described in this study.

8.4.1 Downstream sediment transfer

Downstream sediment sorting may be predicted from the magnitude and velocity of tracer waves. Existing predictive methods may be categorised according to the mechanism responsible for the downstream trends: (1) selective transfer (e.g. Hoey and Ferguson 1994); (2) abrasion (Kodama 1992); (3) sediment patches (Seal et al. 1993); (4) aggradational waves and abrasion (Parker 1991). All these methods consider one or two process excluding other mechanisms, for example, Seal et al. show that the effects of patches may be quantified in a hiding factor combining lateral and downstream size selective effects. It is important to note that the processes contributing to downstream fining are not mutually exclusive (Werritty 1992). This section presents a brief description of the possibility of predicting downstream fining from tracer wave movement where abrasion is absent, partly analogous with studies of downstream propagation of aggrading waves (Parker 1991).

Downstream propagation of tracer waves with size related velocity were apparent in sub-reaches 3A and 3B (section 5.3.2). These waves are generalised in Figure 8.5 where actual tracer proportions (Figure 5.25) are replaced by best fit lines (significant at $p = 0.05$). Best fit lines are not used for any fractions in reach B (Figure 8.6) or in reach A for the < 180 mm fraction, as study duration was too short for attainment of a tracer peak. The trends presented are consistent with response times (reflecting selective transfer and reach contrasts) where the response velocity (Table 5.6) of coarser fractions in reach A and all sizes in B was small compared with the finer clasts in reach A.

offers considerable advantages over transit and residence times since flux is considered relative to time rather than age.

Response time provides a useful tool for analysing fluvial activity. Although constrained by a prerequisite of 100 % recovery (although these errors are accountable), a prototype study could be developed to assess the recovery of a reach to an imposed input of sediment. Preliminary tracer investigation could be used to predict/alleviate the effects of large scale anthropogenic disturbances such as mining (e.g. Lewin et al. 1977) or forestry (e.g. Robinson and Blyth 1982) upon river systems.

8.3.3 Hydraulic data

Use of a single gauging station provides peak stage data for a whole reach at a general and unrepresentative level of resolution. Local shear stresses (although relative in this study) will vary during an event according to flow depth and slope and hence local transfer fluxes. Data resolution could be improved by monitoring within reach distributions of peak stage per event using a network of crest stage recorders. Such analysis may allow determination of the distribution of depths in for example, 1A providing quantitative evidence for increased flux rates.

8.3.4 Data resolution

The lack of systematic trends (except in grain size) identified within the sediment transfer process in reach B may be a consequence of the level of resolution of data collection. In an inactive system such as reach B changes were at the local scale (a function of within store morphology and relative grain size) so detection of significant trends would require high measurement intensity (both spatial and temporal). Recorded changes are of the same order of magnitude as data uncertainty. Assuming that measurement uncertainty is normally distributed with a mean of zero, use of a higher resolution would decrease uncertainty and may allow detailed trends to be determined. In a more active system such as reach A the measurement uncertainty is a smaller percentage of the change and the level of resolution may be lower and still allow significant changes to be identified.

Conventionally, less active sites are sampled less frequently since changes are assumed less, but, this does not necessarily contribute to understanding of the system. Such systems are difficult to understand using infrequent data collection. The results of this study suggest that in order to monitor a low magnitude process a higher level of resolution is required. Increased resolution in reach B would necessitate frequent monitoring of detailed bed structures and small scale morphology. These factors govern system order at the local scale, the summation of which may provide explanation for partial non systematic behaviour at the larger scale. In reach A such

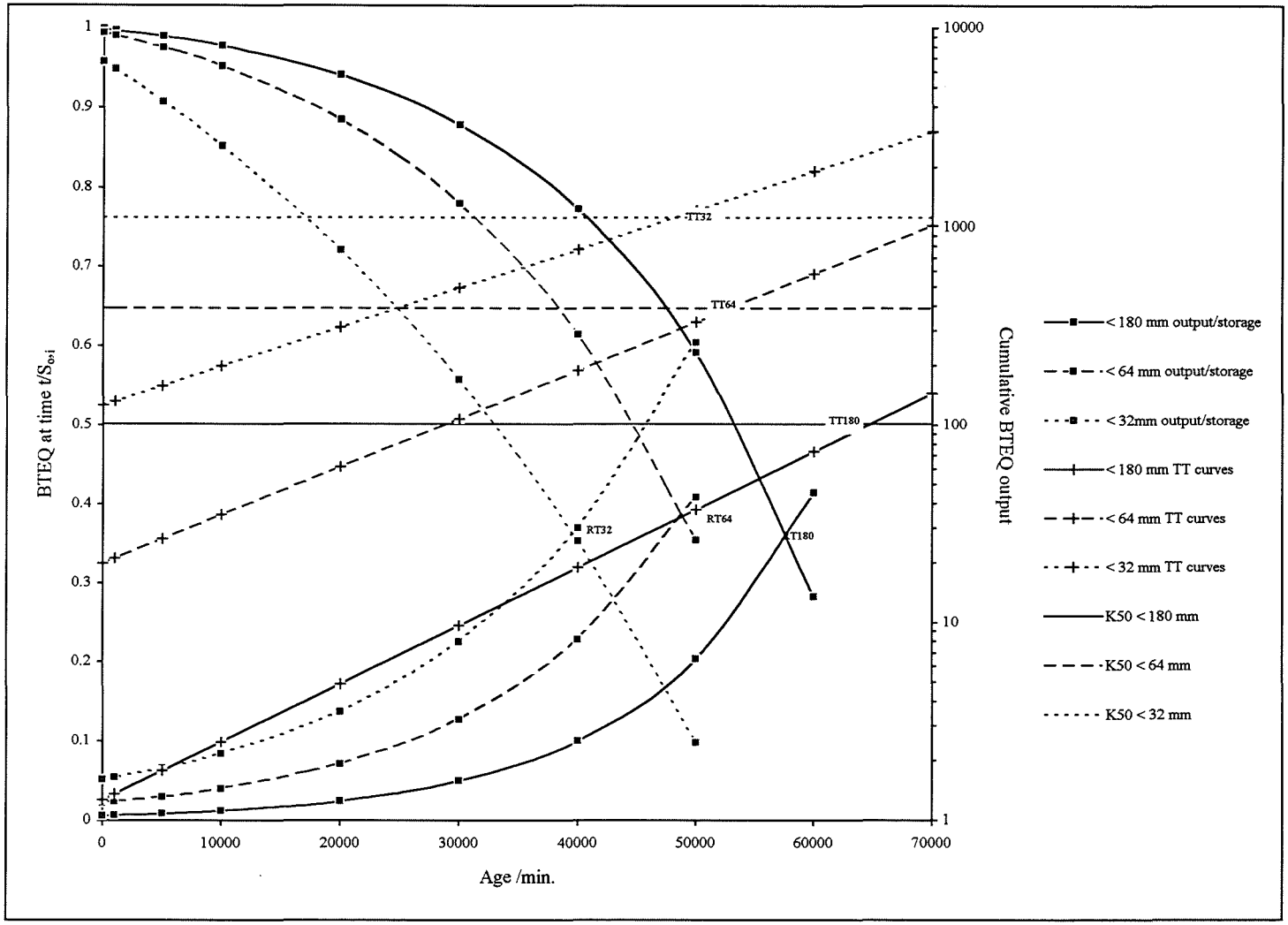

Figure 8.4. Comparison between response time and transit time. Response time is defined by intersection of output and storage curves (RT). Median transit time is defined as the time where output (defined by the transit time curve) of 50% (K50) of the tracer sample is attained (TT). Median transit time should approximate response time where sediment is not added to a store or reach.
Transit time curves were determined using regression (Table 5.4).

more instructive than developing an average transit time for average (in terms of morphology) reach conditions.

Under idealised steady state conditions (in this case zero input to storage), the median transit time (and hence residence time, Eriksson 1971) equals response time. Use of the reach scale ensures this steady state. Median transit time data were calculated for reach A from the regression equations presented in Table 5.4. The median was calculated as the time for half the BTEQ placed in the reach at t = 0 to be output. Response time was derived from Table 5.6, mean data were used for < 64 mm and < 32 mm classes. Results are presented in Table 8.4 and Figure 8.4.

	Γ_i	Median transit time
<180 mm	57900	64800
<64 mm	49050	52900
<32 mm	40150	48030

Table 8.4. Comparison of response time and median transit time for reach A defined as steady state.

The disparity in the data is a reflection of the assumptions used to account for non 100% recovery rate and the problem of exhaustion of supply to the transit time relationships. The slope of the transit time distribution should increase with decreasing grain size. Instead, the opposite occurs, thus overestimation of the true median transit time will increase with decreasing grain size. In addition, response time assumes that the recovery rate errors are evenly distributed between output and storage, whereas mean transit time assumes error only in storage and therefore underestimates output and further overestimates the median. The magnitude of the disparity between Γ_i and median transit time is a function of the proportion at which response time was determined (a function of recovery rate) and the importance of recovery rate and exhaustion to the transit time relationships. This data demonstrate that response time and transit times are only comparable when there is a 100% recovery rate and minimal or equal exhaustion, the latter only possible if all grain sizes are equally mobile. At all other times, the median transit time reflects fractional output rates and the age distribution of the remaining sediment and is therefore not directly related to the more useful response time.

As sediment is added to a store or sub-reach, transit time becomes unrepresentative as contrasting ages of sediment will be output during the same flood event. Response time is also sensitive to this addition where input determines the point at which Γ_i is reached. In some circumstances, Γ_i may be defined twice for the same store (e.g. Appendix E7, F). Whilst problematic, response time still

8.3.2 Tracer particle flux

Tracer data were used to determine fractional transfer fluxes relative to volumetric storage. Sample size is crucial to the accuracy of the estimates derived from these particles (Church and Hassan 1992). Logistical factors constrained tracer numbers, but, sample sizes compare favourably with previous studies (e.g. Laronne and Duncan 1992 used 970 tracers across 2 reaches, Drew 1992 used 200 per reach), although study objectives differ. In the absence of recommended sample sizes, it must therefore be assumed that the small sub-sample of the bed material occupied by tracers represents an accurate estimate of overall sediment fluxes. Some stores contained insufficient tracers, particularly at the sub-reach scale. A future study may reduce spatial resolution and concentrate upon a sub-reach using a large number of tracers documenting detailed storage behaviour.

The tracer data may be assessed with reference to the three prerequisites crucial to accurate representation of sediment fluxes and transit time development (Dietrich et al. 1982): (1) Accurate storage definition, this was addressed in the sub-section 8.3.1.1; (2) tracer grain size distributions should match that of the bed; this was achieved by accurate scaling of tracer data into bed tracer equivalent (BTEQ); (3) attainment of 100% recovery rates; this is rarely achieved in any tracer studies (Hassan et al. 1984) and the present study is no exception (Table 4.4, 4.5). If a systematic trend in non recovery is apparent then the results presented will not completely describe the sediment transfer process. Small deviation away from 100% recovery for clasts > 32 mm is the result of random errors in tracer relocation in each reach and data quality is unaffected. Finer fractions were less accurately represented, particularly the < 23 mm clasts. However, where transfer is size selective, any systematic error will reflect the increased mobility of finer clasts and associated greater probabilities of deep burial (Church and Hassan 1994) hindering relocation. On this basis, the inferences regarding the effect of absolute tracer grain size upon transfer remain robust.

An accurate transit time cannot be calculated if sediment of different ages is free to mix (section 5.2), as the age of output sediment would not accurately reflect the incidence of flooding. An accurate estimate can be made only if hydraulic conditions are kept constant, as in conditions attainable within flume studies. An initial aim of this study was transit time function development at different scales, but this was only possible at the reach scale or by defining a single input or output point and even then exhaustion effects decreased the accuracy of the data. The idealised study advocated by Dietrich et al. (1982) where sediment was monitored through regular river sections would identify transit times but not within channel differentiation. In a detailed sediment budget study, examination of storage and output fluxes per storage type using response time is far

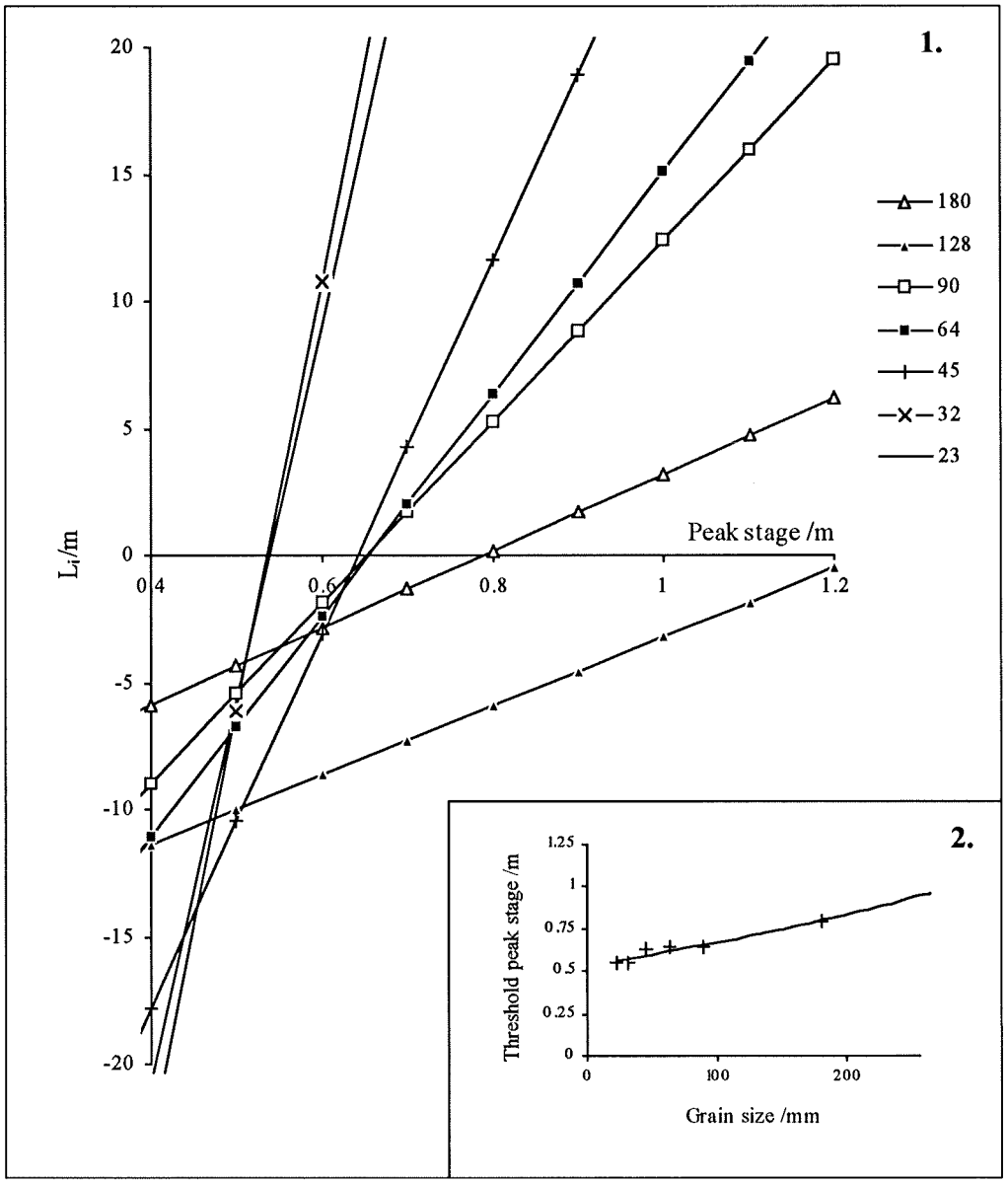

Figure 8.3. Mean distance moved per half phi class *i* in reach A predicted from peak stage at Q3 using regression relationships presented in Table 7.1. Duration above threshold is 0. 1. Predicted relationships, axes are truncated at ± 20 m. Threshold stage for motion per size class, H_{Ti} is determined from the intercept on the abscissa. 2. Threshold according to grain size D_i. Best fit line derived from regression where $H_{Ti} = 0.53e^{2.20*10^{-3}D_i}$, $r^2 = 0.92$, $p<0.05$. < 128 mm data are excluded from regression.

8.3.1.2 The bedload threshold

The bedload threshold used in this study (derived from bedload traps downstream of reach B) determines the duration used to describe and compare the tracer and volumetric fluxes. The accuracy of this threshold may be assessed with reference to the multiple regression relationships derived between distance of transfer, stage and duration in reach A (Table 7.1); relationships for reach B were not significant. Duration is assumed to be zero therefore a threshold stage is identifiable for fraction *i* from the regression relationships (Figure 8.3). It is assumed that such conditions are representative of an initial rise in stage prior to which sediment entrainment is prevented. The fractional threshold is determined from the intercept through the abscissa. The regression relationship between intercept and grain size (Figure 8.3, 2) demonstrates that the threshold for motion is significantly related to grain size ($p < 0.05$). An exponential curve more accurately accounts for the reduction in competence for coarser grain sizes compared with linear predictions. The threshold stage comparable with that derived from the bedload traps (0.49 m at Q5 corresponded with a threshold stage of 0.36 m at Q3, section 4.4.3) is the intercept of the regression line, in this case 0.53 m.

Non correspondence (Q3 threshold used = 0.36 m and Q3 threshold from tracers = 0.53 m) is a result of using tracers to define a threshold, thus it is likely that the figure of 0.53 m is closer to a tracer rather than total sediment transfer threshold. The effect upon duration of each threshold (assuming that one is for tracers and the other for all sediment) is not too significant since hydrographs are generally fairly steep (Appendix B), however where hydrographs are less steep or do not exceed both thresholds, the error may be up to 50 %. The threshold used in this study (section 4.4.3) was derived for total transfer rather than gravel alone and represents a consistent basis for comparing tracer dispersion. A gravel threshold stage could not be defined from the bedload traps since significant quantities of > 16 mm particles did not move until flow was overbank at Q5, thus accurate extrapolation to Q3 was not possible. No transfer rate calculations were made from tracers and the bedload transfer rates obtained from volumetric fluxes relative to the total sediment transfer threshold remain valid. The qualitative role of duration to the levels presented in this chapter (1a, 2a and 2b) remains unaffected since this refers to the probability of morphological change (i.e. all material, not just tracers). The only area where non application of a tracer threshold may be a problem is assessment of the role of duration upon fractional transfer. However, if it is assumed that the relative magnitude of the duration data used is consistent whether a tracer or total transfer threshold was used then the conclusions (based upon p values, Table 7.1) remain valid (in relative terms). This assumes that duration of the lower part of the hydrograph (above the total threshold) is proportional to the upper (above the tracer threshold), providing both thresholds are exceeded. Most major floods exceeded both thresholds, those which did not were small duration minor events and thus have a minimal effect upon the results presented herein.

point sampling is acceptable in reach B where bedload can be related to local hydraulics. However, finer sediment beyond the scope of volumetric or tracer data may derive from far upstream and pass through the reach as a throughput load, particularly in a size selective system (Wathen et al. in prep. 1994). The problem is rather more acute in reach A. Size selectivity in tracer fluxes, particularly those propagated furthest downstream suggests that a point sample would overestimate the proportion of fine sediment in relation to point hydraulic conditions, although exact magnitudes are dependant upon the relative difference between local size selective entrainment and reach scale size selective transfer. Where supply limited conditions prevail, a suitable point sampling programme should attempt to separate throughput load (where fine material in transfer is locally over represented) from locally derived transfer. Without detailed reference to bedload source areas, this remains an insurmountable problem and an inherent inaccuracy with all point samples.

Transfer estimates derived from cross sections are not subject to the same disadvantages as point samples as data are usually width integrated and input load is determined. Data derived from such studies are useful where erosion is limited to pool-bar units (e.g. meandering reaches of the Waimakiriri river, Carson and Griffiths (1989), the braided reach of the Sunwapta river, Goff and Ashmore, 1994) or the thalweg (reach B). For larger more active reaches, the spatial pattern of sediment transfer and coarse temporal resolution between surveys may contradict the true fluxes and inevitably leads to underestimation (Figure 6.8). No single methodology is appropriate to estimate at a point bedload transfer and consideration should be made of the drawbacks associated with each one relative to the aims of the data collection (Ferguson and Ashworth 1992).

8.3.1.1 Storage definition

A completely objective method of storage definition is probably not attainable, but potential activity quantified from the shear stress index (SSI) provides the least subjective method to date. Previous methods all use a degree of qualitative definition, for example potential activity (Kelsey et al. 1987), presence of vegetation (Nakamura 1986) and presence/absence of bedload transfer (Hoey and Sutherland 1991). Accurate survey data converted to depth and slope provided an objective rule driven definition parameter. Inevitably, categorisation into storage type was partly subjective although subdivision remained strictly numerical. The method adopted is vindicated by results from reach A in which storage type is a crucial factor. However, in the less active reach B the method was less successful, primarily due to the low imposed excess shear stress associated with shallow gradient and the importance of local within store variability, particularly within the submerged channel. These results suggest that the storage definition method may require modification for application to contrasting reach types.

8.2.4.2 Local within store morphology

At a detailed scale, the distribution of small scale features such as avalanche faces and temporary scour deposits affects transfer data derived from storage types. For example, in reach B stable storage was unusually active compared with other intermediate stores (Table 5.8). Whilst partly a function of reduced shear stress gradients in the channel, stable storage included fine grained mobile scour deposits derived from lateral pool scour (Markham and Thorne 1992). These important local effects are difficult to accurately quantify for two reasons: (1) the extent of these features is overlooked even using a 1 m survey resolution; (2) few tracers were located in such small areas. Such small scale effects induce noise around the relationships particularly in reach B, more systematic behaviour may be determined using a more detailed level of resolution.

8.3 Evaluation of data collection and analytical methods

Evaluation of the data collection programme provides an assessment of the techniques used, the level of resolution and the assumptions used in the analysis providing recommendations for future studies of sediment movement. The methods will be divided into volumetric flux, particle flux, hydraulic data and the level of resolution of the data collection programme.

8.3.1 Volumetric flux

Volumetric data derived from cross sections were used to define stores and determine volumetric fluxes. The accuracy of the latter is a function of the spatial and temporal resolution of the surveying programme (Lane et al. 1994). A survey interval of 1 m (advocated by Lane et al.) represents an improvement over previous studies where a c5 m interval was used (e.g. Ferguson and Ashworth 1992, Goff and Ashmore 1994). Survey interval is a function of study aims and river type (particularly slope), the extent to which increased resolution affords no advantages to data accuracy thereby becoming counterproductive should be assessed. Temporal resolution was sufficient to meet the aims of this study, namely the linkage of tracer and volumetric fluxes within a sediment budget framework. However, any future studies should attempt to ensure that the temporal interval is no more than a single flood (where possible). Relating volumetric fluxes to tracer dispersion over composite study periods introduces a degree of inaccuracy.

At a point sediment transfer rates reflect the interaction between local and upstream fluxes, the latter dominating in reach A by virtue of their magnitude, but are absent from B (Figure 6.5). This contrast is indicative of the imposed shear stress and reflects the difference in overall sediment activity at each site posing an interesting problem for measuring bedload transfer. Clearly use of

channel shear stress (maintaining the bars) and associated downstream sediment delivery may have prompted braiding and storage in 3A. On this basis, the distribution of sub-reach channel patterns in a transitional system may represent spatial variations in morphology induced sediment transfer. An example of the sensitivity of 3A to upstream supply is the plugging of the right anabranch at the head of bar III after 21000 min. associated with subsequent downstream changes to the local channel pattern (Appendix F13). Sub-reaches 1A and 2A appear to rapidly transfer all sediment delivered, most material being subsequently deposited and stored in 3A. From these results, transitional patterns associated with a process continuum (Ferguson 1987) such as in reach A reflect imposed slope and additionally, morphology induced variations in sediment transfer (Lane et al. in prep).

The contrast in sub-reach morphology in reach A defines the spatial distribution of flood effectiveness (e.g. Wolman and Gerson 1978) with imposed flooding affecting sub-reaches with contrasting results. Flooding in 1A and 2A is less effective than 3A; sub-reach morphology in the former did not alter. More permanent changes were induced in 3A, partly as a function of upstream sediment delivery, less effective upstream floods transfer sediment from 1A and 2A, usually as a throughput load (Appendix F), into 3A where reduced competence results in deposition. Sub-reach 3A may be defined as temporarily over aggraded (probably in response to insufficient slope to support an active braided system) characterised by transient storage features. The spatial distribution of sub-reach stability defines effectiveness. For example, the sediment wave which passed through 1A and 2A between 36000 and 57110 min. resulted in aggradation which was subsequently evacuated from the submerged channel whilst remaining on the fixed bars. The effectiveness of this flood was small in 1A and 2A as channel stability and overall morphology was maintained. Positive feedback operated as fixed bars aggraded further and constrained the main channel increasing sediment supply to 3A where the width:depth ratio increased. Rather than defining a flood as effective, it is more instructive to define effectiveness on the basis of reach or sub-reach responsiveness, reflecting local morphology and the downstream effect of upstream stability. Such a definition may be used to assess the significance, maintenance and permanence of transfer and storage zones (e.g. Church and Jones 1982, Lane et al. in prep).

The duration of this study has provided insight into temporary stability within transitional reaches and downstream linkages which govern channel pattern stability. Historical evidence suggests that fixed bars are also transient in the longer term (particularly in reach A), with the mechanisms responsible for such changes gradual (most likely in B) or abrupt (reach A). Any changes are linked to sediment supply, probably in response to extreme flooding required to destabilise such features.

scatter attributable to the influence of storage factors upon local dimensionless shear stress. Although impossible to quantitatively separate all the factors, the relative importance of variables pertinent to sediment transfer are presented. Any future study should concentrate upon quantification of these factors at various levels of spatial (according to morphology and storage type) and temporal (duration relative to peak stage) resolution. This may necessitate increased tracer samples or reduced scales of study (e.g. pool-bar units) to account for these specific characteristics of the transfer system.

8.2.4 Morphological controls upon sediment transfer

8.2.4.1 Sub-reach morphology

At the sub-reach scale, morphology was precisely quantified and tracer numbers were high allowing detailed inferences regarding sub-reach variability. Reach A consists of two meandering sub-reaches (1A and 2A) and a braided sub-reach (3A). Given the classic relationship between slope and channel pattern (Leopold and Wolman 1957, Schumm and Khan 1972), it is interesting to note the occurrence of both meanders and braiding within an overall transitional channel pattern overlying a relatively high imposed slope. It is likely that this is a function of sediment supply where the upstream meanders transfer sediment into 3A resulting in over aggradation (Lane et al. in prep.) and a braided pattern. By contrast, reach B is a straight/meandering reach characterised by high fixed alternate bars (Seminara and Tubino 1989) and a meandering thalweg. Increased slope associated with reach orientation non parallel to the valley slope (where lateral valley slope is locally greater than downstream gradient) permits a more pronounced meandering pattern compared with the straight reaches immediately up and downstream.

Minimal interaction between tracers and the dominant fixed bars characterised sub-reaches 1A and 2A and reach B. Tracers reseeded 15 m upstream of reach A were not transferred to fixed bars, but some T3 tracers (Figure 3.1) were relocated in bar I suggesting that the sediment source was from far upstream. Fixed bars in both reaches indirectly affect sediment transfer by constraining flow within the submerged channel increasing local depth and shear stresses. In addition, the location of fixed bars controls channel change; in reach A, aggradation of bar I (Figure 3.6) resulted in bank erosion and an increase in channel width without migration (Figure 6.2).

Tracer data (response times and descriptive matrices) suggest that the meandering patterns in reach A are transfer dominated and braided systems are storage based. Historical evidence indicates a recent avulsion where sub-reach 3A was meandering in 1971 and 1988 whilst 1A and 2A were generally braided. Once fixed bars began to establish in 1A and 2A, increased within

8.2.3 Level 2b: High shear stress, long duration

High shear stress and long duration flooding is associated with morphological change in reach A. During such periods (e.g. 36000 - 57110 min.), sediment transfer is a function of enhanced surficial entrainment (level 2a) and release of stored material due to morphological change.

Peak stage retains primary importance where the within bank constraint ensures variable average imposed shear stress (Table 8.4). Absolute grain size is also of primary importance despite differentiation in fractional transfer distances being reduced during long duration high shear stress events (Appendix I). Field evidence documenting an approach towards equal mobility during highest flood events (e.g. Kuhnle 1992) may reflect the duration of the imposed shear stress. At high duration, relative size effects during transport (rather than at entrainment) result in increased trapping of finer sediment as duration rises with simultaneous enhancement of the mobility of coarser particles which are less likely to be trapped. Higher shear stress reduces the role of D_i* at entrainment to secondary importance, although it remains important for transfer distances through a depositional and subsequent entrainment effect (section 7.2.1 and Table 7.1).

Descriptive matrices presented in chapter 6 demonstrate that the relationship between sediment transfer and storage type is reduced (although still important) for level 2b events compared with smaller events. Intense flooding was associated with free bar migration and evacuation of the stored sediment increasing the apparent activity of storage based stores. As morphological change released tracers stored in bars up to a depth of approximately 0.25 m (Appendix L), burial is assigned secondary status. This reflects the lack of importance of burial once a sediment store is eroded/mobilised during such intense flood events, although deeply buried material (> 0.4 m) did remain immobile. Sediment excavation depths increase during higher stage indicating that buried sediment is more accessible although this is dependant upon storage type. As already intimated, the role of morphology is crucial to these trends and, to a certain extent, determines the linkages between them. For example, in sub-reaches 1A and 2A, burial is more important since the stable morphology restricts bar migration whereas free bars are frequently eroded in 3A thus burial is less of a constraint on sediment transfer.

These results demonstrate the importance of reach contrasts and levels of spatial and temporal resolution to explanations of sediment transfer. Previous studies describe tracer transfer according to average hydraulics, grain size and general reach conditions (e.g. Laronne 1987, Church and Hassan 1990, Drew 1992, Schmidt and Ergenzinger 1992). More detailed analysis of the effect of bed structure (locked, surface or buried) has improved understanding of sediment transfer distributions (Laronne and Carson 1976, Hassan and Church 1992), but considerable unexplained scatter remains. This study has adopted a morphological approach providing explanation for this

described in this study. Whilst not directly applicable to reach A, such factors may dominate in channels where morphological stability is apparent even during intense flooding.

Peak stage remains a primary variable reflecting the infrequency of overbank flow even during intense flooding in reach A. Absolute grain size is also a primary determinant of sediment fluxes despite fractional transfer rates at high stage suggesting tendency towards equal mobility (Kuhnle 1993, Wathen et al., in prep.). Reach scale size selectivity was most pronounced in response to low duration intense flooding (e.g. Appendix I1 A, 62010 min.), a result of the dependence of coarser fractions upon duration for increased transfer, and fine fraction mobility in response to high peak stage (Table 7.2). Although partly conjectural, it is suggested that relative grain size effects are overcome by higher excess shear stress with increased probabilities of entrainment corresponding with absolute grain size (Kirchner et al. 1990, Buffington et al. 1992); D_i^* is therefore assigned secondary status during high flow. Burial remains a primary factor, though depths of evacuation increase with stage (according to storage type, Appendix L), sediment mobility is still constrained in the absence of major morphological change.

Level	**2a**	**2b**
Condition	**High τ/ Low T**	**High τ/ Long T**
Factor	**Reach A**	**Reach A**
Reach slope	Primary	Primary
Peak stage	Primary	Primary
Di	Primary	Primary
Storage type	Primary	Primary
Morphology (local)	Secondary	Secondary
Morphology (sub-reach)	Primary	Primary
Burial	Primary	Secondary
Di*	Secondary	Secondary

Table 8.4. Classification of the importance of factors determining τ^*_i upon sediment transfer at high imposed shear stress with varying duration. See Table 8.2 for definition of levels.

Morphology and storage type affect the rate of transfer. In the absence of significant morphological change, relative mobility of different storage types will be proportional to those at lower stress. VA stores will transfer more sediment as depth of scour and frequency of entrainment increases with flow depth (demonstrated by response time data and movement of buried sediment). Mobility in S and IA is likely to be restricted to surface particles, morphological change being required for release of buried sediment. These storage type effects vary according to sub-reach. Flux rates from the submerged channel in 1A and 2A increase in response to fixed bars which restrict flow width and increase local depth and hence τ^*_i (resulting in significant transfer), whilst in 3A τ^*_i is smaller.

Bed material grain size. Hiding and protrusion effects alter the probability distribution of friction angles for a particular grain size (Kirchner et al. 1990, Buffington et al. 1992) reducing the importance of absolute tracer grain size. Data derived from reach B demonstrate this process. Hiding of fine sediment in coarse riffles and protrusion of coarse particles on bar surfaces affects relative sediment mobility in response to small scale local entrainment processes (Appendix I4). These results reflect local grain size distributions relative to tracers in reach B. However, it is reasonable to assume that, in the absence of morphological change, relative grain size effects also influence mobility in reach A during small floods (although this was not documented) where local influences are more important. Relative grain size is therefore of primary importance in both reaches when shear stress is low, although this is inevitably conjectural in the absence of detailed grain size, bed micro roughness and packing data.

Summarising, sediment transfer processes in response to small imposed shear stresses differ between reaches reflecting location, morphology and the local distribution of shear stress in the channel. MSS analysis presented in chapter 6 demonstrated the irrelevance of storage type and shear stress to sediment transfer in B, consistent with response time (section 5.3.3) and fractional movement distances (section 7.2.3). Once a threshold is reached, sediment transfer is a function of grain size and local factors controlling the resistance of sediment to motion. In reach A, shear stress, storage type and grain size were relevant and related in a complex way. The preceding discussion demonstrates that whilst sediment transfer is a function of τ^*_i, the relative magnitudes of the contributory factors must be ascertained before explanation of transfer patterns can be sought. Future research into transfer at low shear stress should focus upon quantification of the importance of each factor (particularly relative grain size). Detailed process measurement is required to ascertain the magnitudes of these factors which tend to operate at local scales under low intensity flow conditions.

8.2.2 Level 2a: High shear stress, short duration

This level is only applicable in reach A as the low slope at B precludes attainment of high shear stresses. It is assumed that, in the absence of significant duration, morphological change does not occur, instead, level 2a is associated with increased rates of surficial entrainment and scour/fill (Hassan 1990, Hassan et al. 1992, Drew 1992). The majority of factors are classified the same as level 1 but with significant deviation (Table 8.4). Results presented for this level are conceptual as it is likely that morphological change will occur at high shear stress levels (Goff and Ashmore 1994) and exert the dominant influence on the results. However, insight is provided into contrasts between high and low shear stress effects upon sediment transfer on the basis of the results

type and burial (chapter 7). Interaction and the relative importance of each varies according to incident stage and duration as will become apparent when levels 1 and 2 are compared.

Storage type. The distribution of storage types determines the spatial variation in flow depth and within channel shear stress. The dependence of local stress upon depth is reflected in the reduced (or non) activity of storage based stores at this level. Response time and descriptive matrix data indicate that transfer declined from VA to IA stores in reach A vindicating the use of elevation (e.g. Williams and Rust 1969, Lekach et al. 1992) as a partial determinant of storage type. Output fluxes from S and IA stores were minimal after 36000 min. in reach A whilst some tracers were mobilised from VA stores (Appendix E4. A). In reach B transfer from storage did not provide such a clear distinction and is thus assigned secondary status. In general, VA and IA represented two extremes (see response times, Table 5.8), the other 3 storage types being much less discriminatory at level 1a. Storage type was less important in reach B reflecting reduced elevation differentiation in the submerged channel, increased variation in local morphology within intermediate storage types, and reduced shear stress gradients between stores.

Morphology. Morphological effects upon sediment transfer may be considered at within store and sub-reach levels. The former is partly responsible for variability about the uniform progression of transfer activity according to storage type (Table 5.8), reflecting the heterogeneity of sediment and morphology at small scales. This is more pronounced in reach B where local factors exert a more significant influence upon sediment transfer than in A where broader trends are much clearer.

Sub-reach morphology provides explanation for the spatial distribution of sediment transfer. In 1A and 2A fixed bars ensure relatively high shear stresses within the submerged channel resulting in transfer during small events. Transfer in 3A was minimal during intermediate events reflecting the high width:depth ratio (hence non attainment of sufficient shear stress) and dominant mode of storage within free bars (Appendix E6. C). In reach B, fixed bars induce a narrow range of shear stresses in the submerged channel in all sub-reaches. A more complete evaluation of the importance of morphology is described in section 8.2.4.1.

Burial. Increased burial depths reduce the relative mobility of tracer sediment (Hassan 1990, Schick et al. 1987b), although this varies according to imposed shear stress and local morphology (Drew 1992). Exponential envelope curves (section 7.4.2) indicate that at low shear stresses, mobility is a function of burial depth (Hassan and Church 1994) in both reaches, so burial is a primary factor. Active layer depth determines the importance of burial and varies between stores particularly in reach A (Appendix L). Burial is a more significant constraint upon mobility in storage based stores (and all reach B stores) where shear stress is insufficient to attain a significant depth of local scour.

Level	**1a**	**1a**	**1b**	**1b**
Condition	**Low τ/ Low T**		**Low τ/ Long T**	
Factor	**Reach A**	**Reach B**	**Reach A**	**Reach B**
***Reach slope*, S**	Primary	Primary	Primary	Primary
Peak stage	Primary	Secondary	Primary	Secondary
D_i	Primary	Primary	Primary	Primary
Storage type	Primary	Secondary	Primary	Secondary
Morphology (local)	Secondary	Primary	Secondary	Primary
Morphology (Sub-reach)	Primary	Primary	Primary	Primary
Burial	Primary	Primary	Primary	Primary
D_i*	Primary	Primary	Primary	Primary

Table 8.3. Classification of the importance of factors determining τ^*_i upon sediment transfer at low imposed shear stress τ with varying duration T.

Reach slope. Absolute shear stress varies according to reach slope which is thus categorised as primary at all levels, defining the average responsiveness of a reach and the frequency of competent events. Peak shear stresses are insufficient for large scale volumetric change in reach B (shown by volumetric data, section 6.2.1). This contrast may provide partial explanation for the frequent non correspondence of tracer data derived from different reaches and different rivers (e.g. Hassan et al. 1992) lending support to the contention that a morphological approach is essential to understand sediment flux characteristics (Hassan and Church 1992).

Peak stage: Peak stage is used as a surrogate for shear stress at the bed during flood events of differing size. Although sensitive to within reach bed and water surface slopes and local morphology, it is an adequate general measure of the relative magnitude of hydraulic conditions. Overbank flow in reach A occurs only in extreme events (peak at Q3 c0.75 m) so a wide range of average within channel shear stress values are attainable. Bimodal transit time distributions indicate the sensitivity of transfer to imposed shear stress (section 5.3.1), so variation in peak stage is a primary factor in reach A. Frequent overbank flow and reduced slope restricts the range of reach average shear stress values in reach B. Reach scale transit time distributions and MSS analysis (section 6.3.3) indicate no correspondence between peak stage and sediment transfer. Once a reach averaged threshold for motion is exceeded, shear stress has only secondary importance.

Tracer grain size. In a size selective system such as the Allt Dubhaig (Ferguson and Ashworth 1991), finer sediment is transferred preferentially further than less mobile coarse tracers. In the absence of abrasion, this process is largely responsible for observed rates of downstream fining (Hoey and Ferguson 1994). Grain size is a primary variable as transfer fluxes are directly proportional to size in both reaches. The exact magnitude of these fractional fluxes is conditioned by relative grain size (hiding and protrusion effects, Fenton and Abbot, 1977), morphology, storage

Flood type (expressed as peak stage and duration) conditions the interactions and relative importance of the factors documented in Figure 8.1, particularly the relative magnitudes of inertial variables. Of crucial importance is the incidence of morphological change (a function of flood type, section 6.3.2) and the effect of this upon the transfer related variables. The following subsections describe the effect of flooding upon these factors at entrainment, transport factors are considered in the model conceptualisation presented in section 8.4.

The factors affecting τ^*_i and hence sediment transfer may be assessed using binary classification of peak stage and duration (Table 8.2). Thresholds between the resulting 4 semi-quantitative levels are assumed gradational rather than abrupt (Newson 1992). Each level will be considered in isolation and the factors affecting τ^*_i classified as having either primary or secondary significance. A primary influence indicates that this variable is an important determinant of sediment mobility, a secondary factor is less important, its effect is overcome by primary factors.

Level	Maximum imposed shear stress	Duration
1a	Low	Low
1b	Low	High
2a	High	Low
2b	High	High

Table 8.2. Levels of resolution describing the distribution and relative magnitude of factors conditioning local and reach scale sediment fluxes according to flood event characteristics.

8.2.1 Level 1a and 1b: Low shear stress

Low shear stresses characterise reach B at all times and apply in intermediate flood events (e.g. 36000 min.) in reach A. The relative influence of each factor on τ^*_i under such conditions is demonstrated in Table 8.3. Each factor is assessed individually and linkages addressed.

Transfer in response to such shear stresses is local scale, and an increase in duration is unlikely to alter this (Table 8.3). Volumetric change during level 1b type events was restricted to local scour and fill, sediment fluxes extending a few metres downstream (Appendix F). In reach A such fluxes were slightly more important, but small compared with the results from higher magnitude floods. Integration over time (Eq. 8.2) indicates that duration is relatively unimportant to transfer at low shear stresses since local effects dominate with marginal transfer conditions (Andrews and Smith, 1992) so all factors are classified the same as level 1a. The following discussion concentrates upon the effects of low imposed shear stresses.

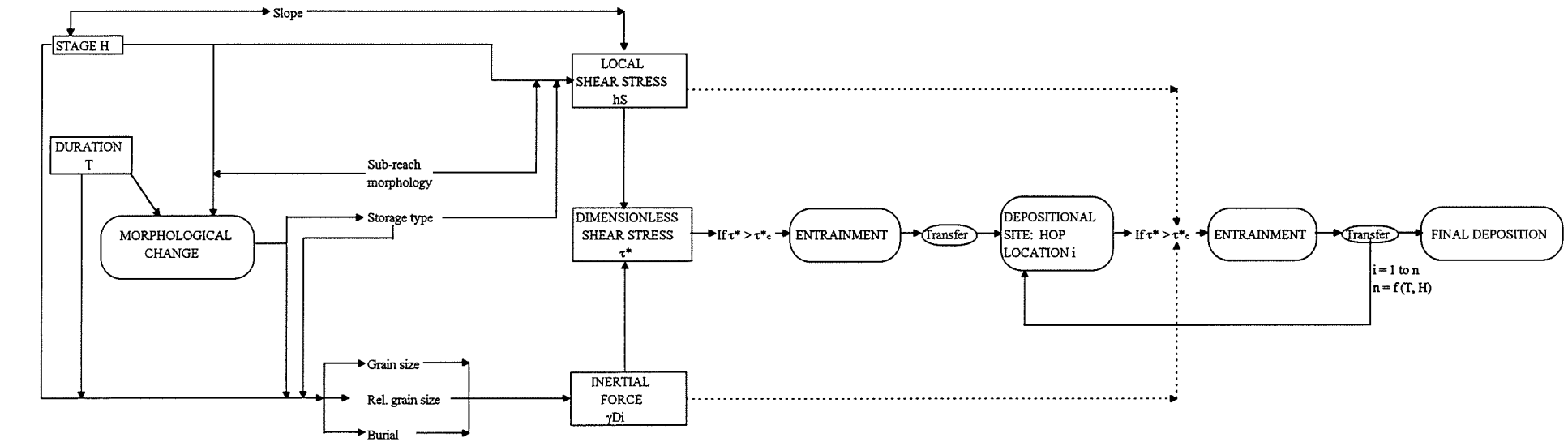

Key:

- Priniciple variable
- Principle process
- Text — Governing factor or proviso
- Direction of influence
- Operation at hop location i

Figure 8.2. Conceptualisation of the sediment transfer system during a single flood. Refer to Eq. 2.2 for key to symbols.

function of grain interaction (D_i*) and friction angle (Li and Komar 1986, Kirchner et al. 1990). The magnitude of entrainment and local scour increases with stage and duration where, additionally, the probability of morphological change rises (Goff and Ashmore 1994). During intense flooding tracers are entrained from storage due to large scale scour and fill together with morphological change associated with reworking of barforms and pool/riffle migration (Hassan and Church 1992).

Reach A			
Factor	**Promote τ_i***	**Reduce τ_i***	**Evidence**
Reach slope S	High slope		TT_i, Γ_i, DM, L_i
Peak stage	High stage	Low stage	TT_i, Γ_i, DM, L_i
Tracer grain size (D_i)	Fine	Coarse	Γ_i, DM, L_i
Storage type	VA, A	S, IA	Γ_i, DM, L_i
Morphology (local)		Avalanche faces	Γ_i, DM, L_i
Morphology (sub-reach)	Fixed bars	Free bars	Γ_i, DM, L_i
Burial	Shallow b_{max}	Deep b_{max}	L_i
Relative grain size(D_i)*	D_i*<1	D_i*>1	L_i
Reach B			
Reach slope S	Low S		TT_i, Γ_i, DM, L_i
Peak stage	NA once above threshold		TT_i, Γ_i, DM, L_i
Tracer grain size (D_i)	Fine	Coarse	Γ_i, DM, L_i
Storage type	VA only	IA only	Γ_i, DM, L_i
Morphology (local)	See section 8.2.4.2.	Avalanche faces	Γ_i, DM, L_i
Morphology (sub-reach)	Fixed bars		Γ_i, DM, L_i
Burial	Shallow B_{max}	Deep B_{max}	L_i
Relative grain size (D_i)*	D_i*<1	D_i*>1	L_i

Table 8.1. The effect of factors conditioning τ^*_i upon sediment mobility considered in isolation from other influences. Data sources are indicated. Key to symbols: TT_i, - transit time function, Γ_i - response time, DM - descriptive matrices, L_i - distance of transfer. NA - no affect upon sediment mobility. In reach B, the absolute magnitude of excess shear stress is unimportant.

The role of event duration T upon sediment transfer may be conceptualised as the integral of τ_i* over time, where

$$\int_0^T \tau_i * dt = \sum_{j=0}^{j=T-1} \left(\frac{hS}{RD_i} \right) (t_{j+1} - t_j) \qquad (8.2)$$

subscript j indicates successive time periods. In the absence of detailed information regarding the distribution of shear stresses during an event, it is sufficient to state that greater duration increases the time for which a particular shear stress may operate. In turn, this affects the relative magnitudes of the factors described in Figure 8.1. The linkages between these factors are summarised as a flow diagram (Figure 8.2).

transient forms whilst in reach B it is probably less than 1 where the recurrence interval of effective events is very high (only very extreme floods would cause any significant channel alteration), consistent with reach stability and the dominance of characteristic morphology. Adopting the terminology of Brunsden and Thornes (1979), reach A may be thought of as a mobile fast responding unstable subsystem (as defined by the incidence of effective flooding) whereas reach B is slowly responding and insensitive.

The following discussion focuses upon the factors responsible for sediment transfer within these contrasting reaches.

8.2 The sediment transfer process

Transfer is promoted by increased shear stress with numerous other factors combining to add inertial effects or directly reduce local stress (Figure 8.1). The ratio of these factors at the entrainment location and subsequent hop positions for fraction *i*, summarised as dimensionless shear stress, τ_i^*, determines the local rate and distribution of sediment transfer. A summary of the effect of each factor acting in isolation is summarised in Table 8.1 together with the data source from which the information is derived.

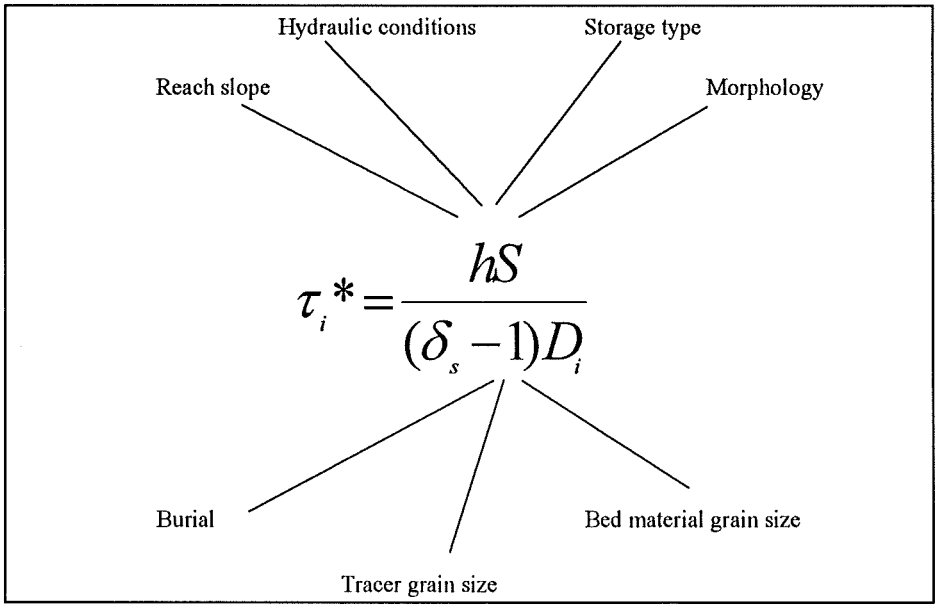

Figure 8.1. Factors controlling mobilisation of sediment from the bed.

Small scale entrainment dominates in the more active stores during minor floods where the depth of scour is limited to a surface layer a few grain diameters thick (varying according to storage type, section 7.4.3). The rate of entrainment from a bed of mixed sized sediment during such events is a

was the dominant control. These trends are linked to activity with insufficient excess shear stress available for morphological change and within channel storage differentiation in reach B.

The contrast in activity may be assessed with reference to local reach characteristics and recent channel change. However, inferences regarding the nature of reaches A and B are constrained by the presence of only 18 months of data so it is instructive to asses the consistency of the data describing present fluxes in relation to the history of channel alteration. Historical maps suggest that reach A is unstable, usually dominated by transient forms whereas reach B has gradually evolved to its present form (Figures 3.7 and 3.11).

The January 1993 flood was the highest on record during this study (Appendix B13, B14), although, its significance to the longer term hydrological record is unknown. Volumetric and tracer data indicate morphological change and substantial sediment evacuation from reach A in response to this event, whereas reach B retained its original morphology and exhibited limited sediment transfer. This contrast in the level of responsiveness in reaches A and B complements the historical trends. Responsiveness also varies within reach A; 1A and 2A are fairly stable (morphology at the start of the study remained throughout) whereas 3A is predominantly transient characterised by frequent morphological change. The significance of this contrast is assessed sub-section 8.2.6.1.

Of crucial importance to reach contrasts is the effectiveness of flooding, a function of: (1) flood magnitude; and (2) the ability of the reach to maintain stability (stable reaches define less effective flooding since response is usually minimal), rather than the ability to return to stability as in the original definition of Wolman and Gerson (1978). Flood effectiveness varies spatially along the long profile, characterised by an increasing return period for major competent floods in the downstream direction associated with the decline in reach slope. The probability of exceedence of critical dimensionless shear stress is higher in A than B for the same flood. As a result, reach A is less stable than B. The increased frequency of effective floods seems to prevent recovery in reach A. This may be expressed by the transient form ratio (Brunsden and Thornes 1979) where,

$$TF_r = \textit{mean relaxation time / mean recurrence interval of events} \qquad (8.1)$$

Evidence from this study suggests that reach A is not evolving or pertaining to a more stable state. Recovery since an effective flood such as January 1993 provides no indication of a systematic gradual return to pre flood conditions and morphological adjustments due to this flood were still present in May 1994 (e.g. Anderson and Calver 1977); and relaxation time (the time for recovery of the landform) is thus high. It is therefore valid to assume that mean relaxation time is in excess of the recurrence interval of effective floods. TF_i is thus in excess of 1, indicative of the presence of

8. Discussion: A semi-quantitative conceptualisation of the sediment transfer process

The preceding chapters demonstrate the importance of storage location for sediment transfer fluxes. Adoption of a morphological approach provides some explanation for previously reported stochastic transfer distributions (Hassan and Church 1992). The role of storage type and morphology was ascertained using response time. Descriptive matrices extended this detailing the effects of flood type, tracer grain size and source store to transfer distribution patterns. A relative measure of activity (MSS) was introduced, demonstrating the relative magnitude of factors operating to condition dimensionless shear stress, τ^*_i, at the point of entrainment. Mobility in reach A was attributable to hydraulic conditions, grain size and storage type whilst grain size was the only influential variable in B. These factors were analysed in more detail with reference to absolute and relative fractional transfer distances. Hydraulic conditions were broken down according to peak stage and duration with grain size divided into relative and absolute effects. The general conclusion from these analyses is that sediment transfer is dependant upon the relative magnitude of factors affecting τ^*_i, the distribution of which are controlled by flood type, morphology and reach contrasts (principally the incidence of morphological change). The following discussion summarises and expands upon the relevance of these results through conceptualisation of sediment transfer in each reach according to flood characteristics. The conclusions depend upon the quality of the data available, so it is instructive to evaluate the data collection programme relative to the aims of this study. Finally, the findings of this study are incorporated within a conceptual model of downstream and within reach sediment transfer.

8.1 Reach contrasts

Sediment transfer may be regarded as a function of dimensionless shear stress and its controlling factors (e.g. Hassan and Church 1992) but differences between reaches A and B indicate that this conceptualisation may vary between sites. The results from this study consistently demonstrate the extent of this disparity. Response time, transit time, volumetric change and fractional transfer distances all suggest that reach A is more active than B. For example, the reach scale response time of the tracer fraction containing the mean reach surface D_{50} is 57900 min. in reach A and 117518 min. in reach B. This contrast in activity also affects the dominant transfer processes. Reach B did not undergo significant morphological change since shear stresses were insufficient hence mobility of sediment was confined to the surface, buried particles were only mobilised due to local scour. Matrix dimensionless shear stress (MSS) analysis revealed that transfer in reach A was the result of complex interaction between hydraulics, grain size and storage whereas in B grain size

3. Morphological change releases large numbers of tracers reducing size selectivity. This was not present in reach B where selectivity was reduced due to relative grain size effects.

4. The previous conclusions consider factors in isolation, in reality, sediment transfer is affected by a range of implicitly related factors operating together at various spatial and temporal scales.

5. Conditions at entrainment are the prime determinant of transfer distances although transport pathways and intermediate rest locations are important and must be considered.

6. The temporal sequence of morphological changes and cross stream currents alter the pathway of sediment transfer, especially for fine tracers scoured from pool sites.

7. Lateral sorting promotes downstream fining (Seal et al. 1993), but, lateral storage must also be considered, possibly in a combined model predicting the influence of lateral effects upon sediment transfer and sorting.

8. The active layer depth varies according to storage type and hydraulic conditions, the spatial and temporal distribution of which affects the importance of burial for sediment transfer.

size effects, particularly protrusion on bar surfaces and vertical winnowing into riffles, resulting in local reductions in the degree of size selectivity.

Examination of burial effects introduces a third dimension to the study of transfer fluxes. In reach B the absence of morphological change ensures that buried sediment is generally less mobile than surface particles. Similarly, this also characterises reach A until flow is sufficient to instigate morphological change whence burial ceases to be a major determinant of sediment mobility. This temporal and spatial variation in the importance of burial alters conventional hypotheses developed in the absence of detailed morphological information. Burial cannot be considered relative to a fixed active layer depth, as this varies with storage type and incident flooding. Accordingly, buried sediment may not be assumed to be less mobile (Hassan 1990, Schick et al. 1987b) or more mobile than surface sediments (Drew 1992) at the reach scale until detailed morphological analysis specific to the measurement site is carried out.

Whilst as comprehensive as possible, there are still some influences which have not been considered. Pocket geometry and particle shape effects condition entrainment (Fenton and Abbott 1977, Kirchner et al. 1990). In the absence of data, the importance of these factors is recognised but will not be included in a conceptual model of sediment transfer which is presented in the following chapter.

Results from this chapter and 5 and 6 have documented the importance of storage type, hydraulics (peak stage and duration), tracer grain size and relative grain size effects at the location of entrainment to fractional transfer patterns. All these factors are altered by local conditions providing a complex overview of the interactions within the transfer system. However, adoption of a morphological approach has demonstrated some degree of order; this will be assessed in the following chapter.

7.6 Conclusions

1. Selective transfer dominates in both reaches, its absolute magnitude being a function of hydraulic conditions, sub-reach morphology and storage type.

2. Relative fractional transfer is affected by the absolute magnitude of stage and duration between searches in reach A. Where both are large, size selectivity is reduced due to relative grain size effects decreasing fine sediment mobility once in transport and duration promoting coarse sediment transfer.

morphological change. Whilst impossible to quantitatively separate out all the factors affecting transfer, the dominance of conditions at entrainment indicates that the approximation represented by the MSS analysis (section 6.3.3.2) is valid.

Previous chapters document the local importance of hydraulics, grain size and storage type to transfer. Analysis of the mode of transfer presented in this chapter allows detailed determination of the importance of these factors for fractional transfer patterns. The effect of peak stage and duration alters fractional transfer due to importance of relative grain size. Relative grain size effects may be subdivided according to influences on entrainment and during transport. The former are important at low peak stage whilst the latter determine transfer distances during intense flooding, although the absolute magnitude is conditioned by storage type. Size selectivity was reduced during high intensity flooding due to two factors: (1) as peak stage increases, fine sediment is more readily transported, although the probability of trapping and subsequent incorporation within the bed increases as duration rises where $D_i^*<1$. Simultaneously, coarse sediment is mobilised in response to peak stage and, providing that duration is sufficient, will remain in motion due to momentum and protrusion effects; (2) during such intense flooding conditions the probability of morphological change is enhanced. Associated with bar migration is the release of all sizes of stored sediment where relative mobility is reduced compared with entrainment from the bed surface. These two factors suggest that when deriving inferences regarding selective transfer from tracer results, the flood type and morphological change must be accounted for to provide explanation and interpretation of the degree of size selectivity.

The effect of the above reach scale factors varies spatially. Data quality is insufficient to allow detailed assessment of (1). However, the distribution of morphological change and associated tracer release due to (2) is documented. Size selectivity was reduced for less active stores and sub-reach 3A, all of which are subject to morphological change during intense flooding. In addition, sediment stored in IA and S storage is temporarily removed from the transport system until release due to bar erosion or migration. Whilst no preferential fluxes were associated with these storage based stores, lateral storage does reduce the mobility of coarse sediment (released fine sediment was more mobile, section 6.3.2.4) promoting downstream fining. Results from reach A demonstrate the importance of the adoption of a tracer and morphology based approach (Hassan and Church 1992) to provide understanding of the spatial and temporal variability in the transfer system.

Morphological change was absent from reach B, so it may therefore be assumed that transfer is a result of small scale scour and fill processes (Hassan 1990). MSS analysis suggested that tracer grain size was the dominant factor governing transfer distances and hence the size selectivity apparent in this reach. Reduced activity allowed recognition of the importance of relative grain

morphological change or shear stress variation, there is no systematic variation in the depth of the active layer and the estimation of $2*D_{84}$ used in the previous subsection is acceptably accurate (especially in view of the error of ± 0.025 m.). Active layer depth in B is a function of imposed small shear stress (associated with low reach slope) and storage contrasts are unimportant. The active layer is generally deeper in reach A due to high overall shear stress, and is conditioned by the incidence of flooding (particularly in relation to morphological change) and storage type.

	Active layer depth (m)					
Time (min.)	**VA**	**A**	**SA**	**S**	**IA**	**Reach**
Reach A						
26900	0.03	0.07	0.05	0.08	0.04	0.05
32450	0.03	0.04	0.04	0.10	0.06	0.06
36000	0.04	0.05	0.04	0.02	0	0.05
57110	0.06	0.05	0.11	0.10	0.02	0.10
62010	0.05	0.07	0.09	0.08	0.06	0.08
Reach B						
23100	N/A	0.03	0.04	0.05	0.05	0.05
32100	N/A	0.03	0.03	0.05	0.02	0.04
38400	N/A	0.05	0.05	0.04	0	0.05
66450	N/A	0.05	0.04	0.05	0.04	0.05
72750	N/A	0.06	0.08	0.06	0.05	0.06

Table 7.4. Storage type active layer depths.

This analysis has indicated that in reach A burial is an important determinant of sediment mobility with evacuation dependant upon storage type and the incidence of flooding. In reach B, whilst burial is important, there is no systematic variation according to storage type or shear stress but scour and fill operate in a random way (Hassan 1990). This process also contributes to the data scatter in reach A. The trends in mobility due to burial are consistent with the overall pattern of sediment mobility according to storage type and sub reach.

7.5 Discussion

The analysis presented in this chapter verifies and extends the conclusions from previous chapters. Comparison of response time and transfer distances suggests that conditions at entrainment dominate transfer patterns, but a non perfect relationship indicates that other processes must be considered. The distance a particle travels is a function of its potential mobility at the location of initial entrainment and at subsequent depositional locations associated with particle hops. For example, if a < 45 mm particle was transported onto a coarse facies in an inactive store then the rest period would be longer than the corresponding period for the same sized tracer temporarily located in an active store. The probability of deposition in less active locations is a function of both distance moved and deviation from the transfer pathway. The latter may alter due to morphology induced cross stream currents (especially important to fine tracers) and

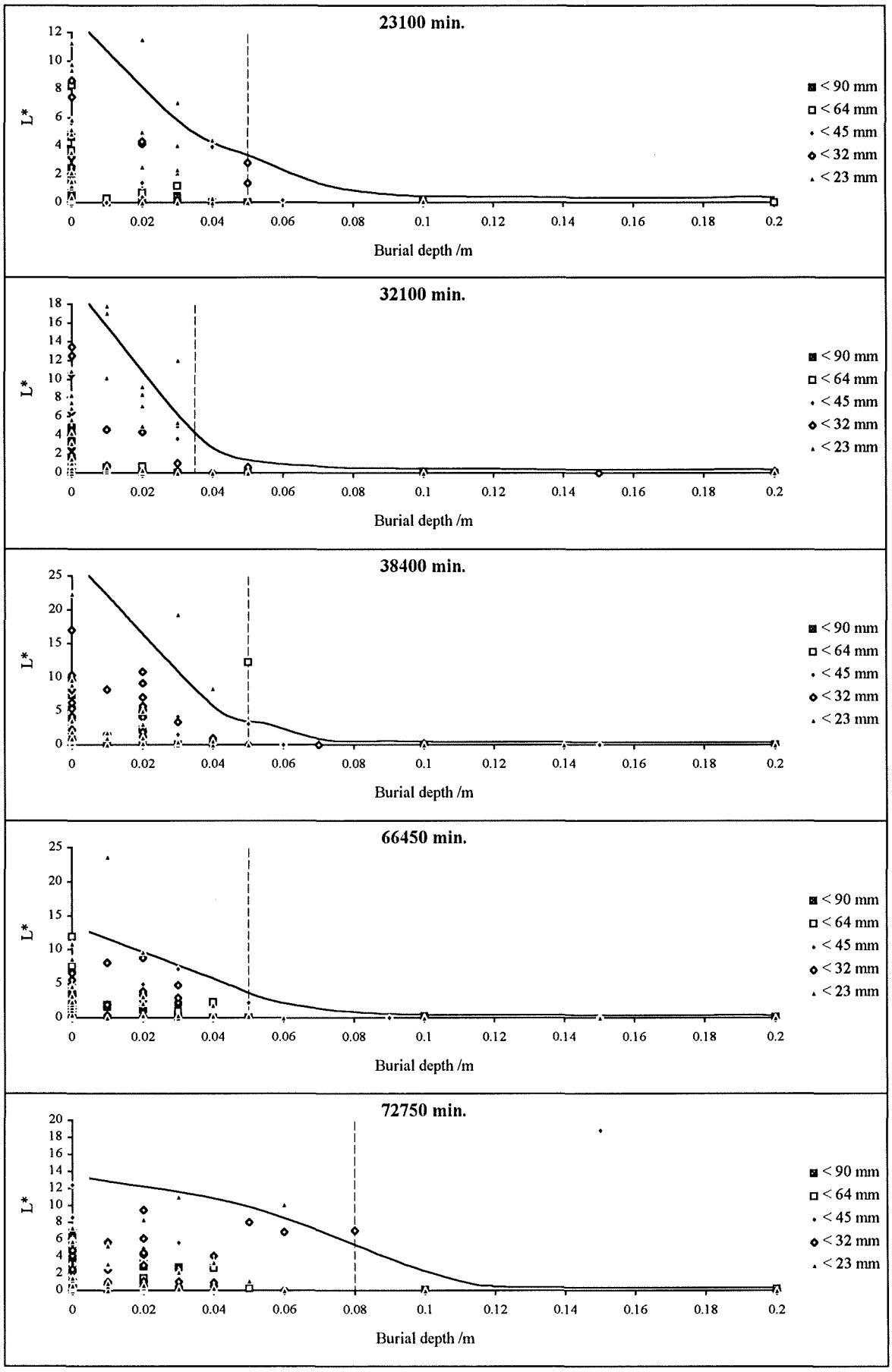

Figure 7.16: Reach B normalised transfer distance according to burial location. L* refers to distance moved by each particle normalised by the reach average per search, $L^* = L/L_{MEAN}$. Burial data are truncated at 0.2 m. Dashed line - estimated active layer depth. Solid line - approximate envelope curves. Immobile tracers in seeding pools are excluded. Note different interval vertical scales.

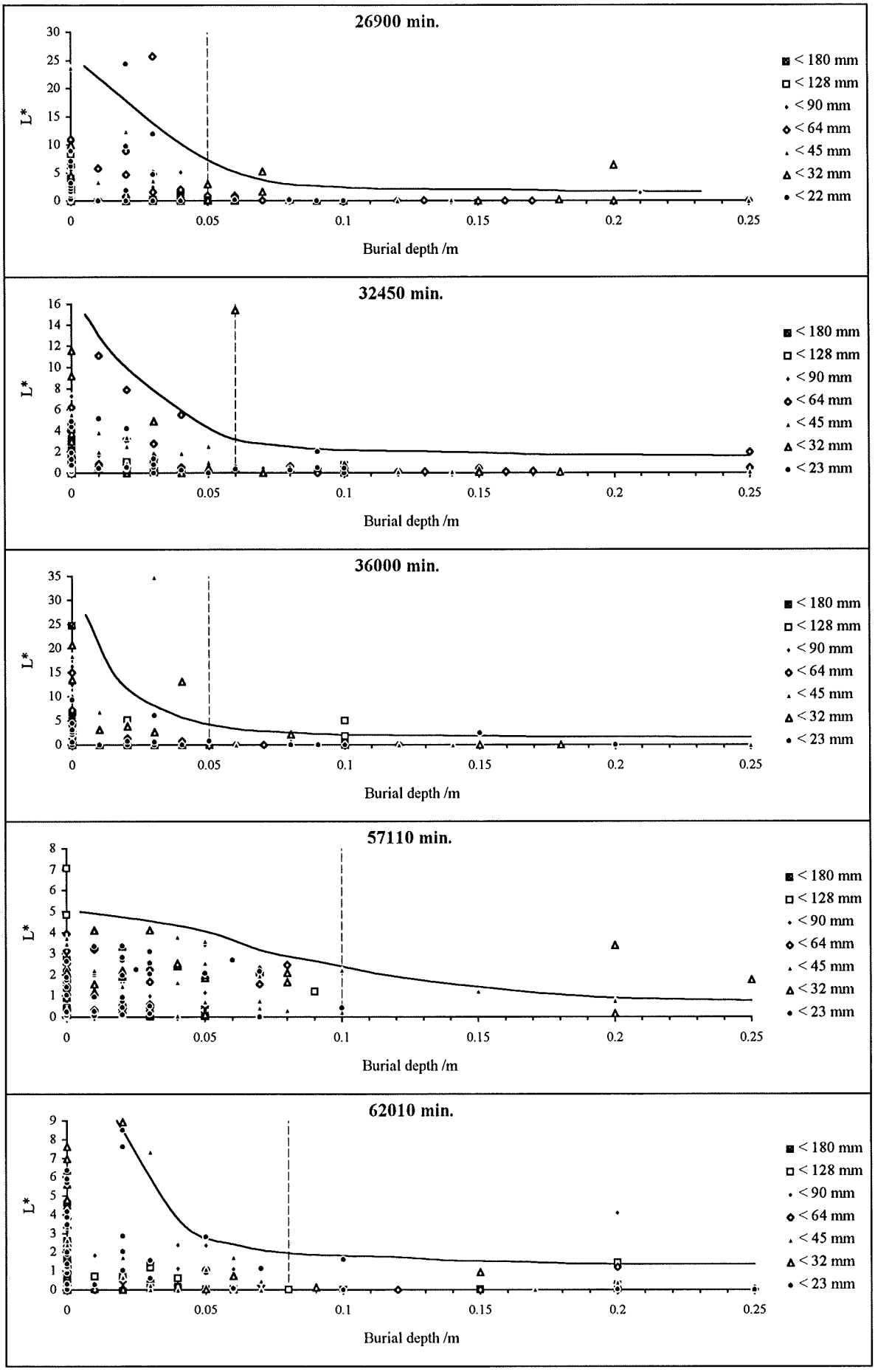

Figure 7.15: Reach A normalised transfer distance according to burial location. L* refers to distance moved by each particle normalised by the reach average per search, $L^* = L/L_{MEAN}$. Burial data are truncated at 0.25 m. Dashed line - estimated active layer depth (see p224 for definition). Solid line - approximate envelope curves. Note different interval vertical scales.

The horizontal distance moved by each tracer particle, L was normalised by the reach average distance L_{MEAN} of all the tracers per search. Only five data sets are available as during the first hop movement was exclusively from surface locations. The distribution of these data was then compared with burial depth. In reach A, most sediment which moved more than the mean was either on the surface or shallow buried prior to 36000 min. (Figure 7.15). Exponential envelope curves may be fitted indicating that at the reach scale buried sediment is less mobile than surface particles in small and intermediate flood events (the curves are approximations including the majority but not all of the data). Burial is a less important control during intense flooding, as demonstrated by the results after 36001 min., when scour and morphological change increases and most previously buried sediment is mobilised.

Results from reach B indicate similar negative exponential envelope curves for each search (Figure 7.16). Immobile sediment in the seeding pools is deemed unrepresentative and is excluded from this analysis. All searches suggest a similar limit to the depth of scour attributable to the absence of morphological change and the imposed consistent shear stresses. The curves are less well developed than in reach A due to the dominance of local random scour and fill in the absence of significant morphological change.

The distribution of the depth of scour was also determined for each storage type (Appendix L). Reach A, VA storage displays a poorly developed relationship, probably reflecting the occurrence of local scour. In other stores, buried sediment is immobile prior to 36000 min., especially in the less active stores. After 57110 min. all sediment is mobile and an exponential bounding relationship is not valid. Morphological change in association with intense flooding is essential for mobilisation of sediment in less active stores, and results in mobility of most deeply buried sediment. Increased mobility in more active stores not only reflects morphological change but also the increased probability of deeper local scour in response to higher shear stress (Hassan 1990). In reach B, there is a tendency for buried sediment to be transferred less distance than surface sediment but there is no period of significant evacuation of buried sediment from any storage type.

Depth of evacuation data permits estimation of an active layer depth in each search. This is defined as the depth of scour above which most material is evacuated. It is not maximum scour since this is a function of local random scour and fill, but it is the readily identifiable depth below which evacuation of sediment is restricted to a few particles. The depths were fitted by eye and are indicated on Figures 7.15, 7.16 and in Appendix L; summary data are presented in Table 7.4.

In reach A active layer depth increases with flood intensity. These results are a function of morphological change in less active stores and demonstrate that the bed cannot be generalised as a uniform layer for a whole reach without lateral variation. However, in reach B, in the absence of

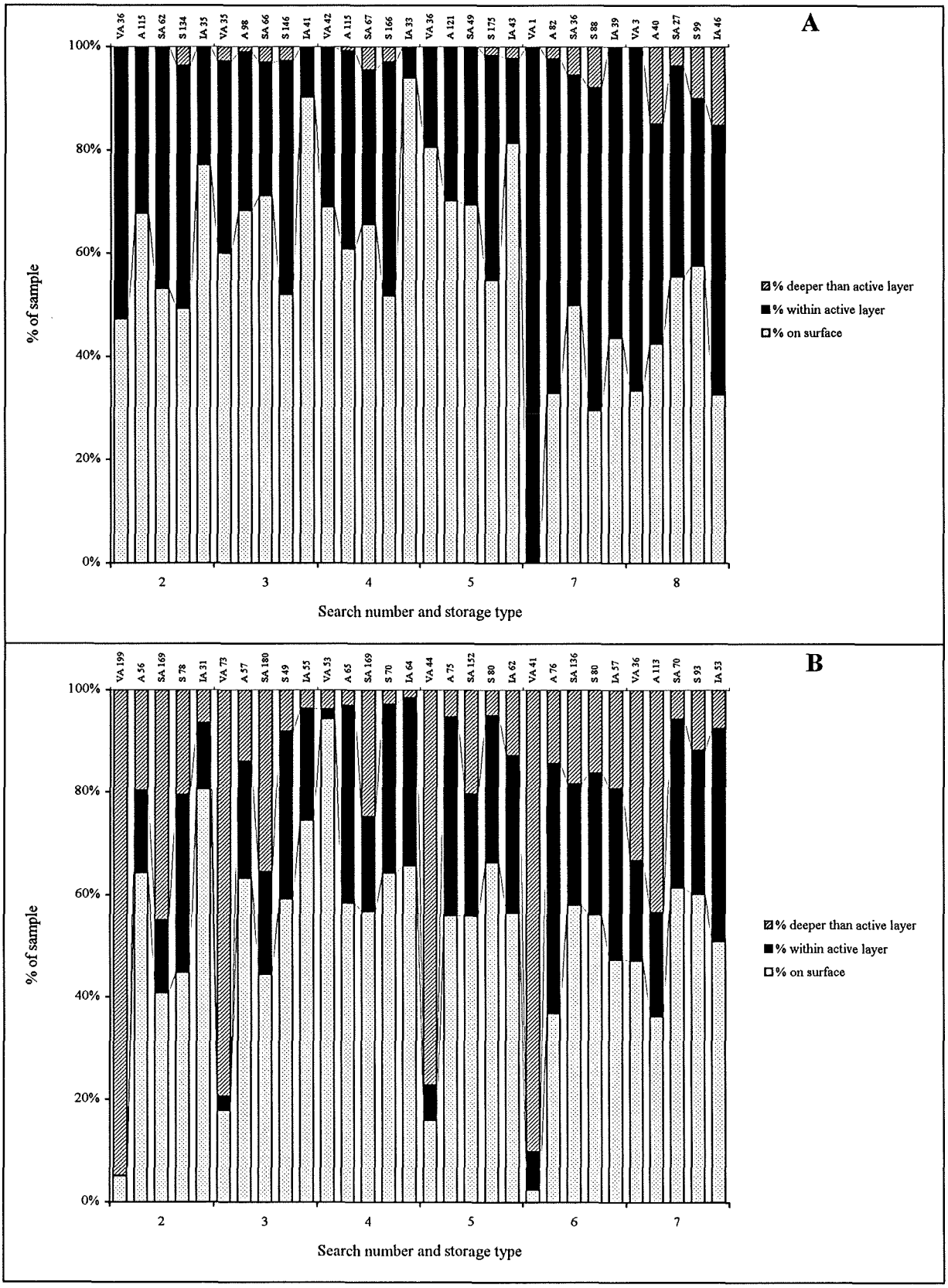

Figure 7.14. Distribution of burial depths of tracers in each storage type relative to an active layer defined as 2*D_{84}. Numerical labels indicate sample size per storage type.

hydraulic conditions responsible for store formation and migration. The less active SA and S storage types form due to unit bar migration, scour, and local redeposition of sediment or repeated aggradation. These all result in increased tracer incorporation and burial depths. The distribution of sediment is a reflection of unit bar size, hydraulics and fractional mixing during migration. In addition, scour of sediment from upstream pools may lead to aggradation in riffles (SA) or bars (S). In reach B, the maximum depth of burial is closer to $2*D_{84}$ reflecting the lack of migration and morphological change; where such three dimensional processes are dominant the conventional simplification of a 2 dimensional regular layered bed is altered.

Comparison of the percentage of tracers within each layer in reach A (Figure 7.14) indicates increased incorporation within less active stores (excluding IA). Burial of sediment increases for less active stores and also after 57110 min. in all storage types. The latter is a response to local aggradation associated with passage of a sediment wave through the reach. The percentage buried after the first hop remained approximately constant until the passage of the wave suggesting that seeding of tracers in pools resulted in almost complete sediment incorporation into the storage system in both horizontal and vertical dimensions. Approximately 50 % of the tracers were buried in reach A suggesting that burial is an important characteristic of the storage system and hence sediment redistribution. Most of this sediment was situated within the assumed active layer although a small amount of deeply buried material was found in later searches, especially within less active stores.

The situation in reach B is complicated by the immobility of sediment in some seeding pools (Figure 7.14). In general, there is no discernible pattern of burial depth according to storage type, consistent with b_{MAX} data. Some irregularities result from resetting of previously immobile buried tracers in seeding pools (e.g. VA storage 35 tracers were reset after 32100 min.). On average, approximately 50% of the tracers were buried, this figure remaining consistent throughout in the absence of large scale aggradation. The active layer did not account for all of the buried particles; many were deeply buried suggesting that $2*D_{84}$ may be an underestimate of active layer thickness in finer grained reaches where local scour and fill dominate.

7.4.3 The depth of scour

The contrast in sediment burial depths suggests that active layer depth varies according to storage type. The data presented thus far result from both scour and fill processes and do not represent the true depth of the active layer as determined from tracers (Hassan and Church 1994). An accurate estimate of the active layer depth according to storage type and reach hydraulic conditions can be obtained by examining the mobility of sediment in each storage type relative to burial depth.

7.4.2 The distribution of burial depths

The distribution of depths of stored sediment may be used to draw inferences regarding the spatial distribution of the depth of the active layer. Table 7.3 presents summary statistics detailing maximum burial depth during the study (b_{MAX}). These data were calculated for reach B excluding the tracers which were immobile and subsequently passively buried in the seeding pools. In reach A burial depths are greatest in the storage based sub-reach 3A associated with widespread stable and semi active storage. This is consistent with Hassan (1990) who found that the deepest burial was associated with bars. The anomalous figure for IA storage is a reflection of the inactivity and inaccessibility of these sites. It is unlikely that the highest bars will aggrade by over 50 cm (and hence bury tracers to that depth) except in response to exceptional flood conditions and morphological changes at the sub-reach scale. In reach B the maximum burial depth shows less systematic variation. The lack of a relationship between burial and storage type is consistent with previous analyses where storage activity was not related to the shear stress index, SSI. In both reaches, burial depths in VA storage are surprisingly low, reflecting small sample sizes associated with rapid sediment evacuation from VA storage and pool water depth precluding tracer searching more than 15 cm below the surface.

Reach A	**Max. burial depth b_{MAX} (m)**	**Reach B**	**Max. burial depth b_{MAX} (m)**
Sub-reach		*Sub-reach*	
1A	0.35	1B	0.25
2A	0.30	2B	0.30
3A	0.60	3B	0.30
Storage type		*Storage type*	
VA	0.15	VA	0.05
A	0 35	A	0.25
SA	0.50	SA	0.15
S	0.60	S	0.25
IA	0.45	IA	0.09

Table 7.3. Maximum burial depth in each sub-reach and storage type.

The distribution of depths may be assessed by categorising the bed into layers. The surface layer is defined by sediment with burial depth of 0; the active layer is $2*D_{84}$ thick as conventionally used by Hoey and Ferguson (1994), [in reach A this is 0.24 m and 0.08 m in B], the third layer containing deeply buried sediment is located at depths greater than the lower boundary of the active layer. D_{84} was taken from reach averaged grain size samples described in chapter 3.

If $2*D_{84}$ were to provide a consistent basis for estimation of the depth of the active layer then sediment in more active stores should display greater burial depths since D_{84} is coarser than in less active stores (section 4.3.2). In fact, the reverse is true in reach A (Table 7.3), reflecting the

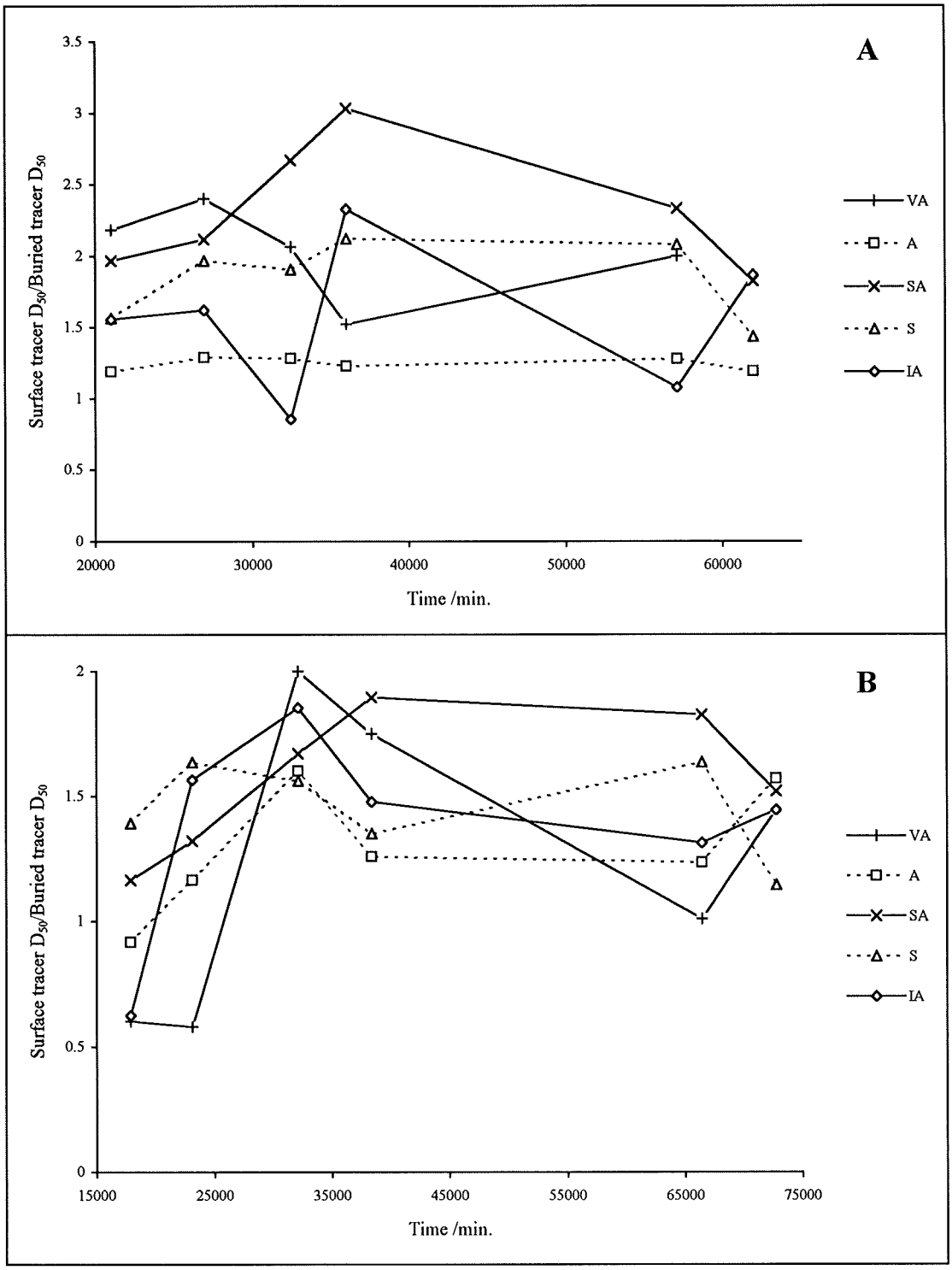

Figure 7.13. D_{50} ratio between surface and buried tracer samples per storage type.

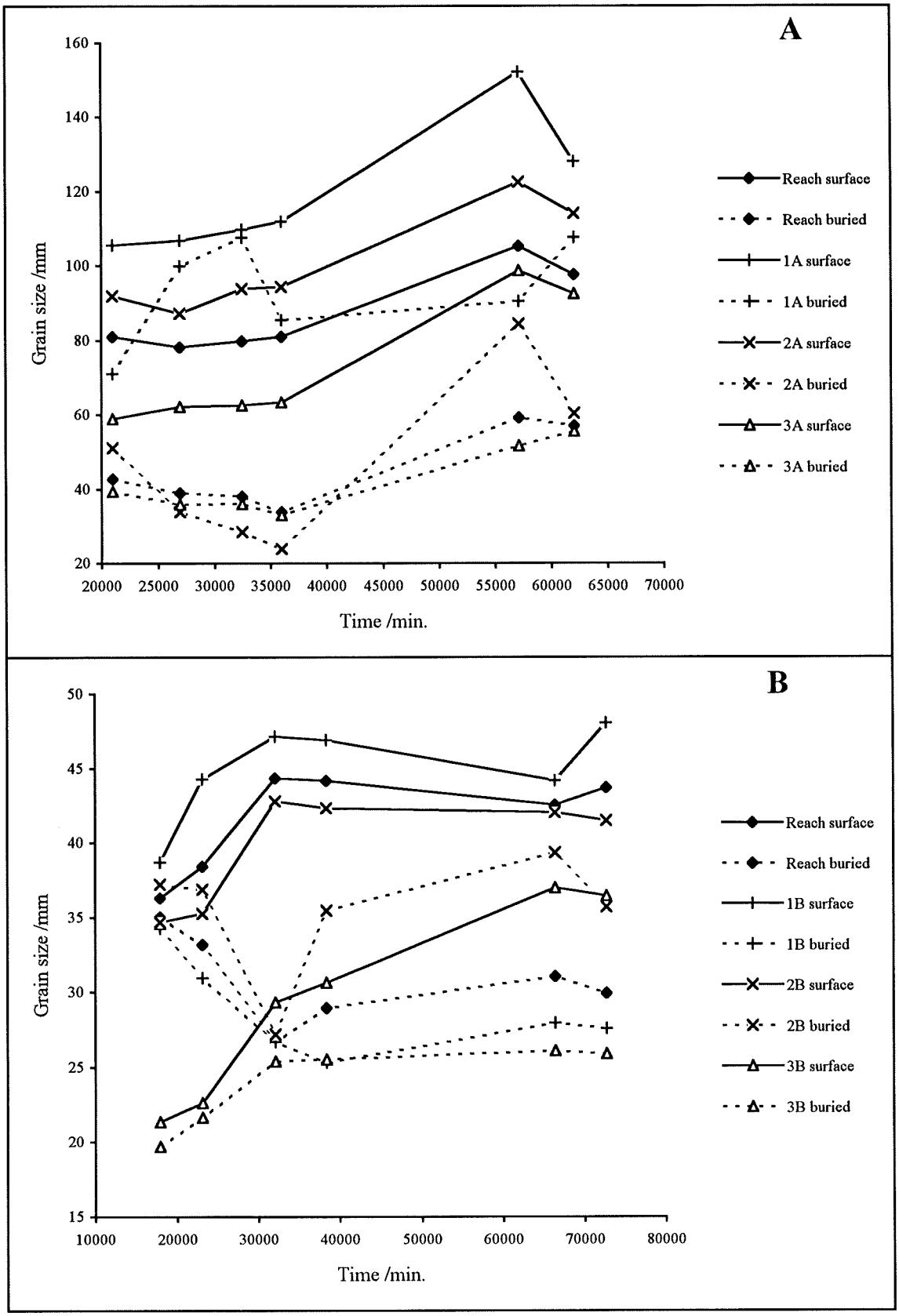

Figure 7.12. D_{50} of surface and buried tracer samples per sub-reach. Reach data are presented for comparison.

Depth of burial was measured from the base of the tracer to the bed surface (accurate to 0.025 m). This figure reflects the minimum scour prior to subsequent entrainment and maximum net fill since tracer deposition (Hassan and Church 1994). The distribution of burial depths will be used to assess three characteristics of vertical sediment exchange: (1) the grain size distribution and relative proportions of surface and buried tracers; (2) the distribution of burial depths throughout this study relative to an assumed active layer depth; and (3) the mobility of buried sediment compared with surface tracers and the maximum scour (as indicated by evacuation of buried sediment) per search according to storage type and sub-reach.

7.4.1 The grain size distribution of buried tracers

Finer sediment, by virtue of increased relative mobility and subsequent burial (Hassan and Church 1994) in a size selective transfer system should become increasingly incorporated within the active layer, leaving a coarser sub set on the surface (unless tracers are passively buried). At the reach scale (Figure 7.12), surface tracer D_{50} is approximately twice that of buried sediment in reach A and one and a half times greater in B. The increase in D_{50} with time indicates the loss of fine sediment out of reach storage during the study due to selective transfer and downstream fining of the traced material. These trends are less pronounced in reach B, where low activity in response to reduced gradients reduces the rate of fining (see Figure 3.4). Sub-reach trends are consistent with the overall reach. The downstream decrease in surface D_{50} reflects increased evacuation of finer sediment from upstream sub-reaches. Close correspondence between the reach average and 3A reflects transfer from upstream sub-reaches where sample sizes progressively declined. In reach B prior to 36000 min. buried D_{50} decreases sharply as a result of the increased mobility of fine sediment which is consequently incorporated into the bed. This is less pronounced in reach A where tracer sediment of all sizes is evacuated.

Increased incorporation of fine tracer sediment below the surface occurred in all storage types, the exact extent varying both in space and time (Figure 7.13). VA and SA storage types in reach A have the greatest degree of vertical sorting, although the results from VA stores should be viewed with caution as sample sizes are low. IA storage is the least sorted, suggesting that sediment supply to such areas is a function of mobilisation of mixed sized sediment (for example, scour from pools) which is deposited without vertical sorting and the effects of frequent inundation and reworking (Diplas and Parker 1992). There is no temporal progression in sorting in either reach, indicating that tracer storage is a composite of a number of flood events and sediment transfer processes.

coarse tracers left in storage. There is no obvious differentiation between other stores except a fine median in IA reflecting tracer availability in local source areas. In reach B no obvious trends are apparent. Only reach average data are presented as insufficient data were available to differentiate sub-reaches. Appendix K tabulates the number of tracers in each storage type per sub-reach according to grain size and shows no obvious pattern of deposition location relative to tracer size fraction. The distribution of sediment reflects the spatial distribution of the factors controlling transfer.

Fractional transfer rates and hence size selective transfer are affected by the individual storage types rather than by lateral sorting. Although less size selective than more active stores, inactive and stable stores release sediment during intense flooding according to grain size (section 6.3.4.2). During such periods relatively more fine sediment was transferred. This process of release and gradual removal of coarser sediment from the transported load demonstrates that lateral storage rather than lateral sorting is an important contributor to downstream fining on the Allt Dubhaig. However, in more active reach A stores and all of reach B, transfer in the submerged channel was the sole factor determining the sub-reach size selectivity. It is also possible that there was a minor element of lateral transport in reach B with a small percentage of material finer than D_{50} transferred non parallel to the thalweg. These results demonstrate that whilst size selectivity at an average scale, such as a reach, can be used to explain downstream fining the exact manifestation and contributory factors vary according to morphology and the effects of hydraulic conditions.

Seal et al. (1993) suggest a model predicting preferential mobility of finer fractions in response to cross sectional variation in grain size and the occurrence of patches, increasing the degree of downstream fining. Their analysis omitted elevation and storage effects. This present study has demonstrated that sediment mobility is a function of storage type, principally in response to increased elevation of less active stores (e.g. Williams and Rust 1969).

7.4 The effect of burial upon sediment mobility

Thus far no distinction has been made to account for tracers below the surface. The distribution and subsequent reactivation of buried sediment is a reflection of the temporal and spatial distribution of the active layer. The extent of the active layer is controlled by hydraulic conditions, bed grain size and local morphology (Hassan and Church 1994). Previous analyses of burial have ascertained sediment mobility relative to burial locations (Hassan 1990, Drew 1992) and developed two and three dimensional models of vertical sorting (Schick et al. 1987a, Hassan and Church 1994). Rather than replicate such analyses, this section concentrates upon the mobility of buried sediment and assesses controlling factors, principally the distribution of the active layer at sub-reach and storage type scales.

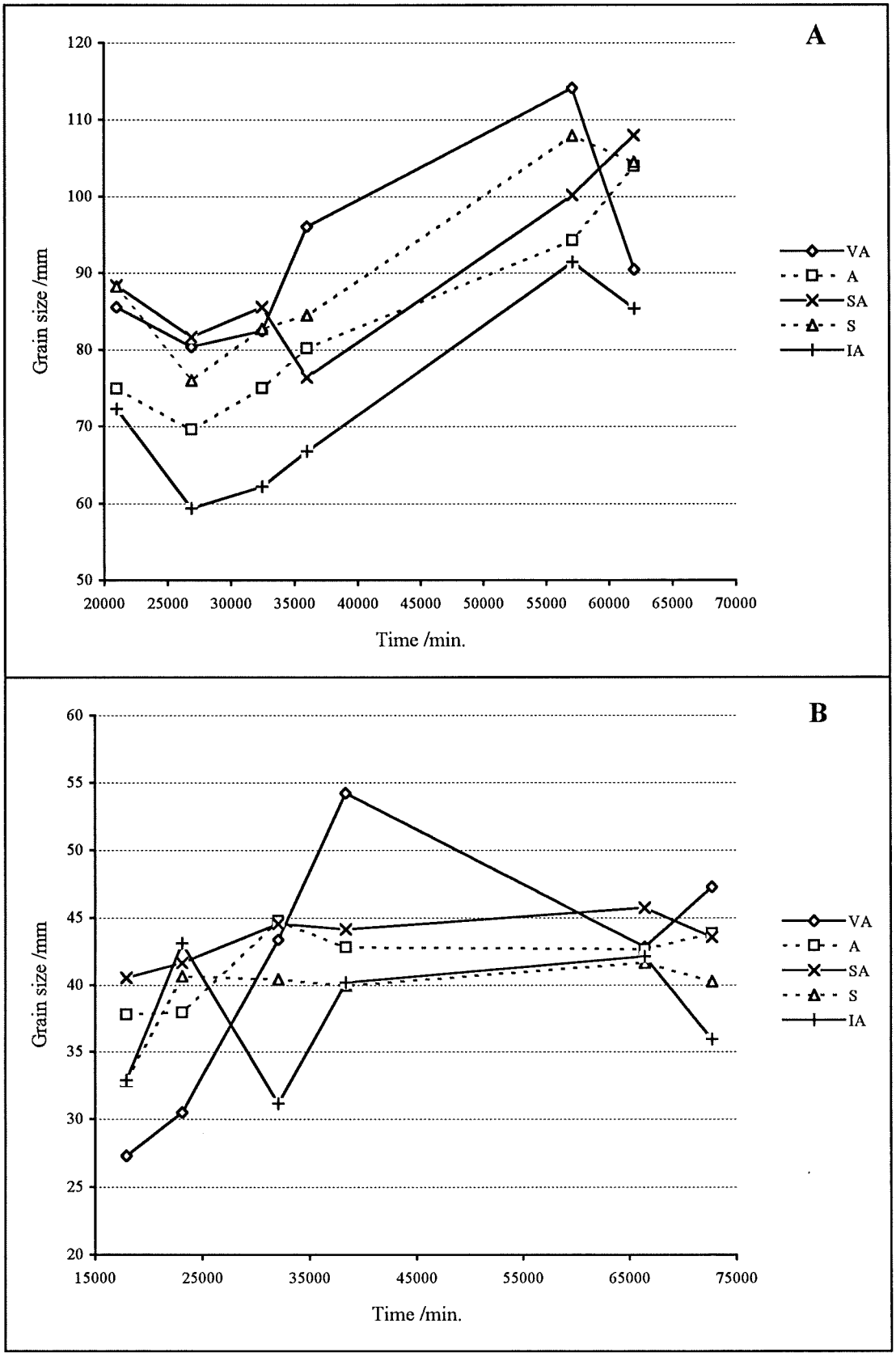

Figure 7.11. Reaches A and B, D_{50} of tracers stored in each storage type per search.

consistent with set I where scatter and distance of transfer increases with decreasing size (Appendix J5). Frequency distributions indicate a clear shift in the mode with fine sediment transported obliquely towards SA5 (Figure 7.10). Results from set II are somewhat anomalous. Most sediment was transported onto IA3 (Appendix J4), but modal angles reveal fine and coarse sediment transported at angles closer to the bank (Figure 7.10). These results probably reflect seeding of the tracers in the pool tail, but also demonstrate that size segregation may occur in other directions where shear stresses and grain size are locally small.

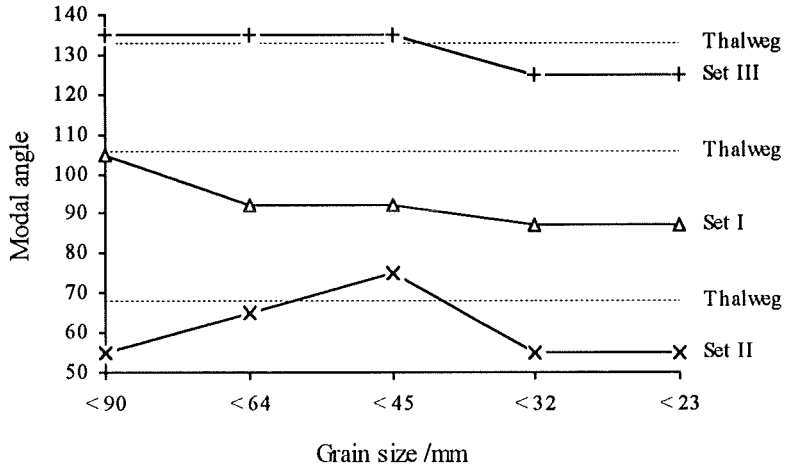

Figure 7.10. Modal angle of evacuation from all tracer sets in reach B. Thalweg angles are calculated relative to tracer seeding lines. Set II thalweg angle is an approximation due to complex pool-bar-riffle local morphology and associated flow directions.

The preceding discussion indicates that although minor, lateral transfer should not be overlooked. Whilst evident in both reaches, the mechanisms responsible for the observed trends differ. Lateral transfer in A is mainly due to distance of transfer (hence hop locations) with finer clasts more mobile and hence more dispersed, whereas in B it is also a function of morphology induced secondary circulation.

7.3.2 Lateral sorting of sediment

Lateral sorting of sediment describes the process where particles are preferentially transported according to grain size into less active stores with subsequent release dependant upon attainment of high τ^* values. For example, if < 32 mm fractions were transported exclusively into inactive storage then reach scale size selectivity would decline in response to the preferential immobility of these finer fractions. Conditions affecting transfer through entrainment and transport related factors have been reported in this study whereas the end result, deposition, has not been considered. The median grain size of tracers in each storage type (Figure 7.11) indicates no preferential deposition in either reach. In reach A, VA is the coarsest reflecting the small sample number and

circulation along the left anabranch leaving a coarser sub set behind. This initial transport is possibly responsible for the decreased recovery rates of finer fractions associated with increased movement distances and vertical exchange (Hassan and Church 1994). Most of the remaining tracers became part of the aggradation blocking the right anabranch with sediment (Appendix F13). The tracers located here were of intermediate size; only 9 out of 64 < 32 mm clasts were found. Any sediment remaining in the pool was subsequently transported along the left anabranch and was not transported into S4 which was a fine grained accumulation formed at a different time from the evacuation of the remaining fairly coarse set III tracers (as shown by set I and II tracers).

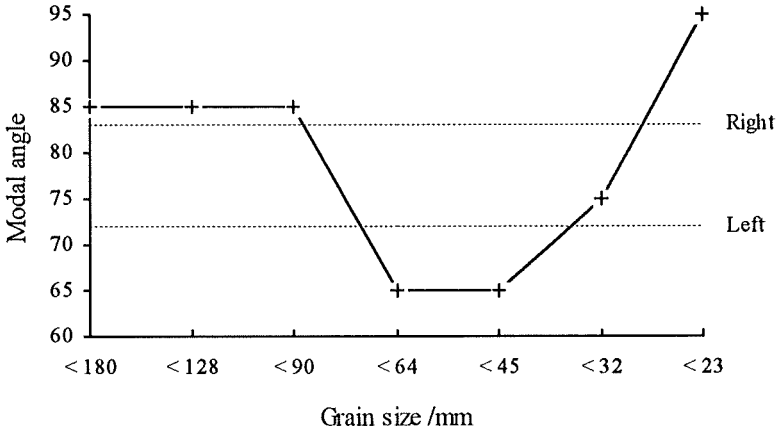

Figure 7.9. Modal angle of evacuation from tracer set III. Approximate anabranch angles, indicated by dotted lines, were calculated using the mid point of tracer line 1 and subjective selection of anabranch mid point.

Whilst realistic, the explanations presented are somewhat speculative. Absolute size effects seem more important for sediment transfer than lateral transport effects, but, the activity of this reach and the large number of possible hops associated with transfer prevent any firm conclusions regarding lateral transport from being derived. Use of radio tracers (e.g. Schmidt and Ergenzinger 1992) would improve the dataset identifying precise trajectories and temporary deposition locations.

7.3.1.2 Reach B

Reduced activity at this site should make any lateral size sorting effects evident; small movement distances allow detailed examination of the evacuation trajectory of each tracer from the seeding pools. Maps for set I (Appendix J3) indicate size related dispersion, although no particles are transported around the downstream bend. A gradual reduction in the modal angle is apparent as grain size decreases (Figure 7.10). A small number of particles close to the local D_{50} are transported laterally towards IA1 probably in response to secondary currents, scour of fine gravel sheets from this pool was partly responsible for maintenance of this bar. Data from set III are

the first hop relative to the tracer seeding lines (approximately perpendicular to flow) per half phi class. Analysis was only possible where evacuated tracers remained in the approximately straight channel downstream of the seeding site. Tracers moving less than 3 m were excluded since the accuracy of the angle calculation was sensitive to small scale data variability. It is assumed that the angle calculated is the angle of evacuation. Data are presented as maps of successive tracer positions and modal angles. The maps (Appendix J) are plotted relative to store location after search 1, corresponding to the spatial extents in Figures 5.3 and 5.9. The xy scales are unequal thus plotted angles are not exact and do not precisely correspond with the modal angle calculations.

7.3.1.1 Reach A

Data from sets I and II cannot be used to assess evacuation angle due to movement around the main bend in reach A. However, the distribution of transfer plotted according to half phi class (Appendix J1) allows inferences regarding transport patterns. Most fine tracers were deposited in store S4 (Figure 5.3) attached to the left bank in sub-reach 3A. Almost no tracers were deposited at the head of S3 and IA3, stores which contained a significant number of tracers derived from set III seeded in the pool upstream (Figure 3.6, 4). The absence of tracers in stores S2 and IA2 (located on the point bar at the apex of the main bend, bar II) suggests that sediment from sets I and II was transported along the thalweg rather than across the bar; thus the tracers passed through the set III seeding site, yet deposition locations contrast. Explanation for these differing pathways is a function of grain size, morphological change and the timing of tracer transport through the set III seeding site relative to morphological change, changing stage and therefore hydraulics. Aggradation occurred at the head of S3 and IA3 effectively blocking the right anabranch around bar III, in response to which, the left anabranch was incised prior to 21000 min. (Appendix F, F7). The aggradation was a result of scour from the set III seeding pool from which tracers were deposited 20 m downstream. Upstream tracers reached and subsequently passed through the pool and exited via the left anabranch since the other side had filled, so the sediment was deposited in different areas. This demonstrates the importance of morphology on tracer distributions and that tracer locations reflect a temporal sequence during bedload transporting flows.

Whilst most set III sediment was deposited in IA3 and S3, some did move down the left anabranch (Appendix J2). Angle of evacuation data may be used to assess size related transport relative to the timing of the local aggradation discussed herein. Summarising these data as modal angles (Figure 7.9) reveals a decrease in the mode as grain size declines below 90 mm indicating that finer sediment is more prone to move down the left anabranch. Data for the <23 mm fraction is anomalous due to reduced recovery rates. The shift in the mode and the pattern of transfer pathways may be attributable to the sequence of events described above. Prior to aggradation and blocking of the right anabranch, fine sediment was transported out of the pool due to secondary

transport factors do not appear to have a major influence upon transfer distances. However, it is impossible to categorically exclude the effect of transport upon transfer distances since the cause of scatter around the relationship may not be attributed to any single factor. In addition to conditions at entrainment, hop location and morphology, factors implicit in tracer transport distributions may also influence transfer (Thorne and Lewin 1979, Laronne and Duncan 1992).

Similar trends are evident at reach B (Figure 7.8) although the data are more scattered. This increased scatter reflects reduced sample size (many Γ_i values = ∞) and the absence of any regular trends in reach B (apart from grain size) according to sub-reach, storage type, hydraulic conditions or bed material. The insignificance of the relation derived for storage types is consistent with the results from chapters 5 and 6 where storage type was found to have little control upon transfer fluxes. The improved significance for sub-reaches is a result of average data reducing some of the variability.

7.3 Tracer transfer patterns

The preceding analysis demonstrated that in addition to operating at the point of entrainment, hydraulic conditions, grain size and storage type during transport may also affect transfer distances since the probability of stopping and subsequent re-entrainment is also a function of local dimensionless shear stress. The exact magnitude of this is impossible to ascertain in the absence of representative data, however, some understanding of modifications to transfer pathways whilst tracers are in transport, primarily in response to morphologically induced cross stream currents, can be determined with reference to tracer trajectories.

7.3.1 Lateral variation

The pathway of a tracer in transport is affected by local morphology, hydraulic conditions (in response to morphology) and tracer grain size. For example, secondary circulation effects in meander bends (e.g. Markham and Thorne 1992) tend to transport a proportion of the sediment moving as bedload onto point bar surfaces (Thorne and Lewin 1979). Morphologically induced currents often cause deviation of transport paths non parallel to the thalweg (Laronne and Duncan 1992).

Angles of evacuation from seeding pools after the first search provide the most reliable data on transport pathways. Tracers in subsequent searches are too scattered to allow further analysis due to complicating factors such as relative grain size and burial. Within each seeding pool, the tracers were unconstrained with pool location providing the opportunity to examine lateral transport in response to secondary currents. The angle of evacuation was calculated from tracer location after

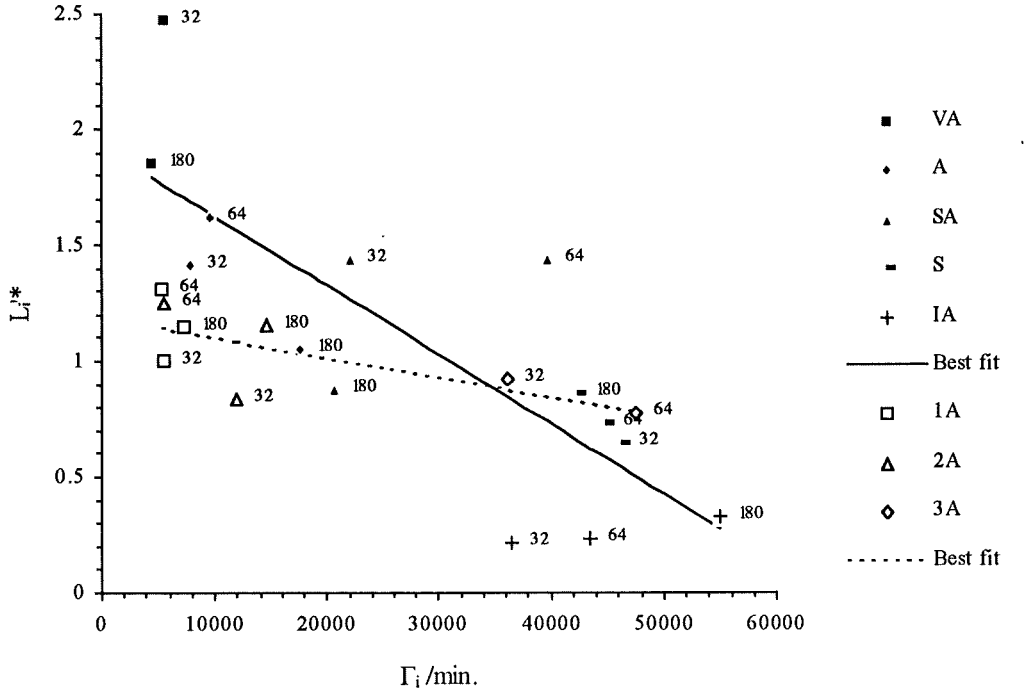

Figure 7.7. Reach A, mean fractional transfer distance (normalised by reach mean) plotted against response time according to storage type and sub-reach. Best fit lines are calculated by regression of sub-reach and storage type data separately, r^2 sub-reach (dotted line) = 50.6%, storage type (solid line)= 64.0%. Figures indicate upper limit size fraction of data point.

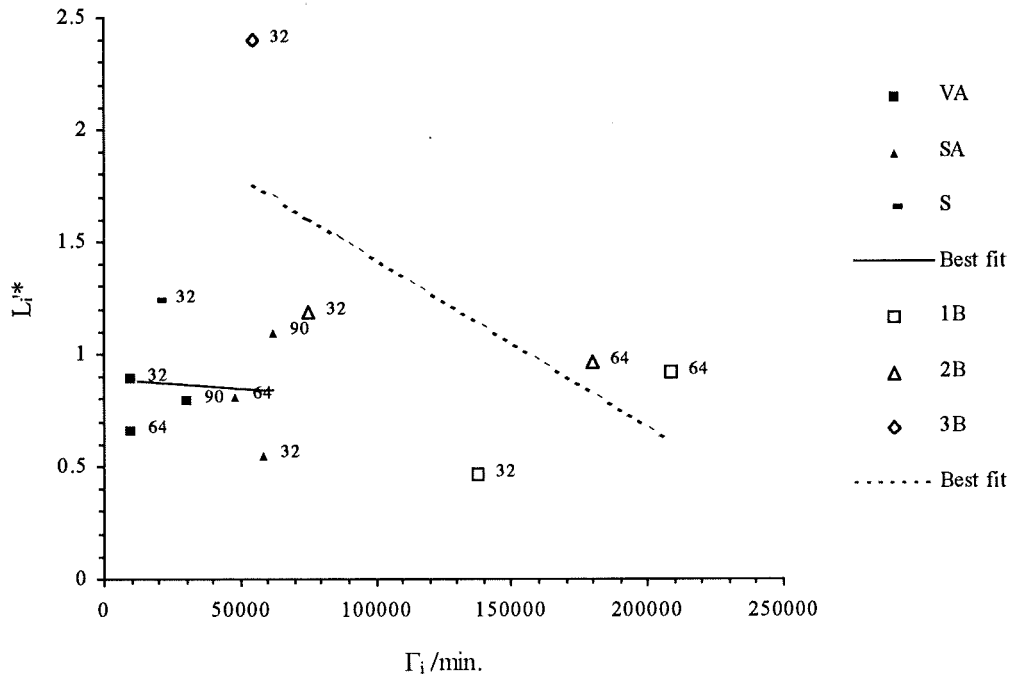

Figure 7.8. Reach B, mean fractional transfer distance (normalised by reach mean) plotted against response time according to storage type and sub reach. r^2 sub-reach (dotted line) = 45.3%, storage type (solid line) = 0.0%.

c. the distribution of transfer distances in each sub-reach is a reflection of the combination of storage types present and the factors governing transfer from such stores, particularly the importance of morphological change;

d. transfer distributions contrast due to between reach differences in hydraulic, morphological and sedimentological characteristics;

e. there is a regular hierarchy in storage type activity at reach A which is not apparent in B. This progression is poorly defined where $D_i^*<1$;

f. semi active storage in reach B displays reduced mobility of finer sizes due to vertical winnowing into a coarse riffle;

g. transfer from storage based S and IA stores contains relatively high proportions of coarse sediment, reflecting the interaction of hydraulic conditions and morphology in reach A and relative grain size effects at B.

7.2.5 Distance moved and response time

Differentiation between transport and entrainment effects may be made by comparing response time, Γ_i, and mean fractional transfer distance normalised by the reach average, $L_i'^*$. The former is based upon the occurrence of entrainment, whilst the latter, described in preceding sections, is based upon transfer distances (a function of factors controlling entrainment and transport). Data are presented at sub-reach and storage type scales. Perfect correspondence between Γ_i and $L_i'^*$ would indicate that transfer distances are only a function of τ^* conditions at the initial location of the tracer per event. Deviation away from a perfect relationship would be symptomatic of three factors, none of which may be isolated: (1) the random nature of entrainment (Buffington et al. 1992); (2) small tracer sample sizes; (3) conditions during transport affecting the magnitude of transfer distances.

In reach A transfer distance is related to response time (Figure 7.7). The best fit lines reflect relative sub-reach and store activity (Figure 7.5 and Table 7.2), with the shallower gradient for sub-reaches associated with the narrower range of transfer conditions at this scale since the data are an average of all 5 storage types. Increased scatter in the storage data reflects the range of morphology. These results suggest an imperfect dependence of transfer upon conditions at entrainment. However, at a more detailed scale, no systematic trends in the scatter are apparent from grain size data per store or sub-reach possibly reflecting the random entrainment process. On this basis, the MSS analysis presented in the previous chapter is valid as an approximation since

stores display less size selectivity. Transfer from these stores requires morphological change (associated with intense flooding) with most sizes having similar high potential mobility. A high proportion of the sediment stored in 3A was located in these storage types leading to the decreased selectivity at this site identified in the previous subsection. In reach B (Figure 7.6) transfer based stores display more size selectivity than storage based ones, particularly inactive storage. Results from 32100 and 66450 min. indicate that coarser sediment travels further from IA storage than finer clasts (Appendix I4, J). In the absence of morphological change in reach B it is likely that coarser sediment may be more mobile due to protrusion effects as the only IA store containing sediment was IA3 (Figure 5.9) where coarse tracers were located on the surface.

	L'*	
	Reach A	*Reach B*
VA	3.21	0.77
A	1.31	1.68
SA	1.19	0.76
S	0.76	1.16
IA	0.26	0.47

Table 7.2. Distribution of mean distance of sediment transfer relative to the reach average according to storage type. Data in excess of 1 are indicative of transfer distances greater than the reach average.

The distribution of $L_i'^*$ in both reaches is particularly scattered (Appendix I5) reflecting the combination of factors influencing sediment transfer at small scales. Simplifying these data using mean L'* across all size fractions during the study indicates a clear hierarchy of storage types at A, and a less obvious trend at B (Table 7.2), consistent with the results discussed in previous chapters.

7.2.4 Summary

The previous sub sections have examined the factors responsible for the dominant mode of transfer at various scales. Whilst consistent with the results from the previous chapters, some additional interactions are apparent. These are summarised as follows:

a. fractional transfer distances depend upon hydraulic conditions (peak and duration), storage type, local morphology and relative grain size. This represents a detailed breakdown of the MSS analysis presented in chapter 6;

b. the trends in activity at all scales discussed in previous chapters are conditioned by relative grain size;

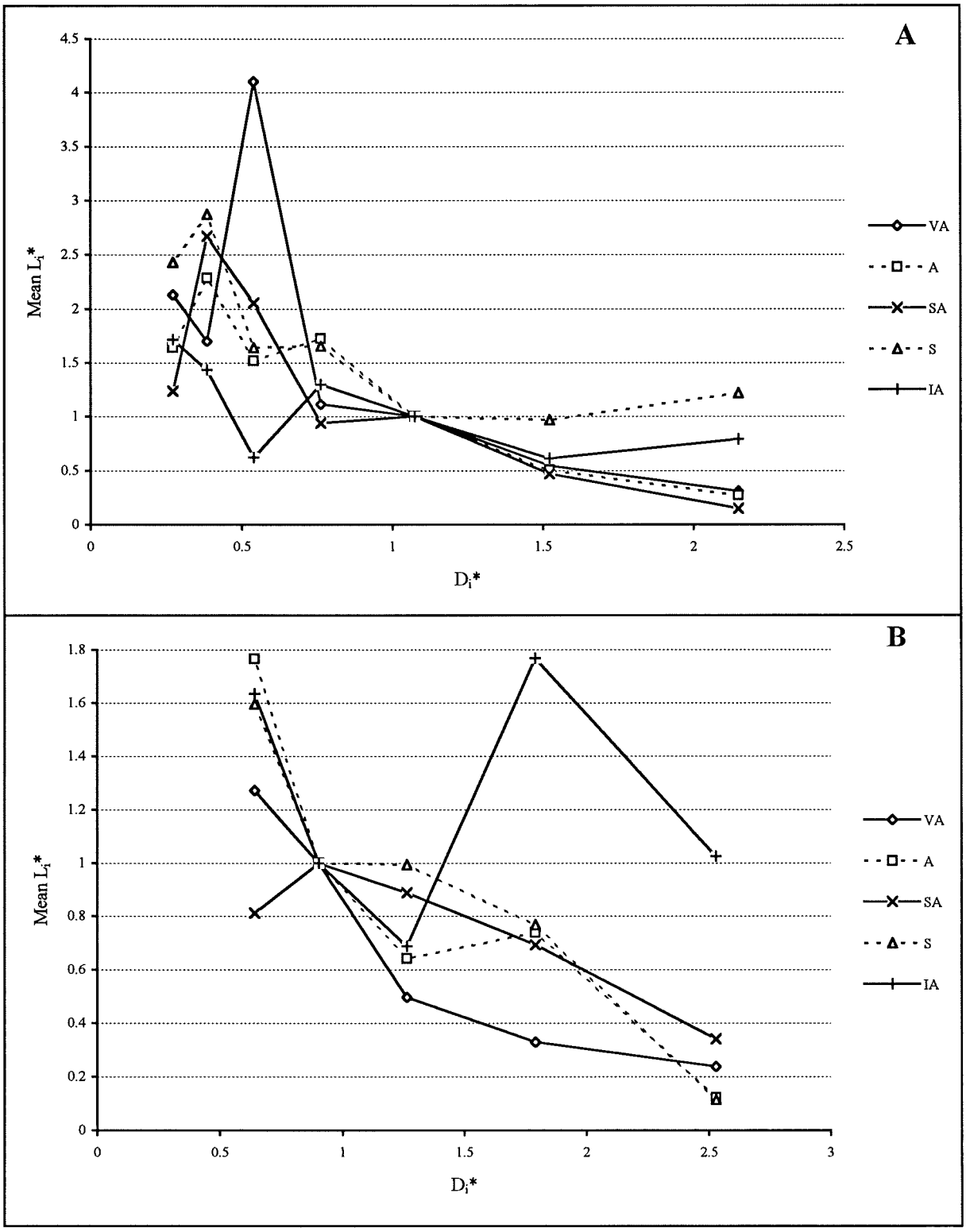

Figure 7.6. Reach A and B, mean dimensionless fractional distance moved from each storage type averaged over the whole study.

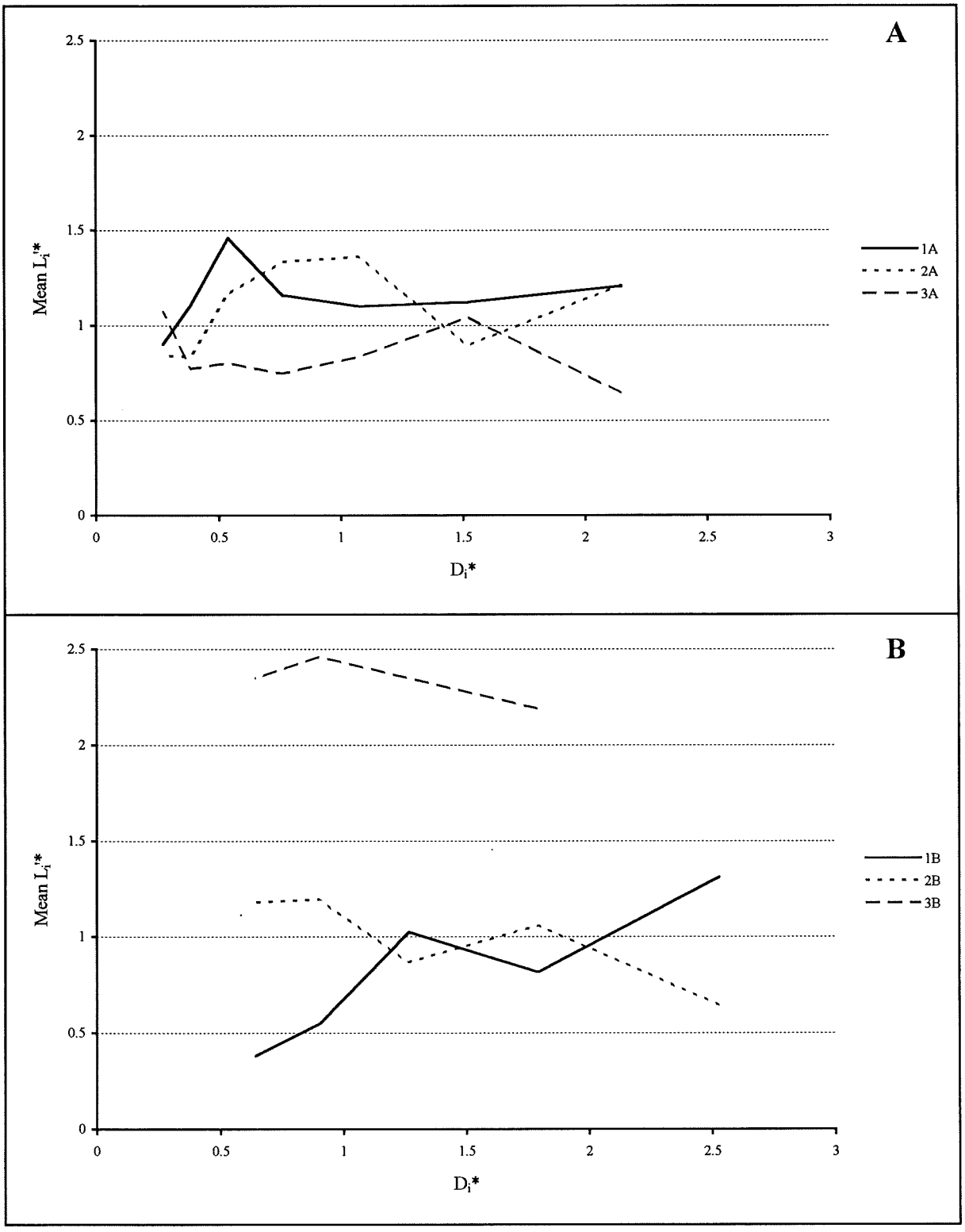

Figure 7.5. Reach A and B relative sub-reach activity represented by mean fractional transfer distance relative to the reach mean. Data are an average over the whole study.

Yatsu, E. (1955) 'On the longitudinal profile of the graded river', *Trans. Am. Geophys. Union*, **36**, 655 - 663.

Young, W. J. and Davies, T. R. H. (1991) 'Bedload transport processes in a braided gravel-bed river model', *Earth Surface Processes and Landforms*, **16**, 499 - 512.